

TRANSLATION

FLOATING GYROSCOPES AND THEIR APPLICATIONS

By G. A. Slomyanskiy, Yu. N. Pryadilov

August 1960

AD618874 32 Pages

#61-13412

339-P

COPY	OF	
HARD COPY	\$.	7.00
MICROFILM	\$.	1.75

MASTER

DDC
RECEIVED
AUG 12 1965
DDC-IRA E

PREPARED BY
LIAISON OFFICE
TECHNICAL INFORMATION CENTER
MCLTD
WRIGHT-PATTERSON AIR FORCE BASE, OHIO

G. A. Slonyanskiy and Yu. N. Pryadilov

ПОПЛАВКОВЫЕ ГИРОСКОПЫ И ИХ ПРИМЕНЕНИЕ

ГОСУДАРСТВЕННОЕ ИЗДАТЕЛЬСТВО ОБОРОННОЙ ПРОМЫШЛЕННОСТИ

Москва 1958

244 pages

This translation was prepared under the auspices of the Liaison Office, Technical Information Center, Wright-Patterson AFB, Ohio. The fact of translation does not guarantee editorial accuracy, nor does it indicate USAF approval or disapproval of the material translated.

Comments pertaining to this translation should be addressed to:

**Liaison Office
Technical Information Center
MCLTD
Wright-Patterson Air Force Base, Ohio**

This volume presents a brief survey of the fundamental properties of gyroscopes and their use for the purpose of determining the orientation of a given object (an aircraft, guided missile, etc.) with respect to a certain system of coordinates, which may be fixed or rotating in space in a prescribed manner; the type designations and capabilities of typical differentiating and integrating gyroscopes are examined.

Detailed consideration is given to the design, theory, and analytical procedures applied to floating differentiating and integrating gyroscopes, and to certain problems attendant upon their application. The volume contains data pertaining to American floating gyroscopes. The physical bases for inertial navigation systems are outlined briefly.

The book is intended for use by engineers working in the field of gyro-mechanism engineering, and may also prove useful to students in the instrument-engineering specialties.

Reviewer: Dr. Tech. Sci. Prof.
G. O. Fridlender

Editor: Eng. I. L. Yanovskiy

Editor-in-Chief: Eng. A. I. Sokolov

PREFACE

Floating gyroscopes are capable of sensing both extremely small and quite large absolute angular velocities, and of functioning reliably under heavy vibrational and shock loads.

Floating gyroscopes were originally intended only for use in the inertial-navigation systems which determine the altitude of flying objects (aircraft, rockets, guided missiles, etc.) with respect to the earth by double integration of their acceleration with respect to time. A navigational system of this type was first worked out in the Soviet Union in 1932 by E. B. Levental. It underwent further development in our country at the hands of B. V. Bulgakov, G. O. Fridlender, L. I. Tkachev, and other scientists and engineers. A great deal of attention has also been devoted to these systems in other countries.

Because of the advantages which they offer, floating gyroscopes have recently found an increasingly wider range of application extending far beyond the field of inertial-navigation system.

The present volume sets forth the considerations basic to the design, theory, and methods of analysis of floating integrating and floating differentiating gyroscopes; consideration is given to the operation of the floating integrating gyroscope in conjunction with a servo drive (Chapters II, III, IV, and V). Chapter VI provides a brief outline of the physical basis of the inertial-navigation system.

In order to clarify the considerations which led to the development of the floating gyroscope and to establish its relationship to the ordinary gyroscope--from which it does not differ in principle--Chapter I presents a brief survey of the

application of gyroscopes for the purpose of determining the orientation of some object (an aircraft, guided missile, etc.) with respect to a certain system of coordinates erected in inertial space: the functions and capabilities of ordinary differentiating and integrating gyroscopes are discussed (Chapter I, Sections 3, 4, 5, 6, 7). However, Chapter I is concerned not only with our previous store of knowledge, but also presents a number of new conclusions. These include derivation of a formula for gimbaling error which includes a consideration of the pitching moment and an expression for the moments which must be applied (in the general case) to a gyroscope with three degrees of freedom in order to impart the proper mode of rotation in inertial space to the spin axis, study of the operation of a typical integrating gyroscope in conjunction with a servodrive, etc. To render the book more understandable to readers unfamiliar with the general and applied theories of the gyroscope, the first two sections of Chapter I give brief discussions of gyroscopes with two and three degrees of freedom.

The concrete data concerning the design and parameters of floating gyroscopes and the equipment used in their analysis have been borrowed from American scientific literature, a bibliography of which is given at the end of the book. These generally unrelated references were systematized, generalized, and subjected to analysis. The theory of floating integrating and floating differentiating gyroscopes set forth in this volume takes the special design characteristics of these devices into account. In the development of this theory special attention has been devoted to definition and study of the parameters which govern the operation of the instruments in use, and also to presentation of these parameters in a form which lends itself to experimental investigation of them. As a rule, all theoretical derivations are accompanied by detailed analyses of the physical aspects of the operation of the instrument and its various elements. The paper by C. S. Draper, W. Wrigley, and L. R. Grohe entitled "The Floating Integrating Gyroscope and its Application to Solution of the Problem of Geometrical Stabilization in Moving

Objects," presented at the 23rd Annual Conference of the United States Institute of the Aeronautical Sciences and published as a separate document has been used as a point of departure.

Considerable attention has been devoted in the present volume to discussion of the procedures used in analysis of floating gyroscopes and their theoretical foundations.

The book has frequent recourse to material from the series of lectures on aviation instruments and automatic devices given at the Moscow Institute of Aviation by G. A. Slomyanskiy.

Chapters I, II, III, IV, and V were written by G. A. Slomyanskiy and Chapter VI by Yu. N. Pryadilov under the editorship of G. A. Slomyanskiy, who made certain additions (this chapter is an abridged and slightly revised translation of an article by Philip I. Klass published in the magazine Aviation Week). Yu. N. Pryadilov also supplied auxiliary translations of some of the American literature references from which the practical data on the floating gyroscopes were borrowed. In addition to this, Yu. N. Pryadilov is also responsible for the technical preparation of the manuscript and of the majority of the illustrations. The remainder of the illustrations were designed by V. N. Pappe.

The authors consider it incumbent upon them to express their gratitude to Doctor of Technical Sciences Prof. G. O. Fridlender for the valuable suggestions which he offered while reviewing the manuscript.

The authors are indebted to V. G. Denisov and G. T. Astavin for the assistance which they rendered in selecting the literature references.

CHAPTER I

BRIEF SURVEY OF THE CHARACTERISTICS AND CERTAIN APPLICATIONS OF GYROSCOPES

The high-speed gyroscopes used in various types of gyroscopic instruments and mechanisms may be classified under two basic headings: gyroscopes with two degrees of freedom and gyroscopes with three degrees of freedom. Each of these two types is endowed with its own special nature and characteristics. The class of gyroscopes with three degrees of freedom is the most widely used. Recently, however, an increasing number of uses have been found for the gyroscope with two degrees of freedom. The basic properties of gyroscopes of both types are considered briefly in the following paragraphs.

Section 1. Brief Consideration of Gyroscopes With Two Degrees of Freedom

The gyroscope with two degrees of freedom (Fig. 1.1) consists of a rotor 1 and a frame 2. The rotor is mounted in bearings situated in the frame and rotates at high speed with respect to the latter about its own axis of symmetry z at a constant angular velocity Ω , which is referred to as the velocity of proper rotation of the gyroscope. Here and in the material which follows we shall consider the vector of angular velocity to be extended along the corresponding axis in a direction such that rotation appears to proceed counterclockwise when viewed from the end of the vector. The same rule will also be observed for moments of force and moments of momentum.

The pivot journals of the gyroscope frame are carried in the bearings 3, which are rigidly attached to the base 4. A gyroscope of this type has two degrees of freedom: first, rotation of the rotor with respect to the frame at an angular velocity Ω ; and second, rotation of the frame with the rotor about the x axis (see Fig. 1.1) relative to the base 4. In actual applications, the outer case of a gyroscope with two degrees of freedom, i.e., the housing of the device itself, is most frequently used as the base.

The axis of symmetry z is designated the spin axis of the gyroscope. The positive direction of the z axis must coincide with the direction of the vector of the angular velocity Ω of the proper rotation of the gyroscope.

The frame and rotor are carefully balanced about the axis of rotation of the frame x . As already noted, the proper-rotational velocity imparted to the gyroscope is high--that is, of the order of 12,000 to 24,000 rpm or more. A gyroscope possessing a high proper-rotational velocity is called a high-speed gyroscope.

The moment of momentum of a gyroscope about the rotor-spin axis z is generally designated the angular momentum of the gyroscope and is represented by the letter H .

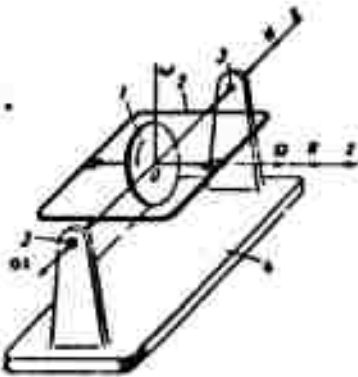
$$H = C\Omega \text{ gf-cm-sec.} \quad (1.1)$$

where C is the axial moment of inertia of the gyroscope (the moment of inertia of the gyroscope about its spin axis) in gf-cm-sec^2 .

It is a known fact in gyroscope theory that if the base gyroscope with two degrees of freedom is rotated with an angular velocity ω whose vector is perpendicular to the axis of rotation of the gyroscope frame and forms some angle θ with the vector H , a "gyroscopic moment" (a Coriolis inertia equal to the vector product of the vector H by the vector ω) will be exerted on the frame. Thus the gyroscopic moment

(1.2)

perpendicular to the plane containing the vector of the proper moment \underline{H} and vector ω (i.e., it acts about the axis of rotation of the frame) and is so



directed that the first vector tends to bring itself into coincidence with the second by the shortest possible path (Fig. 1.1). If the gyroscopic moment encounters no resistance it will turn the frame with the rotor into a position in which the vector \underline{H} will coincide with the vector ω . Rotation of the base of a gyroscope with two degrees of freedom about axes coinciding

Fig. 1.1. Gyroscope with two degrees of freedom:

- 1) gyroscope rotor; 2) frame; 3) bearings; axis of rotation of the frame cannot
- 4) base.

with or parallel to the spin axis or the give rise to a gyroscopic moment, since

no Coriolis inertia arises under these conditions.

It should be noted that the gyroscopic moment—all other factors considered equal—will assume a maximum value at the point where the angle $\theta = 90^\circ$, i.e., when the vector of the rotational velocity of the base ω is perpendicular to the vector of the proper gyroscopic moment \underline{H} . This follows immediately from Formula (1.2).

If an external moment \underline{M} is applied about the axis of rotation \underline{x} of the frame (Fig. 1.1) of a gyroscope with two degrees of freedom, the gyroscope will, under the influence of this moment, behave like any other solid object having a fixed axis of rotation (in our case, the \underline{x} axis). In other words, the rotation of the frame

with the gyroscope about the \underline{x} -axis is subject in this case to the equation (neglecting friction):

$$J\ddot{\theta} = M, \quad (1.3)$$

where J is the moment of inertia of the frame with the gyroscope relative to the \underline{x} axis in gf-cm-sec^2 and θ is the angle through which the frame rotates about the \underline{x} axis.

The only difference between this gyroscope and the solid object will consist in the fact that the bearings of the frame will receive an additional load due to the gyroscopic moment which arises from the angular velocity $\dot{\theta}$ of the spin axis and is proportional to this velocity. However, if the frame carrying the gyroscope is given a velocity $\dot{\theta}_0$ about the \underline{x} -axis at the instant $t=0$ and is thereafter left unhindered, it will continue to rotate at this velocity for an indefinite period like any other solid body. In practice, however, friction in the bearings and air resistance will eventually bring this motion to a halt. Thus a gyroscope with two degrees of freedom cannot persistently maintain the position originally imparted to it.

The capacity of a gyroscope with two degrees of freedom to react to an angular velocity ω by generating a gyroscopic moment Γ proportional to ω and applied to the frame of the gyroscope is an extremely valuable one from a practical standpoint, since it permits such gyroscopes to be used as units which are sensitive to angular velocities. Highly important gyroscopic devices, such as the differentiating and integrating gyroscopes, which will be considered later, have been constructed on the basis of this property of the gyroscope with two degrees of freedom.

Section 2. Brief Consideration of Gyroscopes With Three Degrees of Freedom

The gyroscope with three degrees of freedom (Fig. 1.2) consists of the rotor 1,

the inner frame 2 of the gimbal suspension and the outer frame 3 of the gimbal suspension. The rotor is mounted in bearings carried on the inner frame, and revolves rapidly with respect to the latter with a constant angular velocity Ω about the spin axis z . The inner frame may rotate with respect to the outer frame about the x axis. The outer frame is, in turn, mounted in bearings fixed in the base 4, and may rotate with respect to the latter about Y axis.

Thus the rotor of the gyroscope has three degrees of freedom: first, the rotation of the rotor itself with respect to the inner frame about the spin axis z ; second, the rotation of the inner frame carrying the rotor about its x axis relative to the outer frame; and third, the rotation of the outer frame carrying the inner frame with the rotor about its Y axis with respect to the base. The spin axis of the gyroscope has two degrees of freedom. The point O , at which the x axis, the Y axis of the gimbal suspension and the spin axis z intersect, is the fixed point of the gyroscope. All of the motions of the gyroscope reduce to its rotation with a certain instantaneous angular velocity relative to the fixed point O . In a mechanical sense, therefore, the gyroscope with three degrees of freedom represents a solid body secured at a single point--the fixed point O .

All components of the gyroscope with three degrees of freedom are subjected to careful static balancing with respect to the axes of rotation of the gimbal-suspension frames so that the center of gravity of the entire frame-and-rotor system will coincide with the fixed point O . When this condition is established, the gyroscope is referred to as astatic. The rotors of gyroscopes with either two or three degrees of freedom are balanced dynamically about their spin axes z .

Let us consider the basic characteristics of the high-speed gyroscope with three degrees of freedom.

1. If a certain direction in inertial space, e.g., the direction of a certain fixed star, is imparted to the spin axis at the initial moment of the time, and the gyroscope is thereafter left unhindered and free from the influence of any external

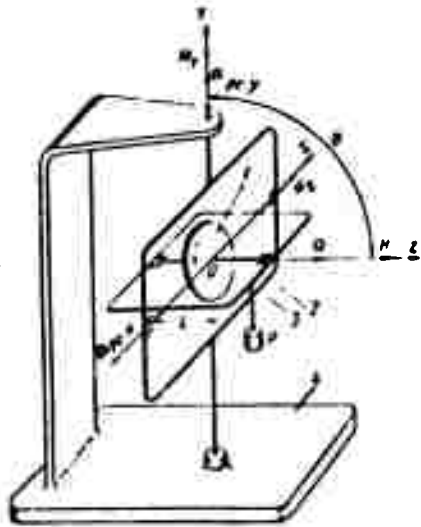


Fig. 1.2. Gyroscope with three degrees of freedom.

1) Rotor of gyroscope; 2) inner gimbal-suspension frame; 3) outer gimbal-suspension frame; 4) base; O) fixed point of gyroscope; x) axis of rotation of inner gimbal-suspension frame; Y) axis of rotation of outer gimbal-suspension frame; z) spin axis of gyroscope.

moments, it will rigidly retain the direction in inertial space which was originally imparted to it; this rigidity will increase with increasing magnitude of the proper moment H . In practice, however, it is impossible to attain complete freedom from effects exerted on the gyroscope by external moments; consequently, ideal maintenance by the gyroscope of the direction originally imparted to it is not possible.

This is explained as follows:

First, it is impossible in practice to fabricate acceptable gimbal-suspension bearings with virtual freedom from friction, and consequently to free the

gyroscope completely from the influence of the frictional moments which arise in these bearings. Secondly, it is impossible to construct an ideally astatic gyroscope. As a result of noncoincidence of the center of gravity of the gyroscope with its fixed point O , a gravitational moment will be exerted on the gyroscope, and, when the base is subject to accelerated motion, a moment of transfer inertia as well.

*(Author's note) Here and throughout, the term rigidity refers to the capacity of a high-speed gyroscope with three degrees of freedom to resist the influence of externally applied moments. Thus, the greater the rigidity of the gyroscope, the smaller will be its deflection from its original position under the action of a given applied moment.

Any gyroscope with three degrees of freedom used in practice will accordingly depart in the course of time from the direction in inertial space which was originally imparted to it. This departure is frequently referred to as gyroscopic drift. The drift velocity will be a function of the parameters of the gyroscope and the quality of its construction. The drift velocity of a real gyroscope has both systematic and accidental components. The systematic component of the drift velocity may be compensated by applying an appropriate moment to the gyroscope, but it is impossible to compensate the accidental drift-velocity components.

2. An external moment \underline{M} , acting on the gyroscope about the axis of rotation of one of the gimbal-suspension frames, will cause the spin axis to rotate (precession) about the axis of rotation of the other gimbal frame at a velocity

$$\Omega_{pr} = \frac{M}{H \sin \theta} \quad (1.4)$$

where θ is the angle between the gimbal frames.

This rotation has a tendency to superpose the vector \underline{H} on the vector \underline{M} . If the external moment \underline{M} acts about the axis of rotation of the outer gimbal-suspension frame, the spin axis (the vector \underline{H}) will, in the course of time, coincide with the axis of rotation of this frame. If the moment \underline{M} acts about the axis of rotation of the outer frame this coincidence will not occur, as will readily be seen from Fig. 1.2.

In cases where the moment applied to the gyroscope does not coincide in direction with the axis of rotation of either of the gimbal frames, only its projections to these axes will give rise to precession. Formula (1.4) and its accompanying explanation are referred to as the law of precession of the high-speed gimbal-suspended gyroscope, and the motion of the gyroscope under the influence of an external moment which they characterize is known as gyroscopic

precession. Let us consider examples which serve to illustrate this law.

Suppose that an external moment M_x --due, say, to a load of weight P suspended on the arm \underline{l} (see Fig. 1.2) from the outer frame--acts on the gyroscope about the axis of rotation \underline{x} of the inner frame of the gimbal suspension. This moment will be equal to

$$M_x = Pl \sin \theta,$$

where θ is the angle between the gimbal frames.

In accordance with the law of precession (1.4), the gyroscope will rotate, or "precess" under the influence of the moment M_x at a velocity

$$\Omega_{pr} = \frac{M_x}{H \sin \theta} = \frac{Pl}{H}$$

about the axis of rotation \underline{y} of the outer frame. This precession will continue until the load P is removed, i. e. as long as the moment M_x remains effective.

Now let an external moment M_y be applied to the gyroscope about the axis of rotation of the outer frame (Fig. 1.2). Thereupon the gyroscope will precess about the axis of rotation of the inner frame at a velocity

$$\Omega_{pr} = \frac{M_y}{H \sin \theta},$$

in accordance with the law of precession.

If the moment M_y acts for a sufficiently long period, this precession will sooner or later bring the spin axis \underline{z} into coincidence with the axis \underline{y} of the outer frame. Here the gyroscope loses one degree of freedom, and consequently will no longer possess the characteristics of gyroscopes with three degrees of freedom; hence it is no longer subject to the law of precession. For this reason, coincidence of the gimbal frames must not be permitted to occur under actual operating conditions.

Referring back to Formula (1.4), we should note that the given moments acting along the axes of the gimbal frames will produce higher precessional velocities as the angle between the gimbal frames departs increasingly from 90° . The smallest precessional velocities are obtained when the gimbal frames are mutually perpendicular ($\theta = 90^\circ$). Accordingly, a high-speed gyroscope will achieve maximal rigidity with respect to the disturbance moments acting upon it when its gimbal frames are mutually perpendicular. Formula (1.4) for the precessional velocity of the gyroscope takes the following form for the case of mutually perpendicular frames:

$$\Omega_{pr} = \frac{M}{H}. \quad (1.5)$$

The actual motion of a gyroscope with three degrees of freedom under the influence of an external moment is somewhat more complex than that indicated by the law of precession. Let us consider this motion.

Let us again apply an external moment \underline{M}_x to the gyroscope about its \underline{x} axis; this may be done, as before, by means of a load \underline{P} (Fig. 1.3). Assume that the spin axis is stationary at the moment of application of the load \underline{P} and that the load is applied without imparting a velocity to the spin axis. In accordance with the law of precession, the gyroscope will precess (rotate) about the \underline{y} axis under the influence of the moment \underline{M}_x at an angular velocity

$$\Omega_{pr.y} = \frac{M_x}{H}.$$

The end of the spin axis will now describe the circular arc \underline{aa} (Fig. 1.3). In actuality, however, the gyroscope will move in such a way that the end of the spin axis describes the trajectory represented by the heavy line in Fig. 1.3. The spin axis will revolve about the \underline{y} axis in one direction with a periodically varying velocity whose mean value during a period \underline{T}_p will be equal to the velocity

$$\Omega_{pr} = \frac{M_z}{H}$$

It will oscillate simultaneously about the axis to which the external moment is applied (the x axis) with an amplitude $\beta^* = \frac{2AM_x}{H^2}$ and a period $T_P = 2\pi \frac{A}{H}$, where A is the equatorial moment of inertia of the gyroscope in gf-cm-sec^2 , i.e. the moment of inertia of the gyroscope rotor about any axis passing through the point O perpendicular to the spin axis z (neglecting the inertia of the gimbal frames, although they also exert an influence on β^* and T_P).

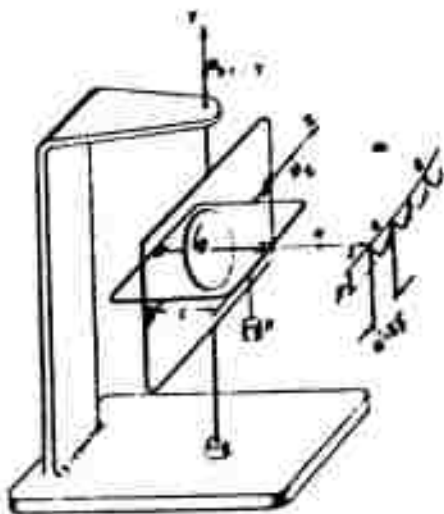


Fig. 1.3 Precession and nutation of a gyroscope with three degrees of freedom.

This oscillation of the spin axis about the axis to which the external moment is applied is called nutation.[†] It can be seen from the formulas for β^* and T_P that nutation becomes less pronounced as H increases. Consequently, the higher the velocity of proper rotation of the gyroscope, the smaller β^* and T_P will be. The actual trajectory described by the end of the spin axis may also assume looped or wavy forms, depending on the initial conditions.

In high-speed gyroscopes, the amplitude β^* and the period T_P are so small as to be practically imperceptible. Therefore nutation is usually neglected in studies of the motion of high-speed gyroscopes under the influence of external moments, i.e. only the fundamental precessional motion of the spin axis as determined by the law of precession is taken into account.

Let us justify this procedure in an example using a gyroscope with relatively

[†] Nutation (Latin): nodding.

small \underline{H} . We shall assume that \underline{C} for this gyroscope is 1 gf-cm-sec², $\underline{A} = 0.6\underline{C}$,
 $\Omega = 12,000 \text{ rpm} = 400\pi \text{ rad/sec}$. Then, applying the formulas for β^* and \underline{T}_p and
 Formula (1.1) we find that

$$\beta^* = \frac{2 \cdot 0.6 \cdot 1}{(1 - 400\pi)^2} \cdot M_x = 76 \cdot 10^{-3} M_x$$

or, expressing β^* in seconds with \underline{M}_x in gf-cm,

$$\beta^* = 0.157 M_x$$

Even with $\underline{M}_x = 100 \text{ gf-cm}$ --a very high figure for gyroscopes of this type--

$$\beta^* = 15.7;$$

$$\underline{T}_p = 2\pi \frac{0.6 \cdot 1}{1 - 400\pi} = 0.003 \text{ sec.}$$

Such oscillation is virtually unnoticeable and, as we said, is usually neglected. Since nutation is highly undesirable in gyromechanisms, they are usually designed in such a way that the amplitude of nutation is quite small with the result that nutation is imperceptible in operation.

3. The high-speed gyroscope with three degrees of freedom is practically inertialess. This means that precession ceases immediately the external moment act-

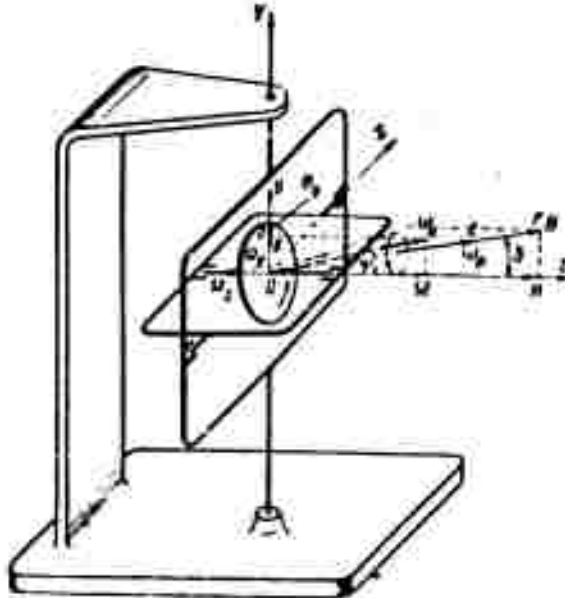


Fig. 1.4. Inertial motion of gyroscope with three degrees of freedom.

ing upon the gyroscope is removed. The inertial motion of the spin axis which arises when precession ends proceeds with such a small amplitude and such a high frequency that it is virtually imperceptible. Furthermore, this inertial motion is rapidly damped by air resistance and the inevitable bearing friction.

To clarify the nature of the inertial motion of a gyroscope with three degrees of freedom, let us refer to Fig. 1.4. Let us assume that the gyroscope has a proper-rotational velocity Ω and is fixed immovably in inertial space. Now, by striking the frame, for example, let us impart to it an additional angular velocity Ω_y about the y axis, which is perpendicular to the x and z axes and, with them, forms a trihedron (at the initial instant, the y axis coincides with the Y axis); then let us leave the gyroscope to itself, without exerting any external

moment upon it.

Since the instantaneous absolute angular velocity of the gyroscope

$\vec{\omega}_a = \vec{\Omega} + \vec{\Omega}_y$ will now no longer coincide in direction with the spin axis \underline{z} , but form an angle ψ with it (see Fig. 1.4) such that $\tan \psi = \Omega_y / \Omega$, the spin axis will no longer be fixed in inertial space, but will begin to move relative to it. The motion which begins will be an inertial motion since we have imposed the condition that no external moments act on the gyroscope. In its inertial motion, the spin axis of the gyroscope will describe a circular cone with a constant angular velocity ω_θ about the stationary vector θ of the kinetic moment of the gyroscope with respect to the fixed point O . The magnitude and direction of the vector θ are constant since no external moments are applied to the gyroscope (kinetic-moment theorem).

The kinetic moment θ of a gyroscope is the result of rotation of the gyroscope about its spin axis \underline{z} as well as of rotation of the spin axis itself. The proper moment H of the gyroscope is equal to the projection of the vector θ onto the spin \underline{z} axis. The second component of the vector θ , which is perpendicular to the \underline{z} axis, is referred to as the equatorial component of the kinetic moment of the gyroscope. Since the velocity with which the spin axis of a high-speed gyroscope can rotate is small by comparison with its proper-rotational velocity, the equatorial component of the kinetic moment θ of a high-speed gyroscope is negligibly small by comparison with the angular momentum of the gyroscope H .

The apical angle of the cone (2θ) is determined from the expression

where \underline{C} and \underline{A} are the axial and equatorial moments of inertia of the gyroscope (the inertia of the gimbal frames is neglected).

moment upon it.

Since the instantaneous absolute angular velocity of the gyroscope $\vec{\omega}_a = \vec{\omega} + \vec{\omega}_y$ will now no longer coincide in direction with the spin axis \underline{z} , but form an angle ψ with it (see Fig. 1.4) such that $\tan \psi = \omega_y / \omega$, the spin axis will no longer be fixed in inertial space, but will begin to move relative to it. The motion which begins will be an inertial motion since we have imposed the condition that no external moments act on the gyroscope. In its inertial motion, the spin axis of the gyroscope will describe a circular cone with a constant angular velocity ω_θ about the stationary vector Θ of the kinetic moment of the gyroscope with respect to the fixed point O . The magnitude and direction of the vector Θ are constant since no external moments are applied to the gyroscope (kinetic-moment theorem).

The kinetic moment Θ of a gyroscope is the result of rotation of the gyroscope about its spin axis \underline{z} as well as of rotation of the spin axis itself. The proper moment \underline{H} of the gyroscope is equal to the projection of the vector Θ onto the spin \underline{z} axis. The second component of the vector Θ , which is perpendicular to the \underline{z} axis, is referred to as the equatorial component of the kinetic moment of the gyroscope. Since the velocity with which the spin axis of a high-speed gyroscope can rotate is small by comparison with its proper-rotational velocity, the equatorial component of the kinetic moment Θ of a high-speed gyroscope is negligibly small by comparison with the angular momentum of the gyroscope \underline{H} .

The apical angle of the cone (2θ) is determined from the expression

$$\tan \theta = \frac{A}{C} \tan \psi = \frac{A}{C} \frac{\omega_y}{\omega},$$

where \underline{C} and \underline{A} are the axial and equatorial moments of inertia of the gyroscope (the inertia of the gimbal frames is neglected).

The velocity ω_Θ is the component of the velocity ω_y directed along the vector Θ and is obtained on decomposition of ω_y in the directions of the vector Θ and the spin axis z (see Fig. 1.4). Using the similar triangles OBE and ODF , we obtain the value of the velocity ω_Θ in the form

$$\omega_\Theta = \frac{\Theta}{A} = \frac{1}{A} \sqrt{H^2 + \Theta^2} = \frac{H}{A} \sqrt{1 + \left(\frac{\Theta}{H}\right)^2} = \Omega \frac{C}{A} \sqrt{1 + \tan^2 \theta},$$

where $\Theta = \frac{A}{\Omega} \Omega_y$ is the equatorial component of the gyroscope's kinetic moment.

It is evident from the expression for $\tan \theta$ that this angle is very small, since the velocity which may be imparted in practice to the spin axis of a high-speed gyroscope without damaging the gyroscope (in our case, the velocity Ω_y) is considerably smaller than the proper-rotational velocity Ω . Moreover, $A < C$ in production gyroscopes. Let us consider an example.

Suppose we have a gyroscope with comparatively small H whose characteristic values are as follows: $C = 1 \text{ gf-cm-sec}^2$, $A = 0.6C$, $\Omega = 12,000 \text{ rpm}$. Let us impart to it a secondary angular velocity $\Omega_y = 10 \text{ rpm}$ (Fig. 1.4) which we know to be larger than the velocity which can be given the spin axis of a gyroscope of this type. Then, applying the formula for $\tan \theta$, we obtain

$$\tan \theta = \frac{0.6 \cdot 1}{1} \cdot \frac{10}{12,000} = 0.0005; \quad \theta = 1' 44''.$$

In this example, therefore, the total apical angle of the cone described by the spin axis in its inertial motion will be $3' 28''$.

As seen from the expression given for the velocity ω_Θ , this is greater than the proper-rotational velocity Ω .

Accordingly, the inertial motion of the spin axis may always be kept practically

imperceptible by proper selection of the gyroscope parameters. This condition is invariably met in the case of high-speed gyroscopes. At the instant at which the external moment applied to the gyroscope ceases to act—as a result of which precession also stops—the instantaneous absolute angular velocity of the gyroscope will be composed of the proper-rotational velocity and the velocities of precession and nutation which prevailed at this instant, and will consequently be directed at a certain small angle to the spin axis. The inertial motion will begin as a result of this. As indicated previously, however, the amplitude of this motion will be so small in high-speed gyroscopes that the spin axis will, in practice, become stationary as soon as the external moment ceases to act. Also mentioned above was the fact that friction in the gimbal-suspension bearings and air resistance lead to rapid decay of the inertial motion of the spin axis. It is this which causes the practically inertialess character of the high-speed gyroscope.

4. The high-speed gyroscope with three degrees of freedom is characterized by rigidity toward disturbing forces which act for short periods. This means that when a short-term disturbing force acts upon this gyroscope, its rotor spin axis will experience virtually no change of direction in space.

It should be remembered, however, that even very small external moments which act for considerable periods in one direction are capable of producing considerable deflections of the gyroscope spin axis from its original position.

The fundamental properties of the high-speed gyroscope with three degrees of freedom which we have outlined above are such as to ensure its use over a broad range of technical fields. In certain cases, however, the degree of precision with which it is necessary to maintain the direction in inertial space originally imparted to the gyroscope is so high that it is frequently impossible to ensure this precision by means of the designs ordinarily used for gyroscopes with three degrees of freedom.

Section 3. Certain Specific Applications of the Gyroscope

With Three Degrees of Freedom

The technical applications of gyroscopes with three degrees of freedom are exceedingly numerous and varied with respect to both the purpose involved and the way in which the gyroscope is put to use.

Here we shall consider, in one of its variants, the practice of using a gyroscope with three degrees of freedom to determine the orientation of some object (an aircraft, rocket, etc.) with reference to a certain coordinate system which may be either fixed or revolving in a prescribed manner in inertial space. This application of the gyroscope is of the highest importance in controlling the

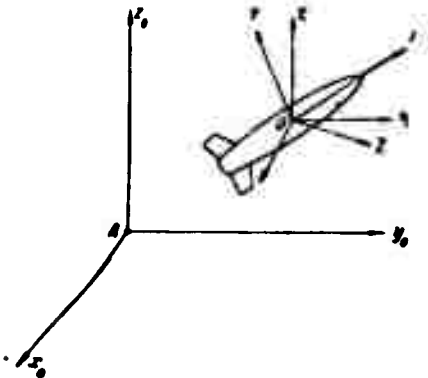


Fig. 1.5. Determination of the position of an object moving in space.

motion of aircraft, rockets, etc. We shall not, however, make it our purpose to study this problem in detail, but shall consider it in general terms and only to the extent necessary to explain why the so-called floating gyroscope has now been adopted as a means of solving the most critical cases of the above problem.

Let $Ax_0Y_0Z_0$ be some earth-related or inertial system of coordinates (Fig.1.5). It will be recalled that a system of measurement is termed inertial when Newton's first law (the law of inertia) applies to it. Suppose further that some object, e.g., a rocket, is moving with respect to this system of coordinates. The trihedron $OXYZ$, whose origin occurs at the object's center of gravity O , is permanently attached to it. The X and Y axes lie in the object's longitudinal plane of symmetry,

with the \underline{X} axis directed along the longitudinal axis of the object. We shall designate \underline{X} the longitudinal axis, \underline{Y} the normal axis, and \underline{Z} the transverse axis. The positive directions of these axes, as well as those of all the other axes represented in Fig. 1.5, are indicated by the arrows. Further, let us take a system of axes $\underline{O\xi\eta\zeta}$ which have their origin at the same point \underline{O} and proceed parallel to the axes of the $\underline{Ax_0y_0z_0}$ -system or possess a definite orientation with respect to the earth.

The position of the object in question with respect to the coordinate system $\underline{Ax_0y_0z_0}$, or with respect to the earth when the axes $\underline{Ax_0y_0z_0}$ are referred to the earth and the axes $\underline{O\xi\eta\zeta}$ are related to it in a definite manner, is determined

by the three coordinates of its center of gravity \underline{O} and the three angles ψ , ϑ , and γ which describe the position of the \underline{OXYZ} -system with respect to the axes $\underline{O\xi\eta\zeta}$. Let us examine these angles.

The system $\underline{O\xi\eta\zeta}$ may be shifted to the position of \underline{OXYZ} by three rotational operations, as follows (Fig. 1.6). First, we must turn the system of axes $\underline{O\xi\eta\zeta}$ through an angle ψ about the axis $\underline{\zeta}$, bringing the axes $\underline{\xi}$ and $\underline{\eta}$ into the positions $\underline{Z_1}$ and $\underline{X_1}$; next, the system $\underline{OX_1Z_1}$ should be turned through an angle ϑ about the $\underline{Z_1}$ axis, so that the axes $\underline{X_1}$ and $\underline{\zeta}$ occupy the positions \underline{X} and $\underline{Y_2}$; finally, the system $\underline{OXY_2Z_1}$ must be rotated through an angle γ about the \underline{X} -axis, whereupon the axes $\underline{Y_2}$ and $\underline{Z_1}$ assume the

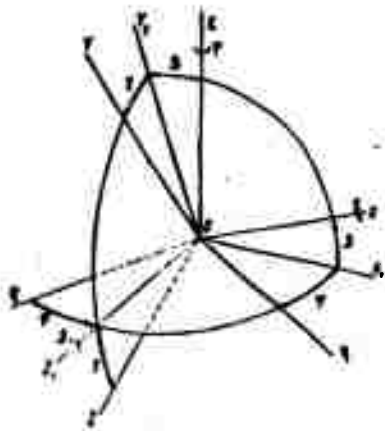


Fig. 1.6. The angles ψ , ϑ , and γ , which characterize the position of the axes \underline{OXYZ} of the object with respect to the axes $\underline{O\xi\eta\zeta}$, which have a fixed orientation in space.

positions Y and Z and the system Oξηζ has been made congruent with the system OXYZ. The cosines of the angles formed by the axes X, Y, and Z with the axes ξ, η, and ζ are presented in the following table:

	<u>ξ</u>	<u>η</u>	<u>ζ</u>
<u>X</u>	$-\sin \psi \cos \theta$	$\cos \psi \cos \theta$	$\sin \theta$
<u>Y</u>	$\cos \psi \sin \gamma$	$\sin \psi \sin \gamma$	$\cos \theta \cos \gamma$
<u>Z</u>	$\cos \psi \cos \gamma$	$\sin \psi \cos \gamma$	$-\cos \theta \sin \gamma$

(1.6)

The three angles under consideration -- ψ , θ , and γ -- fully determine the directions of the axes OXYZ of the object, or, in other words, its position with respect to the axes Oξηζ. Since the angles ψ , θ , and γ are the angles of rotation of the object about the axes ξ, Z₁, and X, the latter will be referred to as the axes of measurement, i.e. the axes to which measurements of the above angles are referred.

Thus in order to determine the position of the object with reference to the system Ax₀Y₀Z₀ (Fig. 1.5), it is necessary to have the three coordinates of its center of gravity O, which determine the location of the object, and the three angles ψ , θ , and γ , knowledge of which is necessary for control of the object's motion. The coordinates of the center of gravity O are measured by means of the so-called navigation systems, which perform this operation either semi-automatically or automatically. If the moving object is an airplane and is not equipped with an automatic or semi-automatic navigation system, its location with reference to the earth -- in other words, its location with respect to the system Ax₀Y₀Z₀, which in this case is referred to the earth -- is determined by the pilot or navigator, using aerial-navigation techniques and the appropriate immediate-

evaluation devices.

There are in existence several types of navigation systems which differ from one another in operating principle. One of these -- the inertial-navigation system, for which floating gyroscopes have also been developed -- will be discussed in general terms in the last chapter of this book.

Although determination of the coordinates of the center of gravity O of the object, i.e. its location, is possible and was accomplished for some time without the aid of gyroscopes, no generally reliable method exists for direct determination without the use of gyroscopes of the angles ψ , θ , and γ for an object moving through the air.

Let us assume that the system $Ax_0y_0z_0$ is inertial and that the axes $O\xi\eta\zeta$ are respectively parallel to the axes $Ax_0y_0z_0$; now consider the manner in which it will be possible, using gyroscopes with three degrees of freedom, to determine the angles ψ , θ , and γ for this case. The case is characterized by the necessity of determining these angles with reference to the axes $O\xi\eta\zeta$, which, like the axes $Ax_0y_0z_0$, have fixed orientations in inertial space. To make it possible to measure the angles ψ , θ , and γ , therefore, it will first be necessary to reproduce the axes $O\xi\eta\zeta$ in a concrete form -- either together or separately -- in the moving object. For this purpose we may use a gyroscope with three degrees of freedom, which, as indicated in Sec. 2, will possess the ability to maintain its spin axis rigidly in a given direction in inertial space.

A simplified drawing showing the design of a gyroscope with three degrees of freedom appears in Fig. 1.7. The gyroscope rotor and the inner frame of the gimbal suspension together form, the so-called gyromotor. The gyroscope shown in Fig. 1.7 has an alternating-current gyromotor, which is usually built as an asynchronous motor with a short-circuited rotor which revolves at constant speed. As a rule, the inner frame 2 of the gimbal suspension is given the form of a closed

shell -- a practice based on considerations of principle.

Let us mount the gyroscope housing 5 in a moving object, e.g., the rocket shown in Fig. 1.5, in such a way that the fixed point O of the gyroscope (Fig. 1.7) coincides with the center of gravity O of the object, and the axis of rotation of the outer gimbal frame is directed along the normal Y axis of the object. The longitudinal and transverse axes of the instrument housing are made to coincide with the longitudinal (X) and transverse (Z) axes of the object, respectively. (Figs. 1.5 and 1.7). Let us further direct the spin axis (z) of the gyroscope along the η axis of the system $O\xi\eta\zeta$. This arrangement makes the spin axis a concrete reproduction of the η axis. With $\psi = \theta = \gamma = 0$, the axis of rotation Y of the outer frame will coincide with the ξ axis, and the axis of rotation of the inner frame with the axes Z and ζ , which are coincident in this instance.

The disposition of the axes for $\psi = \theta = \gamma = 0$ is shown in Fig. 1.7. We

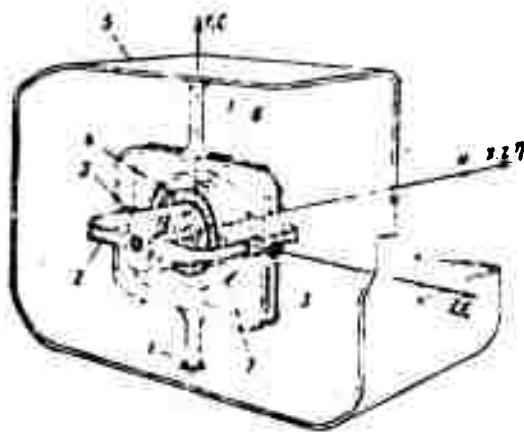


Fig. 1.7. Simplified drawing showing construction of gyroscope with three degrees of freedom. 1) Bearings of outer gimbal frame; 2) inner gimbal frame; 3) bearings of inner frame; 4) gyromotor stator; 5) gyroscope housing; 6) outer gimbal frame; 7) gyroscope rotor.

have noted that the device is positioned in such a way that the fixed point O of the gyroscope coincides with the center of gravity O of the object. This condition is by no means obligatory, however, and has only been made to make the discussion clearer.

If the object, together with the gyroscope housing, is now rotated with reference to the system of axes $Oxyz$, the following will take place as a result of the directional stability of the spin axis in space:

- 1) the housing of the gyroscope will turn through a certain angle ψ' about its axis of rotation with respect to the outer frame;
- 2) the outer frame will turn through a certain angle θ' with respect to the inner frame about the latter's axis of rotation;
- 3) the inner frame will turn through a certain angle γ' about the spin axis z of the gyroscope.

In the general case, these three angles ψ' , θ' , and γ' will not be equal to the angles ψ , θ , and γ , but will be known functions of these three angles. As will be seen upon examination of Fig. 1.7, however, the gyroscope shown in this figure can only be used in one way or another to measure the angles ψ' and θ' . It will be impossible to measure the angle γ' because the body of the gyroscope rotor is in continuous rotation relative to the inner frame. In whatever position we place the gyroscope with three degrees of freedom, it can only be used to measure two angles--the angle of rotation of the housing with respect to the outer frame, and the angle of rotation of the outer frame relative to the inner frame. We cannot measure the angle of rotation of the inner frame about the spin axis because the rotor spins uninterruptedly. To render it possible to measure all three angles with a single instrument, the device would need a component whose orientation in space was constant, rather than an axis of the type which is found in the case of the gyroscope with three degrees of freedom; in this case we would have only two equations for determination of the three angles ψ ,

ϕ , and γ :

$$f_1(\phi, \theta, \gamma) = \phi' \dots f_2(\phi, \theta, \gamma) = \theta'.$$

Thus it is impossible to determine all three angles ϕ , θ , and γ by means of a single gyroscope with three degrees of freedom. In practice, two such gyroscopes are used for this purpose. It is desirable to install these gyroscopes in the object in such a way that they produce direct measurements of the angles which interest us: ϕ , θ , and γ . However, this can be accomplished only in the cases of θ and γ . The reason for this is as follows. The axis of the device about which the angle that it measures directly is reckoned will be designated the instrument's measurement axis. For the angle measured directly by the device to be equal to the angle in which we are interested, it would be necessary for the measurement axis of the instrument to coincide with the measurement axis of that angle. The measurement axis of the angle ϕ is the f axis (Fig. 1.6), whose orientation in space is fixed.

The spin axis z of the gyroscope alone retains its fixed orientation in space when the object is subjected to arbitrary motion. However, it is impossible to make use of this as the measurement axis of the instrument, since -- as we have already noted -- it is impossible to measure angles of rotation about it. All the accessible measurement axes of the instrument are subject to one form of variation or another in their orientation in space when the object is moved in an arbitrary fashion. Thus direct measurement of the angle ϕ is not possible in the general case.

In order to obtain signals proportional to the angles which are measured directly by the gyroscopes, we must equip them with contact-type or contactless detectors (pickoffs) of one kind or another. Let us assume that our gyroscopes

are provided with potentiometer pickoffs.

Let us consider the problem of positioning the gyroscopes for measurement of the angles ψ , θ , and γ . One of the pair of gyroscopes used for the measurement of these angles will be used to determine θ and γ , and the other for measurement of ψ . Let us examine first the gyroscope with which it is intended to measure θ and γ , referring to Fig. 1.8. The housing of the instrument is installed in the object in such a way that the axis of rotation 1 of the outer gimbal frame lies along the longitudinal axis of the object (Fig. 1.8), while the transverse axis of the instrument housing (the axis of rotation of the bail ring 10) coincides with the object's transverse axis Z . The coincidence of these axes is not mandatory, however; it is adopted here as an aid to description. It is only necessary for the axis of rotation of the outer frame and the transverse axis of the housing to be parallel to the longitudinal and transverse axes of the housing, respectively.

The spin axis z of the gyroscope must be directed along the f axis of the system $O\xi\eta$ in order to reproduce the latter axis in a concrete form. In this case, the Z_1 axis will coincide with the geometric axis of rotation of the inner gimbal frame 2 (Figs. 1.6 and 1.8). With the instrument housing and gyroscope in this position it develops that for $\psi = \theta = \gamma = 0$, the X axis coincides with the η axis, the Y axis with the z and f axes, and the Z axis with the ξ axis, as shown in Fig. 1.8. The measurement axes of the device are the X and Z axes; the angle γ must be measured about the former, and the angle θ about the latter. Since the X axis is the measurement axis for the angle γ (Fig. 1.6), this angle will be subject to direct measurement. Since the Z axis does not generally coincide with the measurement axis Z_1 of the angle θ , the measurements of this angle will be subject to error. What is done to measure the angle θ directly will be described below.

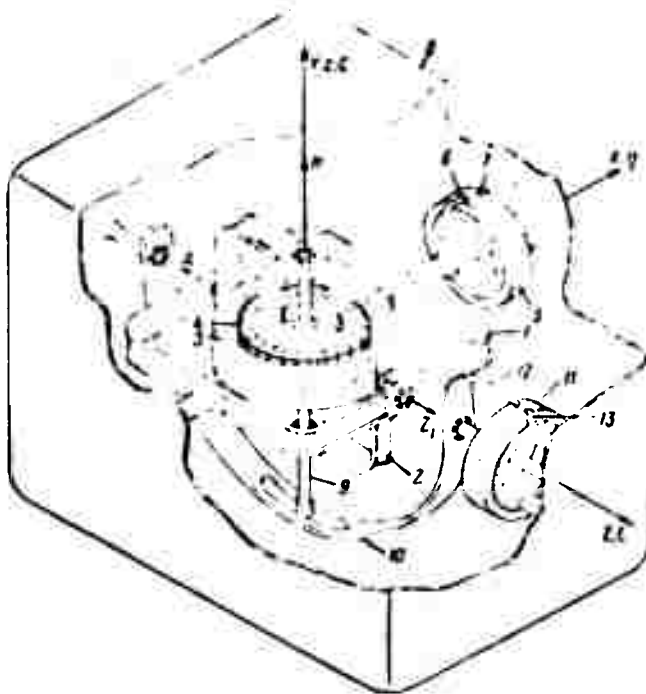


Fig. 1.8. Simplified drawing showing construction of a gyroscope designed for measurement of the angles θ and γ .

- 1) Outer gimbal frame; 2) inner gimbal frame; 3) gyroscope rotor; 4) gyromotor stator; 5) potentiometer for angle γ ; 6) wiper of potentiometer for angle γ ; 7) center-point tap of potentiometer for angle γ ; 8) gyroscope housing; 9) dog; 10) ball ring; 11) potentiometer for angle θ ; 12) wiper of potentiometer for angle θ ; 13) center-point tap of potentiometer for angle θ .

Potentiometer pickoffs are mounted on the measurement axes of the device.

The wound potentiometer carcasses 5 and 11 are attached to the instrument housing 8 at the X and Z axes, respectively. The wiper 6 of the potentiometer 5 is mounted on the outer gimbal frame. The wiper 12 of the potentiometer 11 is attached to the ball ring 10, which is carried in bearings located in the instrument housing on the measurement axis Z . This enables the ball ring to rotate relative to the instrument housing about the Z axis. The roller of the dog 9, which is mounted on the inner gimbal frame and coincides with the negative part of the

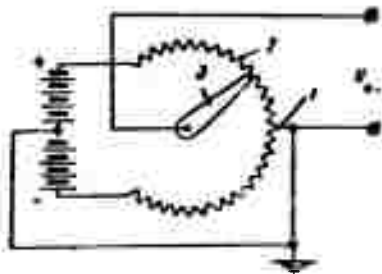


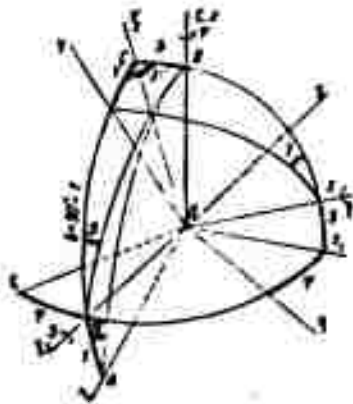
Fig. 1.9. Potentiometer circuit diagram. 1) Center point of potentiometer winding; 2) potentiometer winding; 3) potentiometer wiper.

\underline{z} axis, inserts into the slot of the ball ring. This roller is free to travel along the ball-ring slot. When $\theta = \gamma = 0$, i.e. when the \underline{Y} axis coincides with the \underline{z} axis, the wipers 6 and 12 are located opposite the center taps 7 and 13 of the potentiometers. Under these circumstances, their output voltages will be zero, as will be seen from the potentiometer circuit diagram presented in Fig. 1.9. When the \underline{Y} axis does not coincide with the \underline{z} axis, the output voltage U_{out} of each potentiometer is proportional to the

angle of rotation of the wiper about the centerpoint of the potentiometer. The polarity of the output voltage is determined by the direction in which the wiper is deflected.

Let us find the angles of rotation of the wipers with respect to the potentiometer centerpoints as they appear on rotation of the housing through the angles ψ , θ , and γ . We shall refer for this purpose to Fig. 1.10, in which the axes \underline{OXYZ} occupy arbitrary positions with respect to the axes \underline{Oxyz} . The centerpoint 7 (see Fig. 1.8) of the potentiometer 5 lies in a plane which passes through the \underline{X} and \underline{Y} axes, i.e., in the plane \underline{XOY} . The wiper 6 of this potentiometer is situated in a plane passing through the \underline{X} axis and the gyroscope spin axis \underline{z} , i.e., in the plane \underline{XOz} . Thus the angle of rotation of the wiper 6 relative to the centerpoint 7 of the potentiometer 5 will be equal to the dihedral angle between these planes. It is obvious from Fig. 1.10 that this angle is the angle γ . Accordingly, the output voltage of the potentiometer 5 will be directly proportional to the angle γ . In other words, measurements of the angle γ will not be subject to error.

The centerpoint 13 of the potentiometer 11 lies in the plane of the Y and Z axes, or in the plane YOZ (Fig. 1.10). The wiper 12 of this potentiometer occupies the plane of the axes Z and z, i.e., the plane ZOz. The angle of rotation of the wiper 12 with reference to the centerpoint 13 will be equal to the dihedral angle between these planes. Let this be denoted by θ' . To determine this



angle we refer to the right spherical triangle ABC (Fig. 1.10). From this we have

$$\sin \theta = \sin(90^\circ + \gamma) \sin \theta'.$$

It follows that

$$\sin \theta' = \frac{\sin \theta}{\cos \gamma}. \quad (1.7)$$

Thus the angle θ' , which is measured directly by the instrument, will not be equal to the angle θ . Measurements of the angle θ will be subject to an error which increases as γ . The reason for this was explained earlier.

To obtain a literal measurement of θ ,

it would be necessary to place the potentiometer not on the Z axis of the housing, but rather on the axis of rotation x of the inner frame, which, in the instance under consideration, invariably coincides with the measurement axis Z₁ of the angle θ (Figs. 1.6, 1.8 and 1.10); the positive directions of the x and Z₁ axes are directly opposed. For this purpose it would be necessary to mount the wound carcass of the potentiometer on the outer gimbal frame and attach the potentiometer wiper to the inner frame of the gyroscope (the converse arrangement could also be used, but this would be less convenient from an engineering standpoint). In this case the angle of rotation of the wiper relative to the potentiometer will be equal to the dihedral angle between the planes YOZ₁ (the plane of the potentiometer).

ter centerpoint) and $\underline{xOZ_1}$ (the plane of the potentiometer wiper), which (angle) is equal to θ , as seen from Fig. 1.10. As a rule, however, the θ potentiometer of an automatic pilot is placed on the \underline{Z} axis of the instrument housing, as shown in Fig. 1.8. The reason for this is the fact that elevator control must be a function of θ' rather than θ for correct automatic piloting. Furthermore, this location of the potentiometer permits reduction of the number of current leads to the outer frame of the gyroscope and relieves its bearings of the weight of the potentiometer. It will be seen from Formula (1.7) that the angle θ' is practically equal to θ at small angles γ , since we may assume, in this case, that $\cos \gamma \approx 1$. However, if it is required that an electrical signal proportional to the angle θ be developed with the potentiometer located on the instrument housing, it will be necessary to multiply the voltage obtained from the potentiometer for θ (more properly, θ') by the cosine of the angle recorded by the γ potentiometer.

Let us turn now to consideration of the gyroscope whose function it is to measure the angle ψ (Fig. 1.11). The instrument is placed in the object in the manner outlined in connection with Fig. 1.7. The measurement axis of the device is the \underline{Y} axis (Fig. 1.11). The wound carcass of the potentiometer is accordingly mounted on the instrument housing, while the potentiometer wiper is attached to the outer gimbal frame. For determination of the angle of rotation ψ' of the wiper with respect to the potentiometer, given an arbitrary position of the object (of the axes \underline{OXYZ}) with respect to the axes \underline{Oxyz} , let us turn to Fig. 1.12. The centerpoint 6 of the potentiometer 7 (see Fig. 1.11) is situated in a plane which passes through the \underline{X} and \underline{Y} axes, i.e., lies in the plane \underline{XOY} (Fig. 1.12). The potentiometer wiper 5 falls in a plane passing through the \underline{Y} and \underline{z} axes (Fig. 1.11), i.e., lies in the plane \underline{YOz} (Fig. 1.12). The angle of rotation of the wiper 5 with respect to the potentiometer 7 is equal to the dihedral angle between the above planes, i.e., the angle ψ' (Fig. 1.12). Applying the cotangent formula for

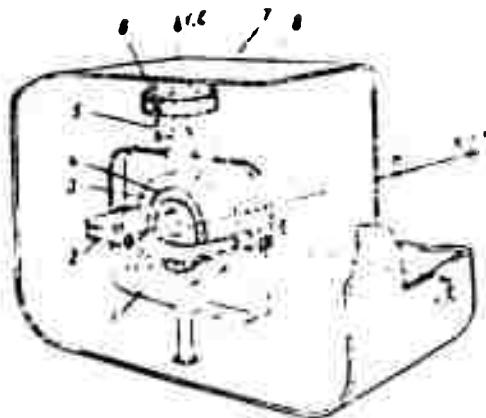


Fig. 1.11. Simplified drawing showing construction of gyroscope designed for measurement of angle ψ .
 1) Outer gimbal frame; 2) inner gimbal frame;
 3) gyromotor rotor; 4) gyromotor stator; 5) potentiometer wiper; 6) center-point tap of potentiometer; 7) potentiometer; 8) gyroscope housing.

the spherical triangle ABC , we obtain

$$\cos(90^\circ - \psi) \sin(90^\circ - \gamma) = \cos(90^\circ - \gamma) \cos(90^\circ + \theta) + \sin(90^\circ + \theta) \sin(90^\circ - \psi').$$

This gives

$$\tan \psi' = \frac{\tan \psi \cos \gamma + \sin \gamma \sin \theta}{\cos \theta}. \quad (1.8)$$

It is seen from this formula that the angle ψ' will be equal to our sought angle ψ only for $\gamma = \theta = 0$. The error in the determination of the angle ψ , which we shall designate the gimballing error, will be equal to

$$\Delta\psi = \psi' - \psi = \arctan \frac{\tan \psi \cos \gamma + \sin \gamma \sin \theta}{\cos \theta} - \psi. \quad (1.9)$$

This is the most general form of the formula. If we set θ here equal to zero, we shall obtain the formula usually presented in the literature for the gimballing

error due solely to the presence of an angle γ .

A voltage proportional to the angle ψ may be obtained by correcting the output voltage of the potentiometer, which is proportional to ψ' , in accordance with the formula

$$\tan \psi = \frac{\tan \psi' \cos \theta - \sin \gamma \sin \theta}{\cos \gamma} \quad (1.10)$$

-- which is derived from Equality (1.8)-- using the output voltages of the potentiometers for the angles γ and θ .

It will be seen from Formula (1.8) that if the angles θ and γ are such that the product of their sines may be neglected and their cosines assumed equal to unity, the angle ψ' will be equal for practical purposes to the angle ψ .

Thus we have seen how two gyroscopes with three degrees of freedom may

be used to determine the angles ψ , θ , and γ , which characterize the position of an object (aircraft, rocket, etc.) with reference to a system $O\{x\}$ (see Fig. 1.5) having a fixed orientation in inertial space.

Now let us consider means of determining the position of an object, e.g., an aircraft, with respect to the earth by the use of gyroscopes with three degrees of freedom. We shall relate the axes $Ax_0y_0z_0$ (see Fig. 1.5) to the earth, for example, by placing their origin A at the point of take-off. Let the z_0 axis be directed vertically upward, then the x_0 and y_0 axes will lie in the horizontal plane. We shall assign "geographical" orientations to these axes: the x_0 axis will be directed to the east, and the y_0 axis to the north. The origin of the axes $O\{x\}$ (Fig. 1.5) will be connected to some point of the moving object

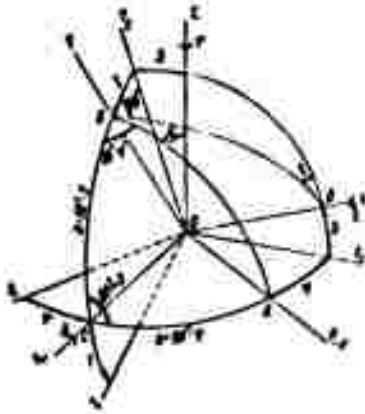


Fig. 1.12. Determination of angle of rotation of wiper with reference to gyroscope potentiometer designed to measure the angle ψ .

(aircraft, etc.)--e.g., to its center of gravity O --and we shall assign orientations to these axes similar to those given the axes $Ax_0y_0z_0$. Here the ζ axis will be directed vertically upward; the ξ and η axes will be horizontal, with the ξ axis pointed eastward and the η axis toward the north (Fig. 1.13). As previously, we shall only concern ourselves with determination of the position of the object, or, in other words, the axes $OXYZ$ connected to it (Fig. 1.5), with reference to the axes $O\xi\eta\zeta$. As before, this position will be characterized by three angles: ψ , ϑ , and γ (Fig. 1.6). In this case these angles bear the following designations: ψ is the course angle (or, more properly, the course with its sign changed), ϑ is the pitch angle, and γ is the roll angle. However, the orientation of the axes

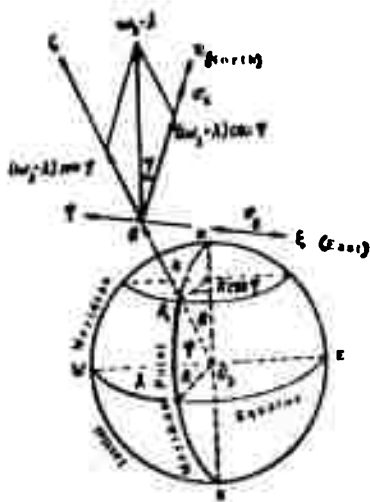


Fig. 1.13. Orientation of axes $O\xi\eta\zeta$ in determining position of object (e.g., an airplane) with respect to the earth. R) Radius of earth; λ, φ) geographical coordinates (longitude and latitude) of point A_1 directly beneath object; h) altitude; v_E, v_N) east-and north-directed components of ground speed of object; ω_e) angular velocity of earth's diurnal rotation; $\dot{\varphi}, \dot{\lambda}$) angular rates of change in latitude and longitude due to motion of object with velocities v_N and v_E .

$O\xi\eta\zeta$ in inertial space, although fixed in our previous discussion, will now vary continually, even in cases where the object is stationary with respect to the earth. The instantaneous angular velocity of the axes $O\xi\eta\zeta$ in inertial space is the sum of the following three velocities (Fig. 1.13):

1. ω_e the angular velocity of the earth's diurnal rotation, since the system $O\xi\eta\zeta$ rotates with the earth;

2. $\dot{\varphi}$, the rate of change in latitude due to motion of the object with reference to the earth along a meridian arc at a velocity v_N .

Since angular velocity is equal to circumferential velocity divided by the

radius, we may write (neglecting h as small by comparison with R)

$$\dot{\varphi} = -\frac{v_N}{R}. \quad (1.11)$$

The velocity v_N is considered positive when directed toward the north. Thus when v_N is positive, the velocity $\dot{\varphi}$ is in the negative direction of the ξ axis.

3. $\dot{\lambda}$, the rate of change in longitude due to motion of the object with respect to the earth along a parallel with a velocity v_E , which is considered positive when directed eastward. Dividing the circumferential velocity v_E by the radius of the parallel, which is equal to $R \cos \varphi$, we obtain

$$\dot{\lambda} = \frac{v_E}{R \cos \varphi}. \quad (1.12)$$

The vector of the velocity $\dot{\lambda}$ is directed along the axis of diurnal rotation of the earth, just as is the vector of the velocity ω_e .

For the sake of convenience, we shall transfer the composite vector $\omega_e + \dot{\lambda}$ to the origin O of the system of axes $O \xi \eta \zeta$. Let u_ξ , u_η , and u_ζ denote the projections of the instantaneous angular velocity of the system $O \xi \eta \zeta$ onto the ξ , η , and ζ axes. It is seen from Figure 1.13 and Formulas (1.11) and (1.12) that

$$\left. \begin{aligned} u_\xi &= -\dot{\varphi} = -\frac{v_N}{R}; \\ u_\eta &= (\omega_e + \dot{\lambda}) \cos \varphi = \omega_e \cos \varphi + \frac{v_E}{R}; \\ u_\zeta &= (\omega_e + \dot{\lambda}) \sin \varphi = \omega_e \sin \varphi + \frac{v_E}{R} \tan \varphi. \end{aligned} \right\} \quad (1.13)$$

In the case under examination, as in the case where the orientation of the system $O \xi \eta \zeta$ in space remained invariant, two gyroscopes with three degrees of

freedom, disposed in the object as shown in Figs. 1.8 and 1.11, are used to measure the angles ψ , θ , and γ . In addition, everything said in connection with the relationships between the angles measured directly by the gyroscopes and the angles ψ , θ , and γ remains fully valid. Here, however, in order to create combined or individual concrete reproductions of the axes $O\xi\eta$ in the object, it will be necessary to correct (to vary) constantly the directions of the spin axes of both gyroscopes in inertial space, i.e., to set the spin axes rotating in inertial space in such a way that they maintain the required positions with reference to the earth. The spin axis z of the gyroscope to be used for measurement of the angle ψ must be horizontal and directed toward the north, i.e., must coincide with the η axis (Fig. 1.13); the spin axis z of the gyroscope whose function is measurement of the angles θ and γ should retain its vertical position, that is, coincide with the ξ axis (Fig. 1.13).

It follows from the law of precession that a corresponding external moment must be applied to the gyroscope in order to shift the spin axis in inertial space at the desired velocity. The devices used to generate this moment are extremely varied in nature, but the commonest one at the present time is the torque generator (we shall refer to it as the torquers) which is installed on the axes of the outer and inner gimbal frames. Torquers vary in design and working principle. Flat, asynchronous two-phase multipole reversible motors with short-circuited rotors of the squirrel-cage type, operating in the short-circuited condition, are frequently used as torquers. A torquer of this kind is often termed a motor-corrector or a correction motor.

A torquer fitted to the axis of the outer frame and applying to the gyroscope a moment which acts about this axis will be referred to as an outer-frame torquer; similarly, a torquer applying a moment to the gyroscope about the axis of rotation of the inner frame and mounted on this axis will be called an inner-

frame torquer.

Instead of mounting the inner-frame torquer on the inner gimbal frame, we may locate it on the Z axis of the instrument housing with the stator on the left-hand wall of the housing and the rotor on the shaft of the bail ring 10 (see Fig. 1.8; the torquer does not appear here). In this case the torquer moment would be transmitted to the gyroscope through the bail ring 10 and the dog 9. This position is to be preferred in certain cases; in others, however, it is generally unsuitable. Moreover, it considerably complicates the laws governing the moment generated by the torquer and makes it a function of the angle ψ , even with $\theta = \gamma = 0$, which is a highly undesirable situation. Accordingly, we shall assume that the inner-frame torquer is mounted on its axis of rotation, with the stator on the outer frame and the rotor on the inner frame.

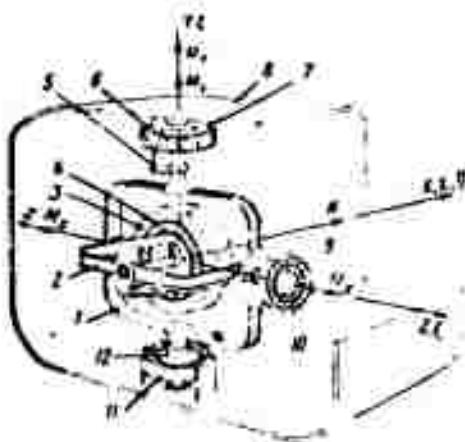


Fig. 1.14. Simplified drawing showing design of gyroscope equipped with two torquers for measurement of the angle ψ .

- 1) Outer gimbal frame; 2) inner gimbal frame; 3) gyroscope rotor; 4) gyromotor stator; 5) potentiometer wiper; 6) center-point tap of potentiometer; 7) potentiometer; 8) gyroscope housing; 9) stator of inner-frame torquer; 10) rotor of inner-frame torquer; 11) stator of outer-frame torquer; 12) rotor of outer-frame torquer.

As previously noted, the outer-

frame torquer is mounted on the axis of rotation of this frame, with its stator on the instrument housing and its rotor on the outer frame.

Figure 1.14 presents a schematic drawing showing the construction of a gyroscope equipped with two torquers and designed for measurement of the angle ψ . The position of the housing with reference to the axes Ox, y, z in Fig. 1.14 corresponds to the case in which $\psi = \theta = \gamma = 0$.

The spin axis z of the gyroscope must be horizontal and directed toward

the north, i.e., must coincide with the ν axis (Fig. 1.13) at all times. To do so it must rotate in inertial space about the ξ and ζ axes with the velocities \underline{u}_ξ and \underline{u}_ζ , given by Equalities (1.13). Let us establish the moments which the torquers must develop in order to effect the required rotation of the spin axis in inertial space. The argument will refer throughout to Fig. 1.15, in which the axes OXYZ occupy an arbitrary position, characterized by the angles ψ , θ , and γ , with respect to the axes Oξηζ. The gyroscope spin axis \underline{z} is drawn coincident with the ν axis, i.e., in the required position. The system Oξηζ is oriented as shown in Fig. 1.13. Let us determine first the position of the axis of rotation of the inner gimbal frame. It is clear from Figs. 1.14 and 1.15 that this axis must coincide with the line of intersection of two planes which pass through the point O: the plane XOZ, which is perpendicular to the axis of rotation \underline{Y} of the outer frame and the plane $\xi \underline{O} \zeta$, which is perpendicular to the spin axis \underline{z} . Extending these planes, we find their line of

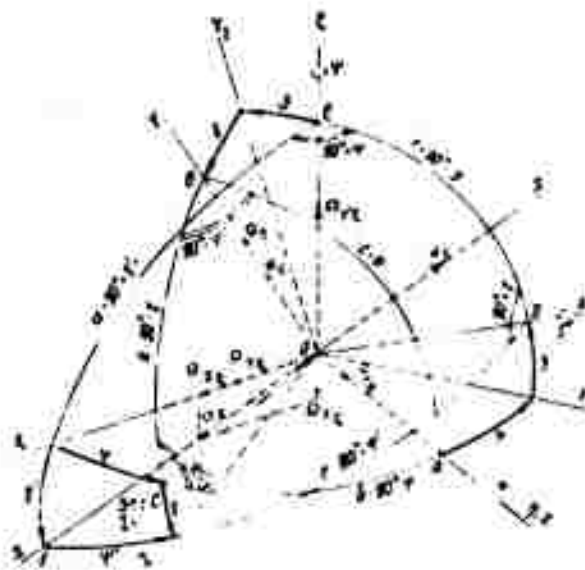


Fig. 1.15. Determination of moments \underline{M}_X and \underline{M}_Y for gyroscope designed to measure angle \underline{x} ψ .

intersection, which is the negative part of the axis of rotation \underline{x} of the inner frame. Extending this axis through the point Q , we obtain the positive axis of rotation \underline{x} of the inner frame.

The position of the \underline{x} axis is determined by the two angles ψ' and γ' . The angle ψ' is given by Formula (1.8). Let us determine the angle γ' from the spherical triangle DEF. Applying the law of sines, we have

$$\frac{\sin(90^\circ + \gamma')}{\sin(90^\circ + \gamma)} = \frac{\sin(90^\circ + \psi')}{\sin(90^\circ + \psi)}$$

It follows from this that

$$\cos \gamma' = \cos \gamma \frac{\cos \psi'}{\cos \psi} \quad (1.14)$$

Now let us determine the angle between the frames of the gimbal suspension, which we shall designate θ . Applying the law of sines to the spherical triangle ABC, we may write

$$\frac{\sin \theta}{\sin(90^\circ + \theta)} = \frac{\sin(90^\circ - \psi)}{\sin(90^\circ - \psi')}$$

This gives

$$\sin \theta = \cos \theta \frac{\cos \psi}{\cos \psi'} \quad (1.15)$$

The moment \underline{M}_x generated by the inner-frame torquer and the moment \underline{M}_y generated by the outer-frame torquer are represented in Fig. 1.15 in the positive sense of their vectors. The moment \underline{M}_x gives rise to precession of the gyroscope about the axis of rotation \underline{y} of the outer frame at a velocity which, in accordance with Formula (1.4) is equal to

$$\Omega_y = \frac{M_x}{H \sin \theta} \quad (1.16)$$

Correspondingly, the moment \underline{M}_Y causes precession at a velocity

$$\Omega_x = - \frac{M_Y}{H \sin \theta} \quad (1.17)$$

about the axis of rotation \underline{x} of the inner frame. The minus sign in Equality (1.17) signifies that positive moments \underline{M}_Y produce precessional velocities directed along the negative part of the \underline{x} axis.

Let us project the velocities $\Omega_{\underline{x}}$ and $\Omega_{\underline{y}}$ onto the ξ , η , and ζ axes. Fig. 1.15 gives

$$\begin{aligned} \Omega_{\xi} &= -\Omega_x \cos \gamma', \\ \Omega_{\eta} &= 0, \\ \Omega_{\zeta} &= \Omega_x \sin \gamma'. \end{aligned}$$

Substituting Equality (1.17) in the above, we obtain

$$\left. \begin{aligned} \Omega_{\xi} &= - \frac{M_Y}{H \sin \theta} \cos \gamma', \\ \Omega_{\eta} &= 0, \\ \Omega_{\zeta} &= - \frac{M_Y}{H \sin \theta} \sin \gamma'. \end{aligned} \right\} \quad (1.18)$$

Using the direction cosines given in Table (1.6), we may determine the projections of the velocity $\Omega_{\underline{y}}$ on the ξ , η , and ζ axes:

$$\begin{aligned} \Omega_{\xi} &= \Omega_Y \cos \psi \sin \gamma, \\ \Omega_{\eta} &= \Omega_Y \sin \psi \sin \gamma, \\ \Omega_{\zeta} &= \Omega_Y \cos \psi \cos \gamma. \end{aligned}$$

Substituting Equality (1.16) in the above, we obtain

$$\left. \begin{aligned} \Omega_{\eta} &= \frac{M_x}{H \sin \theta} \cos \psi \sin \gamma, \\ \Omega_{\xi} &= \frac{M_x}{H \sin \theta} \sin \psi \sin \gamma, \\ \Omega_{\zeta} &= \frac{M_x}{H \sin \theta} \cos \theta \cos \gamma. \end{aligned} \right\} \quad (1.19)$$

Thus the velocities of rotation of the gyroscope spin axis about the ξ and ζ axes under the influence of the moments \underline{M}_x and \underline{M}_y are

$$\left. \begin{aligned} \Omega_{\xi} = \Omega_{\eta} + \Omega_{\zeta} &= \frac{1}{H \sin \theta} (M_y \cos \gamma' + M_x \cos \psi \sin \gamma), \\ \Omega_{\zeta} = \Omega_{\eta} + \Omega_{\xi} &= \frac{1}{H \sin \theta} (-M_y \sin \gamma' + M_x \cos \theta \cos \gamma). \end{aligned} \right\} \quad (1.20)$$

These velocities should be equal, respectively, to the velocities \underline{u}_{ξ} and \underline{u}_{ζ} . Replacing Ω_{ξ} and Ω_{ζ} in Equations (1.20) by \underline{u}_{ξ} and \underline{u}_{ζ} , respectively, and solving for \underline{M}_x and \underline{M}_y , we obtain

$$\left. \begin{aligned} M_x &= H \frac{(u_{\xi} \sin \gamma' + u_{\zeta} \cos \gamma') \sin \theta}{\cos \psi \sin \gamma \sin \gamma' + \cos \theta \cos \gamma \cos \gamma'}, \\ M_y &= H \frac{(u_{\xi} \cos \theta \cos \gamma - u_{\zeta} \cos \psi \cos \gamma) \sin \theta}{\cos \psi \sin \gamma \sin \gamma' + \cos \theta \cos \gamma \cos \gamma'}. \end{aligned} \right\} \quad (1.21)$$

The velocities \underline{u}_{ξ} , \underline{u}_{ζ} and the angles γ' , θ are determined from Equalities (1.13), (1.14) and (1.15). It will be seen from Formula (1.21) that the moments \underline{M}_x and \underline{M}_y are rather complex functions of the velocities \underline{u}_{ξ} and \underline{u}_{ζ} and the three angles ψ' , θ , and γ measured by the two gyroscopes with three degrees of freedom.

Thus we see that it will be necessary for the torquers to apply the moments \underline{M}_x and \underline{M}_y -- as determined by Formulas (1.21) -- to the gyroscope if its spin

axis is to remain at all times horizontal and directed northward. Let us assume that the moment generated by the torquer is proportional to the control current supplied to it. For this it is necessary that the control currents of the torquers be governed by the same laws (1.21) as the moments M_x and M_y . Computing amplifiers may be used to obtain such currents. Voltages proportional to $\dot{\alpha}$, $\dot{\beta}$, and $\dot{\gamma}$ must be delivered to the amplifier input. It should produce currents at its output corresponding to the laws governing the moments (1.21).

The laws governing the moments which must be generated by the torquers of the gyroscope used to measure the angles θ and γ may be determined in a similar fashion.

Throughout the discussion we have assumed that the gyroscope is not subject to drift, and consequently that the spin axis rigidly maintains the direction in inertial space originally imparted to it, or rotates in exact conformity to the control signals supplied to the torquers. However, every gyroscope of the type under consideration is in practice subject to drift arising from friction in its bearings, noncoincidence of the center of gravity of the gyroscope with its fixed point, and a number of other factors. The drift velocity (or drift rate) is not constant, and includes considerable accidental components. As noted previously, the systematic component of the drift velocity may be compensated by the application of moments generated expressly for this purpose by the torquers. Compensation for the accidental drift-velocity components is impossible. The problem of attaining maximal drift suppression by all practical means is therefore highly important in the design and manufacture of the gyroscopic instruments under discussion. Considerable progress has been achieved in this regard.

The most general formulas are those given in (1.21). In a number of cases it is possible to resort to simplification, which consists in neglecting

individual values which appear in them, or disregarding them for reasons of principle. It should be noted that the moment applied to the gyroscope to establish the desired motion of the spin axis in inertial space (its position with respect to the earth) may be generated by a variety of technical means, and not necessarily by the use of torquers of the type described here.

In the majority of devices constructed and used in practice for measurement of the angles ψ , θ , and γ , the gyroscope spin axis is maintained horizontal (or vertical) not by applying to the gyroscope moments which are definite functions of the velocities \dot{u}_ξ , \dot{u}_η , and \dot{u}_ζ and the angles ψ' , θ , and γ by means of torquers, but by another method. A device whose gyroscope spin axis is to retain a vertical direction is provided with a mechanism sensitive to the position of the spin axis with respect to the vector of gravity, i.e., with respect to the vertical. If the spin axis deviates from the required position with respect to the gravitational vector, this mechanism actuates torquers (which, in this case, would be termed correction motors). The latter apply moments to the gyroscope which make it precess back to the required position. As soon as the spin axis has returned to the required position, the sensing elements switch off the torquers, with the result that the moments developed by them revert to zero. In this case the moments are functions of the angles through which the spin axis deviates from the required position. In instruments of this type, whose function is measurement of the angle ψ , the position of the spin axis with respect to north may be left totally uncorrected, but is most frequently corrected in a similar manner by a magnetic or induction compass. In this case the instrument is equipped with a device which senses the deflection of the spin axis from the north and actuates the torquer on the inner gimbal frame. The outer-frame torquer is switched on by a mechanism which senses the position of the spin axis with reference to the horizontal plane or, which amounts to the same thing, with reference to the gravity vector (the vertical). In this case, however, as seen from Fig. 1.15, the moment

\underline{M}_Y will not only restore the spin axis to the horizontal, but also simultaneously produce a change in its azimuthal position; the moment \underline{M}_X , whose purpose is to correct the spin-axis azimuth, will simultaneously cause deflection of this axis from the plane of the horizon.

Due to the small magnitude of the precessional velocity, the oscillations of the pendulum which reproduces the gravitational vector and those of the compass card (magnetic needle) which reproduces the northerly direction will hardly exert any influence on the gyroscope.

This method of maintaining the spin axis in the required position is the one most widely used at the present time. It ensures a comparatively high degree of precision.

An ever greater demand for precision in maintaining the system $O\xi\eta\zeta$ in the required position--a particularly important function in self-contained navigation systems--has led to a situation in which the precision attainable by the methods considered above, using ordinary gyroscopes, is clearly inadequate. A way out of this situation has been found in the use of floating gyroscopes. Before turning to study of these devices, however, let us consider very briefly the means by which it is possible to create a system capable of measuring directly not only the angles θ and γ , but the angle ψ as well.

Section 4. The Stabilized Platform

To be able to make direct measurements not only of the angles θ and γ , but also of ψ , we must have an object which is stabilized with respect to the three axes $O\xi\eta\zeta$, and thus constitutes a concrete reproduction of these axes. It is customary to refer to such an object as a stabilized platform. Stabilization is accomplished by means of gyroscopes and the motors which they control. It may be effected by a variety of mechanisms differing in operating principle. In the

following we shall consider the manner in which the platform is stabilized with respect to the axes $O\xi\eta\zeta$ by means of three ordinary integrating gyroscopes, or--a superior arrangement from the viewpoint of precision--by three floating gyroscopes equipped with servodrives. We shall not concern ourselves with other stabilization methods. It is pointed out that the precision stabilization required in the most critical self-contained navigation systems, and in inertial navigation systems in particular, can apparently be attained only by the use of floating integrating gyroscopes and properly selected servosystems.

From the standpoint of mechanics, the stabilized platform should represent a solid body with one fixed point with respect to the instrument housing, i.e., it should possess three degrees of freedom with reference to the latter. With this in view, the platform is installed in the instrument housing in the manner shown schematically in Fig. 1.16.

The stabilized platform 1 is mounted on the shaft 9, which is carried in bearings located in the inner gimbal frame 7. To avoid cluttering the drawing, the shaft 9 is shown in Fig. 1.16 with only one end supported, and the frames of the gimbal suspension is shown as open brackets. In actuality, both frames are closed to obtain the necessary rigidity, and the shaft is supported at both ends. Thus the platform and each of the frames are carried in two bearings.

This permits the platform 1 to rotate with respect to the inner frame 7 about the axis ζ , which is the geometric axis of the shaft 9. The inner frame 7 is mounted within the outer frame 5 of the gimbal suspension in such a way as to permit it to rotate with respect to the latter about the x axis (or, which amounts to the same thing, about the Z_1 axis, whose positive direction is opposed to that of the x axis), which is perpendicular to the ζ axis. Finally, the outer frame 5 is installed in the instrument housing 2 in a manner which permits it to rotate with respect to the latter about the X axis, which is perpendicular to the x axis.

The axes $O\xi\eta\zeta$ are attached to the platform and bear a fixed relation to it. The axes $OXYZ$ bear a fixed relation to the object, and thereby to the instrument

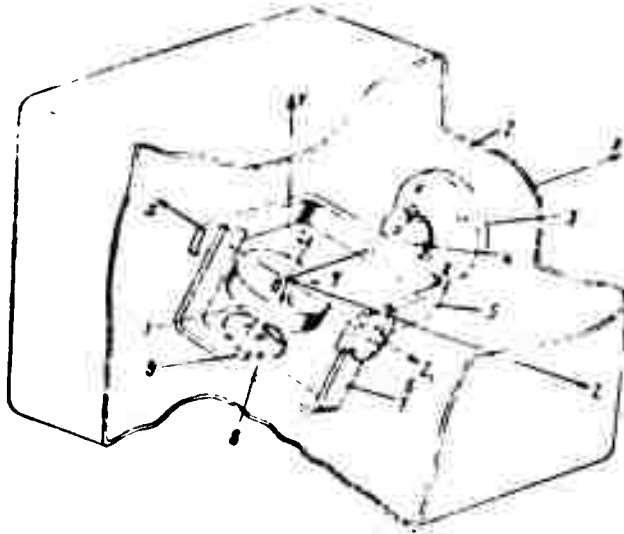


Fig. 1.16. Stabilized Platform. 1) Platform; 2) instrument housing; 3) flange with bearing for outer gimbal frame; 4) circle showing angle of rotation of instrument housing with respect to outer frame (read-off scale for angles γ); 5) outer gimbal frame; 6) circle showing angle of rotation of outer frame with respect to inner frame (read-off scale for angles ϑ); 7) inner gimbal frame; 8) circle showing angle of rotation of inner frame with respect to platform (read-off scale for angles ψ), 9) axis of platform.

housing 2. All of the above axes have their origins at the point O .

The instrument is installed in the object in such a way that the axis of rotation of the outer frame 5 is directed along the longitudinal X axis of the object, and at $\psi = \vartheta = \gamma = 0$ (see Fig. 1.6) the ξ and Z_1 axes coincide with its /sic/ transverse Z axis, the η axis with its X axis, and the ζ axis with its normal Y axis.

Let us assume that the platform 1, and therefore the axes $O\xi\eta\zeta$ attached to it, are in one way or another either stabilized in inertial space or made to rotate with respect to it in a specified manner, e.g., in the same manner as the axes shown in Fig. 1.13. If the object, together with the instrument housing, now rotates in some arbitrary manner with respect to the axes $O\xi\eta\zeta$, which are reproduced by the platform 1, the result in the general case will be as follows (see Figs. 1.16 and

1.6):

1. The inner frame 7 will rotate through an angle ϕ with respect to the platform 1 about the ξ axis. The rotation will amount to exactly this angle by virtue of the fact that the ξ axis is the measurement axis for the angle ϕ . The angle reading may be taken with the aid of the indicator 8, which consists of a scale attached to the frame 7 and an arrow attached to the shaft 9.

2. The outer frame 5 will rotate about the Z_1 axis, which is always located in the plane $\xi O \eta$, passing through an angle θ with respect to the inner frame 7, since the Z_1 axis is the measurement axis for the angle θ . The scale 6 provides readings of the angle θ .

3. The instrument housing 2 rotates about the X axis through an angle γ relative to the outer frame 5, since the X axis is the axis of measurement of the angle γ . The reading for this angle is taken from the scale 4.

In the actual instruments, pickoffs, which emit electrical signals proportional to the angles ϕ , θ , and γ are used instead of the angle-reading devices.

Thus the construction described above permits measurement of the angles ϕ , θ , and γ directly, i.e., it is unaffected by any gimbaling error.

Let us consider the similarities and differences between the present device (see Fig. 1.16) and the gyroscope with three degrees of freedom represented in Fig. 1.8. It has been shown above that the gyroscope in Fig. 1.8 enables us to obtain direct measurements of the angle γ , and also the angle θ , provided the potentiometer is installed on the Z_1 axis in the same manner as the visual indicator of the device shown in Fig. 1.16. Measurement of the angle ϕ with the gyroscope in Fig. 1.8 was impossible due to the fact that the gyroscope rotor is in continuous motion about the spin axis, so that its position in space is subject to continuous variation; only the spin axis z retains a fixed direction. Hence, if it were possible for a gyroscope to retain all of its properties with the rotor stationary, it could be used to measure the angle ϕ as well, and could do this directly.

However, no gyroscope retains all of its characteristics when the proper rotation of its rotor ceases.

The device shown in Fig. 1.16 embodies the concept of a gyroscope with three degrees of freedom and a nonrotating rotor. The gimbal-suspended stabilized platform 1 simulates the gyroscope with three degrees of freedom and nonrotating rotor. The platform itself represents the rotor, the shaft 9 its axis, and the axis the spin axis. The platform is capable of rigid retention of a position in inertial space imparted to it, or of varying it in a specified manner in response to appropriate correcting signals. The measurement axes ξ , \underline{Z}_1 , and \underline{X} of the platform coincide with the measurement axes of the angles ψ , θ , and γ (see Fig. 1.6). Thus the platform, which is stabilized with respect to the three axes $O\xi\eta\zeta$, renders possible direct measurement of all three angles ψ , θ , and γ . In inertial-navigation systems, two accelerometers, which measure the acceleration of the object in inertial space in the directions of the ξ , and η axes are mounted on the platform 1. Sometimes a third accelerometer is included to detect acceleration along the ζ axis. The output signals of the accelerometers are subjected to double integration with respect to time. The first integration yields the projections of the linear velocity of the object onto the ξ and η axes; the second gives the component distances traveled along these axes.

As already noted, either ordinary or floating gyroscopes may be used to stabilize the platform. However, the platform drift obtained in the use of ordinary gyroscopes is inadmissibly large for the purposes of inertial-navigation systems. In this case the basic factors producing drift are the considerable magnitude and variability of the frictional moments which arise in the gimbal-suspension bearings of the gyroscopes, and imperfect balancing. These factors are virtually eliminated in the floating gyroscope--a fact which ensures stabilization with a high degree of precision.

Section 5. The Differentiating Gyroscope

The differentiating gyroscope is a gyroscope with two degrees of freedom (see Fig. 1.1) equipped with some device (mechanical or electrical) which, upon deflection of the gyroscope frame from a given position (referred to as its initial position), applies to it a moment proportional to the angle through which the frame is deflected and tending to return it to its initial position. Such gyroscopes are generally further provided with dampers the function of which is to suppress oscillations of the frame about its axis of rotation. The damper generates and applies to the frame a moment proportional to the angular velocity of the frame about its axis of rotation.

The differentiating gyroscope serves to measure the angular velocity of rotation of its housing about an axis perpendicular to the axis of rotation of the gyroscope frame and to the initial position of the spin axis (the position occupied by the spin axis when the measured angular velocity is zero). The construction of a differentiating gyroscope is shown schematically in Fig. 1.17. The rotor 3 is carried in the frame 4 and rotates with respect to the latter about the z axis with a constant angular velocity Ω . The frame 4 is mounted in turn in the instrument housing 5 in a manner which permits it to rotate with respect to the latter about the x axis. The two springs 7 are fastened to the frame 4 at a certain distance from its axis of rotation. The other ends of these springs are attached to the instrument housing. They serve to subject the frame to a moment proportional to the angle of its deflection in any direction from its original position and directed in such a way as to return it. Since the springs are elastic components, we shall designate the moment which they generate by M_{el} .

The dashpot 2 serves to suppress oscillations of the frame with respect to the housing. The remaining components of the design will be considered somewhat

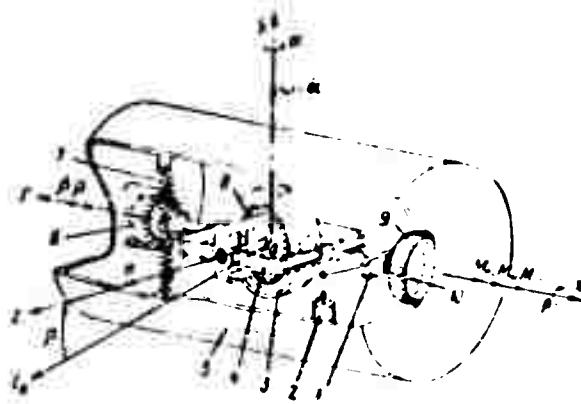


Fig. 1.17. Simplified representation of construction of differentiating gyroscope. 1) Potentiometer wiper; 2) dashpot; 3) gyroscope rotor; 4) gyroscope frame; 5) gyroscope housing; 6) torquer; 7) springs; 8) gyromotor stator; 9) potentiometer; 10) center tap of potentiometer.

later.

Let the system of mutually perpendicular axes $Oxyz_0$ be attached immovably to the instrument housing; this system has its origin at the point O , which is the point of intersection of the gyroscope spin axis z with the x axis of rotation of the frame. As noted previously, the x axis is directed along the axis of rotation of the gyroscope frame. The y and z_0 axes are perpendicular to the x axis. Here the z_0 axis is made to coincide with the direction occupied by the spin axis z when the moment applied to the frame by the springs is zero, i.e., when the measured angular velocity assumes zero value.

We shall designate the y axis the measurement or input axis of the gyroscope in view of the fact that our gyroscope is intended to measure the angular velocity of rotation ω of its housing about the y axis. The direction of the z_0 axis will be termed the initial direction of the spin axis z , since the z axis coincides with the z_0 axis at $\omega = 0$. Finally, the x axis will be designated the output axis of the gyroscope, since (see Fig. 1.1) rotation of the housing with the angular

velocity ω results in rotation of the frame about the \underline{x} axis.

Accordingly, when the angular velocity ω of the housing about the measurement axis is zero, the spin axis \underline{z} coincides with the \underline{z}_0 axis and the moment generated by the springs $M_{e1} = 0$.

If now the gyroscope housing rotates about the measurement axis with a constant angular velocity ω (see Fig. 1.17), a gyroscopic moment is created which tends to turn the frame about its \underline{x} axis of rotation. This moment is called the restorative moment of the differentiating gyroscope.

The restorative moment will be resisted by the moment M_{e1} generated by the springs. As a result, the frame will be deflected from its original position until the gyroscopic moment is balanced by the counteracting moment generated by the springs and the frictional moment applying to the axis of rotation of the frame.

Let us derive the equation of motion of the frame. When the instrument housing rotates about the measurement axis at an angular velocity ω , which is considered positive when its vector coincides with the direction of the positive part of the \underline{y} axis, the following moments will act on the frame about its \underline{x} axis of rotation. (Here and henceforth, a moment will be considered positive when its vector is directed along the positive part of the \underline{x} axis for positive values of the quantity of which it is a function):

1. A gyroscopic moment, which, according to Formula (1.2), will be given by

$$M_g = -H\omega \sin(90^\circ - \beta) = -H\omega \cos \beta. \quad (1.22)$$

where β is the angle of deflection of the frame (or of the spin axis) from its initial position; this angle is considered positive in the direction indicated by the arrow in Fig. 1.17.

2. A moment generated by the springs. By specification this is proportional

to the angle θ and directed so as to return the frame to its initial position ($\theta = 0$). Accordingly, the moment generated by the springs will be equal to

$$M_{s1} = K_{s1} \theta. \quad (1.23)$$

where K_{s1} is a proportionality coefficient equal to the moment generated by the springs when θ is equal to one radian; dimensions, gf-cm/rad.

3. A damping moment generated by the dashpot. This moment is proportional in value and opposed in direction to the velocity $\dot{\theta}$. Thus (the velocity $\dot{\theta}$ is positive when its vector is directed along the negative x axis) it is given by:

$$M_{d1} = K_{d1} \dot{\theta}. \quad (1.24)$$

where K_{d1} is the specific damping moment, or the moment generated by the dashpot when the velocity $\dot{\theta}$ is 1 rad/sec; dimensions, gf-cm-sec.

4. A moment of inertia equal to (the acceleration $\ddot{\theta}$ is positive when its vector is directed along the negative part of the x axis)

$$M_{i1} = J \ddot{\theta}. \quad (1.25)$$

where J is the moment of inertia applied to the axis of rotation of the frame by all parts of the instrument moving with it; dimensions, gf-cm-sec².

5. The referred frictional moment $\pm M_{fr}$ (the plus sign is used for $\dot{\theta} > 0$, and the minus for $\dot{\theta} < 0$). This value is equal to the sum of all frictional forces and moments arising on rotation of the frame and referred to the x axis. We shall

consider the value of this moment constant, although it will be to some extent a function of the angle β in the design represented schematically in Fig. 1.17.

Equating the sum of all these moments to zero, we obtain the equation of motion of the gyroscope frame in the form

$$J\ddot{\beta} + K_{\phi}\dot{\beta} + K_{\beta}\beta \pm M_{fr} = H\omega \cos \beta. \quad (1.26)$$

The device is constructed in such a way that the angle β will remain small throughout the entire range of measurement of the velocity ω . When this condition prevails, we may assume $\cos \beta \approx 1$, whereupon Equation (1.26) takes the form

$$J\ddot{\beta} + K_{\phi}\dot{\beta} + K_{\beta}\beta \pm M_{fr} = H\omega. \quad (1.27)$$

The frame can be set into motion only in cases where the gyroscopic moment $H\omega$ is greater than the frictional moment M_{fr} . Thus by making these moments equal to one another, we obtain the following expression for the smallest angular velocity to which the instrument will be sensitive:

$$\omega_{min} = \frac{M_{fr}}{H}.$$

Therefore the smaller the angular velocity to which the device is to respond, the smaller must be its frictional moment M_{fr} . At the present time it is frequently necessary to measure angular velocities so small that this can no longer be accomplished by means of differentiating gyroscopes of the usual design (see Fig. 1.17), due to considerable frictional moments. It is consequently necessary

in these cases to use floating differentiating gyroscopes, in which the frictional moment is reduced to zero for all practical purposes.

Solving Equation (1.27) for β , we obtain the following expression for the current value of this angle:

$$\beta = \frac{1}{K_{\sigma 1}} (H\omega \mp M_{11} - K_{\sigma 2} \dot{\beta} - J\ddot{\beta}). \quad (1.28)$$

In the equilibrium position, which is reached a certain period after the instrument housing starts rotating with the constant velocity ω , $\dot{\beta} = \ddot{\beta} = 0$, so that the angle of deflection of the frame from its original position becomes equal to

$$\beta = \frac{H}{K_{\sigma 1}} \omega - \frac{M_{11}}{K_{\sigma 1}}. \quad (1.29)$$

In the equilibrium position, the gyroscopic moment is balanced by the moment generated by the springs and the referred frictional moment. An effort is made to construct the device in such a way that the second term in the right-hand member of Formula (1.29) will be negligibly small. Let us assume that this is the case. Then, instead of Formula (1.29) we obtain the following expression for the value of the angle β in the equilibrium position:

$$\beta = \frac{H}{K_{\sigma 1}} \omega. \quad (1.30)$$

It will be seen from this expression that in the equilibrium position corresponding to some given measured velocity ω , the angle of deflection of the frame from its

initial position will be directly proportional to ω , so that it may be used as a measure of this angular velocity for constant values of H and K_{e1} .

Formula (1.30) is an approximate one, since it was obtained on the basis of the conditions that $\cos \beta \approx 1$ and $M_{\Gamma} = 0$. In exact measurements, therefore, it is necessary to estimate the errors which these assumptions introduce. Furthermore, it should be borne in mind that when the spin axis z is deflected through an angle β from its initial position (the z_0 axis), the device will also exert a reaction upon the angular velocity about the z_0 axis. At small values of β , the resulting error will be small. In exact measurements, however, it must also be taken into account.

The reason for referring to the present device as a differentiating gyroscope becomes clear from Formula (1.30). The designation is explained by the fact that the output quantity of the gyroscope, the angle β , is proportional to the first-order derivative with respect to time of the input quantity, the angle α of rotation of the gyroscope about the measurement axis, or of the angular velocity

$$\omega = \dot{\alpha} = \frac{d\alpha}{dt}.$$

If the gyroscope housing rotates with a variable angular velocity ω , the value of the angle β at a given instant will no longer be determined by Formula (1.29) or (1.30), but by Expression (1.28). In order to obtain the closest possible correspondence here between the current values of the angle β and the instantaneous values of the measured velocity ω , the parameters of the device should be selected in such a way that the influence of the last two terms in the right-hand member of Expression (1.28) will be minimal. To achieve this as well as small values of M_{Γ} in the frames of the design shown in Fig. 1.17 is exceedingly difficult. A device built in accordance with this design will often be

incapable of providing the high-precision measurements of ω required for contemporary navigational systems, and particularly for the self-contained ones. The so-called floating differentiating gyroscope, which we shall consider later, is markedly superior in this respect. ✓

Direct use of ϕ as an output signal is feasible only in direct-evaluation devices. In order to use a differentiating gyroscope in any type of telemetering or automatic control system it is necessary to convert this angle into an electrical signal proportional to it, e.g., into a voltage.

The potentiometer pickoff 9 serves this purpose in the diagram shown in Fig. 1.17. The wound carcass of the potentiometer is mounted on the instrument housing, and the wiper 1 is rigidly attached to the gyroscope frame. The wiper is positioned in such a way that when $\omega = 0$ and $M_{\text{exl}} = 0$, the voltage registered by the potentiometer is also zero. The potentiometer is made strictly linear so that the voltage which it registers will be proportional to the angle ϕ and characterized by a sign (or phase) corresponding to the sign of this angle.

Other types of output-signal pickoffs having the properties necessary to meet the above requirements, e.g., inductive devices may be used instead of the potentiometer pickoff.

In isolated special applications, the differentiating gyroscope is also equipped with a torquer device similar in construction to that seen in the gyroscope with three degrees of freedom. The function of the torquer 6 (Fig. 1.17) is to apply to the gyroscope frame a moment proportional to the correction (control) current delivered to its input. A moment (e.g. an imbalance moment) created by deflection of the frame from its initial position at $\omega = 0$ may be compensated by the moment generated by the torquer.

Section 6. The Integrating Gyroscope

The integrating gyroscope consists of a gyroscope with two degrees of freedom (Fig. 1.1) equipped with a damping device which applies to the gyroscope frame a moment acting about its x axis of rotation and proportional to the angular velocity of the frame about this axis.

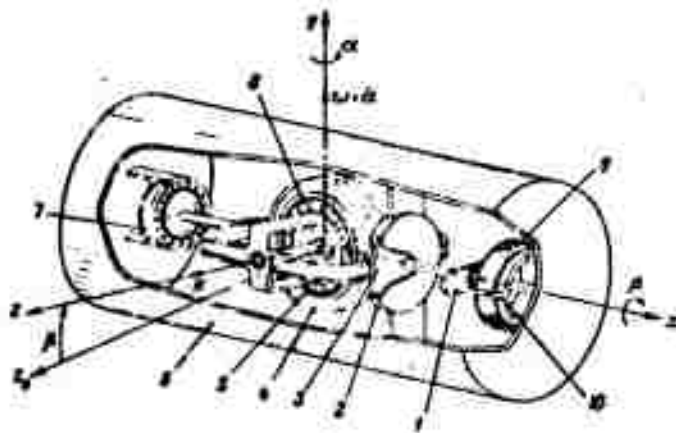


Fig. 1.18. Simplified drawing showing design of integrating gyroscope. 1) Potentiometer wiper; 2) shell of damper (rigidly mounted in gyroscope housing); 3) disk of damper (rigidly attached to gyroscope frame); 4) gyroscope rotor; 5) gyroscope frame; 6) gyroscope housing; 7) torquer; 8) gyromotor stator; 9) potentiometer; 10) center tap of potentiometer.

A gyroscope of this type serves to measure the angle of rotation of its housing about an axis perpendicular to the axis of rotation of the frame and to a given initial position of the spin axis. The design of an integrating gyroscope is represented schematically in Fig. 1.18. This is similar to that of the differentiating gyroscope (Fig. 1.17) but differs in the following respects: the integrating gyroscope is not equipped with springs or other devices performing a similar function. A liquid damper is used with it instead of a dashpot, since

the latter, which is used in the differentiating gyroscope only for the purpose of suppressing oscillations of the frame, cannot fully meet the specifications for the damper of an integrating gyroscope. In contrast to the air damper, the liquid damper is virtually free of dry-surface friction. Its characteristics are more stable and it permits the generation of considerably larger damping moments.

The liquid damper is represented schematically in Fig. 1.18 as consisting of the shell 2, which is mounted in the gyroscope housing 6, and the disk 3, which is rigidly connected to the axis of the frame 5. The gap between the shell and the disk is filled with a viscous liquid.

The axes represented in Fig. 1.18 are identical in significance to those shown in Fig. 1.17. As before, the angle of deflection of the frame (the spin axis z) from its original position (the z_0 axis) is denoted by β . ϵ denotes the angle of rotation of the gyroscope housing about its measurement (input) axis y . Hence ω , the angular velocity of the gyroscope about the measurement axis, is equal to $\dot{\epsilon}$.

Using this notation, we may state that the integrating-gyroscope problem formulated above revolves about the proportionality of the angle β to the angle ϵ or, in other words, to the integral of the angular velocity ω with respect to time. This last also explains why the present device is termed an integrating gyroscope.

If we neglect the friction and inertia of the gyroscope frame and the related components of the device, the operation of the integrating gyroscope may be presented in general terms as follows: a gyroscopic moment arises upon rotation of the housing about the measurement axis y at an angular velocity ω . The frame begins to rotate under the influence of this moment. The moment generated by the damper resists the rotation of the frame. According to Formulas (1.22) and (1.24), these moments are respectively equal to

$$\dot{\alpha} = -H\omega \cos \beta \approx -H\omega, \quad M_{dp} = K_{dp} \dot{\beta}.$$

Under the assumed conditions, the sum of these two moments should be equal to zero at all times, i.e., $K_{dp} \dot{\beta} = H\omega$; it follows from this that

$$\dot{\beta} = \frac{H}{K_{dp}} \omega, \quad (1.31)$$

i.e., at any given instant, the velocity of rotation $\dot{\beta}$ of the frame is proportional to the angular velocity of rotation ω of the housing about the axis of measurement.

Integrating this last equality and assuming that $\beta = 0$ at the initial instant $t = 0$, we obtain

$$\beta = \frac{H}{K_{dp}} \int_0^t \omega dt, \quad (1.32)$$

i.e., the angle of rotation of the integrating gyroscope frame is equal to the time integral of the angular velocity ω . Since $\omega = \frac{d\alpha}{dt}$, the integrand $\omega dt = d\alpha$, so that

$$\beta = (H/K_{dp}) \int_0^t d\alpha(t).$$

Since $\alpha(0) = 0$ and $\alpha(t) = \alpha$, integration yields

$$\beta = (H/K_{dp}) \alpha. \quad (1.33)$$

i.e., the angle of rotation of the frame is directly proportional to the angle of rotation of the housing of the integrating gyroscope about its measurement axis.

As in the case of the differentiating gyroscope, the smallest angular

velocity to which the integrating gyroscope can respond is given by $\omega_{min} = \frac{M_{fr}}{H}$, where M_{fr} is, as before, the referred frictional moment. Taking M_{fr} into consideration and neglecting the inertia of the design members which rotate about the x axis, we find that for $\omega > \omega_{min}$, the angle

$$\beta = \left(\frac{H}{K_{dp}} \right) \int_0^t \omega dt - \left(\frac{M_{fr} K_{dp}}{H} \right) t.$$

The second term in the right-hand member is the instrument error due to the frictional moment. This error is directly proportional to the time during which the device rotates at the velocity ω . It is to be noted that the error of a differentiating gyroscope due to the moment M_{fr} is a constant value when $M_{fr} = \text{const.}$ At the present time, integrating gyroscopes with frictional moments practically equal to zero are required for the solution of a number of highly important technical problems. This requirement is satisfied only by floating integrating gyroscopes.

When an integrating gyroscope is used in a telemetering or automatic control system, it is necessary to convert the angle β into an electrical signal proportional to it, such as a voltage. The potentiometer pickoff 9 performs this function in the design shown in Fig. 1.18; this is completely analogous in construction and operation to the one described for the differentiating gyroscope.

The torquer 7 (Fig. 1.18) serves to compensate any constant-value and unidirectional disturbance moments which may act on the frame of the gyroscope about its axis of rotation. These include, for example, imbalance moments, moments generated by the leads to the gyromotor (these are not shown in Fig. 1.18), and so on. A current I_{con} supplied to the torquer causes it to generate a moment equal in value and opposite in direction to the moments of the above disturbances. Another very important function of the torquer will be discussed later.

Let us now consider the operation of the integrating gyroscope in somewhat

greater detail, taking into consideration the inertia of the gyroscope frame and the components of the device attached to it. Suppose that the instrument housing rotates about the measurement axis y at an angular velocity ω . Under these conditions the following moments will act on the frame about its x axis of rotation:

1. A gyroscopic moment equal to

$$g = -H\omega \cos \beta.$$

As a rule, the operating conditions created for integrating gyroscopes in the mechanisms in which they are used are such that the angle β remains small at all times. This virtually eliminates the effect on the instrument of the angular velocity of rotation of its housing about the initial position z_0 of the spin axis, and renders the gyroscopic moment in practice proportional to ω , since $\cos \beta$ may be assumed equal to one with a very small error. Thereupon the expression for the gyroscopic moment takes the form

$$g = -H\omega = -H\dot{\alpha}.$$

2. A moment generated by the damper and given by

$$M_d = K_d \beta.$$

3. A moment of inertia, equal, as in the case of the differentiating gyroscope, to

$$M_{i, \alpha} = J \ddot{\beta}.$$

4. A referred frictional moment $\pm M_{fr}$. The instrument is designed in such a way that this moment is held to a minimum. We shall accordingly disregard it for the sake of simplicity.

Equating the sum of the first three moments to zero, we obtain the equa-

tion of motion of the integrating-gyroscope frame in the form

$$J\ddot{\beta} + K_{sp}\dot{\beta} = H\dot{\alpha}. \quad (1.34)$$

A single integration of this equation for the initial conditions $\alpha = \beta = \dot{\beta} = 0$ at $t = 0$ yields

$$T\dot{\beta} + \beta = \frac{H}{K_{sp}} \alpha, \quad (1.35)$$

where

$$T = \frac{J}{K_{sp}}, \quad (1.36)$$

the time constant of the integrating gyroscope.

Integrating Equation (1.35) for the same initial conditions, we obtain

$$\beta = \frac{H}{J} e^{-\frac{t}{T}} \int_0^t \alpha(\tau) e^{\frac{\tau}{T}} d\tau.$$

Integrating the right-hand member of this equality by parts, we obtain

$$\beta = \frac{H}{K_{sp}} \left(\alpha - e^{-\frac{t}{T}} \int_0^t \dot{\alpha} e^{\frac{\tau}{T}} d\tau \right) = \frac{H}{K_{sp}} \left[\alpha - \int_0^t \dot{\alpha}(\tau) e^{-\frac{t-\tau}{T}} d\tau \right]. \quad (1.37)$$

Here τ is a variable of integration.

It will be seen from this equality that to permit measurement of the angle α , the bracketed integral, in which $t \gg \tau$, must at all times remain vanishingly small. For this purpose the parameters of the instrument design must be chosen so that the value of the time constant T becomes sufficiently small and the value of $\dot{\alpha}$ not excessively large. As seen from Equality (1.36), this in turn

necessitates making the moment of inertia J as small as possible and the specific damping moment K_{dp} as large as possible. If the small- T condition is satisfied, we may drop the second term in the bracketed notation of Equality (1.37). We shall then have the familiar ratio (1.33)

$$\beta = (H/K_{dp})\omega.$$

The use of an integrating gyroscope to measure the angle ϵ by direct (immediate or remote) measurement of the angle of rotation β of the gyroscope frame with respect to the instrument housing is expedient only in those cases where the range of possible values of the angle ϵ and the parameters of the instrument are such that the angle β remains small enough at all times during operation to permit setting $\cos \beta = 1$ and $\sin \beta = 0$ with a sufficiently small error. Otherwise the operation of the instrument will be complicated by the following circumstances: first, if the angle β is such that $\cos \beta$ may not be assumed equal to unity, the gyroscopic moment becomes $H\dot{\epsilon} \cos \beta$ (instead of $H\dot{\epsilon}$, as when $\cos \beta = 1$); this results in nonlinear dependence of β on ϵ . Secondly, if it is inadmissible to set $\sin \beta = 0$, the angular velocity of the instrument housing about the initial position of the spin axis \underline{z} , i.e., about the axis \underline{z}_0 , will affect the value of the angle β .

When arbitrary values of the angle ϵ are to be measured, therefore, the integrating gyroscope must be used in conjunction with a servomechanism. A system formed in this way constitutes a spatial angular-velocity integrator which operates on the principle of an integrating drive. In this system, the integrating gyroscope serves as the sensing unit. We apply the designation "spatial" to this integrator in view of the fact that it detects rotational velocity relative to inertial space and integrates it with respect to time (like the integrating gyroscope).

Section 7. The Spatial Angular-Velocity Integrator and Applica-
tion of the Integrating Gyroscope to Geometrical
Stabilization

A schematic representation of the uniaxial spatial angular-velocity integrator appears in Fig. 1.19. The integrator is termed uniaxial because its purpose is to integrate the angular velocity of rotation in inertial space about a single arbitrary axis, with which the measurement (input) axis of the integrator must be brought into alignment (or parallelism). The integrator must not be sensitive to rotations about the axes perpendicular to its measurement axis. The principal components of the integrator are the integrating gyroscope and the servomechanism.

The integrating gyroscope 2 is held in the clamp 1, which is mounted rigidly on the shaft 3. The latter is carried in the bearing 6 of the flange 7, which is fixed to the integrator housing 8. The geometric axis of the shaft 3 is the measurement axis of the integrator, or (a term by which we shall refer to it from now on) its input axis. The integrating gyroscope 2 is inserted in the clamp 1 in such a way that its measurement (input) axis coincides with the input axis of the integrator. We shall therefore refer to the input axis of the integrator as the y axis. To avoid complicating the drawing, the gyroscope housing 2 in Fig. 1.19 is not sectioned. Nevertheless, the disposition of the gyroscope elements is readily understood on comparison of Figs. 1.19 and 1.18. The x axis is the axis of rotation of the gyroscope frame in both illustrations, and the z_0 axis represents the initial position of the spin axis z . The arrows indicate the positive directions of the angles ϵ and β . The slave motor 5 of the servosystem is mounted on the flange 7; this functions to rotate the gyroscope housing 2 about

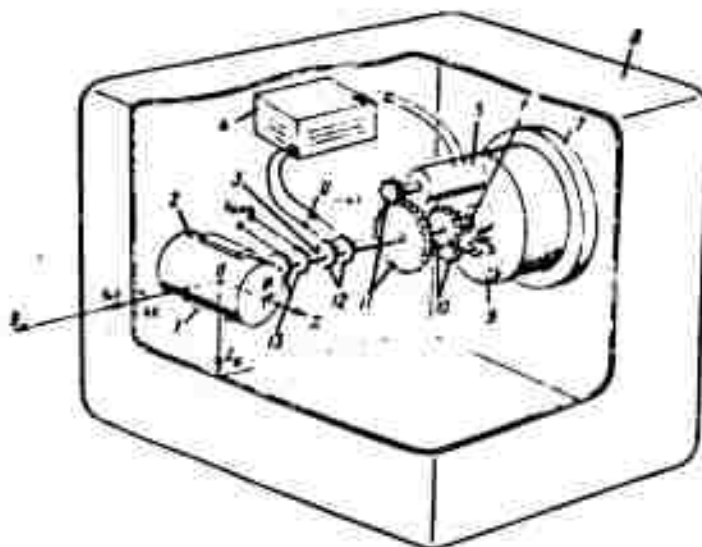


Fig. 1.19. Schematic representation of uniaxial spatial angular-velocity integrator with integrating gyroscope and servomechanism. 1) Clamp rigidly attached to shaft 3; 2) integrating gyroscope; 3) shaft; 4) amplifier; 5) slave motor; 6) bearing; 7) flange; 8) integrator housing; 9) indicator; 10) gear train; 11) reduction gearing; 12) wipers and contact rings for pickoff of output voltage U_{out} from integrating-gyroscope potentiometer; 13) wipers and contact rings for delivery of current I_{con} to torquer of integrating gyroscope.

the input axis y with respect to the integrator housing. The angle of rotation α of the integrator housing 8 in inertial space about the input axis y is indicated by dial 9 which is driven from the shaft 3 by the gear train 10. The voltage U_{out} of the potentiometer 9 (see Fig. 1.18) is delivered via the wipers and contact rings 12 (Fig. 1.19) to the input of the amplifier 4. The slave motor 5 is connected to the amplifier output.

The integrator operates as follows: let us assume first that the servodrive is shut off, i.e., that the amplifier input is disconnected from the wipers 12. Now let us turn the integrator housing 8 in inertial space through a certain angle α about its input axis y at an angular velocity ω . The housing 2 of the integrating gyroscope, which functions in this case as a sensing element, will

turn with it through the same angle. Then, in accordance with the foregoing, the gyroscope frame will turn through an angle ϕ , proportional to the angle ϵ , with respect to the instrument housing. An output signal, an electrical voltage U_{out} proportional to ϕ and thereby to the angle ϵ , will appear at the output of the integrating-gyroscope potentiometer 9 (see Fig. 1.18) as a result.

Let us switch on the servodrive and apply the voltage U_{out} to the input of its amplifier 4. After amplification, this voltage will set the slave motor 5 into operation. The latter, working through the reduction gear 11 and the shaft 3, will begin turning the integrating-gyroscope housing 2 in the opposite direction. The angle ϵ , and therefore the angle ϕ and the voltage U_{out} , will become smaller. This process will continue until the operation of the servodrive ceases; this occurs when the voltage U_{out} is reduced to zero. The voltage U_{out} becomes equal to zero, however, only when the angle ϕ and therefore the angle ϵ are zero, i.e., when the servodrive returns the integrating-gyroscope housing to its original position. The angle of rotation of the integrating-gyroscope housing 2 with respect to the integrator housing 8 will be indicated by the dial 9 (see Fig. 1.19). This angle is equal to the angle of rotation ϵ of the integrator housing 8 in inertial space.

We have considered the operation of the integrator in separate phases. In actual operation, the servodrive is "on" at all times. The process is as follows: let us assume that the integrator housing 8 rotates in inertial space about the input axis y of the integrator with a certain angular velocity ω . At the initial instant of this rotation, the integrating-gyroscope housing 2 will also rotate together with the integrator housing. As a result, an output signal, the voltage U_{out} , will appear at the output of the integrating gyroscope. This voltage will actuate the servodrive. The latter, which is highly sensitive and responds rapidly, will keep turning the gyroscope housing in the opposite direction at a velocity equal in magnitude and opposite in direction to the velocity ω .

Consequently the integrating-gyroscope housing will remain stationary in inertial space. In so doing it will be deflected from its initial position through a very small angle, which will depend on the sensitivity thresholds of the integrating gyroscope and the servodrive. Thus the angle θ will remain small at all times, which, as noted above, is extremely important.

The rotation of the integrating-gyroscope housing relative to the integrator housing about its input axis y is transmitted to the indicator dial 9 (see Fig. 1.19). Thus the integrator indicator will show the angle of rotation of the integrating-gyroscope housing with respect to the integrator housing. It is clear from the preceding discussion that this angle will be equal to the time integral of the angular velocity of rotation ω of the integrator housing 8 in inertial space about the integrator input axis y , i.e., to the angle α .

Thus the uniaxial spatial angular-velocity integrator only integrates the angular velocity of rotation of the housing about its input axis y , since the rotations of the integrator housing relative to all other axes perpendicular to the input axis cannot create an output signal, a voltage U_{out} , in the integrating gyroscope, and cannot, therefore, operate the servodrive.

Let us suppose that the integrator housing may only rotate in inertial space about the y axis, or, in other words, that the orientation of the y axis in inertial space does not change. It follows directly from analysis of the operation of the integrator that under these conditions the clamp 1 and the integrating gyroscope 2, mounted within it, will retain fixed orientations in inertial space during any rotation of the housing 8 about its input axis y . With reference to the clamp 1 the integrator under examination, which consists of an integrating gyroscope 2 and a servodrive, functions as a uniaxial stabilizer which effects geometrical stabilization of the clamp 1 in inertial space with respect to the y axis. Consequently, if we have a platform which must be stabilized geometrically with

respect to a single axis in inertial space, an integrator of the type discussed above may be used to accomplish it. Let us consider this extremely important application of the integrator in somewhat greater detail.

Suppose that the platform 4 (Fig. 1.20) requires geometrical stabilization in inertial space with respect to the axis Y_{pl} . The axes $O_1X_{pl}Y_{pl}Z_{pl}$ are fixed to the platform. The platform must be stabilized with respect to the axis Y_{pl} . This means that the orientation of the X_{pl} and Z_{pl} axes must remain stationary during all rotations of the base 1 about the Y_{pl} axis in inertial space, and also when there are moments which tend to turn the platform 4 about the axis Y_{pl} . The platform 4 is mounted on the base 1 via the two journals 5, which are directed along the axis Y_{pl} . The integrating gyroscope 6 is attached to the platform. The input (measurement) axis y of the gyroscope must be parallel to the stabilization axis Y_{pl} of the platform; let the x axis run parallel to the X_{pl} axis and the z_0 axis coincide with the Z_{pl} axis. Let the slave motor 8 of the servodrive be mounted on the base 1 of the stabilizer. The motor torque is transmitted to the platform 4 via the reduction gear 9. In principle, the scheme shown in Fig. 1.20

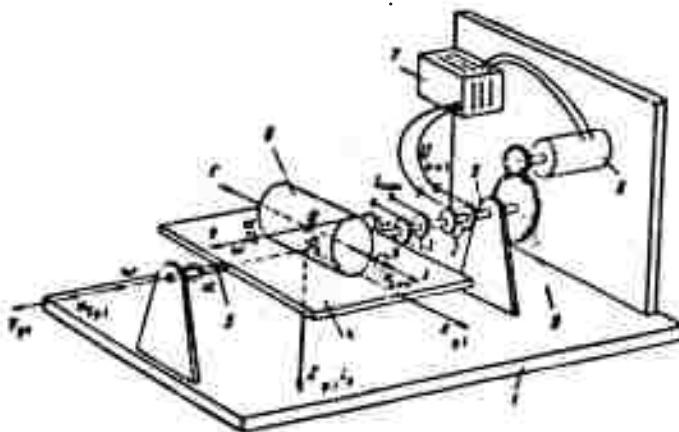


Fig. 1.20. Uniaxial stabilizer. 1) Base of stabilizer; 2) brushes and contact rings for pickoff of output voltage U_{out} from integrating-gyroscope potentiometer; 3) brushes and contact rings for delivery of current I_{con} to torquer of integrating gyroscope; 4) platform to be uniaxially stabilized; 5) platform axis journals; 6) integrating gyroscope; 7) amplifier; 8) slave motor; 9) reducing gear.

differs in no respect from that of Fig. 1.19. Thus the position of the platform 4, i.e., the orientation of the X_{pl} and Z_{pl} axes in inertial space, will remain unchanged during all rotations of the base 1 about the Y_{pl} axis.

Let us now assume that a disturbance moment $M_{Y_{pl}}$ has begun to act on the platform about the Y_{pl} axis. Under the influence of this moment the platform will begin to rotate about the axis Y_{pl} . This results in the appearance at the output of the gyroscope potentiometer 9 (Fig. 1.18) of a voltage U_{out} , which, after amplification and suitable transformation by the amplifier 7 (see Fig. 1.20), sets the slave motor 8 of the servosystem into operation. The latter, working through the reducing gear 9, begins to apply to the platform 4 a moment which is opposed in direction to $M_{Y_{pl}}$. Let us suppose that the moment developed by the slave motor is proportional to the voltage U_{out} , i.e., to the angle of deflection α of the platform from its initial position ($\alpha = 0$). The motor torque will then increase as the angle of deflection of the platform from its initial position increases. But, as long as the motor torque remains smaller than the moment $M_{Y_{pl}}$, the platform will continue to deviate from its original position. When, however, the motor torque becomes equal to the moment $M_{Y_{pl}}$ at a certain value of the angle α , further deviation of the axis under the influence of $M_{Y_{pl}}$ will not occur. Thus the servodrive has arrested the rotation of the platform due to the moment $M_{Y_{pl}}$, but has not been able to return it to its initial position. The angle α at which this equilibrium is established may be referred to as the static error of the system. If the moment $M_{Y_{pl}}$ now reverts to zero, the servodrive will turn the platform to its initial position ($\alpha = 0$). The manner in which this occurs is clear from the preceding arguments.

If, however, we use a servodrive equipped with an integral control, the

static error will always be zero. Fixed orientation of the platform 4, both during rotation of the base 1 and under the influence of disturbance moments $M_{Y_{p1}}$, may accordingly be ensured by the use of a rapid-response servomechanism having adequate capacity and a suitable control function. We shall consider this problem in greater detail in Chapter III.

Everything which we have said with reference to the action of the disturbance moment $M_{Y_{p1}}$ upon the platform applies with equal force to the integrator in Fig. 1.19, where the clamp 1 plays the part of the platform.

This mode of operation of the system, in which its function is to maintain the platform in a fixed orientation in space, will be referred to as the geometrical-stabilization regime. Similarly, the operation of the integrating gyroscope in this regime will also be referred to as its operation in the geometrical-stabilization regime.

However, the system under consideration not only enables us to maintain the platform (the axes X_{p1} , Z_{p1}) in a fixed orientation in space, but also to alter it at a prescribed velocity and by a prescribed angle. This is accomplished by supplying a current I_{con} proportional to the desired rotational velocity of the platform in inertial space about the Y_{p1} axis to the torquer 7 (Fig. 1.18) of the integrating gyroscope. This is actually the second function of the torquer which we referred to earlier. The torquer applies to the frame of the gyroscope a moment proportional to the current I_{con} .

Suppose it is required that the platform (the X_{p1} , and Z_{p1} axes) rotate about the axis Y_{p1} at a certain constant angular velocity ω . This necessitates delivery of a current I_{con} to the torquer 7 (Fig. 1.18) such that the moment M_t generated by the torquer as a result will be equal in magnitude but opposite in direction to the gyroscopic moment which arises upon rotation of the gyroscope housing with a constant angular velocity ω about its input axis y . Let us

assume that just such a current I_{con} is supplied. The torquer 7 will then apply the constant moment M_t to the frame of the gyroscope. The presence of this moment is equivalent in its effect on the gyroscope to rotation of the gyroscope housing with a constant angular velocity $\omega_t = -\omega$. Under the influence of M_t , the gyroscope frame begins to rotate and the spin axis z is deflected through a certain angle θ from its initial position z_0 . A voltage U_{out} will then appear at the output of the potentiometer 9 (see Fig. 1.18), setting the slave motor 8 (see Fig. 1.20) of the servodrive into operation. The latter will begin to turn the platform 4 about the Y_{pl} axis in such a way as to return the z axis to its initial position. To do this the servodrive must rotate the platform with the gyroscope in the opposite direction to the angular velocity ω_t . Let ω_{adj} denote the velocity of rotation (adjustment). Rotation of the gyroscope housing at a velocity ω_{adj} will give rise to a gyroscopic moment Γ which opposes the moment M_t . When the velocity ω_{adj} attains the required value ω , which corresponds to the control current I_{con} , the gyroscopic moment Γ will be equal to the moment M_t . The rotation of the gyroscope frame ceases and the platform with the gyroscope and the X_{pl} and Z_{pl} axes attached to it will rotate about the Y_{pl} axis with the required angular velocity ω . Here the angle θ will assume a value determined by the sensitivity threshold of the integrating gyroscope and servodrive, which should be as low as possible.

The above statements may be supported by the following relationships. When the gyroscope housing rotates at a velocity ω the gyroscopic moment is equal to

$$\Gamma = -H\omega.$$

The corrective moment M_t is proportional to the current I_{con} ; that is,

$$M_t = K I_{con}.$$

To prevent the gyroscope frame from rotating about its own axis, we must have

$$\Gamma + M_t = 0.$$

or, substituting the values of Γ and \underline{M}_t in this equality, we obtain

$$H\omega = K_t I_{con}.$$

From this it follows that if

$$I_{con} = \frac{H}{K_t} \omega,$$

i.e., if a current \underline{I}_{con} proportional to the desired velocity of rotation ω of the platform (the \underline{X}_{p1} , and \underline{Z}_{p1} axes) about the \underline{Y}_{p1} axis is supplied to the torquer, the servodrive will rotate the platform at this velocity.

Since $\omega = \dot{\alpha}$ (α is the angle of rotation of the platform in inertial space), the last expression may be rewritten in the form

$$\alpha = \alpha_0 + \frac{K_t}{H} \int_0^t I_{con} dt,$$

where α_0 is the value of the angle α at the instant $t = 0$.

This mode of operation of the uniaxial stabilizer will be termed the spatial-integration regime. This designation is based on the following considerations: an electrical signal, the current \underline{I}_{con} , is supplied to the system input; at the output we obtain the angle of rotation α of the platform in inertial space, which is proportional to the time integral of the input signal. It should be noted that this mode of operation of the uniaxial stabilizer corresponds exactly to the operation of an ordinary electromechanical integrator with the difference that by virtue of the properties of the gyroscope, the output quantity of the uniaxial stabilizer is the angle of rotation in inertial space, while the out-

put quantity of the electromechanical integrator is the angle of rotation with respect to the instrument housing.

Any change in the current I_{con} initiates rotation of the platform with the gyroscope (the X_{pl} , and Z_{pl} axes) at a new angular velocity corresponding to the new value of the current I_{con} . The character of this transient effect is determined by the dynamic properties of the system as a whole. In the unsteady operating state, the output signal of the gyroscope, i.e., the voltage U_{out} , is also a function of the angle of deflection β of the gyroscope frame from its initial position, which angle is determined in this case by the difference between the angular velocity which corresponds to the corrective signal and the actual angular velocity, and also by the acceleration.

The mode of operation of the integrating gyroscope in the presence of a current I_{con} will be designated its operation in the spatial-integration regime.

We have considered the use of the integrating gyroscope and servodrives to form a spatial angular-velocity integrator (see Fig. 1.19) and a uniaxial stabilizer (see Fig. 1.20). Let us now examine the means by which stabilization of the platform 1 (Fig. 1.16) in inertial space with respect to the three mutually perpendicular axes $O\{ = \{$, and, consequently, concrete reproduction of these axes, may be accomplished by the use of three integrating gyroscopes and servodrives.

A simplified schematic representation of such a triaxial stabilizer is given in Fig. 1.21. The housing of the stabilizer is positioned in the object in the same way as in the instance shown in Fig. 1.16. For the sake of clarity, Fig. 1.21 illustrates the case in which the axes $OXYZ$ connected to the object (or with the stabilizer housing) coincide with the axes $O\{ = \{$, which are connected to the platform. The three integrating gyroscopes 10, 17 and 18 (Fig. 1.21) are mounted on the platform to detect its deflections from the position in inertial space imparted to it. The input (measurement) axes Y_{ξ} , Y_{η} , and Y_{ζ} of the gyroscopes are directed parallel to the ξ , η , and ζ axes. The remaining

two axes of each of the gyroscopes are keyed by the same subscripts as the measurement axes. The axis 3 of the platform 1 to be stabilized and the axes of the inner and outer gimbal frames (6 and 11) are equipped with servodrives. The servomechanism amplifiers are not shown in Fig. 1.21. The servodrive of the axis 3 of the platform 1 is controlled exclusively by the gyroscope 18. In combination with the servodrive which it controls, this gyroscope stabilizes the platform in inertial space with respect to the ξ axis. The stabilization process takes place in the manner outlined in the discussion of the operation of the uniaxial stabilizer shown in Fig. 1.20. Stabilization of the platform 1 in inertial space with reference to the ξ and η axes is accomplished in a similar manner by means of the gyroscopes 10 and 17 and the servodrives of the inner and outer gimbal frames, i.e., these gyroscopes and servodrives maintain the platform in the plane $\xi \eta$. To effect this stabilization it is necessary that each of the gyroscopes 10 and 17 be capable of controlling both the inner-frame servodrive and the outer-frame servodrive. Let us illustrate this with examples. Suppose that $\psi = \theta = \gamma = 0$, as indicated in Fig. 1.21; the axis of the inner frame coincides with the ξ axis, and the axis of the outer frame with the η axis. The input (measurement) axes y_{ξ} and y_{η} of the gyroscopes 10 and 17 are therefore respectively parallel to the Z_1 and X axes of the inner and outer gimbal frames. Accordingly, only the inner-frame servodrive should operate upon deflection of the platform about the η axis, which is sensed by the gyroscope 10, and only the outer-frame servodrive should respond to deflection of the platform about the ξ axis, which is sensed by the gyroscope 17. Thus in the given case ($\psi = \theta = \gamma = 0$) the gyroscope 10 controls the servodrive of the inner frame, while the gyroscope 17 controls the outer-frame servodrive.

Now let us turn the stabilizer housing through an angle $\psi = 90^\circ$ about the ξ axis (Fig. 1.22). Now the measurement axis y_{ξ} of the gyroscope 10 will be

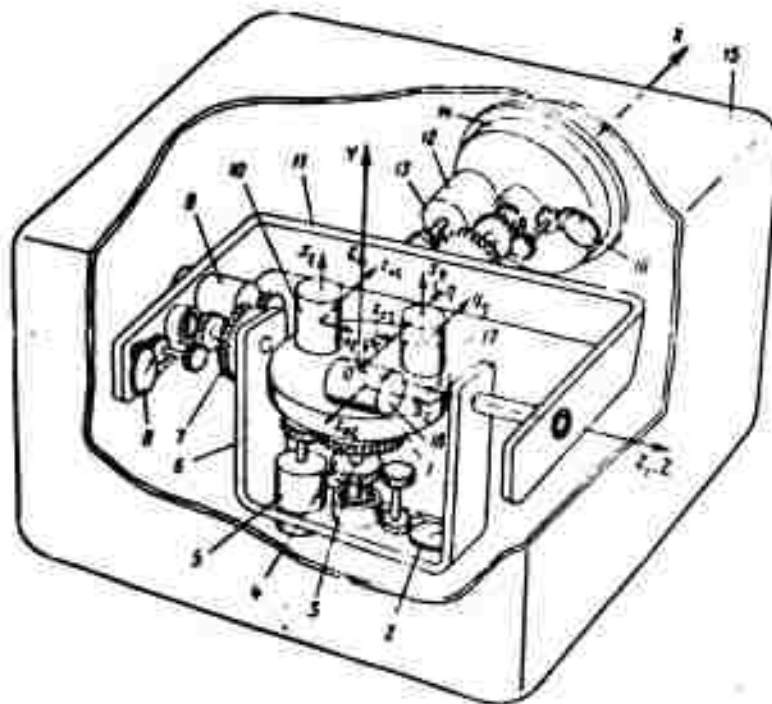


Fig. 1.21. Simplified schematic representation of triaxial stabilizer.

1) Platform to be triaxially stabilized; 2) indicator for angle ϕ ; 3) axis of platform; 4) reduction gear of platform servodrive; 5) slave motor of platform servodrive; 6) inner gimbal frame; 7) reduction gear of inner-frame servodrive; 8) indicator for angle θ ; 9) slave motor of inner-frame servodrive; 10) integrating gyroscope sensitive to angular velocity of platform about X axis; 11) outer gimbal frame; 12) slave motor of outer-frame servodrive; 13) reduction gear of outer-frame servodrive; 14) flange; 15) stabilizer housing; 16) indicator for angle γ ; 17) integrating gyroscope sensitive to angular velocity of platform about Y axis; 18) integrating gyroscope sensitive to angular velocity of platform about Z axis.

parallel not to the axis of rotation Z_1 of the inner frame, as it was at $\phi = 0$, but to the X axis of rotation of the outer frame; the measurement axis Y_n of the gyroscope 17 will become parallel to the Z_1 axis of rotation of the inner frame. Thus with $\phi = 90^\circ$, the gyroscope 10 must control the outer-frame servodrive, while the gyroscope 17 must control the inner-frame servodrive.

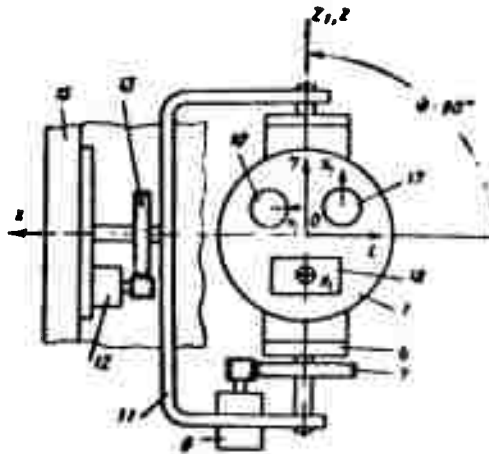


Fig. 1.22. Position of elements of stabilizer shown in Fig. 1.21 after rotation of housing through an angle $\varphi = 90^\circ$ about the ξ axis. Key same as for Fig. 1.21.

If $\varphi \neq 0, 90, 180, \text{ or } 270^\circ$, the measurement axes y_{ξ} and y_{η} will not generally coincide with the axes of rotation of the gimbal frames. In this case, the servodrives of the inner and outer frames should function simultaneously upon deflection of the platform about the axis ξ or upon rotation of the object about this axis. They must be controlled by the gyroscope 10, since it senses rotations about the ξ axis. Similarly, both servodrives function upon rotations about the axis η , but they must be controlled by the gyroscope 17. Finally, when rotations occur simultaneously about the ξ and η axes, both gyroscopes, 10 and 17, contribute simultaneously to control of the inner- and outer-frame servodrives.

Thus the stabilizer must be equipped with a device which will distribute the output voltages of the gyroscopes 10 and 17 appropriately between the amplifiers of the inner- and outer-frame servodrives. Such a device is referred to as a coordinate transformer. It is installed on the axis 3 of the platform 1 (Fig. 1.21). Since the coordinate transformer is there to distribute the gyroscope output voltages according to the size of the angle φ , one of its elements is fixed

to the platform and the other to the inner gimbal frame. The coordinate transformer is not shown in Fig. 1.21, since its treatment is beyond the scope of the present volume.

Thus if the required orientation in inertial space is imparted to the platform 1, or, in other words, to the axes $O\xi = \xi$ (Fig. 1.21), and the stabilizer set in operation, the platform will maintain the orientation imparted to it regardless of the motion of the object. The angles of rotation ψ , θ , and γ of the object about the ξ , Z_1 and X axes will be indicated by the visual indicators 2, 8, and 16. To obtain electrical signals proportional to the angles ψ , θ , and γ , it is necessary to replace the indicators with suitable data-transmitting devices which transform angular displacements into electrical signals.

In this case only the I_{con} -current necessary to suppress the systematic disturbance moments of the gyroscope is supplied to the gyroscope torquer.

Now suppose it is required that the axes $O\xi = \xi$ rotate in inertial space in a certain manner, for example, that they be oriented with respect to the earth in the manner indicated in Fig. 1.13. For this it is necessary that the projections of the instantaneous angular velocities of the platform 1 (of the axes $O\xi = \xi$ of Fig. 1.21) in inertial space onto the ξ , η , and ζ axes be equal to the velocities \underline{u}_ξ , \underline{u}_η , and \underline{u}_ζ as determined by Equalities (1.13).

It was indicated earlier (in discussion of the operation of the uniaxial stabilizer shown in Fig. 1.20) that in order to set the platform rotating in inertial space at a specified angular velocity about the input axis, it is necessary to supply a current I_{con} proportional to this velocity to the torquer. In our case, it is necessary to set the platform into simultaneous rotation about all three axes. To accomplish this, therefore, we must supply currents I_{con} respectively proportional to the velocities \underline{u}_ξ , \underline{u}_η , and \underline{u}_ζ to the torquers of the gyroscopes 10, 17, and 18.

In this way the triaxial stabilizer under discussion enables us to reproduce the axes $O\xi\eta\zeta$ in concrete form, either with fixed orientations in inertial space or with a specified orientation relative to the earth, or rotating in inertial space in some other manner. In all cases, the angles ψ , ϑ , and γ are measured directly and without distortion.

Provided that floating integrating gyroscopes are used in their construction, the devices discussed here, the spatial integrator and the stabilizer, can ensure the high precision required in modern self-contained navigational systems, and particularly in those of the inertial type. Ordinary integrating gyroscopes are unable to provide this degree of precision, due largely to the presence of considerable and variable frictional moments which arise in the gyroscope's frame bearings.

The above treatment of the problem in which the platform is stabilized with respect to one and three axes with the aid of integrating gyroscopes and servo-drives is not, of course, exhaustive. It has only been dealt with to the extent necessary to explain the application of the integrating gyroscope for this purpose. The characteristic feature of this method is that here the gyroscopes do not exercise any direct stabilizing influence on the platform, but are used only as sensing elements. This fact, in particular, differentiates the given method from the method, widespread at present, of direct gyroscopic stabilization, investigated both theoretically and in practice by B. V. Bulgakov, Ya. N. Roytenberg, and others.

CHAPTER II

DESIGN AND BASIC PARAMETERS OF FLOATING GYROSCOPES

The integrating and differentiating gyroscopes designed for use in modern automatic flight-control systems, especially in self-contained inertial-navigation systems, for the gyro-stabilization of radar pathfinding apparatus, and for a variety of other automatic devices should be characterized by high parameter stability, low sensitivity thresholds, high precision, and great strength and stability with respect to vibration and shock. These requirements are not, as a rule, adequately met by the conventional integrating and differentiating gyroscopes, the basic designs of which are shown in Figs. 1.18 and 1.17. The fundamental reasons for the failure of such gyroscopes to meet the above specifications are as follows: the significant and variable frictional moments which arise in the frame bearings of the gyroscope and between the reciprocating elements of the damper; insufficient strength and stability under vibration and shock; and the difficulties encountered in ensuring the required damping. Thus the development of gyroscope designs having great strength and stability, negligibly small frictional moments in the gyroscope-frame supports, and dampers free from dry friction has been a problem whose successful solution has made it possible to use integrating and differentiating gyroscopes to advantage in modern precision systems.

The problem of reducing friction in the bearings of gyroscope suspensions is not a new one. The problem arose in connection with the first gyroscopic device, which was constructed in 1852 by L. Foucault to demonstrate the diurnal rotation of the earth. The practical realization of the marine gyroscopic compass depended in many respects on finding a successful solution to this problem. A

highly successful and effective solution was proposed in 1908 by Dr. Anschütz in his marine gyrocompass. This method consisted in mounting a shell containing the gyrowheel on a float which rode in a bowl filled with a heavy liquid--mercury. A pin attached to the bowl served to center the floating system.

The practice of harnessing the buoyancy of a liquid to relieve supports of their loads has been widely adopted, and not only for gyroscopic devices. For example, to reduce friction in the compass-card supports of modern marine and aviation magnetic compasses, the card is installed in a liquid-filled bowl. The buoyant forces of the liquid, acting in a direction opposed to those of the card's weight, relieves its support almost completely, leaving only the small pendulum effect necessary for normal operation of the compass.

In floating gyroscopes--the most recent and most promising variant of the integrating and differentiating gyroscopes--reduction of frictional moments is also accomplished by exploitation of the buoyancy of a liquid. The liquid serves simultaneously to provide the necessary damping and the high vibration- and shock-resistance and stability characteristic of these devices.

The concept of the floating gyroscope with two degrees of freedom was first put forward in the Soviet Union by Engineer L. I. Tkachev, under whose guidance the first design for a floating integrating gyroscope was worked out at the Moscow Institute of Power Engineering (Moskovskiy Energeticheskiy Institut) in 1945. On the basis of an application dated January 29, 1949, L. I. Tkachev was awarded Author's Certificate No. 113446 for the floating gyroscope, which was designated "A Sensitive Element for Precision Gyroscopic Devices used in Spatial Orientation of Flying Craft."

The design of the MIPE floating gyroscope is presented in Fig. 2.1. The gyromotor 12 is enclosed in the cylindrical shell 3 which, together with the head assemblies, forms a hermetic float. The float containing the gyromotor is installed in the instrument housing on the suspension axes 18 (diam. = 0.6 mm), which are held

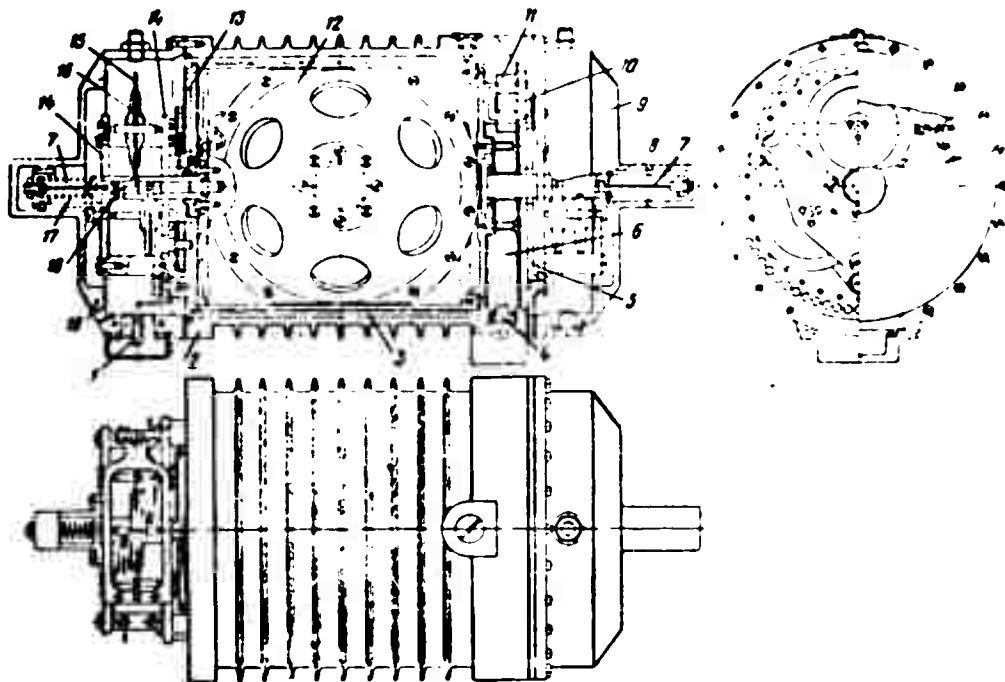


Fig. 2.1. MIPE Floating gyroscope (1945):

1) gyromotor current-supply lead; 2) outer cylinder; 3) inner cylinder (float); 4) inductive pickup; 5) rear wall; 6) textolite plate; 7) axial tension member; 8) balancer disc; 9) rear cap; 10) corrector coil; 11) permanent magnet of corrector; 12) gyromotor; 13) front wall; 14) plates carrying disc bearings; 15) disc; 16) current-supply bands; 17) axial spring; 18) suspension axis; 19) front cap.

under tension by the axial spring 17. The suspension axes bear against the discs 15, which are mounted in turn in jewelled bearings carried in the plates 14. The entire free inner volume of the instrument housing is filled with a heavy liquid. The volume of the float and the specific gravity of the liquid are adjusted in such a way that the buoyancy of the liquid is equal to the weight of the floating gyro-assembly. The current leads to the float are formed by the silver bands 16. Pure liquid damping produced by friction between the float 3 and the film of liquid between it and the inner surface of the cylinder 2, is used exclusively in this device. The inductive pickup 4 functions as an output-signal detector. The corrector consists of the permanent magnet 11 and the coil 10. This first model of the instrument possessed the following characteristics: kinetic moment $\sim 55,000$ gf-cm-sec; frictional moment in the supports of the floating gyroassembly ~ 0.001 gf-cm; error, of the order of $0.05^\circ/\text{hr}$. The device was designed for use with a servodrive.

Work toward the realization of floating gyroscopes was first initiated abroad in 1946 by C. S. Draper in the laboratory which he supervised at the Massachusetts Institute of Technology (USA). A number of experimental models were built and studied under his direction under a contract with the US Army Air Corps. In 1948, working on the basis of data furnished by MIT, the Minneapolis-Honeywell firm developed several variants of the floating gyroscope which were put into batch production; this began in 1951. By the beginning of 1957 approximately 21,000 floating gyroscopes had been produced.

The floating gyroscopes made by MIT, the Minneapolis-Honeywell Company and several other firms will be examined in the following paragraphs.

Section 1. Integrating Gyroscopes

The general design features of the floating integrating gyroscopes are as

follows: the frame carrying the gyrowheel is installed within a hermetic cylindrical shell, and turns in bearings located in the instrument housing. The housing is also cylindrical in form and completely filled with a heavy liquid (a fluoro-organic compound). Thus the gyroassembly behaves as a float immersed in a liquid, which also explains the term "floating" applied to gyroscopes of this type. The volume of the shell and the specific gravity of the liquid are chosen so that the buoyant forces of the liquid will be equal to the weight of the gyroassembly and relieve its bearings of practically their entire load, thus reducing the frictional moment which arises in them to a negligibly small value. It is necessary to ensure correct centering of the gyroassembly with respect to the instrument housing, and the center of gravity of the gyroassembly and its center of pressure must coincide at all times; an attempt should be made to locate the point of coincidence in the axis of rotation of the gyroassembly. The damping moment is provided by friction of the cylindrical surface of the gyroassembly shell against the thin film of viscous liquid in the narrow gap between the cylindrical surfaces of the gyroassembly shell and the instrument housing. Dry friction is completely eliminated by this damping principle. Since disturbing forces of all kinds are generally transmitted from the instrument housing to the gyroassembly through the viscous liquid and not through the bearings, the floating gyroscope possesses, in addition to negligibly small friction in the gyroscope-frame supports, great stability against shock and vibration which, far from damaging it during operation, do not even cause any noticeable deterioration in the quality of its performance.

The design of a floating integrating gyroscope developed, constructed, and tested in the instrument laboratory of the Massachusetts Institute of Technology is presented in Fig. 2.2. The mechanical construction of this instrument is similar to that shown in Fig. 1.18, and consists of the same components as those required for operation of an integrating gyroscope. The x , y , z , and z_0 axes of Fig. 2.2 have the same significance as in Fig. 1.18. The rotor 8 of the gyroscope

is carried in the frame 9. The frame with the rotor and gyromotor stator 12 are enclosed in a hermetic, perfectly cylindrical shell 7 to form a unit to which we shall refer henceforth as the floating gyroassembly. The latter is mounted in the bearings 4, which are located in the hermetic housing 1 of the instrument in a manner which permits it to rotate about the x-axis with respect to the housing. Along the section AB, which covers the floating gyroassembly, the housing 1 is

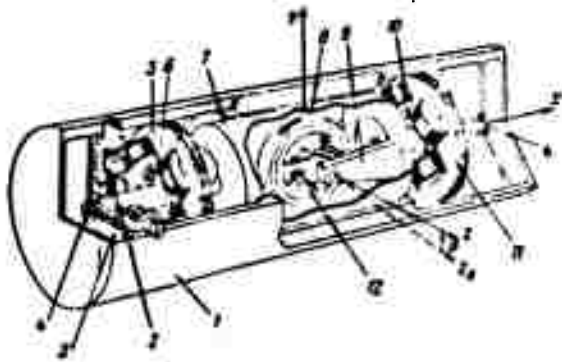


Fig. 2.2. Simplified drawing showing design of floating integrating gyroscope:

- 1) housing; 2) balancer nuts; 3) yokes; 4) gyroscope frame supports; 5) stator of microsyn output-signal detector (pickoff); 6) rotor of microsyn output-signal detector; 7) shell; 8) gyroscope rotor; 9) yoke (gyroscope frame); 10) rotor of microsyn corrector (torquer); 11) stator of microsyn corrector; 12) gyromotor stator.

perfectly cylindrical in form. There is a small uniform gap (of the order of 0.2 mm) in this section between the surface of the floating gyroassembly shell and the inner surface of the instrument housing. The entire unoccupied space inside the instrument housing is filled with a liquid having a high specific gravity. This liquid serves to relieve the bearings of the floating gyroassembly, protect them from shock and vibration, and generate a damping moment. The outer surface of the shell 7 (in the section AB), the inner surface of the housing 1, and the liquid in the gap between them perform the functions of a damper. The liquid and the clearance between the floating gyroassembly shell and the instrument housing are chosen

so that the damping moment will be strictly proportional to the velocity of rotation of the floating gyroassembly, i.e., so that there will be friction proportional to the first power of this velocity, at all operationally possible velocities of rotation of the floating gyroassembly with respect to the instrument housing. Under operational conditions, the entire instrument is placed in a chamber in which the temperature is automatically maintained constant. Automatic regulation of temperature is necessary for the following reasons:

1) the specific gravity of the filler liquid is determined by temperature. By suitable adjustment of the temperature, the specific gravity of the liquid can be made approximately equal to the mean specific gravity of the floating gyroassembly. When this condition is met, the effective load on the bearings of the gyroassembly can be reduced to a very small value. Maintenance of the liquid at the proper specific gravity is the chief purpose of temperature regulation;

2) temperature determines the viscosity of the liquid and the value of the specific damping moment. But since floating integrating gyroscopes are employed in practice in conjunction with servodrives, variation in the specific damping moment, as a rule, only affects the dynamic characteristics of the system;

3) a change in the temperature of the liquid produces changes in the positions of the center of gravity of the floating gyroassembly and the center of pressure with respect to its axis of rotation, which may lead to increased imbalance of the floating gyroassembly and the action of transfer accelerations on the instrument.

It should be noted that, as a rule, the problem of the regulation of temperature and specific gravity is always more complicated than elimination of the difficulties which arise as a result of variation in viscosity.

The virtually complete relief of the bearings permits the use of jewelled instead of ball bearings and reduction of the frictional moment to a negligibly small and stable value, and also enables the position of the x axis with

respect to the instrument housing to remain invariable for practical purposes. Immersion of the gyroassembly in liquid ensures great strength and stability in withstanding shock and vibration without damage, and prevents almost all disturbance of its characteristics at moments when disturbing forces act upon it. It is possible to obtain very high performance levels in a floating integrating gyroscope over a wide range of input angular velocities by appropriate selection of the design of the floating gyroassembly, the instrument housing and the liquid.

The floating gyroassembly is carefully balanced to bring its center of gravity into coincidence with the center of pressure and reduce its buoyancy to zero. Thus a floating gyroassembly immersed in liquid of the required specific gravity and warmed to operating temperature should possess zero buoyancy, be free of x -axis trim, and be in equilibrium with respect to this axis. The elimination of trim and reduction of buoyancy to zero are most efficiently accomplished by means of weights attached to the x axis at either end of the floating gyroassembly (these weights are not indicated in Fig. 2.2). Equilibrium relative to the x axis is established by means of the four nuts 2, which are screwed onto four mutually perpendicular threaded rods attached to the shaft of the floating gyroassembly. One pair of rods is directed parallel to the spin axis z , and the other perpendicular to it. Only two of the rod-and-nut devices appear in Fig. 2.2; the other pair is omitted from the illustration. The floating gyroassembly is balanced prior to installation in the instrument housing. The final balancing operation about the x axis is carried out with the instrument completely assembled, i.e., after its housing has been filled with liquid and hermetically sealed. This should be done under the operating conditions of the instrument. This balancing operation is accomplished by adjusting the same nuts 2. The nuts are turned by means of the yokes 3 which grip them across their flats. The yoke heads extend hermetically out through the housing and are provided with screwdriver slots.

The final balancing about the x axis makes it possible to reduce the

systematic disturbing moments which act on the floating gyroassembly about this axis to a minimum. It was noted above that the entire device is installed in a chamber provided with automatic temperature regulation. The need for automatic maintenance of a constant temperature will become clear when it is remembered that the gyromotor enclosed in the shell continually generates heat in significant quantities while the conditions for loss of heat to the surrounding space may vary considerably. Without positive automatic temperature regulation, therefore, the



Fig. 2.3. External view of microsyn:
1) laminated stator; 2) rotor; 3) stator shaft; 4) wound spools mounted on stator poles; 5) effective air gap.

floating integrating gyroscope could not generally operate with the very high precision required of it. The time required to bring the instrument to the proper operating state is determined by the time needed to establish the necessary stable temperature regime. In designing a

floating integrating gyroscope, therefore, careful attention should be devoted to those of its parameters which charac-

terize it as an object of temperature control. Devices known as microsyns are used in the present instrument (see Fig. 2.2) as the output-signal detector (pickoff) and the corrector (torquer). Their rotors 10 (pickoff) and 6 (torquer) are rigidly fitted to the axle of the floating gyroassembly, while the corresponding stators 11 and 5 are attached to the instrument housing. The two rotors are identical. The laminated stator blocks are also identical. The microsyn is shown separately in Fig. 2.3.

Let us consider, in general terms, the operating principle and design of the microsyns.

The design of the microsyn pickoff and the microsyn torquer is identical; the difference between them consists solely in the purposes for which they are used.

The microsyn pickoff operates on alternating current only, while the microsyn torquer works on both alternating and direct current. The stator 1 of the microsyn (Fig. 2.4) takes the form of a symmetrical, four-pole magnetic circuit and is built up from individual laminae of a ferromagnetic material characterized by the smallest possible hysteresis. The rotor 2 is a two-pole design with 90° pole arcs, and is also composed of separate laminae of a ferromagnetic material with minimal

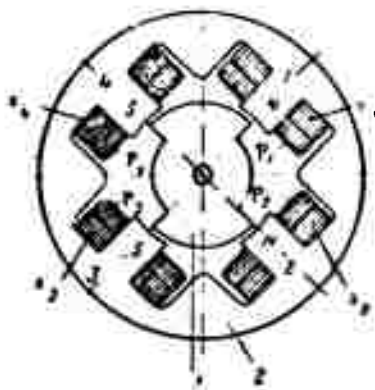


Fig. 2.4. Schematic representation of microsyn:

1) rotor; 2) stator; P_1, P_2, P_3, P_4) coils of primary windings; S_1, S_2, S_3, S_4) coils of secondary winding.

hysteresis. Each pole of the stator carries a primary and a secondary coil. The primary coils are series-connected in the manner shown in Fig. 2.5, and form the excitation winding, which, when supplied with an excitation current of voltage U_{ex} , magnetizes the stator pole as indicated in Fig. 2.4. If the excitation current is a direct current, which it may be in the case of the microsyn torquer, the indicated polarity will remain unchanged. If, however, an alternating current is supplied to the excitation winding, the

polarity of the poles will alternate with the frequency of the alternating current. The secondary coils are also series-connected and form the secondary winding (Fig. 2.5). The coils on opposed (unlike) poles are connected accordingly (coils S_1 and S_3 ; S_2 and S_4). The two pairs of coils produced in this way are counterconnected (Fig. 2.5b). Thus the coils S_1 and S_3 are connected with the coils S_2 and S_4 in such a way that their phases are opposed.

In the starting position, each pole of the rotor overlaps half of each of two unlike poles of the stator (Fig. 2.4). The effective angle of rotation of the rotor is usually small. Thus the total overlap of like poles of the stator

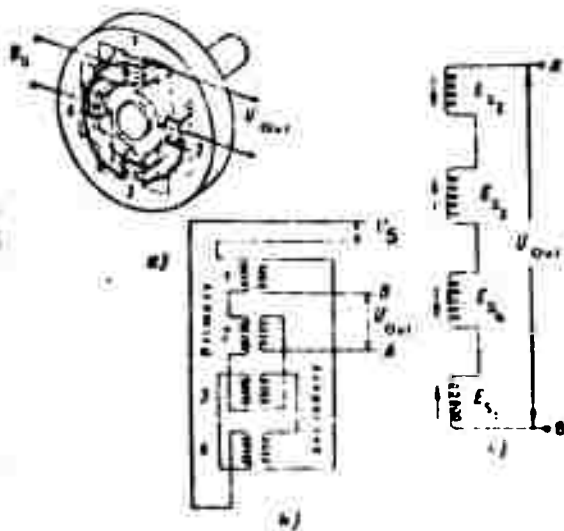


Fig. 2.5. Diagram of microsyn windings: a) disposition of windings in stator; b) relative positions of primary and secondary windings; c) directions of currents induced in secondary coils S_1 , S_2 , S_3 , and S_4 in one half-period.

by the rotor remains the same.

Let us examine the operation of a microsyn as an output-signal detector. In this case it functions as an inductive pickoff acting on the principle of the differential transformer. The job of the microsyn pickoff is to deliver at its secondary-winding output a voltage U_{out} proportional to the angle of deflection β of the rotor from its original posi-

tion ($\beta = 0$), which corresponds to the zero value of U_{out} . The phase of this voltage is determined by the direction

in which the rotor is deflected. With

the rotor in its starting position, the flux created by the coils of the primary winding induce an identical emf in each pair of opposed secondary-winding coils, due to the perfect symmetry of the system in this position (See Fig. 2.4). Since the coils S_1 and S_3 are phase-opposed to the coils S_2 and S_4 (Fig. 2.5b and c), the resulting voltage U_{out} at the secondary-winding output will be zero in the case under examination. For the sake of clarity, the directions of the currents in the secondary-winding coils during one half-period are indicated by arrows in Fig. 2.5c. If the rotor is now deflected from its original position through a certain angle, let us say in a counterclockwise direction, the amount by which it overlaps the poles 2 and 4 will increase, while the overlap of poles 1 and 3 will decrease (see Fig. 2.4). This will result in redistribution of the flux created by the primary-winding coils, so that the emf's E_{S_2} and E_{S_4} induced in the coils S_2 and S_4 become larger and the emf's E_{S_1} and E_{S_3} induced in the coils S_1 and S_3 smaller by comparison with the values for the original position. A voltage U_{out} having

the phase of the emf induced in the coils S_2 and S_4 (see Fig. 2.5c) will therefore appear at the secondary-winding output. The amplitude of this voltage will be proportional to the angle of deflection θ of the rotor from its starting position.

Upon deflection of the rotor from its starting position through an identical but oppositely-directed angle, the phase of the voltage U_{out} will be reversed, but its amplitude will remain the same.

We have stated that U_{out} will be proportional to the angle of rotation θ of the rotor with respect to the stator. This will apply, however, only in cases where the total flux created upon rotation of the rotor by the primary coils remains constant, and its redistribution among the poles of the stator, which serve as the cores of the coils, proceeds in strict proportion to the angle of rotation of the rotor from its center position. The extent to which this requirement is fulfilled will depend on the precision with which the geometrical shape and dimensions of the rotor and stator are maintained, the precision with which the proper air gap is maintained between the poles of the rotor and stator, the degree of uniformity achieved in the magnetic properties of the laminated rotor and stator blocks, and the precision with which the windings are fabricated. It is perfectly obvious that the larger the effective angle of rotation of the rotor, the more difficult it will be to keep this angle proportional to the voltage U_{out} . Hence the working angle must be kept small. Moreover, a microsyn pickoff whose parameters have been suitably chosen and which has been carefully made, assembled, and regulated is virtually inertialess at small working angles. The resultant force attracting the rotor to the poles of the stator is also practically zero under these conditions. These last characteristics of the microsyn are highly important since they make it possible to obtain an output signal with the exertion of practically no reactive force on the gyroscope.

One of the principal advantages of the microsyn pickoff over the potentiometer

pickoff is the fact that it does not make use of sliding contacts. In addition, the sensitivity threshold of a wire potentiometer is limited by the diameter of the wire, while in the microsyn it is virtually zero ($1/600^\circ$, which, for a rotor approximately 1.3 mm in diameter, corresponds to a 0.26- μ linear displacement of the rotor pole relative to the stator pole). Thus in all instances where the angle to be measured is small, the microsyn possesses considerable advantages over the potentiometer. In this connection, however, we should not overlook the weight of the microsyn rotor, which is, of course, considerably greater than that of the potentiometer wiper. This fact does not apply to the floating gyroscope.

Although in practice microsyn pickoffs are made in a variety of sizes, the outer diameter seldom exceeds 51 mm. In certain cases in which the dimensions must be kept to a minimum, microsyns are made with outer diameters of approximately 19 mm. The typical microsyn pickoff has an outer diameter of approximately 38 mm, weighs about 57 g and displaces a volume of about 16.4 cm³. For excitation by a current of 50 ma and 400 cps, the amplification factor (sensitivity) of a microsyn pickoff of this kind will be

$$K_{\beta, U_{out}} = \frac{U_{out}}{\beta} = 12 \text{ mv/mrad}$$

for a range of rotor angles of rotation $\beta = \pm 10^\circ$.

Let us turn now to consideration of the operation of the microsyn as a corrector. In this case it must develop a moment proportional to the value of the control current I_{con} delivered to the input of its secondary winding. The direction of the moment must be determined by the phase or polarity of the voltage U_{con} impressed on the secondary winding. In addition, the magnitude of this moment should not depend in practice on the angle of deflection of the rotor from its starting position, even at small values of this angle.

Suppose that the rotor is in its starting position. Let us apply to the secondary-winding input a corrective voltage U_{con} whose polarity (if the microsyn torquer is fed with direct current) or phase (if the microsyn torquer is fed with alternating current) is such that the secondary coils S_2 and S_4 generate fluxes coincident in direction with the fluxes from the primary coils P_2 and P_4 , thereby amplifying the fluxes of poles 2 and 4. Here the fluxes of coils S_1 and S_3 will be opposed to those of coils P_1 and P_3 , and will weaken the latter accordingly. The result is the appearance of a moment which tends to turn the rotor in the direction of increasing magnetic field strength, i.e., to the left. The magnitude of this moment will be proportional to the product of the currents I_{ex} and I_{con} supplying the primary (excitation) and secondary windings. Since I_{ex} is constant, the rotor moment will be proportional only to the value of the current I_{con} fed to the secondary winding.

If the phase (or polarity) of U_{con} is now reversed, the fields of poles 1 and 3 will become stronger while those of poles 2 and 4 will be weakened; this results in a change of sign in the rotor moment. It is noted that some hysteresis appears when the microsyn torquer is fed with direct current. This, however, may be eliminated readily by the use of high-frequency alternating current.

When the primary winding of a microsyn torquer is fed with either alternating or direct current and no current flows in the secondary winding, the effects exerted by the poles 1,4 and 2,3 on the rotor, under ideal conditions, will cancel each other out. Consequently, the rotor moment in the absence of a current I_{con} will be zero.

In conclusion, it is again noted that the microsyn will function satisfactorily only if it is constructed and regulated with extreme care. In the floating gyroscope, as will be seen from Fig. 2.2, the microsyn is immersed in liquid.

Any working design for a floating integrating gyroscope must include a number of components which have been omitted from Fig. 2.2 for the sake of simplicity.

For example, the drawing does not indicate the leads which provide the gyromotor with current from an external source. It is highly important that these current leads be practically inertialess, i.e., that they apply only a negligibly small moment to the floating gyroassembly. This requirement is satisfied by the use of thin band-type leads of high-grade material which are semicircular or spiral in shape in the unstressed state. One end of the lead is fixed to the housing and the other to a component of the mechanism which communicates with the floating gyroassembly. After installation, the lead remains in the unstressed state when

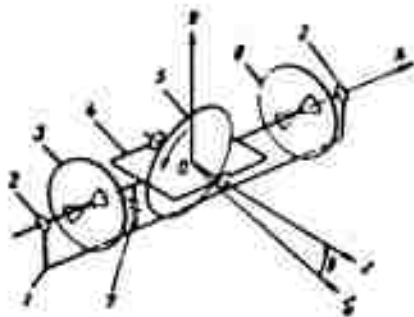


Fig. 2.6. Schematic drawing showing principle of floating integrating gyroscope: 1) instrument housing; 2) bearings of floating gyroassembly; 3) microsyn output-signal detector (pickoff); 4) gyroscope frame; 5) gyroscope rotor; 6) microsyn corrector (torquer); 7) liquid damper; y) input (measurement) axis of instrument; x) output axis; z) spin axis of gyroscope; z_0) initial position of spin axis z ; the axes $Oxyz_0$ are attached to the instrument housing.

position of the spin axis z . In the drawing in Fig. 2.6, the microsyn stators are represented by discs, and the rotors in the form of pairs of triangular petals which represent the two poles of each rotor. We shall use this scheme from now on to represent the floating integrating gyroscope.

An axonometric projection of the Type 10⁴ floating integrating gyroscope

the spin axis of the gyroscope occupies its starting position. Since the floating gyroassembly turns through small angles when the instrument is in operation, the moment which such a current lead applies to it will be negligibly small.

A schematic representation of the principle of the floating integrating gyroscope under discussion is shown in Fig. 2.6. As before, the axes $Oxyz_0$ are attached to the instrument housing. The z axis is the gyroscope spin axis; the y axis is the measurement (input) axis of the instrument; the x axis is its output axis, and the z_0 axis defines the initial

under consideration appears in Fig. 2.7. Type designation is based on the value of the angular momentum \underline{H} of the gyroscope expressed in cgs units. "Type 10^4 " designates a gyroscope for which $\underline{H} = 10^4 \text{ gm} \cdot \text{cm}^2 \cdot \text{sec}^{-1} = 10.2 \text{ gf-cm-sec.}$

The functions of the basic design components of this gyroscope will be readily understood on comparison of Figs. 2.7 and 2.2. Therefore, we shall merely concern ourselves with certain details of the instrument's construction.

The instrument housing may be disassembled and consists of a central section 6, two lateral sections 2 and 10 and a cover 11, which are joined hermetically to one another by means of the bolts 15. The gyromotor is mounted in the yoke 19 (in Fig. 2.2, this is keyed with the number 9). The rotor of the microsyn pickoff is installed to the left of the floating gyroassembly 17, and the torquer rotor to the right of it. The microsyn stators 19 and 16 are attached by the screws 9 to thin-walled ring-shaped components with the flanges 5 and 7, respectively. The flanges are apparently gripped between the components 3 and 6 and 6 and 10 of the instrument housing. The spaces 3 and 7 probably serve to permit adjustment of the positions of the microsyn stators with respect to their rotors. If this is the case, there should be four such spaces located at 90° intervals around each stator. The position of the stator would be adjusted by exerting pressure through these spaces to shift the stator in the desired direction. Whether or not the stator is in the correct position may be judged from the output signal of the microsyn pickoff. The plate 4 appears to be a screen intended to shield the microsyn pickoff from disturbances arising in the gyrometer during its operation. Current is supplied by the gyromotor by means of the band-type leads 12 (of which there should be three) installed in component 13. The compensating-membrane chamber 14, which communicates with the internal cavity of the instrument housing, is installed in the cover 11. The liquid in this chamber serves to compensate variations in the volume of the liquid contained in the instrument housing caused by changes in its temperature. The angle of rotation of the

floating gyroassembly relative to the instrument housing is limited to $\pm 5^\circ$ by a stop pin secured on the right in the central section 6 of the instrument housing. All of the electrical inputs and outputs of the instrument are by way of the contact pins 1 located in the base of the device.

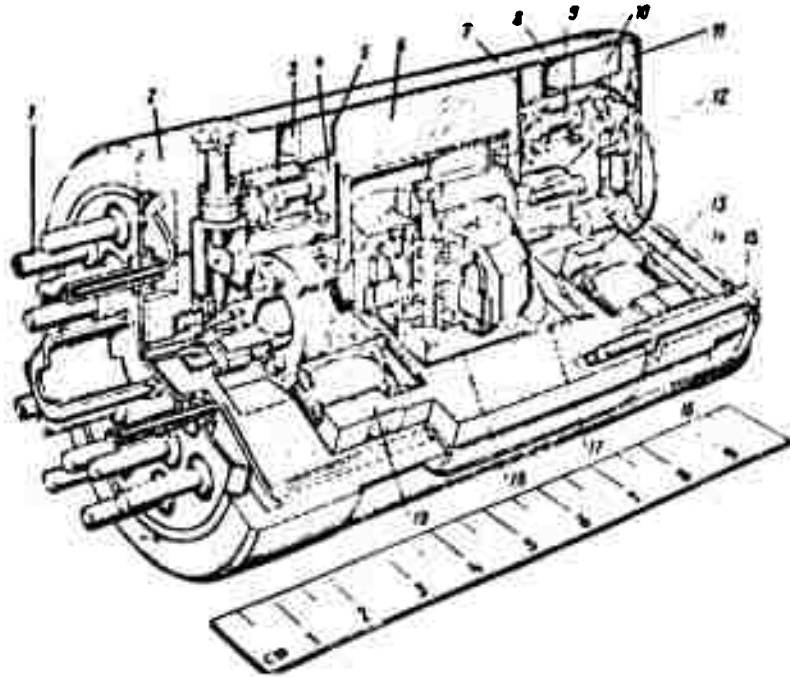


Fig. 2.7. Design of Type 10^4 floating integrating gyroscope:

1) pins for current-supply leads and output-signal pickup; 2, 6, 10) components forming instrument housing; 3, 8) spaces for adjustment of microsyn stator positions; 4) screen; 5, 7) flanges for attachment of microsyn stators to instrument housing; 9) bolts attaching microsyn stators to flanges 5, 7; 11) cover; 12) band-type lead; 13) disc carrying supply leads; 14) membrane chamber; 15) assembly screws for housing components; 16) stator of microsyn torquer; 17) floating gyroassembly; 18) yoke (gyroscope frame); 19) stator of microsyn pickoff.

A conjectural section through the gyromotor is shown in Fig. 2.8b.

The MIT-Type 10^4 floating integrating gyroscope No. 79 has the following characteristics (Tables 1 and 2):

Table 1. Values Determined Prior to Final Assembly of Device

No.	Designation	Symbol	Dimensions	Theoretical Value	Measured Value
1	Weight of gyroscope rotor	-	gf	11.79	11.81
2	Axial moment of inertia of gyroscope rotor	\underline{C}	gf-cm-sec ²	0.0122	0.0122
3	Proper-rotational velocity of rotor for 400-cycle feed current	Ω	rpm	8000	8000
4	Angular momentum of gyroscope	\underline{H}	gf-cm-sec	10.19	10.22
5	Weight of floating gyro-assembly	-	gf	53.5	53.6
6	Moment of inertia of floating gyroassembly with respect to its \underline{x} -axis of rotation	\underline{J}	gf-cm-sec ²	0.036	0.038
7	Maximal angle of rotation of floating gyro-assembly from its initial position with respect to instrument housing (as permitted by stops)	δ_{\max}	degrees	$\pm 5 \pm 0.5$	± 5.6
8	Radial clearance of damper	δ	mm	0.254	0.246
9	Specific gravity of fluid	γ_{fl}	gf/cm ³	$1.93 \pm 1\%$	1.928
10	Viscosity of fluid at 71.1° C	η	centipoises	$650 \pm 5\%$	687
11	Specific damping moment	$\frac{K}{\beta M_{dp}}$	$\frac{\text{gf-cm}}{\text{rad/sec}}$ $\frac{\text{gf-cm}}{\text{c/min}}$	20.39 $5.92 \cdot 10^{-3}$	22.12 $6.43 \cdot 10^{-3}$ (calculated)

Table 1. (continued)					
No.	Designation	Symbol	Dimensions	Theoretical Value	Measured Value
12	Microsyn-torquer moment M_t obtained when primary and secondary windings are supplied with currents I_{ex} and I_{con} whose products $I_{ex} \cdot I_{con} = 1 \text{ ma}^2$	C_t	gf-cm/ma ²	$4.08 \cdot 10^{-4}$	$4.14 \cdot 10^{-4}$
13	Sensitivity of microsyn pickoff for excitation current of 125 ma, 400 cps	$K_{\beta} U_{out}$	mv/mrad	21.0	20.0
			volts/degree	0.366	0.349
			volts/degree	0.366	0.349
14	Ratio of output voltage U_{out} of microsyn pickoff to product $I'_{ex} \frac{f}{P} \beta (I'_{ex}$ and $\frac{f}{P}$ are the magnitude and frequency of the excitation current, and β is the angle of rotation of the floating gyroassembly)	C_P	mv/ma·cps·rad	0.42	0.40
			mv/ma·cps·deg	$7.33 \cdot 10^{-3}$	$6.98 \cdot 10^{-3}$

Table 2. Values Determined after complete Assembly of Device

No.	Designation	Symbol	Dimensions	Theoretical Value	Measured Value
1	Phase voltage of gyromotor supply	U_{ph}	volts	8.0 ± 1	7.5
2	Frequency of gyromotor current supply	f_{gyr}	cps	400 ± 0.4	400 ± 0.04
3	Phase current of gyromotor	I_{ph}	a	0.3	0.2
4	Temperature in damper gap	t	°C	71.1 ± 1.1	71.1
5	Zero-point output signal of microsyn pickoff (signal delivered by device at zero input angular velocity ω and torquer control current I_{con} (spurious signal due to interference harmonics))		mv	< 5 (root-mean-square)	1.9

Table 2. (continued)

No.	Designation	Symbol	Dimensions	Theoretical Value	Measured Value
6	Drift velocity due to imbalance of floating gyro-assembly		rad/sec °/min	10^{-4} 0.344	$0.3 \cdot 10^{-4}$ 0.103
7	Drift velocity due to moments which cannot be taken into account due to their random nature		rad/sec °/min	$< 5 \cdot 10^{-5}$ < 0.172	10^{-5} 0.034
8	Smallest detectable velocity of rotation of device about measurement axis y	ω_{\min}	rad/sec °/min	$< 5 \cdot 10^{-5}$ < 0.172	See Ch. V
9	Largest value of measured input angular velocity	ω_{\max}	rad/sec rpm	> 4.5 > 42	See Ch. V
10	Time constant	T	sec	0.0017	0.0027
11	Ratio of angular velocity $\dot{\beta}$ of floating gyroassembly to input angular velocity ω	$\frac{K}{\omega, \dot{\beta}}$	rad/sec rad/sec	0.5	0.47 (calculated)
12	Ratio of angular velocity $\dot{\beta}$ of floating gyro-assembly to product of currents I_{ex} and I_{con} applied to primary and secondary windings of microsyn torquer	$\frac{K}{I_{\text{ex}} I_{\text{con}}}, \dot{\beta}$	$\frac{\text{rad/sec}}{\text{ma}^2}$ $\frac{\text{°/min}}{\text{ma}^2}$	$2 \cdot 10^{-5}$ 0.115	$1.9 \cdot 10^{-5}$ 0.109
13	Ratio of angular velocity $\dot{\beta}$ of floating gyro-assembly to angular acceleration $\ddot{\gamma}$ of instrument housing about output axis x	$\frac{K}{\ddot{\gamma}, \dot{\beta}} = T$	$\frac{\text{rad/sec}}{\text{rad/sec}^2}$	0.0017	0.0027
14	Ratio of angular velocity ω to which (velocity) application to currents I_{ex} and I_{con} to primary and secondary windings of microsyn torquer is equivalent (in its effect on the floating gyro-assembly), to the product of these currents	$\frac{K}{I_{\text{ex}} I_{\text{con}}}, \omega = \frac{K}{\omega, \dot{\beta}}$	$\frac{\text{rad/sec}}{\text{ma}^2}$ $\frac{\text{°/min}}{\text{ma}^2}$	$4 \cdot 10^{-5}$ 0.229	$4.09 \cdot 10^{-5}$ 0.234

Table 2.(continued)

No.	Designation	Symbol	Dimensions	Theoretical Value	Measured Value
15	Ratio of angular velocity ω to which (velocity) rotation of instrument housing about its output axis x with an acceleration \ddot{y} is equivalent (in its effect on the instrument), to this acceleration	$\frac{k_{\ddot{y}}}{K_{\omega, \beta}} = \frac{T}{K_{\omega, \beta}}$	$\frac{\text{rad/sec}}{\text{rad/sec}^2}$	0.0035	0.0057
16	Ratio of rate of change \dot{U}_{out} of microsyn-pick-off output voltage to input angular velocity ω	$K_{\omega} \dot{U}_{\text{out}}$	$\frac{\text{volts/sec}}{\text{rad/sec}}$ $\frac{\text{mv/sec}}{\text{°/min}}$	10.5 3.053	10.05 2.922
17	Ratio of rate of change \dot{U}_{out} of microsyn-pick-off output voltage resulting from delivery of currents I_{ex} and I_{con} to primary and secondary windings of microsyn torquer to the product of these currents	$\frac{K_{I_{\text{ex}} I_{\text{con}}}}{\dot{U}_{\text{out}}}$	$\frac{\text{mv/sec}}{\text{ma}}$	0.4	0.406

It is seen from Tables 1 and 2 that the weight of the floating integrating gyroscope rotor is very small (~ 12 gf) and that it has a small specific moment of inertia (~ 0.012 gf-cm-sec²). By way of comparison, we might note that the cards of fluid-filled magnetic compasses (types A-4, KI-11, etc.) have approximately the same weight and moment of inertia. At the same time the proper-rotational velocity of the rotor is comparatively rather small at 8000 rpm. It will also be seen from Tables 1 and 2 that the angular momentum of the floating gyroscope is relatively small (~ 10.2 gf-cm-sec). The total weight of the entire floating gyroassembly, 53.6 gf, is quite typical. All this gives some idea of the very small dimensions of the device itself and the high technical requirements

inevitably involved in the manufacture, assembly, regulation and testing of the floating gyroscope.

The device operates at small angles of deflection of the floating gyro-assembly from its original position, since the working angles must be smaller than the angles of rotation permitted by the stops, $\pm 5^\circ \pm 0.5^\circ$. This ensures virtual linearity of both gyroscopic moment and output voltage as functions of the angle of deflection. The operating temperature of the instrument is 71.1°C . This is because the fluid used (more exactly, the medium used to fill the instrument) is too viscous or completely solidifies at normal temperatures, and only acquires the required viscosity at this temperature.

The drift velocities due to imbalance of the floating gyroassembly ($\sim 0.103^\circ/\text{min}$) and to moments of an accidental nature ($\sim 0.034^\circ/\text{min}$) are worth noting. This drift attests to the great difficulty encountered in balancing and regulating the device. It is highly important for the drift velocity to remain constant in magnitude and direction. It can then be reduced with relative ease by supplying the corrector with the appropriate constant current I_{con} .

The time constant of the instrument under consideration is only 0.0027 sec (calculated value 0.0017 sec), a figure which indicates the rapidity with which transient processes run their course.

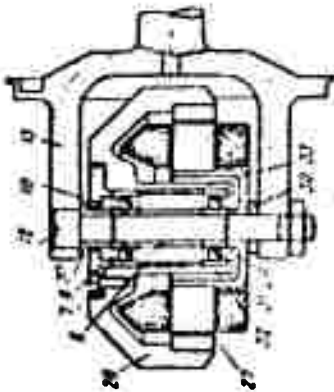
The instrument was designed to detect angular velocities beginning with $5 \cdot 10^{-5} \text{ rad/sec}$ ($0.172^\circ/\text{min}$), or a velocity smaller by a factor of 1.46 than that of the earth's diurnal rotation. In other words, it has to sense an angular velocity approximately equal to one revolution per thirty-six hours. The tests showed that the instrument was able to detect a considerably smaller angular velocity. At the same time it has to be able to measure angular velocities higher than 4.5 rad/sec , i.e., more than 42 rpm. Hence, the theoretical ratio between the maximum ω_{max} and minimum ω_{min} values of the measured angular velocity is $9 \cdot 10^4$. Since the actual value of ω_{min} is less than the theoretical value,

the effective value of the ratio is even greater. It should be pointed out that ω_{\min} is dependent upon both the moment of friction in the supports of the floating gyroassembly and the level of electrical interference which disturbs the correct functioning of the instrument.

Let us consider some of the industrial models of the floating integrating gyroscope made in America, known by the abbreviation HIG (Hermetic Integrating Gyroscope). A figure is usually added to these letters to indicate the power to which the number 10 must be raised to obtain the angular momentum of the gyroscope \underline{H} in cgs units, i.e., in $\text{g-cm}^2 - \text{sec}^{-1}$; for example HIG-3 ($\underline{H} = 10^3 \text{ g-cm}^2 - \text{sec}^{-1}$), HIG-6 ($\underline{H} = 10^6 \text{ g-cm}^2 - \text{sec}^{-1}$), and so on.

Figure 2.8 shows the main features of the design of the HIG-4 made by the Minneapolis-Honeywell firm. Some of the parts may not be reproduced exactly. Basically, the instrument is similar to the one considered earlier, depicted in Fig. 2.7. The floating gyroassembly consists of a hermetically-sealed shell containing an asynchronous gyromotor. The shell is made from two sections 11 and 14, and from the kinematic point of view constitutes the gyroscope frame. The sections 11 and 14 are connected respectively to the shafts 34 and 23 which lie along the geometrical axis of the cylindrical shell, which is the x axis of rotation of the floating gyroassembly. The ends of the shafts are fitted with journals which insert into jewelled socket-bearings attached to the walls of the housing 6 (as in Fig. 2.7, the housing is sectional). There should be jewelled disc bearings behind the sockets to receive axial loads.

The gyromotor, like the one shown in Fig. 2.8b, is mounted on an immovable axle 12 between the brackets 13 and 28 of the unit 14. The axle 12 passes through openings in the brackets 13 and 28, the upper part of it being held by bracket 13. The lower end of the axle 12 is threaded and the nut holding the axle in place is screwed onto it (this is not visible in Fig. 2.8). The parts attached to the axle 12 are the plate 30, the socket 31, to which is fixed the



1) yoke; 2) balancer nuts; 3) winding of microsyn pickoff stator; 4) head of balancer yoke; 5) laminated stator of microsyn pickoff; 6) housing (sectional, as in Fig. 2.7); 7) screw; 8) spacer; 9) cap; 10) rotor bearing; 11) cylindrical section of shell of floating gyroassembly; 12) rotor axle; 13) bracket; 14) cover for shell containing of brackets 13 & 28; 15) stop; 16) winding of microsyn-torquer stator; 17) laminated stator of microsyn-torquer; 18) rotor of torquer; 19) leads; 20) hollow center of membrane chamber; 21) membrane chamber; 22) clamping screw; 23) shaft of unit 14; 24) casing; 25) heating element; 26) gyroscope rotor; 27) gyromotor stator; 28) bracket; 29) rotor bearing; 30) plate; 31) socket; 32) rotor socket; 33) spacer; 34) shaft of unit 11; 35) balancer rod; 36) microsyn-pickoff rotor; 37) socket.

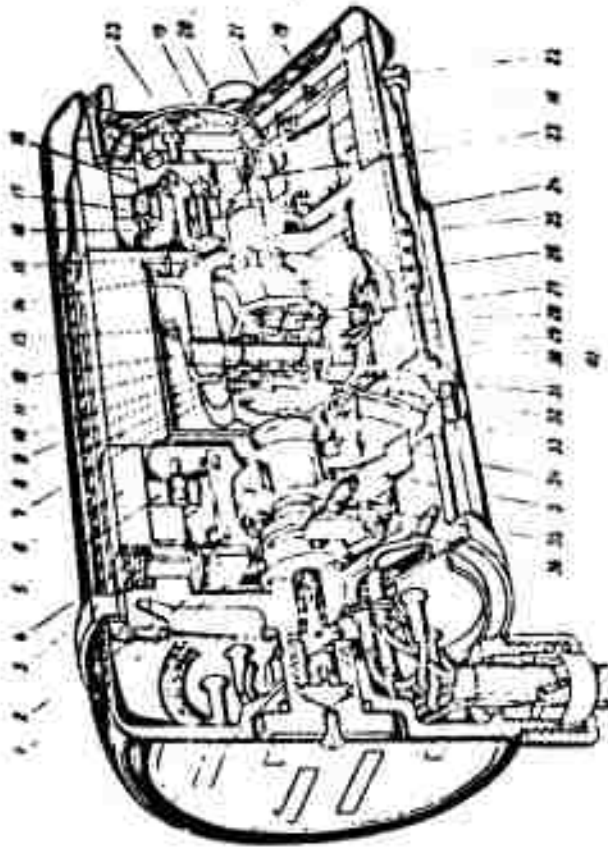


Fig. 2.8. Basic features of design of HIC-4 floating integrating gyroscope.

gyromotor stator 27, and the inner rings of the magnetic-type bearings 10 and 29 of the gyromotor rotor with the spacer 8 between them. The inner ring of bearing 10 bears on the shoulder of the axle 12 while the ring of bearing 29 bears on the end of the stator socket 31. The outer rings of the bearings and the spacer 33 between them are fixed to the socket of the rotor 26; the outer ring of bearing 29 pushes against the shoulder of the rotor socket 32. The outer rings of the bearings in the rotor are kept in place by the cap 9 which is screwed to the gyromotor rotor by the screws 7. The tightness of the bearings is regulated by a nut at the end of the axle 12.

Current is supplied to the floating gyroassembly through band-type leads 19 lying in one plane. The angles of rotation of the gyroassembly are restricted by the stop 15 which is attached to the instrument housing by one end, the other end fitting into an arresting socket in the unit 14.

The rotor 36 of the microsyn-pickoff is attached to the shaft 34, and the rotor 18 of the microsyn-torquer to the shaft 23. The laminated stators 5 and 17 with windings 3 and 16 are fixed to the housing of the instrument. The gyroassembly is balanced by four flat self-braking nuts 2 screwed onto the threaded balancer rods 35. The nuts are turned by means of the yokes 1, the heads 4 of which extend hermetically through the outer surface of the housing.

Variation in the volume of the filler liquid due to temperature change is compensated for by a corrugated membrane chamber 21 communicating with the inside of the housing via the hollow center 20. The sections making up the housing are held together by the screws 22. All joints must be hermetically sealed.

The temperature of the instrument housing is kept constant by an automatic temperature controlling device. This is done by varying the current supplied to the heating element, 25, which is situated on the outside of the housing under the shell 24. The resistance of the temperature sensor is probably located on the housing under the heating element.

Figure 2.9 shows an HIG-5 floating gyroscope made by the same firm, with one section opened. It is similar in design to the HIG-4, but its main difference from the latter and the model shown in Fig. 2.7 is that the gyroscope frame 2 (see Fig. 2.9) is actually a closed frame and not a yoke as in the HIG-4 and the instrument in Fig. 2.7. The face surfaces of the frame take the form of circular disks and are used to secure the cylindrical shell which, together with them, forms a hermetically-sealed float with the gyromotor inside. The disks of the frame have shafts to which are attached the microsyn rotors. The shafts are equipped with journals by means of which the floating gyroassembly is mounted on bearings. At the beginning of 1957 these instruments were being turned out at the rate of 300 a month. The same firm is turning out (at the beginning of 1957 at the rate of 25 a month) an instrument similar in design, the HIG-6, intended for the stabilized platforms of long-range inertial systems. All three types are shown side by side in Fig. 2.10 for comparison of their relative sizes. Each one has its own particular features. The HIG-6 has the lowest threshold of sensitivity and the greatest accuracy.

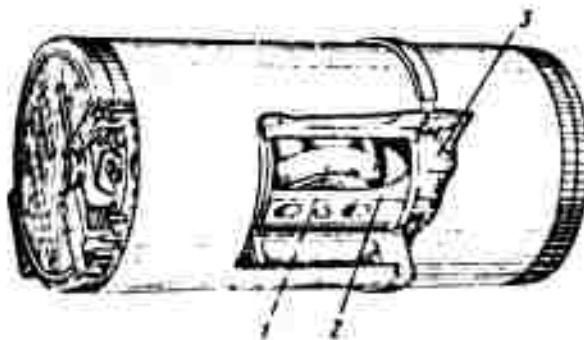


Fig. 2.9. HIG-5 floating integrating gyroscope: 1) gyromotor; 2) gyroscope frame; 3) microsyn rotor.

Figure 2.11 shows an external view of the HIG-4 made by the Greenleaf Company.

Figure 2.12 shows a variation of the floating integrating gyroscope somewhat different in design from those considered above. This instrument has been devel-

oped by Minneapolis-Honeywell. The main feature of its design is replacement of the microsins by a pickoff and torquer of another design; they are both situated at the same end of the instrument. Other differences in construction can easily be seen from a comparison of Figs. 2.12 and 2.8.

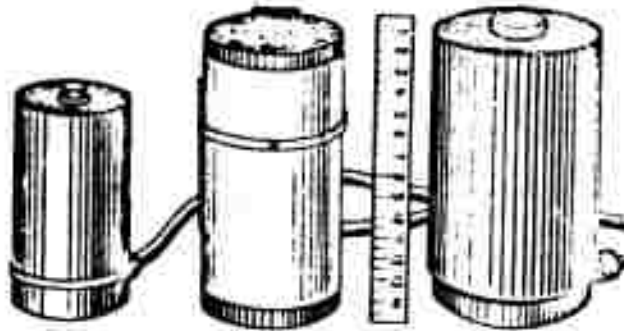


Fig. 2.10. Floating integrating gyroscopes made by Minneapolis-Honeywell: (left to right) the HIG-4, HIG-5 and HIG-6.

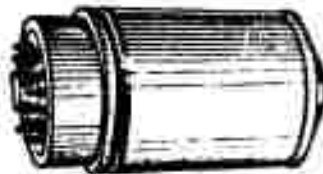


Fig. 2.11. External view of HIG-4 floating integrating gyroscope made by Greenleaf.

Figure 2.13 shows an external view of two floating integrating gyroscopes with angular momentum of $2 \cdot 10^4$ and $6.05 \cdot 10^6 \text{ g}^2\text{-cm-sec}^{-1}$ (20.4 and 6.170 gf-cm-sec) made by the Kearfott firm.

The minimum angular velocities which are detected by these instruments are 4.1 deg/hr and 0.01 deg/hr respectively. The parts are made from materials with practically identical linear temperature coefficients of expansion, which

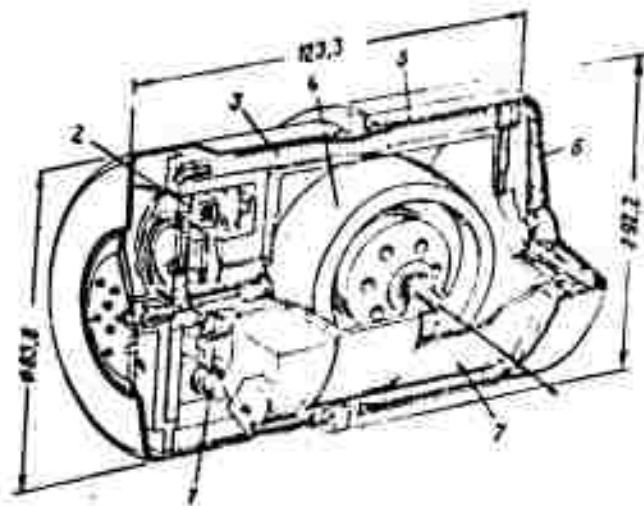


Fig. 2.12. Floating integrating gyroscope:
1) torquer; 2) pickoff; 3) housing; 4) gyroscope
rotor; 5) heating element; 6) compensation-
membrane chamber; 7) floating gyroassembly.

prevents the possibility of the gyroassembly becoming unbalanced over a wide range of variation in the temperature of the surrounding medium. These instruments contain both dc and ac correctors, and also dc linear detectors. Deviation from linearity throughout the working range does not exceed 0.1% in the former and 0.17% in the latter. The time constants T are respectively 0.0025 and 0.0035 sec. The weight of the instruments is 626 gf and 2.95 kgf. In addition, the firm produces instruments with angular momentums of $2.5 \cdot 10^6$ and $12.5 \cdot 10^6$ g-cm²-sec⁻¹ (2,550 and 12,750 gf-cm-sec).

One of the very important uses of floating integrating gyroscopes is in the construction of stabilized platforms. Here the size of the platform is roughly proportional to the cube of the size of the gyroscope. Hence to reduce the size of the platform it is first and foremost necessary to reduce the dimensions of the gyroscope, but without affecting its accuracy.

An example of the design of a miniature floating gyroscope is the MIG

(Miniature Integrating Gyroscope) which was put into production on a small scale (about two per month) by Minneapolis-Honeywell at the beginning of 1957. The instrument is intended for inertial guided missiles of the short-range type, as well as for use in aircraft. The weight of the MIG is about 220 gf, its diameter is 44.5 mm, and its length is 63.5 mm. The angular momentum is $H = 102$ gf-cm-sec and the drift velocity is not more than 0.5 deg/hr. If the instrument is properly regulated when set into operation, the random drift velocity is approximately 0.15 deg/hr.

We should point out that the drift velocity of the MIG is half that of the HIG-5 in which it amounts to 1 deg/hr, although the HIG-5 is six times as heavy and four and a half times greater in volume than the MIG, and also has the same angular momentum. This is because in working out the design of the MIG greater attention was given to achieving stability of dimension under the influence of temperature variation and shock, to reducing the intake so as to reduce such undesirable effects as electromagnetic nonlinearity and asymmetry, and also to eliminating anisoelectricity in order to do away with the vibration and moments caused by it for all practical purposes; the latter constitute one of the main sources of drift.

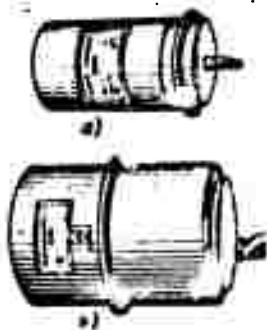


Fig. 2.13. External view of floating integrating gyroscopes made by Kearfott with angular momentum: a) $H = 20.4$ gf-cm-sec, and b) $H = 6170$ gf-cm-sec.

Although the parts of the MIG are small in size, they must nevertheless be manufactured and assembled with an extremely high degree of accuracy. The following facts are indicative in this respect. The diameter of the laminated stator of the gyromotor has to be maintained with an accuracy of up to 7.6μ . Polishing is not permissible since it

causes short-circuiting of the stator plates, which in turn causes magnetic

asymmetry. The journals, which are made from tungsten carbide, and the sapphire bearings of the floating gyroassembly have to be almost ideally cylindrical in shape. Deviations of more than 0.5μ from ideal cylindrical form are not tolerated. The jewel-type bearings used in watches are not satisfactory.

The basic features of the design of the MIG are shown in Figs. 2.14 and 2.15. An external view of the instrument can be seen in Fig. 2.16. Figure 2.15 shows that the float 4, which is made of two sections screwed together, acts directly as the frame of the gyroscope. The 2.5-watt gyromotor is mounted in the left-hand half of the float. The right-hand half is attached after the gyromotor

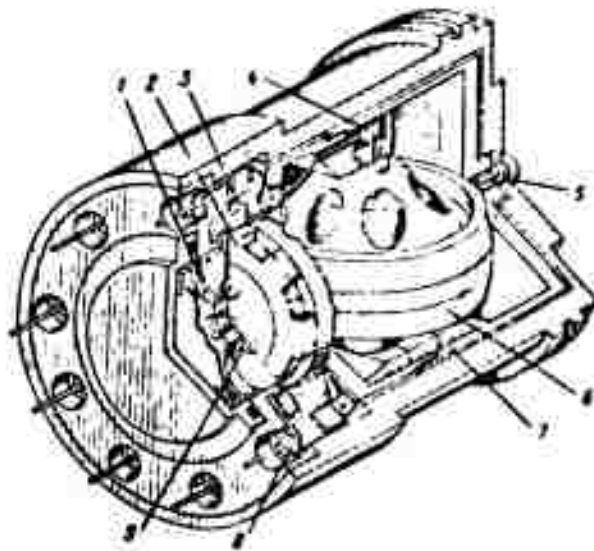


Fig. 2.14. MIG-miniature floating integrating gyroscope (1956):
1) recess for flexible lead; 2) dualsyn rotor; 3) dualsyn stator; 4) gyromotor feed; 5) journal of floating gyroassembly; 6) rotor of gyromotor; 7) floating gyroassembly; 8) and 9) air-tight inlets.

has been completely assembled. The angle of rotation of the floating gyroassembly is $\pm 3^\circ$. The design makes the gyroassembly very convenient to assemble, and at the same time provides great rigidity and practical isotropy of the elastic properties in all planes passing through its rotation axis. At first sight, the design is very simple, but this is not actually so since manufacture of it with the requisite accuracy is extremely complicated from the technological standpoint.

This difficulty, however, is fully compensated for by the advantages of the design when compared with the designs of the gyroassemblies in the instruments we have considered above. The floating gyroassembly has journals made of tungsten carbide 0.46 mm in diameter. They are inserted into jewelled bearings fixed to the instrument housing. The suitable journals and bearings are found by selection. To increase the rigidity of the gyromotor rotor axle, it is made in the form of two cones rigidly attached to the rotor 5. The elastic properties of the design are isotropic for practical purposes. The floating gyroassembly is filled with helium. In the instrument under consideration the microsyn-pickoff and microsyn-torquer are incorporated into one unit called a dualsyn. Thus the dualsyn is both the output-signal detector and the corrector (torque generator). The dualsyn consists of a multipolar rotor 2 (Fig. 2.14) attached to the floating gyroassembly and a corresponding stator 3 attached to the housing. In Fig. 2.15 the stator and

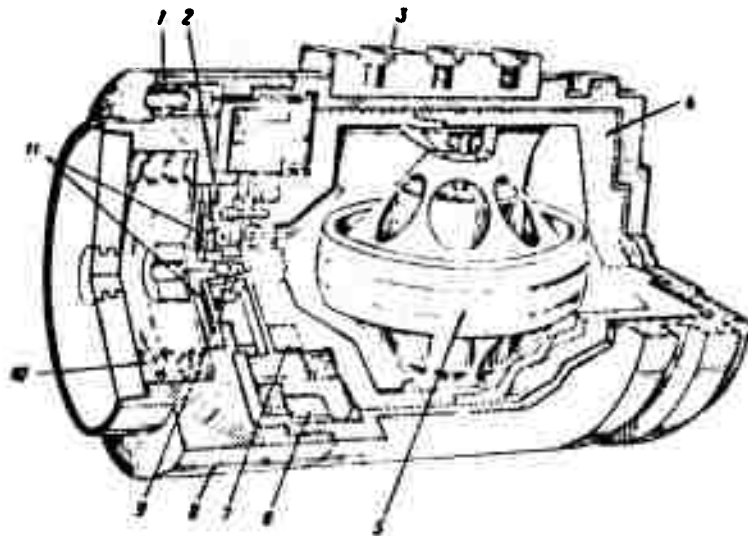


Fig. 2.15. MIG - miniature floating integrating gyroscope (1957): 1) hermetically-sealed inlet; 2) flexible lead; 3) heating and heat-sensitive elements; 4) float (gyroscope frame); 5) gyro-motor rotor; 6) dualsyn stator; 7) dualsyn rotor; 8) instrument housing; 9) jewelled bearing; 10) bellows; 11) flat internal heating element.

the rotor of the dualsyn are marked 6 and 7. The plates of the rotor and stator are made from a ferromagnetic material with strong magnetic properties. The stator

has four windings of 0.11-mm wire, two for the alternating current required by the dualsyn when working as an output signal detector, and two for direct current for when it is working as the corrector. The working principle of the dualsyn is similar to that of the microsyn-detector and microsyn-corrector.

The instrument is filled with "fluorolube" (a fluoro-organic compound) which is solid at normal temperatures. The filling is done in a special way that in effect prevents the formation of air bubbles, which disturb the balance of the gyroassembly. Variation in the volume of the liquid due to temperature is compensated for by the bellows 10.

To maintain the temperature at 82.2°C , the instrument contains the 7-watt internal heating element 11 and heating elements 3 (see Fig. 2.15). The desired temperature is automatically maintained. The resistance of the sensitive element is 980 ohms.

Current is supplied to the gyromotor by the flexible leads 2 (Fig. 2.15) in the recesses 1 (Fig. 2.14). One end is soldered to the element connected to the housing, while the other end is soldered to the hermetically-sealed inlets 9 (see Fig. 2.14) of the floating gyroassembly.

A comparison of the Figs. 2.12, 2.14, and 2.15 makes it clear that the instrument in Fig. 2.12 is the forerunner of the MIG.



Fig. 2.16. External view of the MIG rotor axle (in the form of cylindrical cups, (1957).

In the main it differs from the MIG in the arrangement of the detector and corrector, the elastic compensation chamber (a membrane chamber instead of the bellows in the MIG), the heater and the

cups, whereas in the MIG it consists of

cones). In Fig. 2.12 the pickoff and torquer are at the same end and have moving coils. The fact that they have been replaced by the dualsyn shows the advantages

of the latter in comparison with other arrangements intended for the same purpose.

Besides these instruments, the firm Minneapolis-Honeywell also makes the GG37 floating integrating gyroscope, known as the ISIP (five such instruments were produced at the beginning of 1957). It is designed specially for use in constructing stabilized platforms for long-range inertial systems. Its dimensions are: diameter 83.8 mm, length 116.8 mm, and drift velocity 0.01 deg/hr.

Floating integrating gyroscopes are high-precision instruments. Their accuracy is so great that a comparatively short time ago it was considered that such accuracy could only be achieved in a few individual laboratory models and under laboratory conditions. Many of the parts of the gyroscope have to be made with an accuracy of up to 0.5 microns. A number of complex technological problems had to be solved before it became possible to mass-produce these instruments.

The floating gyroscopes have to be assembled in specially equipped rooms free from practically all dust. The temperature, humidity, and pressure in these rooms must be kept constant. In the Sperry Company's assembly rooms, for example, the air is purified to the extent that no particles of dust larger than 0.3 μ remain. The temperature is kept constant to within half a degree, and the humidity with an accuracy of 5 percent.

The use of paper and pencil in the assembly shops is prohibited so that the air will not be contaminated with fibre particles and graphite dust. All drawings are made on light-sensitive plastic and notes are taken down on sheets of vinyl masticated rubber with ball-point pens. The walls of the rooms are covered with the same material.

Work tools are polished to mirror-like brightness and are cleaned ultrasonically each day. All parts not being used at a given time are kept in plastic bags or under glass covers. Each component part of an instrument goes through a preliminary-treatment section before being taken into assembly. Here, any projecting edges are removed from the parts and they are then electropolished. The

removal of projecting edges is carried out under a microscope with X 45 magnification, with the aid of special instruments similar to those used by dentists.

Before entering the assembly shop the worker has to go through seven special rooms. In the first (outer) sterile room, he washes his hands and face (women are not allowed to use cosmetics). In the second his shoes are thoroughly cleaned. In the third room his clothes are cleaned by a stream of air. In the next room the worker takes off his outer clothing and puts on nylon trousers and a nylon shirt, and over them nylon overalls. On top of his footwear he puts nylon coverings, and on his head a nylon cap. The whole set of nylon clothing is cleaned and sterilized daily. When he has changed his clothes, he enters the fifth room where his clothes are again cleaned in an air-stream. Finally, when he has passed through two more rooms, he reaches the assembly shop.

A serious problem has been the need to build test apparatus with an extremely high degree of accuracy. This can be illustrated by the following instances taken from the experience of Minneapolis-Honeywell. It was mentioned above that the MIG floating gyroassembly is filled with helium. Helium seeping through into the liquid filling the housing of the floating gyroscope creates sudden moments which impair the accuracy of the instrument, since helium bubbles settling on the gyroassembly or on its bearings cause a sudden moment as a result of imbalance, which, in its turn, gives rise to drift. Special mass-spectrometric devices have been constructed to detect the escape of helium and they can measure a leakage rate of 1 cm^3 in 30 years. These instruments are used in the assembly shops.

There are similar devices of still greater sensitivity. One of them, according to available literature, can measure a leak of 1 cm^3 in 3000 years.

Another vital problem is to remove all the air and any other gas from the space to be filled with liquid. The gyroscope is filled in a vacuum. Before the operation, the gyroscope is heated for forty hours to remove the air and other

gases. Warmed "fluorolube" is introduced into the gyroscope in a vacuum. The process of filling takes ten hours. Figure 2.17 shows the work bench at which these operations are carried out. On the left-hand bench the floating gyroassembly is



Fig. 2.17. Photograph of work bench on which the floating gyroassembly is tested for helium leak and the HIG-5 is filled with liquid in a vacuum under glass jars.

being tested for helium leakage with a mass-spectrometer. On the right can be seen two pieces of apparatus for filling the instruments. The gyroscopes are in evacuated glass jars. Two HIG-5 gyroscopes can be seen in each jar. The filling is carried out automatically.

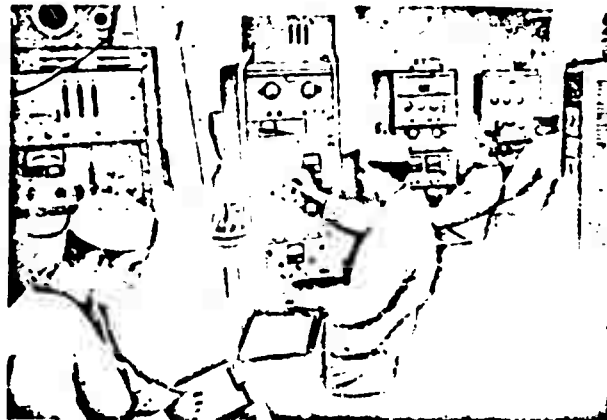


Fig. 2.18. Final adjustment and testing of floating gyroscope:
1) testing stand.

Table 3.

No.	Firm	Type	Angular momentum \bar{M}		Dimensions of housing		Weight kg	no. of phases	Gyromotor		Floating gyroassembly	
			$\text{g} \cdot \text{cm}^2 \cdot \text{sec}^{-1}$	$\text{g} \cdot \text{cm} \cdot \text{sec}$	diam mm	length mm			U, V voltage starting power working power P - 6yr in watts	angle of rotation θ_{\max} in degrees	K, ω , β	constant τ msec
1	Greenleaf	HIG-3	10^3	1.02	25.4	51.6	0.128		$\frac{1}{0.5}$	± 6		
2	Greenleaf	HIG-4	10^4	10.2			0.681	2	12 $\frac{2.2}{1.5}$	± 5		
3	Minneapolis- Honeywell	HIG-4	10^4	10.2	~ 60	101.6	0.681	2	10		1	3.5
4	Kearfott		$2 \cdot 10^4$	20.4	50.8	98.4	0.626					2.5
5	Minneapolis- Honeywell	HIG-5	10^5	102	70	152.4	1.25	3	10	± 6	1	2.8
6	Greenleaf	HIG-5	10^5	102			1.36	3	9.5 $\frac{1}{1.5}$ at $\cos \varphi = 0.35$	± 8	1	2.4
7	Minneapolis- Honeywell	MIG	10^5	102	44.5	63.5	0.220		2.5	± 3		
8	Minneapolis- Honeywell	HIG-6	10^6	1020	~ 85	152.4	2.043	3	115		2.5	3.1
9	Minneapolis- Honeywell	ISTP			83.8	116.8						
10	Kearfott		$6.05 \cdot 10^6$	6170	95.2	155.6	2.95					3.5

*Ratio of rotation velocity of floating gyroassembly β to input angular velocity ω .

**This coefficient is equal to the ratio of the moment created by the microsyn-torquer to the product of the current impressed upon its primary and secondary windings.

*** Approximate value of moment \bar{M}_1 assumed equal to the product $\bar{H}\omega_d$.

† This velocity is equal to one revolution in 15 days.

‡ This velocity is equal to one revolution in 4 years.

Table 3. (continued)

No.	Pickoff		Torquer coefficient C_t gf-cm/mm ²	Angular velocity sensed			Drift velocity ω_{dr} o/hr	Approx. value of moment of in- terference act- ing on floating gyroassembly M_1 gf-cm	Additional information
	amplification factor (sensitivity) K $\frac{V}{\text{deg}}, \frac{V}{\text{hr}}$	greatest deviation from linearity, $\frac{\delta}{\%}$		ω_{min} o/hr	ω_{max} deg/sec	ω_{max} o/hr			
1					1		< 103	0.51	Operating temp $T \approx 93.3^\circ \text{C}$
2	10 with excitation current of 50 ma, 400 cps	± 1			4		≈ 1	0.05	Starting time ≥ 15 sec; Frequency of current feeding gyromotor $f_{gyr} = 400$ cps.
3	25 with excitation current of 100 ma, 400 cps		$1.02 \cdot 10^{-3}$ or $10.2 \cdot 10^{-3}$	1	5	$1.03 \cdot 10^6$	5	0.25	Sensitivity threshold of detector $1/600^\circ \pm 0.1^\circ$.
4				4.1					Works without heating.
5	34 with excitation current of 100 ma, 400 cps		$2.55 \cdot 10^{-3}$ or $35.7 \cdot 10^{-3}$	0.2	1	$1.03 \cdot 10^6$	1	0.5	Sensitivity threshold of detector $1/600^\circ \pm 0.1^\circ$; withstands load up to 50 g; Speed of rotor—12,000 rpm.
6	72 with excitation current of 100 ma, 400 cps	± 1	$44.8 \cdot 10^{-3}$ with dc		1		5	2.5	Frequency of current to gyromotor $f_{gyr} = 400$ cps; Synchronous speed of motor 12,000 rpm; Starting time 45 sec; Zero output signal ≥ 10 mv; Velocity β equals input velocity ω ; Heater power 225 w (two sections 75 w & 150 w) fed by 14 v dc; Working temp $\approx 75^\circ \text{C}$.
7							0.5	0.25	Given correct adjustment when starting velocity of random (sudden) drift $\approx 0.15^\circ/\text{hr}$; Working temp $T \approx 93.3^\circ \text{C}$.
8	25 with excitation current of 100 ma, 400 cps		$2.55 \cdot 10^{-5}$ or $1.02 \cdot 10^{-3}$	0.01	0.04	$0.824 \cdot 10^6$	0.05	0.25	Threshold of sensitivity of pickoff $1/600^\circ \pm 0.1^\circ$.
9							0.01		
10				0.01					Works without heating.

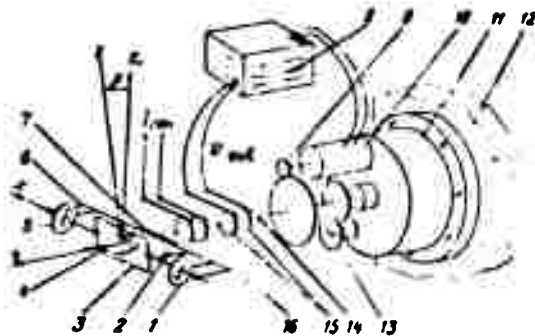


Fig. 2.19. Diagram of uniaxial spatial integrator of angular velocity with floating integrating gyroscope and servodrive: 1) microsyn-pickoff; 2) liquid damper; 3) gyroscope frame; 4) gyroscope rotor; 5) microsyn-torquer; 6) floating gyroscope housing; 7) part fixing gyroscope housing to shaft 14 (which may be considered as a uniaxially stabilized platform); 8) amplifier; 9) reducer; 10) slave motor; 11) flange; 12) integrator (stabilizer) housing; 13) read-out device; 14) shaft (input axis of integrator); 15) brushes and contact rings for picking off output voltage-signal U_{out} from microsyn-pickoff; 16) brushes and contact rings for supplying current I_{con} to secondary winding of microsyn-torquer; y) input axis of gyroscope and integrator; z) output axis of gyroscope; and z_0) initial position of spin axis z .

Each operation in manufacturing a floating gyroscope needs a great deal of time and has to be carried out with the greatest care. Production of the MIG is further complicated by the fact that during its manufacture it has to be assembled and dismantled several times. The most critical operations in the assembly of the MIG-5 are:

- a) checking the microsyn rotor and stator for production of the output signal;
- b) balancing the floating gyroassembly;
- c) selecting the journals and bearings;
- d) testing the load on the bearings from the characteristics of the gyromotor.

All these operations are carried out before the instrument is filled with liquid. Since the comparatively heavy gyroassembly is supported by slender journals of tungsten carbide resting on jewels during these operations, a small jolt can

destroy both the journals and the jewels. Consequently, this process has to be carried out with the greatest caution.

The final tests also take up a great deal of time. It requires about 14 hr to test the HIG-4, 7 hr for the HIG-5, 24 hr for the HIG-6 and 24 hr for the G337.

It is extremely important to choose a suitable place for the tests since one person walking across a concrete floor can cause enough shaking to disrupt the tests completely. Some gyroscopes are tested in the evening when there are fewer people about in the building. The turntable platform is one of the most important and critical pieces of test apparatus.

Figure 2.18 gives some impression of the layout and equipment required for the final testing of floating gyroscopes. The instrument undergoing examination is mounted on the platform 1.

Table 3 gives the basic characteristics of floating integrating gyroscopes produced by different firms.

It was pointed out above that floating integrating gyroscopes are most suitable for use as the sensing components of spatial integrators of angular velocity with servodrives, and for geometric stabilization of platforms in inertial space, which amounts to the same thing in effect. Having familiarized ourselves with the design of the floating integrating gyroscope, we can now turn to consideration of its use in the integrator. The schematic layout of an angular-velocity spatial integrator with an integrating gyroscope and servodrive is shown in Fig. 2.19. The floating integrating gyroscope is represented here in the same way as in Fig. 2.6. In principle the layout is not in any way different from those shown in Figs. 1.19 and 1.20. The only difference is that a floating integrating gyroscope is used here instead of an ordinary integrating one. The gyro housing 6 is firmly fixed by 7 to the axle 14 which is the output axis of the integrator. The input axis y of the gyroscope coincides with the input axis of the integrator. The x axis of rotation of the gyroassembly is perpendicular to the y axis. The z_0 axis, which

is the initial position of the spin axis \underline{z} , is perpendicular to the \underline{x} and \underline{y} axes, and together with them forms a trihedron. All the axes originate at the point O which is the point of intersection of the \underline{x} and \underline{y} axes. In principle the integrator functions in exactly the same way as the integrator and uniaxial stabilizer with an ordinary integrating gyroscope (Figs. 1.19 and 1.20), described in Chapter 1, Section 7.

The floating integrating gyroscope is sensitive to considerably smaller angular velocities than the ordinary integrating gyroscope in which the friction in the frame bearings is extensive. The integrator (stabilizer) with a floating integrating gyroscope, therefore, is much more accurate as an instrument. We will not repeat for Fig. 2.19 everything that has been said with regard to the work of the angular-velocity spatial integrator, but will merely point out the following. Two basic regimes should be distinguished in the operation of the system; the geometric-stabilization regime and the spatial-integration regime. The geometric-stabilization regime is the automatic maintenance of the initial orientation of the \underline{x} and \underline{z}_0 axes connected to the gyro housing in inertial space. It is assumed in this connection that the orientation of the input axis \underline{y} of the integrator in inertial space remains unchanged, irrespective of the functioning of the integrator.

Any rotation of the housing 12 of the integrator about the \underline{y} axis in inertial space causes a voltage U_{out} at the output of the microsyn-pickoff 1. This voltage actuates the servodrive which will keep turning the component 7 (the platform) with the gyroscope housing back to its original position, thus keeping its orientation in inertial space constant. The basic characteristic of the fixed geometric-stabilization regime is the relationship between the constant values of the angular velocity ω_{tra} of rotation of the integrator housing in inertial space about the \underline{y} axis and the corresponding values of the angular velocity ω_{rel} of rotation of the gyroscope housing about the integrator housing (ω_{tra} is the transfer velocity

of the gyroscope housing). It is clear that in an ideal integrator the values of these velocities should be the same.

The spatial-integration regime is the coercive rotation of component 7 (the platform), in other words the gyroscope and connected x and z_0 axes, in inertial space about the y axis with the desired angular velocity ω . This rotation is effected by supplying a current I_{con} to the secondary windings of the microsyn-corrector 5. As was described above, in this case the gyroscope housing rotates in inertial space about the y axis with an angular velocity ω proportional to the current I_{con} . The angle of rotation about the y axis will be proportional to the integral of the current I_{con} with respect to time. The basic characteristic of the fixed spatial-integration regime is the dependence between the constant values of the current I_{con} and the corresponding values of the angular velocity ω .

Thus the study of integrating floating gyroscopes intended for use in integrators and stabilizers of the type we have considered should be conducted with respect to these two regimes.

Section 2. Differentiating Gyroscopes

It has been stated above that at the present time the best-perfected form of differentiating gyroscope is the floating differentiating gyroscope. This instrument differs from the floating integrating gyroscope by the presence of a component, either electrical or mechanical, which is intended to impose upon the floating gyroassembly a moment proportional to the angle of deflection β of the gyroassembly from its initial position, corresponding to a zero value of the measured angular velocity ω and tending to return it to the initial position. As a component of this kind, we can use a torsion rod made of any material with good elastic properties, which, incidentally, are the same under torque towards either side within the working range of angles of twist.

Figure 2.20 shows the construction of a floating differentiating gyroscope

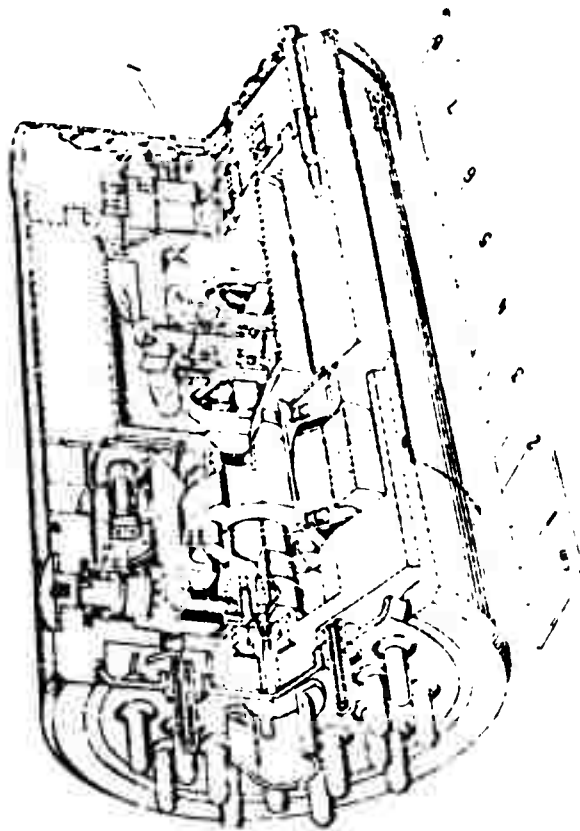


Fig. 2.20. Floating differentiating gyroscope, 10^4 type:
1) torsion rod.

with a torsion rod, designed by the Massachusetts Institute of Technology. In design this instrument is on the whole similar to the floating integrating gyroscope shown in Fig. 2.7. The main difference is that the right-hand support of the floating gyroassembly is made in the form of an elastic torsion rod 1. The other end of the torsion rod, which is elongated and cylindrical, is rigidly fixed to the gyroassembly. The right-hand end of the rod, which is spherical, is rigidly fixed to the instrument housing by means of a conical clamp.

The central, elastic, part of the torsion rod (the working part) smoothly opens out into the thicker ends which serve to hold it. In this way the torsion rod fulfills two functions at the same time: firstly, it is a support (on the right-hand side in Fig. 2.20) for the floating gyroassembly, and, secondly, when the gyroassembly departs from its initial position, it imposes on it a moment proportional to the angle of deflection, tending to return the assembly to its initial position, i.e., it acts as does the spring 4 in the differentiating gyroscope in Fig. 1.17.

In the design shown there is no corrector. A microsyn is used as the detector, as in the floating integrating gyroscope. Its component parts can clearly be seen in Fig. 2.14 to the left of the floating gyroassembly.

The principle of this type of floating differentiating gyroscope is shown in Fig. 2.21, but for the sake of consistency a microsyn-corrector has also been included in this figure.

It is also possible to have differentiating gyroscope designs which use some kind of electrical arrangement instead of a torsion rod. One such version (with a feedback circuit) will be examined later on when we deal with the theory of the floating differentiating gyroscope.

Tables 4 and 5 contain the basic characteristics of the floating differentiating gyroscope with torsion rod, Type 10⁴, No. 55, depicted in Fig. 2.20.

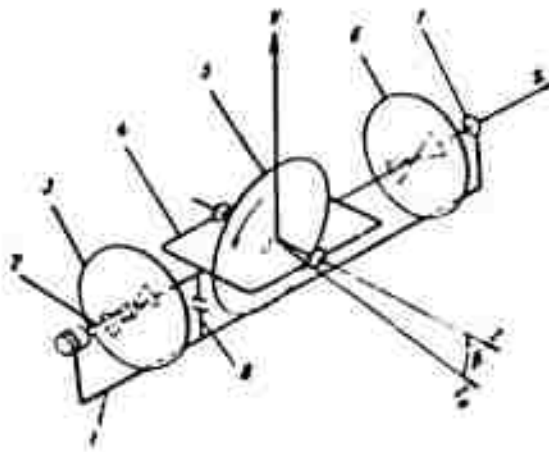


Fig. 2.21. Principle of floating differentiating gyroscope with torsion rod: 1) instrument housing; 2) torsion rod; 3) microsyn-torquer; 4) gyroscope frame; 5) gyroscope rotor; 6) microsyn-pickoff; 7) floating gyroassembly bearings; 8) liquid damper; y) input (measurement) axis of instrument; x) output axis; z) spin axis; z_0) initial position of gyroscope spin axis z ; axes $Oxyz_0$ are connected to the instrument housing.

Table 4.

Values determined prior to final assembly of device

No.	Designation	Symbol	Dimensions	Theoretical Value	Measured Value
1	Weight of gyroscope rotor		gf	11.79	11.84
2	Axial moment of inertia of gyroscope rotor	\underline{C}	gf-cm-sec ²	0.0122	0.0123
3	Proper-rotational velocity of rotor for 400-cycle feed current	$\underline{\Omega}$	rpm	8000	8000
4	Angular momentum of gyroscope	\underline{H}	gf-cm-sec	10.19	10.25
5	Weight of floating gyroassembly		gf	51.8	52.4
6	Moment of inertia of floating gyroassembly with respect to its x axis of rotation	\underline{J}	gf-cm-sec ²	0.035	0.036

Table 4. (Continued)

No.	Designation	Symbol	Dimensions	Theoretical Value	Measured Value
7	Maximal angle of rotation of floating gyroassembly from its initial position with respect to instrument housing (as permitted by stops)	β_{\max}	degrees	± 2.5	± 2.5
8	Radial clearance of damper	δ	mm	0.254	0.272
9	Specific gravity of fluid	γ_{f1}	gf/cm ³	$1.93 \pm 1\%$	1.912
10	Viscosity of fluid at 71.1° C	η	centipoises	$230 \pm 5\%$	232
11	Specific damping moment	K_{β}, M_{dp}	$\frac{\text{gf-cm}}{\text{rad/sec}}$ $\frac{\text{gf-cm}}{^\circ/\text{min}}$	5.1 $1.48 \cdot 10^{-3}$	4.7 $1.36 \cdot 10^{-3}$ (calculated)
12	Natural undamped frequency of floating gyroassembly in absence of damping liquid	f_0	cps	19	20
13	Sensitivity of microsyn-pickoff for excitation current of 250 ma 400 cps	$K_{\beta}, U_{\text{out}}$	mv/mrad volts/deg	42 0.732	40 0.698
14	Ratio of output voltage U_{out} of microsyn-pickoff to product $I'_{\text{ex}} f_p / \beta (I'_{\text{ex}} \text{ and } f_p \text{ are the magnitude and frequency of the excitation current, and } \beta \text{ is the angle of rotation of the floating gyroassembly})$	C_p	mv/ma cps rad mv/ma cps deg	0.42 $7.32 \cdot 10^{-3}$	0.40 $6.98 \cdot 10^{-3}$

Table 5.

Values determined after complete assembly of device

No.	Designation	Symbol	Dimensions	Theoretical Value	Measured Value
1	Phase voltage of gyromotor supply	U_{ph}	volts	3.5	4.0

Table 5. (Continued)

No.	Designation	Symbol	Dimensions	Theoretical Value	Measured Value
2	Frequency of gyromotor current supply	f_{gyr}	cps	400 ± 0.4	400 ± 0.04
3	Phase current of gyromotor	I_{ph}	amp	0.55	0.6
4	Temperature in damper gap	t	$^{\circ}\text{C}$	71.1 ± 1.1	71.1
5	Rigidity of torsion rod	k	$\frac{\text{gf}\cdot\text{cm}}{\text{rod}}$ $\frac{\text{gf}\cdot\text{cm}}{\text{deg}}$	$\frac{494}{8.62}$	$\frac{515}{8.98}$
6	Natural undamped frequency of floating gyroassembly after housing is filled with liquid	f_0	cps	19	25.2
7	Damping ratio (ratio of tone damping factor to critical damping factor)	b	--	0.614	0.436
8	Maximum value of detectable angular velocity (limited by mechanical means)	ω_{max}	rad/sec rpm	2 19.1	1.95 18.6
9	Minimum value of detectable angular velocity (see Chapter V)	ω_{min}	rad/sec $^{\circ}/\text{sec}$		0.17 9.75
10	Ratio of output voltage microsyn-pickoff U_{out} to input angular velocity ω	$K_{\omega}, U_{\text{out}}$	$\frac{\text{mv}}{\text{rad/sec}}$ $\frac{\text{mv}}{^{\circ}/\text{min}}$	830 0.241	819 0.238
11	Drift velocity caused by displacement of torsion rod from center (zero) position. (see Chapter V, Section 5)		rad/sec	0.001	0.0026
12	Drift velocity caused by moments unaccountable because of their random nature		rad/sec	0.0005	0.0007
13	Mechanical hysteresis of torsion rod in units of equivalent input angular velocities		rad/sec	0.0003	0.0001

On the basis of Tables 4 and 5 we can draw the following conclusions with regard to the floating differentiating gyroscope with elastic torsion rod No. 55. The most characteristic feature of this instrument is the comparatively high minimum detectable angular velocity, $\omega_{\min} = 0.17$ rad/sec., and the low value of the ratio $\frac{\omega_{\max}}{\omega_{\min}}$, $\frac{\omega_{\max}}{\omega_{\min}} = \frac{1.95}{0.17} = 11.5$.

The comparatively high value of ω_{\min} does not mean at all that the instrument does not react to angular velocities less than ω_{\min} . The point is that at angular velocities smaller than ω_{\min} the proportionality coefficient between the output voltage U_{out} of the microsyn-detector and the measured angular velocity will be a variable value and, to a certain extent, a random one. In the case of angular velocities ω within the range $\omega_{\min} \leq \omega \leq \omega_{\max}$, this coefficient can be considered constant for practical purposes.

Later on we shall show that in this respect the floating differentiating gyroscope with a feedback circuit is considerably more efficient; its ω_{\min} is equal to 0.0009 rad/sec ω_{\max} equal to 1.8 rad/sec, and, consequently $\frac{\omega_{\max}}{\omega_{\min}} = 2000$.

The floating differentiating gyroscope requires a considerably smaller specific damping moment, and consequently, a less viscous liquid than the floating integrating gyroscope. This is because the moment created by the damper is utilized in the integrating gyroscope as a counteracting moment and has to be large if the instrument is to function properly. In the differentiating gyroscope, however, this moment is used solely to dampen the vibrations of the floating gyroassembly. It can be seen from the Tables that the specific damping moment of the differentiating gyroscope is one quarter of its value in the integrating gyroscope and the viscosity is one third as much.

Figure 2.22 shown an external view of two floating differentiating gyroscopes, types JR and K, made by Minneapolis-Honeywell. According to the advertisements, both these instruments ensure a proportional dependence between the output signal and the input angular velocity in the working range with an accuracy of



Fig. 2.22. External view of the Minneapolis-Honeywell floating differentiating gyroscopes: (a) type JR; (b) type K; 1) graduation line; 2) mounting flange; 3) plate.

+0.25% of the upper limit of measurement, and withstand excess load through vibration up to 15 g at frequencies up to 2000 cps. The JR withstands impact loads up to 100 g applied to any plane, while the type K withstands similar loads up to 50 g. Type K weighs 1.64 kg and has the dimensions 81.3 (diam.) X 146 mm; it is intended for the control and homing of guided missiles, and also for aircraft.

In order that the instrument may be correctly installed, the mounting flange 2, as in other floating gyroscopes, is marked with a graduation line 1 which

indicates the diametric plane of the output (measurement) axis of the instrument. Above the line is a plate 3 with the words "Output Axis" and in addition there is a dot with an arrow round it showing the direction of positive rotation about the input axis.

Type JR has an angular momentum of $H = 10^6 \text{ g-cm}^2\text{-sec}^{-1} \approx 1020 \text{ gf-cm-sec}$ and is equipped with a compensating arrangement which maintains the damping coefficient constant without heating. The dimensions are 20.8 (diam.) X 85.7 mm, and the starting time is less than one minute. The instrument is designed for tactical weapon systems, which apparently explains its comparatively high kinetic moment in relation to the small size.

Figure 2.23 shows a patented design (Wendt H. C. GEC, US Patent, Class 74-5.7, No. 2,731,836 of 1/24/1956) for a floating differentiating gyroscope with a two-rotor asynchronous gyromotor, similar to one developed and constructed by V. A. Pavlov in 1949. The main aim of this particular design is to reduce the error

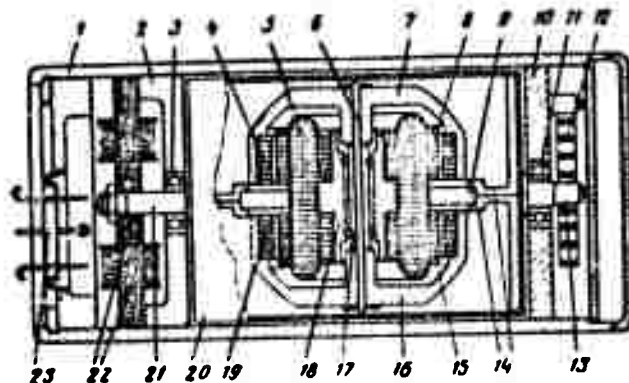


Fig. 2.23. Floating differentiating gyroscope with two-rotor gyromotor: 1) instrument housing; 2) and 10) inner walls of housing; 3) and 11) gyroassembly bearings; 4) and 19) squirrel-cages of rotor; 5) stator winding; 6) rotor axle; 7) and 16) rotors; 8) and 15) laminated stators of gyromotor; 9) disc made in one piece with socket; 18) and 12) spiral spring; 13) and 21) journals of gyroassembly (gyro frame); 14) parts holding gyromotor (disc 9); 17) rotor bearings; 18) socket made in one piece with disc 9; 20) cylindrical shell; 22) pickoff; 23) block with pins.

caused by asymmetry of the parts of the ordinary single-rotor gyromotor with respect to the plane passing through the axis of rotation of the gyroscope frame perpendicular to the axis of rotation of the rotor. The gyromotor is mounted on the disc 9 which is made in one piece with the socket 18. The disc 9 is held by two identical parts 14 and together with them, from the kinematic standpoint, forms the gyro frame. The parts 14 are enclosed in a hermetically-sealed cylindrical shell 20, which together with the gyromotor forms the floating gyroassembly. Its journals 13 and 21 are mounted in the bearings 3 and 11 in the wall 2 and 10 of the instrument housing 1. The space between the shell of the floating gyroassembly and the instrument housing is filled with liquid. The elastic counteracting moment is created by the spiral spring 12, one end of which is attached to the journal 13 and the other to the wall 10 of the instrument. The pickoff 22, which is similar to the microsynchronizer pickoff examined earlier, generates output signal. The

pins in the block 23 are used to supply current and to pick off the output signal.

The stator consists of two sets of identical laminations 8 and 15 attached to the socket 18, with the common winding 5 around them. This design is distinguished by having one common winding rather than two separate ones. It is not altogether easy to make a stator of this kind but the advantages of the symmetrical arrangement and the more uniform distribution of the winding make up for this. The double stator with a single winding takes up considerably less room than one with separate windings. The laminations can be nearer the center of the instrument since there are no windings on the adjacent sides of the sets of laminations. In consequence, the over-all length of the rotor is also reduced.

Each set of laminations is encased by its own rotor. The rotors 7 and 16 are identical; they are bell-shaped and are attached to the common axle 6 mounted in the bearing 17 indicated sketchily in the drawing. The squirrel-cages 4 and 19 fit into the rotors. Thus the gyromotor consists of two asynchronous motors, the rotors of which are attached to a common axle and the stators of which have a common winding. This kind of gyromotor is little affected by loss of balance through variation in temperature, and is almost entirely free from the influence of asymmetrical forces and pressures of various kinds which arise in an ordinary single-rotor gyromotor.

According to information contained in advertisements, the Giannini firm produces a medium-sized floating differentiating gyroscope, No. 36128, intended for aircraft and missile guidance, and for telemetering as well. The liquid used to fill the instrument is oil (apparently silicone oil). It has an internal electrical heating unit which keeps the temperature of the oil constant over a wide range of outside temperatures. The damping coefficient is thus kept the same. The gyroscope works on 400-cps three-phase alternating current. Either a potentiometer-detector made of precious metal or a standard selsyn is used to obtain an output signal. In either case the output signals are high-level and can be used

to measure angular velocities or for automatic control, either directly or after slight amplification. The instrument has a damping ratio of 0.5 to 0.6, and is suitable for the measurement of angular velocities ranging from 15 to $250^{\circ}/\text{sec}$ (0.262 to 4.36 rad/sec). As usual, angular displacements of the floating gyro-assembly are limited by mechanical stops. As in the case of any floating gyroscope, the instrument can withstand great vibrational and impact loads.

The Lear Company produces an ultra-accurate miniature floating differentiating gyroscope (diam. 38.1 mm, length 76.2 mm and weight 318 gf). This is type 2157-F, the design of which differs slightly from the normal. The instrument has an improved torsion rod which is particularly rigid in a transverse direction; this fact considerably helps to remove errors brought about by transverse deformation of the normal-type torsion rod. All parts which join together are made from materials with matching linear coefficients of expansion. This helps to eliminate errors and, in particular, loss of balance by the gyroassembly through change in the dimensions of the parts due to temperature, and makes it possible to have a zero point which for practical purposes is independent of outside temperature. The task of keeping the damping factor constant from -54 to $+74^{\circ}\text{C}$ has been similarly solved in principle.

Vibrations of the floating gyroassembly are damped by means of two hydraulic dampers which consist of thin steel cylinders filled with a special viscous liquid and their plungers. The material from which the damper parts are made and the viscous liquid are selected so that in practice temperature changes do not affect the damping factor. This can be done in the following way: the damping factor is directly proportional to the viscosity of the liquid and inversely proportional to the square of the gap between the cylinder and plunger. Since the viscosity is increased as the temperature falls, to prevent the damping factor depending to any extent on the temperature, the gap has to decrease as the temperature increases, and vice versa. For this to happen, the coefficient of linear

expansion α_{pl} of the plunger must be greater than the corresponding coefficient of the cylinder material α_{cy} . It is advisable to use a material for the cylinder in which $\alpha_{cy} \approx 0$, and for the plunger, one in which α_{pl} ensures the requisite change in the gap, with temperature.

This arrangement has made it unnecessary to have an electric heater and temperature control system in the instrument, and this has to a certain extent made it possible to simplify its design and operation. The output signal is obtained from an electromagnetic detector without sliding contacts. According to data supplied by the firm the instrument has an extremely low threshold of sensitivity, approaching zero.

The floating differentiating gyroscopes which we have considered by no means exhaust all the possible variations in design, which are extremely diverse.

Section 3. Floating Gyroscopes With Three Degrees of Freedom

Alongside the continual perfecting and ever wider application of floating gyroscopes with two degrees of freedom, research is being carried out at present in the construction of suitable floating gyroscopes with three degrees of freedom which will react to angular displacements about two mutually perpendicular axes. They are designed to work together with servodrives, which ensures that the instrument housing remains practically unchanged in position with respect to the spin axis throughout the operation of the instrument, thereby ensuring a high degree of precision.

As an example of this type of design we will take a gyroscope manufactured by the Arma Bosch Corp., shown in Fig. 2.24. In this gyroscope there is practically complete suspension of the gyroassembly without the use of any gimbal bearings, which ensures that the drift does not exceed $0.1^\circ/\text{hr}$.

As is clear from Fig. 2.24, the gyroscope is constructed in the following way.

The two-rotor motor (only one rotor 1 can be seen in the diagram) is placed inside a hermetically-sealed shell float 4, which from the kinematic standpoint represents the inner gimbal frame. The shell float is constructed of two mushroom-shaped parts, a central cylinder and two lateral cross pieces 9, and together with the gyromotor forms the floating gyroassembly 4.

The central cylindrical section of the gyroassembly is encircled by a ring 8, which is a kind of outer gimbal. The cross pieces 9 are on the outside of the

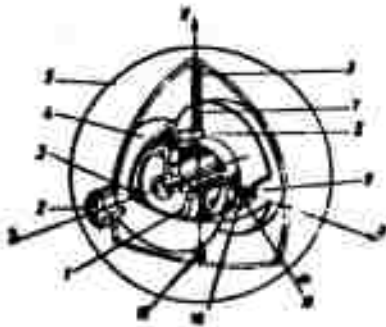


Fig. 2.24. Floating gyroscope with three degrees of freedom: 1) one rotor of a two-rotor gyro motor (the other is not shown); 2) pickoff; 3) pickoff magnet; 4) floating gyroassembly; 5) instrument housing; 6) and 11) leads; 7), 10), 12) suspension wires; 8) ring; 9) cross pieces.

ring 8. The gyroassembly 4 is suspended on two sides from the ring by two thin metal wires 10, which are perpendicular to the spin axis z , and form, as it were, the x axis of rotation of the gimbal frame. Thus, these thin wires replace the journals and bearings of the gimbal frame used in ordinary gyroscopes. The ring 8, with the gyroassembly 4 suspended from it, is in turn suspended by thin wires 7 and 12 from the spherical instrument housing 5. These wires form the y axis of rotation of the outer gimbal frame and replace the usual journals and

bearings. All three axes are mutually perpendicular and intersect at one point, which is the fixed point of the gyroscope.

The inner space between the housing 5 and the gyroassembly 4 is filled with a liquid whose specific gravity is such that the gyroassembly and the ring 8 are in a state of neutral equilibrium, i.e., in a state of complete suspension. Under these conditions the gyroassembly hardly exerts any load at all on the suspension wires. The negligibly small load which does act on these wires is solely due to

the fact that the gyroassembly is not ideally suspended. Hence, the work of the wires is to center the gyroassembly with respect to the ring 8, and to center the ring 8 together with the gyroassembly with respect to the housing 5.

Current is supplied to the gyromotor through the spiral leads 6, 11 and 12. A combined detector is used to pick off the output signals proportional to the angles of rotation about the \underline{x} and \underline{y} axes; one section of it is a permanent magnet 3, fixed inside the gyroassembly 4, and the other section is attached to the housing 5. When the axis of the magnet coincides with the centerpoint of the outside of the detector, the output signal is equal to zero. Whenever the housing 5 turns with respect to either pair of suspension wires, or both pairs of wires simultaneously, the centerpoint of the outside of the detector is displaced relative to the magnet axis 3 and a signal is produced at the output of the detector proportional to the angle through which the housing has turned about the \underline{x} and \underline{y} axes.

A great advantage of this design is the absence of gimbal bearings and, consequently, friction moments in the gimbal axes causing drift that is to a great extent unaccountable and, therefore, uncompensatable.

The gyroscope is mounted on a platform stabilized along two axes by servodrives which are switched on and off by the output signals. As in the case of the floating integrating gyroscope, the use of servodrives makes it possible in stabilizing the platform to keep to very small angles of rotation of the gyroscope housing with respect to its initial position since they are determined by the amplification factor of the amplifiers, the capacity and working speed of the servodrives.

This instrument, like any floating gyroscope, can be expected to withstand a great deal of vibration and to resist impact loads to a high degree.

This gyroscope was developed for the express purpose of constructing a miniature aircraft gyroscope able to work on the principle of the marine compass and

also as a guiding gyroscope. When it is to be used as a guiding gyroscope, the pendulum action can be eliminated without any disturbing moments being imposed.

CHAPTER III

THEORY OF THE FLOATING INTEGRATING GYROSCOPE

The present chapter deals with the fundamentals of the theory of the floating integrating gyroscope, taking into account the characteristic features of its design and singling out the parameters of interest from the standpoint of practical application, testing, and integration of the test results.

The standard design and working principle of this instrument are shown in Figs. 2.2 and 2.6. It should be recalled that in these diagrams the x , y and z_0 axes are connected to the instrument housing; z is the spin axis of the gyroscope, y is the input (measurement) axis, and x is the output axis; z_0 is the initial position of the spin axis z corresponding to zero values of the input angular velocity ω , the output voltage U_{out} of the microsyn-pickoff, and the control current I_{con} of the microsyn-torquer. β designates the angle of deflection of the spin axis from its initial position. In Figs. 2.2 and 2.6 this angle is shown in the positive sense of its vector. The same designations are adopted in Fig. 3.1. Henceforth, when considering both individual parts of the instrument as well as the instrument as a whole, we shall use the concept "amplification factor." In so doing we shall take the amplification factor of a part to mean the ratio between the value obtained at its output and the value reaching its input in the steady state. Let us use the following symbols to express this: x_{in} -- input value; x_{out} -- output value; and $K_{x_{in}, x_{out}}$ -- amplification factor. Then, according to our definition

$$K_{i_{n.s.}} = \frac{x_{out}}{x_{in}}.$$

(3.1)

The amplification factor may be constant or variable. In our theoretical arguments we shall take the amplification factors to be constant.

Section 1. Differential Equation of Motion of the Floating Gyroassembly.

The floating integrating gyroscope consists of the following basic components:

1. Floating gyroassembly
2. Damper
3. Torquer (torque generator)
4. Pickoff

Various types of pickoffs and torquers are used in floating gyroscopes, but the microsins discussed in Chapter II are the commonest. From now on we will consider that microsins are used as the detectors and torquers in order to keep our discussion consistent with what has gone before.

Let us consider the basic relationships of the components of the floating integrating gyroscope.

1. Floating Gyroassembly

Let us use the following symbols (Fig. 3.1):

• rad/sec is the angular velocity of the instrument housing about the input (measurement) axis y , equal to the projection of the instantaneous absolute angular velocity of the instrument housing onto the input axis y . This velocity is considered positive when its vector coincides with the positive direction of the y axis;

ω_{z_0} rad/sec is the projection of the instantaneous absolute angular velocity of the instrument housing onto the z_0 axis. The velocity ω_{z_0} is considered positive when its vector coincides with the positive direction of the z_0 axis;

H gf-cm-sec is the angular momentum of the gyroscope.

When the instrument housing rotates with angular velocities of ω and ω_{z_0} , a gyroscopic moment G is created (Fig. 3.1); on the basis of Formula (1.2)

$$G = -H\omega \cos \beta + H\omega_{z_0} \sin \beta. \quad (3.2)$$

Factoring the product $H\omega$ in the second expression, we obtain

$$G = -H\omega \left(\cos \beta - \frac{\omega_{z_0}}{\omega} \sin \beta \right). \quad (3.3)$$

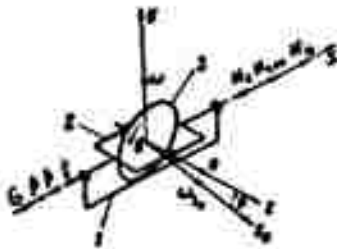


Fig. 3.1. Derivation of equation of motion of floating gyroscope.

1) instrument housing; 2) floating gyroassembly; 3) gyroscope rotor.

The floating gyroassembly, as well as the instrument as a whole, is designed to detect the angular velocity ω alone. To make this possible, the gyroscopic moment, which is the motive moment of the instrument, must be a function of the angular velocity ω alone. As is clear from Equality (3.3), this can only be the case when $\beta = 0$, for only in this case is

$$G = -H\omega \quad (3.4)$$

i.e., there is one single value of G for each value of ω . When the values of ω are positive, the gyroscopic moment G is directed along the x axis (see Fig. 3.1).

But if $\beta \neq 0$, the gyroscopic moment will depend in addition on ω_{z_0} and β , which is not at all desirable.

Thus, even if $\omega_{z_0} = 0$, when $\beta \neq 0$ there will be different gyroscopic moments (equal to $-H\omega \cos \beta$) for the same values of the angular velocity ω at different values of the angle β , i.e., the greater the angle β , the smaller they will be. Since the floating integrating gyroscope is used solely for detection of the angular velocity ω , it is essential when using it to ensure conditions under which the gyroscopic moment depends solely on ω with a high degree of accuracy. For this purpose the angle β must remain insignificantly small - approaching zero - the whole time the instrument is working.

The angular momentum of the gyroscope H can be considered as the amplification factor of the floating gyroassembly.

2. Damper

It has been pointed out that the floating integrating gyroscope uses a liquid damper. The basic components are shown separately in Fig. 3.2. Let us use the following designations:

l is the length of the damper (the length of the gyroassembly shell) in cm,

r is the outer radius of the gyroassembly shell in cm,

δ is the gap between the shell and the instrument housing in cm,

$\dot{\beta}$ is the angular velocity of the floating gyroassembly with respect to the instrument housing about the x axis (it is considered positive when its vector is directed along the negative x axis) in rad/sec (see Fig. 3.1),

$\eta = \eta(r)$ is the absolute viscosity of the liquid filling the damper gap in poises, and

t is the temperature of the damping liquid in $^{\circ}\text{C}$.

As is known, the damping moment created by the liquid damper under consideration is in direct proportion to the first power of the angular velocity of one cylindrical surface with respect to the other. Calling this moment \underline{M}_d and the proportionality coefficient \underline{c} , we arrive at

$$\underline{M}_d = \underline{c} \dot{\beta};$$

here

$$\underline{c} = \frac{2\pi}{981} \frac{lr^3}{\delta} \eta \quad \text{at cm-sec.} \quad (3.5)$$

When the velocities $\dot{\beta}$ are positive, the moment \underline{M}_d is directed along the positive \underline{x} axis (see Fig. 3.1).

Regarding the angular velocity $\dot{\beta}$ as the input value of the damper, and the damping moment \underline{M}_d as its output value, we find that \underline{c} represents the amplification factor of the damper. Calling this $\underline{K}_{\dot{\beta}, \underline{M}_d}$, we obtain

$$\underline{M}_d = \underline{K}_{\dot{\beta}, \underline{M}_d} \dot{\beta}, \quad (3.6)$$

where

$$\underline{K}_{\dot{\beta}, \underline{M}_d} = \underline{c} = \frac{2\pi}{981} \frac{lr^3}{\delta} \eta \quad \text{gf-cm-sec.} \quad (3.7)$$

The factor \underline{c} , or $\underline{K}_{\dot{\beta}, \underline{M}_d}$, which is the same thing, is often called the specific damping moment.

It should be pointed out that since the viscosity η depends on temperature, in order to keep $\underline{K}_{\dot{\beta}, \underline{M}_d}$ constant, the temperature of the damping liquid must be kept constant.

3. Microsyn-Torquer

The construction and working principle of the microsyn-torquer have been considered earlier and are shown in Figs. 2.3, 2.4 and 2.5. The moment \underline{M}_t created by the torquer is proportional to the product of the excitation current \underline{I}_{ex} and the control current \underline{I}_{con} , and can be represented as

$$\underline{M}_t = \underline{C}_t \underline{I}_{ex} \underline{I}_{con} \quad (3.8)$$

The value of the proportionality coefficient \underline{C}_t gf-cm/amp² is determined by the construction parameters of the microsyn. In order to make the moment of the microsyn-torquer a function of the control current \underline{I}_{con} alone, the excitation current \underline{I}_{ex} has to be kept steady. Assuming that this is the case and designating

$$\underline{K}_{I_{con}, \underline{M}_t} = \underline{C}_t \underline{I}_{ex} \text{ gf-cm/amp,} \quad (3.9)$$

we find

$$\underline{M}_t = \underline{K}_{I_{con}, \underline{M}_t} \underline{I}_{con} \quad (3.10)$$

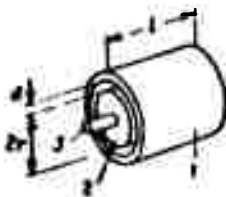


Fig. 3.2. Diagram for use in determining basic characteristics of the damper.

1) Instrument housing; 2) floating gyro-assembly shell; 3) gyroassembly axis.

The constant coefficient $\underline{K}_{I_{con}, \underline{M}_t}$ is the amplification factor of the microsyn-torquer if the control current \underline{I}_{con} is regarded as the input value and the moment \underline{M}_t as the output value. If the microsyn-torquer works on direct current, the direction of the moment \underline{M}_t is determined by the direction of the current \underline{I}_{con} , and if it works on

alternating current, the direction of \underline{M}_t depends on the phase of the current \underline{I}_{con} . Let us agree to consider \underline{M}_t positive when its direction coincides with the positive direction of the \underline{x} axis (Fig. 3.1). In this way, the currents \underline{I}_{con} which are taken as positive, will correspond to positive moments \underline{M}_t , i.e., moments along the \underline{x} axis.

4. Microsyn-pickoff

The construction and working principle of the output signal microsyn-pickoff have been considered earlier and are shown in Figs. 2.3, 2.4 and 2.5. The input value of the microsyn-pickoff is the angle β of rotation of the microsyn rotor from its initial position relative to the stator. The output value is the voltage \underline{U}_{out} which is picked off the secondary, output winding of the microsyn.

This voltage is

$$\underline{U}_{out} = \underline{K}_{\beta, \underline{U}_{out}} \beta, \quad (3.11)$$

where $\underline{K}_{\beta, \underline{U}_{out}}$ is the amplification factor (sensitivity) of the microsyn-pickoff;

$$\underline{K}_{\beta, \underline{U}_{out}} = \underline{C}_p \underline{I}'_{ex} \underline{f}_p \text{ v/rad} \quad (3.12)$$

where \underline{C}_p is a constant coefficient dependent upon the construction parameters of the microsyn-pickoff in v/rad amp cycles,

\underline{I}'_{ex} is the excitation current in amp,

\underline{f}_p is the frequency of the excitation current in cps.

Since the amplification factor $\underline{K}_{\beta, \underline{U}_{out}}$ depends on \underline{I}'_{ex} and \underline{f}_p , to keep it constant, the magnitude and frequency of the excitation current have to be kept invariable with the greatest possible degree of accuracy. Henceforth it will be

considered that the pickoff excitation winding is fed with current from a stabilized source in such a way that it can be considered with a high degree of accuracy that

$$I'_{ex} = \text{constant}; f_p = \text{constant}.$$

As follows from Formula (3.12), the amplification factor of the microsyn-pickoff K_{β} , U_{out} depends both on its construction parameters which determine the coefficient C_p and on I'_{ex} and f_p . Strictly speaking, the coefficient C_p will not have the same value at different angular positions of the detector rotor with respect to the stator. This is because the actual parameter values of the electric and magnetic circuits of the microsyn-pickoff are on the whole slightly different from their nominal values, which in turn is due to inaccuracies in the manufacture and assembly of the parts and units of the pickoff, and also the quality of the material used. Moreover, on account of radial and axial gaps in the supports of the floating gyroassembly the instrument may make random movements with respect to the stator within the limits of these gaps, causing variation in the gap between the rotor and the stator, i.e., random variation in the parameters of the magnetic circuit of the pickoff. This movement of the rotor relative to the stator may be caused by factors both inside and outside the gyroscope. The chief internal factor is the vibration of the gyromotor caused by a rotor which is not perfectly balanced. The rotor must therefore be mounted with the greatest care from the dynamic point of view. There must be no gaps in the bearings of the rotor, nor should gaps appear at any time during the guaranteed life of the instrument. Changes in the magnetic circuit can also be caused by irregularities in the shape of the bearings and the journals of the floating gyroassembly. It will be clear from this that it is essential to reduce the radial and axial gaps

in the bearings to a minimum and to make the highest demands with regard to the correct shape of the bearings and journals.

The fewer the relative changes possible in the parameters of the electric and magnetic circuit when the instrument is functioning, the less the actual values of the voltage U_{out} will depart from its values as determined from Formula (3.11). It should be pointed out that deviations from Formula (3.11) can also be caused by variable magnetic fields created by the working gyromotor. It is essential to aim at reducing these fields to a minimum and also to screen the microsyn-pickoff from the gyromotor.

All these facts, and also the impossibility of keeping I'_{ex} and f_p absolutely constant, lead to a certain discrepancy between the values of the microsyn-pickoff output voltage and the same values obtained from Formula (3.11) when K_{β} , $U_{out} = \text{const}$. In view of this, the actual value of the output voltage, which is the output voltage of the floating integrating gyroscope, can be represented as the sum of the two terms:

$$U_{out} = K_{\beta}, U_{out} \beta + \Delta \quad (3.13)$$

where K_{β} , U_{out} is considered constant and equal to its nominal value. The first term is the voltage produced by the microsyn-pickoff when C_p , I'_{ex} and f_p are constant. This voltage, which can be called nominal, is exactly proportional to angle β . The second term Δ , given careful construction, assembly, and adjustment of the instrument and the use of a stabilized current supply, represents a slight departure of the output voltage from its nominal value caused by the fact that C_p , I'_{ex} and f_p are not constant.

In practice it can be considered that the output voltage K_{β} , $U_{out} \beta$ is proportional to the angle β not only when this angle is constant, but also when it varies. In other words, the voltage does not depend on the rate and

acceleration of the change in the angle β . The voltage Δ , in exactly the same way, does not depend on $\dot{\beta}$ and $\ddot{\beta}$ in practice.

Since the deviation of the values of C_p , I'_{ex} and f_p from their nominal values, observed over a period of time t with the change of the angle β , are indefinite and to a certain extent random in nature, the voltage Δ is an indefinite and to a considerable extent random function of the angle β and the time t . Therefore, in the general case

$$\Delta = \Delta(\beta, t).$$

In an ideal case, when the output angular velocity ω equals zero, the voltage U_{out} must also equal zero. It is extremely difficult, however, to achieve this completely. In the Massachusetts Institute of Technology instrument, for instance, the zero signal of the microsyn-pickoff is equal to 1.9 mv (see Table 2, p. 93).

Thus, in the general case, in Equality (3.13) when $\beta = 0$, the voltage U_{out} will not be zero. In other words, when $\beta = 0$, $U_{out} \neq 0$ but is equal to Δ_0 .

Let us find the expressions for \dot{U}_{out} and \ddot{U}_{out} , the first and second derivatives of U_{out} with respect to time. Differentiating Equality (3.13) with respect to time, we find

$$\dot{U}_{out} = K_p \cdot U_{out} \dot{\beta} + \Delta'_t + \Delta'_\beta \dot{\beta} = (K_p U_{out} + \Delta'_\beta) \dot{\beta} + \Delta'_t. \quad (3.14)$$

where Δ'_t and Δ'_β are partial derivatives of Δ with respect to t and β respectively.

Differentiating (3.14) with respect to time, we obtain

$$\ddot{U}_{out} = (K_p U_{out} + \Delta'_\beta) \ddot{\beta} + \Delta''_t + 2\Delta''_{t\beta} \dot{\beta} + \Delta''_{\beta\beta} \dot{\beta}^2.$$

where Δ''_{tt} , $\Delta''_{t\beta}$ and $\Delta''_{\beta\beta}$ are partial derivatives of the second order of Δ . Substituting the value $\dot{\beta}$ determined from Equality (3.14) in the expression for \dot{U}_{out} , we obtain

$$\begin{aligned} \dot{U}_{out} = & (K_{\beta, U_{out}} + \Delta_{\beta}) \dot{\beta} + \frac{\Delta''_{\beta\beta}}{(K_{\beta, U_{out}} + \Delta_{\beta})^2} \dot{U}_{out} + \\ & + \frac{2}{K_{\beta, U_{out}} + \Delta_{\beta}} \left(\Delta'_{t\beta} - \frac{\Delta'_{\beta\beta}}{K_{\beta, U_{out}} + \Delta_{\beta}} \right) \dot{U}_{out} + \Delta''_{tt} - \\ & - \frac{2\Delta'_{t\beta}}{K_{\beta, U_{out}} + \Delta_{\beta}} + \frac{\Delta'^2_{\beta\beta}}{(K_{\beta, U_{out}} + \Delta_{\beta})^2}. \end{aligned}$$

In an instrument working normally the voltage Δ and the derivatives Δ'_{β} , $\Delta'_{t\beta}$, $\Delta''_{\beta\beta}$, $\Delta''_{t\beta}$ and Δ''_{tt} are small, and in the general case, together with Δ , they are indefinite and to a considerable degree random functions of β and t . An analysis of the physical causes of the dependence of Δ on β enables us to consider that with respect to β the voltage Δ is a continuous and defined function, at least within the range of working values of β . It can therefore be taken that the derivative $\Delta''_{\beta\beta}$ is a second-order infinitesimal with respect to the first derivatives of Δ . On the basis of what has been said, in the last expression for \dot{U}_{out} we can ignore the terms containing the product of the derivatives, and also the term containing $\Delta''_{\beta\beta}$. Having done this, we obtain

$$\dot{U}_{out} = (K_{\beta, U_{out}} + \Delta_{\beta}) \dot{\beta} + \frac{2\Delta'_{t\beta}}{K_{\beta, U_{out}} + \Delta_{\beta}} \dot{U}_{out} + \Delta''_{tt}. \quad (3.15)$$

It can be seen from Eqs. (3.14) and (3.15) that the true sensitivity of the microsyn-pickoff with respect to the angle β will be equal not to $K_{\beta, U_{out}}$, but to $K_{\beta, U_{out}} + \Delta'_{\beta}$. Since, in the general case, the derivative Δ'_{β} is not constant,

the sensitivity will not be constant either. But, as pointed out, in an instrument which is working normally Δ'_{β} is a small value, so it is quite permissible to ignore it as a term extremely small compared to K_{β} , U_{out} . We shall not do so here, however, so that we shall have the chance later on of qualitatively determining the influence of Δ'_{β} on the performance of various types of floating gyroscopes.

The interrelation of the parts of the floating integrating gyroscope which we have examined is clearly illustrated by the block-diagram in Fig. 3.3. This figure gives a diagrammatic representation of the floating integrating gyroscope showing the individual parts of the instrument, their interconnection and their functions. In addition, the figure shows all the physical values affecting the work of the instrument, in particular, the moments acting on the floating gyro-assembly about its x axis of rotation. The symbols used are those which were explained earlier.

The physical values indicated in the diagram are all subdivided into the following three groups:

1. Basic values. These include the angle β , the angular velocities ω and $\dot{\beta}$, the current I_{con} , the voltage U_{out} , and the moments G , M_d and M_t . The interconnection between these values is shown by thick lines.
2. Auxiliary values. These are the currents I'_{ex} and I_{ex} , the gyromotor power consumption P_{gyr} and the temperature τ . The interconnection between them is shown by broken lines.
3. Interference. This includes the velocity ω_{z0} and the acceleration $\ddot{\gamma}$. The direction of their effect is shown by lines consisting of dots and dashes.

The lines showing the interconnection are in all cases marked with arrows to indicate the direction in which the effect travels. Furthermore, the lines showing the influence of the moments are shown with small circles. This means that

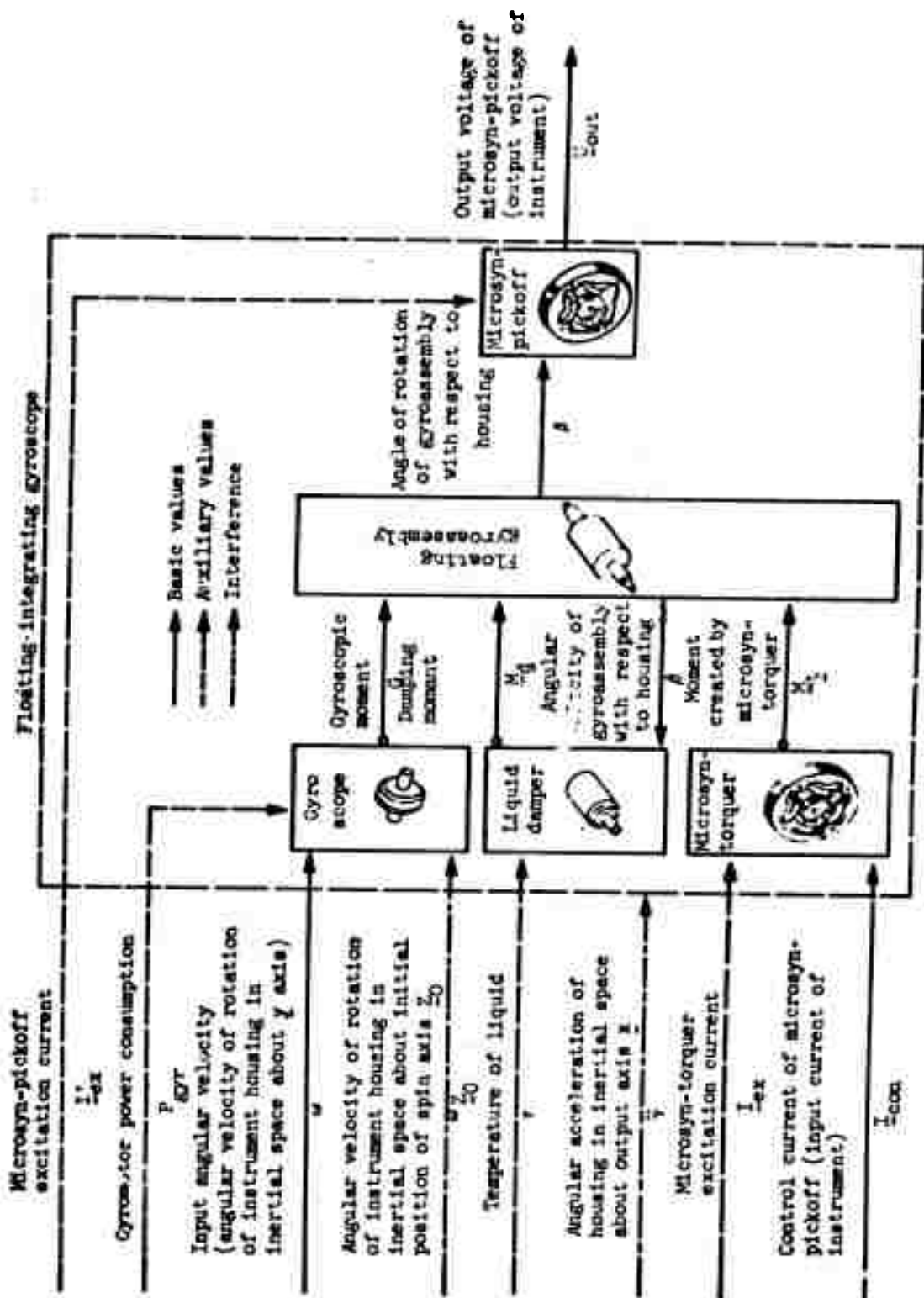


Fig. 3.3. Block-diagram of floating integrating gyroscope.

according to Newton's third law, the component parts which create moments experience an equal and oppositely directed effect from the parts upon which they impose those moments. The moments of inertia \underline{M}_1 and also the components of the interference moment, which inevitably occur when the instrument functions, have not been included.

Let us now proceed to the formulation of the equation of motion of the floating gyroassembly relative to its \underline{x} axis of rotation. Besides the above-considered moments \underline{G} , \underline{M}_d and \underline{M}_t , determined by Formulas (3.3), (3.6), and (3.10), respectively, there is also a moment of inertia acting on the gyroassembly about its \underline{x} axis of rotation (Fig. 3.1)

$$\underline{M}_{in} = \underline{J}(\ddot{\beta} + \ddot{\gamma}),$$

where \underline{J} is the moment of inertia of the floating gyroassembly and all the parts connected to it about its \underline{x} axis of rotation, in gf-cm-sec^2 ,

$\ddot{\beta}$ is the angular acceleration of the gyroassembly about the \underline{x} axis with respect to the instrument housing; it is considered positive when its vector is directed along the negative \underline{x} axis (Fig. 3.1), in rad/sec^2 , and

$\ddot{\gamma}$ is the absolute angular acceleration of the instrument housing about the \underline{x} axis. The angle γ , and consequently the angular velocity $\dot{\gamma}$ and angular acceleration $\ddot{\gamma}$, of rotation of the housing about the \underline{x} axis are considered positive in a clockwise direction when viewed from the positive end of the \underline{x} axis (in the same way as β , $\dot{\beta}$, $\ddot{\beta}$) in rad/sec^2 .

When the acceleration of $\ddot{\beta}$ and $\ddot{\gamma}$ are positive, the moment \underline{M}_{in} is directed along the positive direction of \underline{x} axis (see Fig. 3.1).

Other moments of various kinds which may act on the gyroassembly about its axis of rotation and which cannot be calculated with any accuracy will be designated \underline{M}_1 (the "1" standing for "interference"). Among such moments are, for example, the moment of residual friction in the bearings of the floating gyroassembly,

the moment arising through lack of perfect balance of the gyroassembly, the moment created by the leads, and disturbing moments created by the detector and corrector.

The numerical values of δ , η , r , K_{β} , $M_d \equiv C$, C_t , C_p , K_{β} , U_{out} , and J for the floating integrating gyroscope Type 10⁴ No. 79 are reproduced in Tables 1 and 2 (Chapter II, Sec. 1).

By making the sum of all the moments considered equal to zero (taking their signs into account) we obtain a differential equation of the motion of the floating gyroassembly about its x axis relative to the instrument housing:

$$J(\ddot{\beta} + \ddot{\gamma}) + K_{\beta} \dot{\beta} = H\omega \left(\cos \beta - \frac{\omega_z}{\omega} \sin \beta \right) - K_{I_{con}} I_{con} - M_d. \quad (3.16)$$

In this equation the values H , K_{β} , M_d and $K_{I_{con}}$, M_t are taken as constant. To meet this condition, it is essential that

$$I_{ex} = \text{const}; f_t = \text{const}; r = \text{const}.$$

Here f_t is the frequency of the torquer excitation current. The other symbols are the same as before. In order that $H = \text{const}$, f_{gyr} , the frequency of the current fed to the gyromotor, and P_{gyr} , the gyromotor input power, must be constant, i.e., we must have

$$P_{gyr} = \text{const}; f_{gyr} = \text{const}.$$

Dividing Eq. (3.16) by K_{β} , M_t , transferring the term with $\ddot{\gamma}$ to the right-hand side and introducing new designations for the coefficient constants, we obtain the differential equation of motion of the floating gyroassembly in the following final form:

$$T\ddot{\beta} + \dot{\beta} = K_{\omega} \left(\cos \beta - \frac{\omega_z}{\omega} \sin \beta \right) - K_{I_{con}} I_{con} - K_{M_d} M_d - T\ddot{\gamma}. \quad (3.17)$$

In this equation

$$T = \frac{J}{K_{\beta} M_d} \text{ sec} \quad (3.18)$$

is the time constant of the integrating gyroscope.

$$K_{\beta} = \frac{H}{K_{\beta} M_d} \quad (3.19)$$

is the dimensionless amplification factor of the integrating gyroscope characterizing the dependence of $\dot{\beta}$ on ω in the steady state, with $\beta = 0$ (and with negligibly small values of β as well in practice).

$$K_{I_{con}} = \frac{K_{I_{con}} M_t}{K_{\beta} M_d} \frac{\text{rad/sec}}{\text{sec}} \quad (3.20)$$

is the amplification factor of the floating integrating gyroscope characterizing the dependence of $\dot{\beta}$ and I_{con} in the steady state. Replacing $K_{I_{con}}$, M_t in (3.20) by the value for it determined from Eq. (3.9), and introducing the designation

$$K_{I_{ex} \dot{\beta}} = \frac{C_T}{K_{\beta} M_d} \frac{\text{rad/sec}}{\text{sec}} \quad (3.21)$$

we obtain

$$K_{I_{con} \dot{\beta}} = K_{I_{ex} \dot{\beta}} I_{ex}. \quad (3.22)$$

The amplification factor $K_{I_{ex} \dot{\beta}}$ characterizes the dependence of $\dot{\beta}$ on the product of the currents $I_{ex} I_{con}$ in the steady state.

$$K_{M_i \dot{\beta}} = \frac{1}{K_{\beta} M_d} \frac{\text{rad/sec}}{\text{g} \cdot \text{cm}} \quad (3.23)$$

is the amplification factor of the gyroscope describing the dependence of $\dot{\beta}$ on M_z in the steady state.

The experimental values of T , K_ω , $\dot{\beta}$, $K_{I_{ex}}$, I_{con} , $\dot{\beta}$ for the floating integrating gyroscope developed by the Massachusetts Institute of Technology - Type 10⁴ No. 79 - are given in Table 2 (Chapter II, Sec. 1).

In Eq. (3.17) the term

$$\frac{\omega_z}{\omega_0} \sin \beta$$

denotes the influence of the angular velocity ω_z on the work of the integrating gyroscope when $\beta \neq 0$. If the gyroscope is being used in systems which ensure low values of the angle β , this term can be ignored. For instance, if the angle is never greater than 0.05°, $\sin \beta < 0.001$ and, consequently, the term in question will be insignificantly small compared to $\cos \beta$, and in practice equal to unity in this case.

We will not consider Eq. (3.17) in detail since in the final analysis we are interested in the output voltage U_{out} of the microsyn-pickoff, and not the angle β .

Section 2. Equation for the Floating Integrating Gyroscope.

When the floating gyroassembly turns through an angle β relative to the instrument housing, a voltage U_{out} is created in the secondary, output winding of the microsyn-detector. This voltage is defined by Eq. (3.13). We should point out that since it is taken that the angles of rotation of the gyroassembly relative to the housing should not be greater than 0.001 rad the whole time the instrument is functioning, the microsyn-pickoff has to be a high-precision sensitive device. This can be understood when it is considered that given $\beta = 0.001$ and a

microsyn rotor radius of about 10 mm, the greatest possible displacement of the rotor pole relative to the stator will only be 0.01 mm.

In general, floating integrating gyroscopes are installed in automatic systems as units sensing angular deviations and control signals, and producing output signals which operate the slave motors of servodrives. In any smoothly working system the servodrive slave motors restrain the object being guided and, consequently, the floating integrating gyroscope mounted in it, from deviation from its initial path within such narrow limits that the angle of rotation of the floating gyro-assembly relative to the instrument housing remains close to zero all the time the gyroscope is functioning. The reaction of these systems to control signals, or in other words, their work as spatial integrators, takes place, likewise, at angles of β close to zero. We will therefore take it that the angle β is always so small that for practical purposes we can assume $\sin \beta = 0$ and $\cos \beta = 1$. The small value of angle β ensures that in practice the work of the instrument does not depend on the angular velocity ω_z . Hence, assuming in Eq. (3.17) $\sin \beta = 0$ and $\cos \beta = 1$, and replacing $\dot{\beta}$ and $\ddot{\beta}$ by means of Eqs. (3.14) and (3.15), we obtain

$$T\ddot{U}_{out} + \left(1 - \frac{2T\Delta_{ip}}{K_{p,U_{out}} + \Delta_p}\right)\dot{U}_{out} = \\ = (K_{p,U_{out}} + \Delta_p)[K_{u,\beta}\omega - K_{i,\beta}I_{con} - K_{v,\beta}\ddot{\gamma} - K_{M,\beta}M_i] + T\Delta_{it} + \Delta_i.$$

In view of the small value of the time constant T we can ignore the term containing the product $T\Delta_{ip}$ in this equation, and also the term $T\Delta_{tt}$. Having done so, we will rewrite the equation in the form

$$T\ddot{U}_{out} + U_{out} = \left(1 + \frac{\Delta_p}{K_{p,U_{out}}}\right)[K_{u,\beta}\dot{\omega}_{out} - \\ - K_{i,\beta}\dot{U}_{out}I_{con} - K_{v,\beta}\ddot{\gamma} - K_{M,\beta}\dot{U}_{out}M_i] + \Delta_i. \quad (3.24)$$

where

$$K_{\omega, \dot{U}_{out}} = K_{\omega, \dot{U}_{out}} K_{p, U_{out}} = \frac{H}{K_{p, M_1}} K_{p, U_{out}} \frac{1/\text{sec}}{1.20 \cdot \text{sec}} \quad (3.25)$$

$$K_{I_{con}, \dot{U}_{out}} = K_{I_{con}, \dot{U}_{out}} K_{p, U_{out}} \frac{1/\text{sec}}{s} \quad (3.26)$$

$$K_{\ddot{U}_{out}} = T K_{p, U_{out}} \frac{1/\text{sec}}{\text{rad/sec}^2} \quad (3.27)$$

$$K_{M_1, \dot{U}_{out}} = K_{M_1, \dot{U}_{out}} K_{p, U_{out}} \frac{1/\text{sec}}{\text{rad/sec}} \quad (3.28)$$

The amplification factors $K_{\omega, \dot{U}_{out}}$, $K_{I_{con}, \dot{U}_{out}}$, $K_{\ddot{U}_{out}}$, $K_{M_1, \dot{U}_{out}}$, and $K_{M_1, \dot{U}_{out}}$ characterize the dependence of \dot{U}_{out} , the rate of change in the output voltage, on the values ω , I_{con} , \ddot{U} and M_1 , respectively. Using Eq. (3.22) and introducing the designation

$$K_{I_{con}, \dot{U}_{out}} = K_{I_{con}, \dot{U}_{out}} K_{p, U_{out}} \quad (3.29)$$

the amplification factor $K_{I_{con}, \dot{U}_{out}}$ can be put in the following form:

$$K_{I_{con}, \dot{U}_{out}} = K_{I_{con}, \dot{U}_{out}} I_{con} \quad (3.30)$$

The experimental values of K_{ω} , $\dot{\theta}_{out}$ and $K_{I_{ex}} I_{con} \dot{\theta}_{out}$ for the floating integrating gyroscope Type 10⁴ No. 79 are given in Table 2 (Chapter II, Sec. 1).

Equation (3.24) can be written as follows after the elementary transformations:

$$\begin{aligned} T\ddot{\theta}_{out} + \dot{\theta}_{out} = K_{\omega} \dot{\theta}_{out} \left(1 + \frac{\Delta_{\theta}}{K_{\theta} \dot{\theta}_{out}} \right) \times \\ \times \left[1 - k_{I_{con}} - \frac{I_{con}}{\omega} - k_{\ddot{\theta}} \frac{\ddot{\theta}}{\omega} - k_{M_{\theta}} - \frac{M_{\theta}}{\omega} \right] + \Delta_{\theta} \end{aligned} \quad (3.31)$$

where

$$k_{I_{con}} = \frac{K_{I_{con}} \dot{\theta}_{out}}{K_{\omega} \dot{\theta}_{out}} = \frac{K_{I_{con}} M_{\theta}}{H} \quad (3.32)$$

$$k_{\ddot{\theta}} = \frac{K_{\ddot{\theta}} \dot{\theta}_{out}}{K_{\omega} \dot{\theta}_{out}} = \frac{T}{K_{\omega} \dot{\theta}} = \frac{J}{H} \quad (3.33)$$

$$k_{M_{\theta}} = \frac{K_{M_{\theta}} \dot{\theta}_{out}}{K_{\omega} \dot{\theta}_{out}} = \frac{1}{H} \quad (3.34)$$

Equation (3.31) will be called the equation of the floating integrating gyroscope.

The second expression for the coefficients in Formulas (3.32), (3.33) and (3.34) have been obtained by substitution of Eqs. (3.18), (3.19), (3.20), (3.23), (3.25), (3.26), (3.27), and (3.28) into the first expression in the coefficients.

Each of the coefficients $k_{\underline{I}_{con}}, \omega$; $k_{\ddot{\gamma}}, \omega$; and $k_{\underline{M}_1}, \omega$ is numerically equal to the value of the ratio between the velocity ω and the value for its first index, at which the output voltage \underline{U}_{out} of the integrating gyroscope will remain constant, and, consequently, the equality

$$\dot{\underline{U}}_{out} = \ddot{\underline{U}}_{out} = 0$$

will be valid if the values for the first indices in the other two amplification factors are equal to zero (or insignificantly small), and $\Delta_{\underline{t}}' = 0$.

Let us examine the physical meaning of each one of these three factors separately. In so doing we will consider that $\Delta_{\underline{t}}' = 0$.

1. Amplification factor $k_{\underline{I}_{con}}, \omega$. Let us assume that $\ddot{\gamma} = 0$ and that $k_{\underline{M}_1}, \omega = \frac{\underline{M}_1}{\omega}$ is insignificantly small compared with unity. Moreover, let us consider that

$$\left. \begin{array}{l} \underline{I}_{ex} = \text{const}; \underline{I}_{ex}' = \text{const}; f_{\underline{p}} = \text{const} \\ \underline{P}_{gyr} = \text{const}; f_{gyr} = \text{const}; r = \text{const.} \end{array} \right\} \quad (3.35)$$

Then, as follows from Eq. (3.31) in order that $\dot{\underline{U}}_{out} = \ddot{\underline{U}}_{out} = 0$, it is first necessary that the equality

$$\left| \frac{\omega}{\underline{I}_{con}} \right| = k_{\underline{I}_{con}}, \omega \quad (3.36)$$

be satisfied and, secondly, that the sign of the control current \underline{I}_{con} be the same as that of the input angular velocity ω . When these conditions are met, the moment created by the microsyn-torquer will be equal in magnitude and opposite in direction to the gyroscopic moment occurring when there is an input angular

velocity ω . As a result, the floating gyroassembly will be in equilibrium and the output voltage U_{out} will therefore remain constant.

It ensues directly from Eq. (3.36) that from the size of the current I_{con} required by the secondary winding of the microsyn-torquer for the output voltage U_{out} to remain constant (for example, equal to zero) we can judge the magnitude of the input angular velocity ω . In this case the value of the angular velocity ω will be determined from the equality

$$\omega = k_{I_{con}} I_{con} \quad (3.37)$$

The sign of ω will be the same as that of the current I_{con} .

The amplification factor $k_{I_{con}}$ has the following meaning in addition. Numerically it is equal to the angular velocity ω to which the application of a current I_{con} of one ampere to the microsyn-torquer is equivalent in its action on the floating gyroassembly.

Expression (3.32) for $k_{I_{con}}$ is sometimes more conveniently represented in a slightly different form. Let us substitute Eq. (3.30) into (3.32) and introduce the amplification factor

$$k_{I_{con}} = \frac{K_{L_{con}} \dot{\theta}_{out}}{K_{\omega} \dot{\theta}_{out}} = \frac{K_{L_{con}}}{K_{\omega}} = \frac{C_T}{H} \frac{r_{ad} \omega_{cc}}{a^2} \quad (3.38)$$

we obtain as a result

$$k_{I_{con}} = k_{I_{ex}} I_{ex} \quad (3.39)$$

The amplification factor $k_{I_{ex}} I_{con}$ is numerically equal to the angular velocity to which the application of currents I_{ex} and I_{con} , the product of which is 1 amp²,

is equivalent in its action on the floating gyroassembly. The experimental value of the factor $k_{\dot{\gamma}, \omega} I_{con}$ for floating integrating gyroscope Type 10⁴ No. 79 is given in Table 2 (Chapter II, Sec. 1).

2. Amplification factor $k_{\ddot{\gamma}, \omega}$. Let us consider that $I_{con} = 0$ and that the value $k_{M_1, \omega} \frac{M_1}{\omega}$ is insignificantly small compared with unity. Furthermore, let us assume that Equalities (3.35) are satisfied. Then, as in the previous case, it follows from Eq. (3.31) that for $\dot{U}_{out} = \ddot{U}_{out} = 0$, it is first necessary to satisfy the equality

$$\left| \frac{\omega}{\dot{\gamma}} \right| = k_{\dot{\gamma}, \omega} \quad (3.40)$$

and, secondly, for the signs of the input angular velocity ω and the the angular acceleration of the instrument housing $\ddot{\gamma}$ to be equal. When these conditions are met, the floating gyroassembly will be stationary with respect to the instrument housing and, consequently, the output voltage U_{out} will be constant. In this case the angular velocity ω will be

$$\omega = k_{\dot{\gamma}, \omega} \ddot{\gamma} \quad (3.41)$$

Thus, the amplification factor $k_{\ddot{\gamma}, \omega}$ is equal to the angular velocity ω , to which the rotation of the instrument housing about the x axis with an angular velocity of 1 rad/sec² is equivalent in its action on the floating gyroassembly.

The experimental value of the factor $k_{\ddot{\gamma}, \omega}$ for floating integrating gyroscope Type 10⁴ No. 79 is given in Table 2 (Chapter II, Sec. 1).

3. Amplification factor $k_{M_1, \omega}$. Let us consider that Eqs. (3.35) are satisfied, that the current $I_{con} = 0$, and that the angular velocity of the instrument housing $\dot{\gamma} = 0$. Then, as follows from Eq. (3.31), in order that $\ddot{U}_{out} = \dot{U}_{out} = 0$, it is first necessary that the equality

$$\left| \frac{\omega}{M_i} \right| = k_{M_i} \quad (3.42)$$

be satisfied, and, secondly, that the signs of the input angular velocity ω and moment M_i be the same. When these conditions are met, the floating gyroassembly will remain stationary with respect to the instrument housing, and consequently, the output voltage U_{out} will be constant. In this case the angular velocity will be

$$\omega = k_{M_i} M_i \quad (3.43)$$

The amplification factor k_{M_i} is equal to the angular velocity ω to which the application of a moment M_i of 1 gf-cm about its x axis is equivalent in its action on the floating gyroassembly.

Thus the work of the floating integrating gyroscope is defined by Eq. (3.31). We should point out that if the rate of change of the output voltage is taken as the output value of the instrument, i.e. \dot{U}_{out} , then Eq. (3.31) will be transformed into an equation of the first order, that is to say the work of the integrating gyroscope will be defined by a differential equation of the first order.

Section 3. Transfer Function and Frequency Characteristic of the Floating Integrating Gyroscope

Assuming in Eq. (3.31) for the floating integrating gyroscope that $\Delta'_g = \Delta'_t = 0$, i. e. considering that the output voltage U_{out} of the microsyn-pickoff is determined by Eq. (3.11) when $K_g, U_{out} = \text{const}$, we can rewrite the equation in the form

$$T\ddot{U}_{out} + \dot{U}_{out} = K_{out} \dot{U}_{in} [-k_{I, out} \dot{I}_{in} - k_{\dot{I}, out} \ddot{I}_{in} - k_{M, out} \dot{M}_I] \quad (3.44)$$

and we will consider that all the Eqs. (3.35) are satisfied. Equation (3.44) is the differential equation for the floating integrating gyroscope, given an ideally working microsynchronizer. Using the differential symbols,

$$p = \frac{d}{dt}, \quad p^2 = \frac{d^2}{dt^2},$$

we can rewrite Eq. (3.44) in the following form as an operator:

$$(Tp^2 + p)U_{out} = K_{out} \dot{U}_{in} [-k_{I, out} \dot{I}_{in} - k_{\dot{I}, out} \ddot{I}_{in} - k_{M, out} \dot{M}_I].$$

Dividing this equation by $Tp^2 + p$, we obtain

$$U_{out} = W_{i.e.}(p) [-k_{I, out} \dot{I}_{in} - k_{\dot{I}, out} \ddot{I}_{in} - k_{M, out} \dot{M}_I], \quad (3.45)$$

where

$$W_{i.e.}(p) = \frac{K_{out} \dot{U}_{in}}{p(Tp + 1)} \quad (3.46)$$

is the transfer function of the floating integrating gyroscope.

We should point out that under working conditions a certain small, and generally variable, voltage of an indeterminate nature (caused by the factors mentioned earlier) is added algebraically to the voltage U_{out} as determined from Eq. (3.45).

To obtain the frequency characteristic of the floating integrating gyroscope we will assume that we have a steady state in which the output voltage U_{out}

changes according to a harmonic law with a frequency of \underline{f} cps, so that

$$U_{out} = U_{out} e^{j2\pi f t},$$

where $2\pi f$ is the angular frequency of oscillation. Then

$$\frac{dU_{out}}{dt} = j2\pi f U_{out}.$$

Using the differential $p = \frac{d}{dt}$, we can rewrite this equality in the form

$$pU_{out} = j2\pi f U_{out}.$$

From this we find that for steady-state harmonic oscillation of the voltage U_{out}

$$p = \frac{d}{dt} \rightarrow j2\pi f.$$

Substituting this value of p into Formula (3.46), we obtain the following expression for the frequency characteristic of the floating integrating gyroscope:

$$\begin{aligned} W_{ig}(jf) &= \frac{K_{out} U_{out}}{j2\pi f (j2\pi/T + 1)} \\ &= \frac{K_{out} U_{out}}{2\pi f \sqrt{1 + (2\pi/T)^2}} e^{-j \left[\arctan(2\pi/T) + \frac{\pi}{4} \right]}. \end{aligned} \quad (3.47)$$

Multiplying the numerator and denominator in Expression (3.47) by \underline{T} , and introducing the designations

$$q = fT \quad (3.48)$$

$$A(f) = \frac{TK_{out} U_{out}}{2\pi q \sqrt{1 + (2\pi q)^2}}. \quad (3.49)$$

$$\varphi(f) = - \left[\arctan(2\pi f) + \frac{\pi}{2} \right]. \quad (3.50)$$

the frequency characteristic of the floating integrating gyroscope can be further represented in the following form:

$$W_{\text{out}}(f) = A(f) e^{j\varphi(f)}. \quad (3.51)$$

Expression (3.49) represents the amplitude-frequency characteristic of the floating integrating gyroscope. It gives the ratio of the amplitudes of the output (voltage U_{out}) and input values of the gyroscope in a steady state with the input value varying harmonically with a frequency f . The value $A(f)$ can also be regarded as the amplification factor of the floating integrating gyroscope when an effect varying harmonically with frequency f is impressed upon its input, for example, when the input angular velocity is

$$\omega = \omega_{\text{max}} \sin 2\pi ft.$$

Expression (3.50) is the phase-frequency characteristic of the floating integrating gyroscope. It gives the phase shift of the output value with respect to the input value under identical conditions.

If the amplitude of the effect at the input of the integrating gyroscope is equal to unity, $A(f)$ is numerically equal to the amplitude of the steady-state oscillations of the output voltage U_{out} , and $\varphi(f)$ is equal to the angle of the phase shift of U_{out} in relation to the input value. It follows from this and from Eq. (3.45) that the basic input values of the floating integrating gyroscope are the angular input velocity ω and the control current I_{con} of the microsynchronizer,

while the subsidiary values are the angular acceleration of the instrument housing $\ddot{\gamma}$ and the moment \underline{M}_1 .

For practical purposes Expression (3.49) is sometimes more conveniently represented in the form

$$A(f) = A_1 A_2(f), \quad (3.52)$$

where

$$A_1 = TK_{\omega} \dot{\omega}_{out} \quad (3.53)$$

$$A_2(f) = \frac{1}{2\pi q \sqrt{1 + (2\pi q)^2}} \quad (3.54)$$

Section 4. Relative Dimensionless Values

Let us look at the relative dimensionless values by means of which the performance of a floating gyroscope (both integrating and differentiating) in a steady state can be conveniently assessed from test results.

These values are:

- i) the relative dimensionless amplification factor,
- ii) the relative error of the output value, and
- iii) the relative dimensionless angular velocity.

Let us consider these values.

We will denote the value reaching the input as x_{in} , and the value obtained at the output as x_{out} . We will consider that, under ideal circumstances, in the steady state the output value is directly proportional to the input value, i.e.

$$\underline{x}_{out} = K_{\underline{x}_{in}} \underline{x}_{in}, \quad \underline{x}_{out} \underline{x}_{in},$$

where the amplification factor

$$K_{\underline{x}_{in}}, \underline{x}_{out} = \text{const.}$$

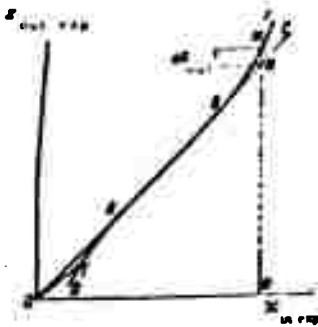


Fig. 3.4. Diagram aiding determination of relative dimensionless values used in assessing performance of floating integrating gyroscopes in the steady state.

Graphically we can represent this dependence, which for the sake of brevity we will simply call the characteristic, by a straight line through the origin of the coordinates; for example, the straight line OC (Fig. 3.4). The angular coefficient of this line will be equal to the amplification factor

$K_{\underline{x}_{in}}, \underline{x}_{out}$. Next, let the graph of the effective dependence of \underline{x}_{out} on \underline{x}_{in} ,

determined experimentally, be shown by the curve DABF (Fig. 3.4). The values of \underline{x}_{in} and \underline{x}_{out} along the axes are

marked "exp" to show their experimental origin. Let us consider that within the sector AB the effective characteristic DABF is proportional to, and to a great degree of accuracy coincides with, the theoretically proportional characteristic OC.

The amplification factor for any arbitrarily chosen point on the actual characteristic, which we shall also mark with "exp", will be equal to the ratio of the coordinates of this point, i.e.

$$(K_{x_{in}, x_{out}})_{exp} = \frac{x_{out, exp}}{x_{in, exp}} = \left(\frac{x_{out}}{x_{in}} \right)_{exp} \quad (3.55)$$

In other words, the amplification factor $(K_{x_{in}, x_{out}})_{exp}$ for any given point on the effective characteristic is equal to the angular coefficient of a straight line drawn from that point to the origin of the coordinates. For example, for the point E (Fig. 3.4) the factor is equal to the angular coefficient of the line OE.

For all the points on the sector AB the factor $(K_{x_{in}, x_{out}})_{exp}$ is the same and we shall call this value the calibration value and denote it $(K_{x_{in}, x_{out}})_{cal}$. For all points on the actual characteristic DABF outside the sector AB the factor value will be different.

For a quantitative estimation of the deviation of the values of the amplification factor $(K_{x_{in}, x_{out}})_{exp}$ from its calibration value we will introduce the concept of the relative dimensionless amplification factor

$$(K_{x_{in}, x_{out}})_{rel} = \frac{(K_{x_{in}, x_{out}})_{exp}}{(K_{x_{in}, x_{out}})_{cal}} \quad (3.56)$$

From what has gone before it follows that the value of this factor for any point on the actual characteristic is equal to the ratio of the angular coefficient of a straight line drawn from the origin of the coordinates to that point to the angular coefficient of a straight line passing through the origin of the coordinates and coinciding with the proportional sector of the effective characteristic. For all points on the proportional sector of the effective characteristic this factor is equal to unity.

The relative dimensionless amplification factor can also be interpreted in the following way. Let us write the value $(K_{x_{in}, x_{out}})_{exp, rel}$ for the point M, for example (Fig. 3.4)

$$(K_{x_{out}})_{exp} = \frac{\frac{NM}{ON}}{\frac{NH}{ON}} = \frac{NM}{NH} = \frac{x_{out,exp}}{x_{out}}. \quad (3.57)$$

It follows from this equality and from the graph in Fig. 3.4 that the relative dimensionless amplification factor is equal to the ratio of the actual output value to that which would be obtained if the dependence between the input and output values were proportional.

The absolute error Δx_{out} in the output value, obtained at any value of the input value is

$$\Delta x_{out} = x_{out,exp} - x_{out}.$$

Here, as before, x_{out} is the output value which would be obtained if the characteristic were proportional; $x_{out,exp}$ is the effective output. Dividing the expression for Δx_{out} by x_{out} , we arrive at an expression for the relative error $\epsilon_{x_{out}}$ in the output value:

$$\epsilon_{x_{out}} = \frac{\Delta x_{out}}{x_{out}} = \frac{x_{out,exp}}{x_{out}} - 1. \quad (3.58)$$

The sign of $\epsilon_{x_{out}}$ is the same as that of Δx_{out} . Consequently, the relative error $\epsilon_{x_{out}}$ in the output value is positive for sectors of the effective characteristic lying above the ideal proportional characteristic (the line passing through the origin of the coordinates and for practical purposes coinciding with the proportional sector of the effective characteristic), and negative for sectors lying below it.

It is clear that this error is zero for the proportional sector of the actual characteristic. For example, for the sector AB (see Fig. 3.4) $\epsilon_{x_{out}} = 0$. For the remaining sectors of DABF the relative error is

$$\epsilon_{\underline{x}_{out}} \neq 0.$$

Since both for floating gyroscopes as a whole and the individual parts of them we have considered, the dependence of the output value on the input value must be proportional, $\epsilon_{\underline{x}_{out}}$, just as the relative dimensionless amplification factor, describes the deviation of the effective characteristic from the required proportional dependence.

Substituting Eq. (3.57) into Expression (3.58), we find the following formula which establishes the dependence of the relative error $\epsilon_{\underline{x}_{out}}$ of the output value on the relative dimensionless amplification factor $(K_{\underline{x}_{in}}, \underline{x}_{out})_{exp. rel}$

$$\epsilon_{\underline{x}_{out}} = (K_{\underline{x}_{in}}, \underline{x}_{out})_{exp. rel} - 1. \quad (3.59)$$

From this

$$(K_{\underline{x}_{in}}, \underline{x}_{out})_{exp. rel} = 1 + \epsilon_{\underline{x}_{out}}. \quad (3.60)$$

Let us now introduce the concept of the relative angular velocity $\omega_{exp. rel}$ defining it by the equality

$$\omega_{exp. rel} = \frac{\omega_{exp}}{\omega_{cal}}, \quad (3.61)$$

where ω_{exp} is any value of the angular velocity arrived at by measurement in testing the gyroscope, and

ω_{cal} is a certain constant value of the angular velocity taken as the calibration value.

Experimentally obtained graphs of the dependence of the relative amplification factors $(K_{\underline{x}_{in}}, \underline{x}_{out})_{exp. rel}$ and relative errors $\epsilon_{\underline{x}_{out}}$ in the output

values on the relative angular velocity $\omega_{\text{exp. rel}}$ are the basic static characteristics of floating gyroscopes.

Section 5. Floating Integrating Gyroscopes Operating in the Steady State

Let us define the steady state as the working conditions under which $\ddot{U}_{\text{out}} = 0$ and $\dot{U}_{\text{out}} = \text{const.}$ Taking it that in Eq. (3.31) $\ddot{U}_{\text{out}} = 0$, we obtain the following equation which describes the steady-state operation of a floating integrating gyroscope:

$$\dot{U}_{\text{out}} = K_{\omega} \dot{U}_{\text{out}} \left(1 + \frac{\Delta_{\dot{\gamma}}}{K_{\dot{\gamma}} \dot{U}_{\text{out}}} \right) [\omega - k_{I_{\text{con}}} I_{\text{con}} - k_{\dot{\gamma}} \ddot{\gamma} - k_{M_{\dot{\gamma}}} M_{\dot{\gamma}}] + \Delta_{\dot{\gamma}} \quad (3.62)$$

Assuming that in this equation $\Delta_{\dot{\gamma}} = \Delta_{\dot{t}} = M_{\dot{t}} = 0$, we obtain the equation describing the steady state of the ideal instrument.

$$\dot{U}_{\text{out}} = K_{\omega} \dot{U}_{\text{out}} (\omega - k_{I_{\text{con}}} I_{\text{con}} - k_{\dot{\gamma}} \ddot{\gamma}). \quad (3.63)$$

From this, when $I_{\text{con}} = \ddot{\gamma} = 0$, we obtain

$$\dot{U}_{\text{out}} = K_{\omega} \dot{U}_{\text{out}} \omega, \quad (3.64)$$

i.e. in the steady state \dot{U}_{out} is directly proportional to ω . Integrating (3.64) under zero initial conditions, and keeping it in mind that in this equation $\omega = \text{constant}$, since, as agreed $\dot{U}_{\text{out}} = \text{const.}$, we have

$$U_{\text{out}} = K_{\omega} \omega t, \quad U_{\text{out}} \propto t.$$

If the time constant T is small enough, Eqs. (3.62), (3.63) and (3.64) are valid in practice even if $\omega \neq \text{constant}$. In such a case integration of Eq. (3.64) gives

$$U_{out} = K_{\omega} \int \omega dt. \quad (3.65)$$

Equations (3.64) and (3.65) describe the work of an ideal floating integrating gyroscope with a small value T and without a servodrive.

For the reasons mentioned in Chapter I, Sec. 6, the floating integrating gyroscope is usually only used, with a servodrive. Hence, from now on when discussing the steady state, we refer to the steady state of a floating integrating gyroscope coupled with a servodrive.

It was shown in Chapter I, Sec. 7 that when a floating integrating gyroscope with a servodrive functions in the steady state, a certain constant voltage U_{out} is created at the output, which is necessary and sufficient for the system to work properly. Thus, when functioning with a servodrive in the steady state $\dot{U}_{out} = 0$.

When $\dot{U}_{out} = 0$, and it is taken into account that in a normal instrument

$$K_{\omega} u_{out} \left(1 + \frac{\Delta_p}{K_{\theta} U_{out}} \right) \neq 0, \quad \text{Eq. (3.62) assumes the form}$$

$$0 = -k_{con} I_{con} - k_{\gamma} \ddot{\gamma} - k_{M, \omega} M_{\gamma} + \frac{\Delta_p}{K_{\omega} U_{out} \left(1 + \frac{\Delta_p}{K_{\theta} U_{out}} \right)}. \quad (3.66)$$

From this equation it is clear that when $\dot{U}_{out} = 0$, i.e. when $U_{out} = \text{const}$, Δ'_p only influences the work of the instrument if $\Delta'_t \neq 0$. It is therefore very important to ensure that $\Delta'_t = 0$, or in other words that the voltage Δ [see (3.13)] should not depend on time.

Let us assume that the acceleration $\ddot{\gamma} = 0$. Then, solving Eq. (3.66) with respect to $k_{I, \text{con}, \omega}$, we obtain

$$k_{I, \text{con}, \omega} = \frac{\omega}{I_{\text{con}}} \left(1 - k_{M, \text{con}} \frac{M_1}{\omega} + \frac{\Delta_1'}{U_{\text{out}, \omega}} \right), \quad (3.67)$$

where

$$\dot{U}_{\text{out}, \omega} = K_{\omega, U_{\text{out}}} \left(1 + \frac{\Delta_2'}{K_{K, U_{\text{out}}}} \right) \omega.$$

The value $\dot{U}_{\text{out}, \omega}$ can be regarded as the rate of change of the output voltage U_{out} caused by the angular velocity ω alone.

Equation (3.67) is the equation for the steady spatial-integration regime, when the floating integrating gyroscope is working as the sensing component of the spatial integrator, shown diagrammatically in Fig. 2.19. This equation has been expressed in a suitable form for evaluation of the amplification factor $k_{I, \text{con}, \omega}$, which is the basic value characterizing the gyroscope working in the spatial-integration regime.

Let us clarify this point. The spatial-integration regime, as explained earlier, is the achievement of rotation of the instrument housing about the input axis with the desired angular velocity ω by impressing a current I_{con} on the control winding of the microsyn-corrector. Hence this regime is characterized by the dependence of ω on I_{con} . From (3.67), when $M_1 = \Delta_1' = 0$ this dependence appears as

$$\omega = k_{I, \text{con}} I_{\text{con}}$$

and, consequently, is defined by the factor $k_{I, \text{con}, \omega}$. When $M_1 \neq 0$ and $\Delta_1' \neq 0$, we have from (3.67)

$$\omega = \frac{k_{I_{con}, \omega}}{1 - k_{M_1, \omega} M_1 + \frac{\Delta_1'}{U_{out, \omega}}}$$

i.e. in this case the dependence of ω on I_{con} is determined by the values of the factor

$$k'_{I_{con}, \omega} = \frac{k_{I_{con}, \omega}}{1 - k_{M_1, \omega} M_1 + \frac{\Delta_1'}{U_{out, \omega}}} \quad (3.68)$$

It is not possible to determine the value of this factor theoretically since the values of M_1 and Δ_1' are indeterminate. It can only be found experimentally for which purpose we have to find the ratio $\frac{\omega_{exp}}{I_{con, exp}}$, which we will denote $\left(\frac{\omega}{I_{con}}\right)_{exp}$. Clearly, the value of this ratio will be equal to $k'_{I_{con}, \omega}$. The value thus obtained can be conveniently used as the experimental value of $k'_{I_{con}, \omega}$, which will relieve us of the need to bring in another factor and will enable us to study and take into account experimentally possible deviations from its nominal values which may also occur when $M_1 = \Delta_1' = 0$. Thus, taking the ratio $\left(\frac{\omega}{I_{con}}\right)_{exp}$ as the experimental value of $k'_{I_{con}, \omega}$, which we shall mark with "exp," we obtain

$$(k'_{I_{con}, \omega})_{exp} = \frac{\omega_{exp}}{I_{con, exp}} = \left(\frac{\omega}{I_{con}}\right)_{exp}$$

The value of the factor $(k'_{I_{con}, \omega})_{exp}$ determined when $M_1 \neq 0$ and/or $\Delta_1' \neq 0$, will not be equal to the value which is determined from Eq. (3.32). In this case $(k'_{I_{con}, \omega})_{exp}$ will be equal to $k'_{I_{con}, \omega}$, determined from Formula (3.32), divided by the parenthesis in the right-hand side of Eq. (3.67), i.e. will be determined

by Formula (3.68). In this way, if none of the terms of Formula (3.67) can be ignored, for $(k_{I_{\text{con}}, \omega})_{\text{exp}}$ we obtain the expression

$$(k_{I_{\text{con}}, \omega})_{\text{exp}} = \left(\frac{\omega}{I_{\text{con}}, \text{exp}} \right) = \frac{k_{I_{\text{con}}, \omega}}{1 - k_{M_{\text{I}}, \omega} \frac{M_{\text{I}}}{\omega} + \frac{\Delta_{\text{I}}}{U_{\text{con}}, \omega}}. \quad (3.69)$$

In every integrating gyroscope used in practice the amplification factor $(k_{I_{\text{con}}, \omega})_{\text{exp}}^*$ will vary with I_{con} and ω . In a quantitative evaluation of this variation it is convenient to use the concept of the relative dimensionless amplification factor which, according to Formula (3.56), in the given case will be

$$(k_{I_{\text{con}}, \omega})_{\text{rel}} = \frac{(k_{I_{\text{con}}, \omega})_{\text{exp}}}{(k_{I_{\text{con}}, \omega})_{\text{cal}}}, \quad (3.70)$$

where the calibration value $(k_{I_{\text{con}}, \omega})_{\text{exp}}$, determined experimentally, is

$$(k_{I_{\text{con}}, \omega})_{\text{cal}} = \frac{\omega_{\text{cal}}}{I_{\text{con}, \text{cal}}} = \left(\frac{\omega}{I_{\text{con}, \text{cal}}} \right). \quad (3.71)$$

It is advisable to determine the value $(k_{I_{\text{con}}, \omega})_{\text{cal}}$ under conditions where the following inequalities are satisfied:

$$\left| k_{M_{\text{I}}, \omega} \frac{M_{\text{I}}}{\omega} \right|_{\text{max}} \ll 1 \quad \text{and} \quad \left| \frac{\Delta_{\text{I}}}{U_{\text{con}}, \omega} \right|_{\text{max}} \ll 1,$$

i.e. when the influence of M_{I} and Δ_{I} are insignificantly small. In this case $(k_{I_{\text{con}}, \omega})_{\text{cal}}$ is in practice equal to the theoretical value of $k_{I_{\text{con}}, \omega}$, taken

*Translator's note. In the original, this factor is usually written $(k_{I_{\text{con}}, \omega})_{\text{exp}}$. Occasionally, it is more accurately rendered as $(k_{I_{\text{con}}, \omega})_{\text{exp}}$; we have followed the original in all cases.

in all the previous arguments as constant. Proceeding from Eq. (3.32), the theoretical value of $k_{I_{con}, \omega}$ is

$$k_{I_{con}, \omega} = \frac{K_{I_{con}, M_t}}{H} \quad (3.72)$$

It is also possible, however, to have cases when this factor will not be constant. For example, if the core of the microsynchronizer becomes saturated, the dependence of the moment M_t , created by it, on the current I_{con} creating it will cease to be proportional. Hence, in the given case the amplification factor K_{I_{con}, M_t} will become variable. This, as can be seen from Eq. (3.72), gives rise to variability of the factor $k_{I_{con}, \omega}$ as well. In view of this, we will mark the factor $k_{I_{con}, \omega}$ and the coefficients through which it is expressed with the index "cur" (current value) in order to cover all feasible values, when considering the factor $(k_{I_{con}, \omega})_{exp. rel}$, and will determine it in accordance with (3.72) by the equality

$$k_{I_{con}, \omega} = (k_{I_{con}, \omega})_{cur} = \frac{(K_{I_{con}, M_t})_{cur}}{H_{cur}} \quad (3.73)$$

In practice, we should choose as $(k_{I_{con}, \omega})_{cal}$ a value of $(k_{I_{con}, \omega})_{exp}$ which corresponds to the working range, i.e. the range over which the angular velocity ω_{exp} is for practical purposes proportional to the current $I_{con. exp}$. In this range the factor $(k_{I_{con}, \omega})_{exp}$ is constant to a sufficiently accurate degree and almost equal to the theoretical value $k_{I_{con}, \omega}$, determined by Eq. (3.72). Therefore, following Eq. (3.72), we can write

$$(k_{I_{con}, \omega})_{cal} = \frac{(K_{I_{con}, M_t})_{cal}}{H_{cal}} \quad (3.74)$$

Since in the general case $(k_{I_{con}, \omega})_{exp}$ is determined by Eq. (3.69), substituting it into Formula (3.70), we obtain

$$(k_{I_{con}, \omega})_{exp. rel} = \frac{k_{I_{con}, \omega}}{(k_{I_{con}, \omega})_{cal}} \frac{1}{1 - k_{M_{i, \omega}} \frac{M_i}{\omega} + \frac{\Delta_i}{U_{out}}}$$

If, instead of $(k_{I_{con}, \omega})_{cal}$, we substitute here its value as obtained from Eq. (3.74), mark $k_{I_{con}, \omega}$ with the index "cur" and substitute its value (3.73), we obtain

$$(k_{I_{con}, \omega})_{exp. rel} = \frac{(K_{I_{con}, M_i})_{cur}}{(K_{I_{con}, M_i})_{cal}} \frac{H_{cal}}{H_{cur}} \frac{1}{1 - k_{M_{i, \omega}} \frac{M_i}{\omega} + \frac{\Delta_i}{U_{out}}} \quad (3.75)$$

The factor $(k_{I_{con}, \omega})_{exp. rel}$ obtainable from this expression has the three following characteristic regions.

I. Working region. In this region

$$\frac{(K_{I_{con}, M_i})_{cur}}{(K_{I_{con}, M_i})_{cal}} \approx 1; \quad \frac{H_{cal}}{H_{cur}} \approx 1 \quad (\text{in practice this condition is always satisfied});$$

$$\left| k_{M_{i, \omega}} \frac{M_i}{\omega} \right|_{max} \ll 1; \quad \left| \frac{\Delta_i}{U_{out}} \right|_{max} \ll 1 \quad (3.76)$$

and, consequently,

$$(k_{I_{con}, \omega})_{exp. rel} \approx 1.$$

Thus, in this region the angular velocity ω will be proportional to the control current I_{con} .

2. Region in which there is considerable influence by indeterminate (random) interference. In this region

$$\frac{(K_{I_{con} M_1})_{c,i}}{(K_{I_{con} M_1})_{c,i+1}} \approx 1; \quad \frac{H_{c,i}}{H_{c,i+1}} \approx 1.$$

But here the absolute values of both terms to be added

$$k_{M_1} = \frac{M_1}{\omega} \cdot \frac{\Delta_i}{U_{out \omega}}$$

(or one of them) are such that they cannot be ignored compared to unity, i.e. in this region the inequalities (or one of them) are not satisfied.

$$\left| k_{M_1} = \frac{M_1}{\omega} \right|_{max} \ll 1; \quad \left| \frac{\Delta_i}{U_{out \omega}} \right|_{max} \ll 1 \quad (3.77)$$

Hence in the region under consideration

$$(k_{M_1})_{c,i+1} = \frac{1}{1 - k_{M_1} = \frac{M_1}{\omega} + \frac{\Delta_i}{U_{out \omega}}} \quad (3.78)$$

and is consequently a variable of random nature because of the random nature of the moment M_1 and the indeterminate nature of Δ_i . This region can be found at very small values of the control current I_{con} , when the moment created under the effect of this current by the microsyn-torquer is commensurate with the moment M_1 , or less than it.

3. Region in which the amplification factor of the microsyn-torquer is variable (region of core saturation). In this region

$$\left. \begin{aligned} \frac{(K_{L, \omega} M_T)_{\text{sat}}}{(K_{L, \omega} M_T)_{\text{sat}}} &\neq 1; \quad \frac{H_{\text{sat}}}{H_{\text{sat}}} \approx 1; \\ \left| k_{M_T} \frac{M_T}{\omega} \right|_{\text{sat}} &\ll 1; \quad \left| \frac{d_T}{U_{\text{sat}}} \right|_{\text{sat}} \ll 1, \end{aligned} \right\} \quad (3.79)$$

by virtue of which

$$(k_{M_T, \omega})_{\text{sat}} = \frac{(K_{L, \omega} M_T)_{\text{sat}}}{(K_{L, \omega} M_T)_{\text{sat}}} \quad (3.80)$$

and is a variable.

This region appears at large values of the control current I_{con} causing saturation of the magnetic circuit of the microsyn-torquer.

To increase the working region, the second region has to be reduced and the boundary of the third region increased in every way. To reduce the second region great care in the manufacture, assembly and adjustment of the instrument is required; the materials used for its parts have to be carefully selected and current supplied from stabilized sources. The systematic interference component can be reduced by impressing a corresponding current I_{con} on the microsyn-torquer. It is possible to increase the boundary of the third region by using materials with the greatest possible induction which are not subject for practical purposes to hysteresis.

How the work of the instrument in a steady geometrical-stabilization regime is evaluated will be dealt with in the next section.

We shall not concern ourselves here with consideration of the steady state of a floating integrating gyroscope when working as an independent instrument without a servodrive and used for measuring angular displacements, since it is

not advisable on the whole to use it for this purpose. We will merely point out that this steady state is characterized by the dependence of the voltage U_{out} on the angular velocity ω , which if need be can easily be obtained from Eq. (3.62). Everything that has been said on this use of the ordinary integrating gyroscope (Chapter I, Sec. 6) applies as well to the floating integrating gyroscope. The only difference is that the floating gyroscope ensures considerably greater accuracy. Equation (3.62) takes into account the factors affecting the work of the instrument more fully than the equations in Chapter I, Sec. 6.

It can be concluded from the analysis of Formula (1.37), made earlier in Chapter I, Sec. 6, that for a floating integrating gyroscope to work the whole time in a steady state, it has to have a fairly small time constant T . To achieve this, the moment of inertia J of the floating integrating gyroscope should be as small as possible, and the specific damping moment $K_{\dot{\theta}}$, M_d as large as possible. As follows from Table 2, this condition is satisfied in practice in the case of the floating integrating gyroscope Type 10⁴, No. 79, since it has a time constant of $T = 0.0027$ sec. It should be pointed out, however, that this considerably exceeds the calculated value of 0.0017 sec. The values of T for certain other integrating gyroscopes are given in Table 5.

Section 6. Floating Integrating Gyroscopes Coupled With a Servodrive

Let us derive the equation for the uniaxial spatial integrator of angular velocity with a floating integrating gyroscope and servodrive, shown in Fig. 2.19. A block diagram of this integrator is shown in Fig. 3.5. Since the gyroscope housing is rigidly connected to the input axis 14 of the integrator by the part 7 (see Fig. 2.19), all our arguments will be conducted with reference to the instrument housing. We will call part 7, to which the gyroscope housing is directly attached, the platform.

In Fig. 3.5, as before, I_{con} is the control current impressed upon the secondary winding of the microsyn-torquer; ω_{tra} is the absolute angular velocity of the integrator housing 12 (Fig. 2.19), or, what amounts to the same, the transfer angular velocity of the gyroscope housing about the input axis y of the integrator; ω_{rel} is the angular velocity of the gyroscope housing with respect to the integrator housing about its input axis y .

The absolute angular velocity of the gyroscope housing about the input axis y of the integrator (let us recall that it coincides with the input axis of the gyroscope) will be

$$\omega = \omega_{tra} + \omega_{rel} \quad (3.81)$$

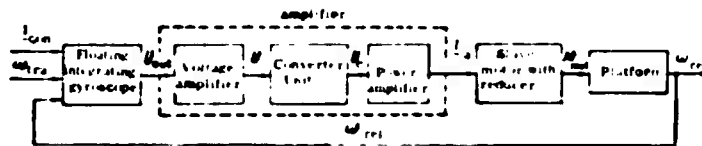


Fig. 3.5. Block-diagram of uniaxial spatial integrator of angular velocity with floating integrating gyroscope and servodrive.

Let us first look at the equations for the separate parts composing the integrator in Fig. 3.5. Let us assume the initial conditions to be zero.

1. Floating Integrating Gyroscope

Its work is described by Eq. (3.45). By replacing the angular velocity ω in this equation by its value (3.81) we obtain the equation for the floating integrating gyroscope in the form

$$U_{in} = W_{in}(p)[\omega_{tra} + \omega_{rel} - k_{I,con} I_{con} - k_{I,a} I_a - k_{M,m} M_m], \quad (3.82)$$

In Fig. 3.5, as before, I_{con} is the control current impressed upon the secondary winding of the microsyn-torquer; ω_{tra} is the absolute angular velocity of the integrator housing 12 (Fig. 2.19), or, what amounts to the same, the transfer angular velocity of the gyroscope housing about the input axis y of the integrator; ω_{rel} is the angular velocity of the gyroscope housing with respect to the integrator housing about its input axis y .

The absolute angular velocity of the gyroscope housing about the input axis y of the integrator (let us recall that it coincides with the input axis of the gyroscope) will be

$$\omega = \omega_{tra} + \omega_{rel} \quad (3.81)$$

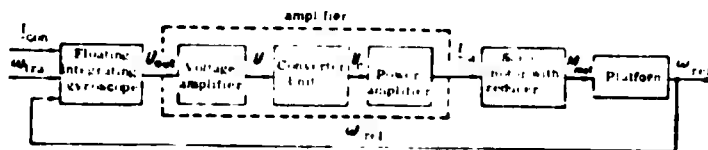


Fig. 3.5. Block-diagram of uniaxial spatial integrator of angular velocity with floating integrating gyroscope and servodrive.

Let us first look at the equations for the separate parts composing the integrator in Fig. 3.5. Let us assume the initial conditions to be zero.

1. Floating Integrating Gyroscope

Its work is described by Eq. (3.45). By replacing the angular velocity ω in this equation by its value (3.81) we obtain the equation for the floating integrating gyroscope in the form

$$U_{gsc} = W_{12}(p) [\omega_{tra} + \omega_{rel} - k_{1con} I_{con} - k_{1cs} \ddot{\varphi} - k_{1M} M_1]. \quad (3.82)$$

where the transfer function of the gyroscope $\underline{W}_{1.g.}(p)$ is determined, as before, by Eq. (3.46).

2. Amplifier

The amplifier consists of the voltage amplifier, converter unit, and power amplifier.

Taking the voltage amplifier to be linear and inertialess, we obtain

$$\underline{U} = K_{\underline{U}_{out}} \underline{U}_{out}, \quad (3.83)$$

where \underline{U}_{out} is the output voltage of the floating integrating gyroscope and the input value of the voltage amplifier, in \underline{v} ;

\underline{U} is the output voltage of the voltage amplifier in \underline{v} , and

$K_{\underline{U}_{out}}$ is the amplification factor of the voltage amplifier.

The converter unit converts the error signal (voltage \underline{U}_{out}) in accordance with a certain desired functional dependence for the purpose of ensuring that the system behaves dynamically and statically as required in the presence of controlling and disturbing effects. The equation for this unit can be written in the form

$$\underline{U}_C = \underline{W}_C(p) \underline{U}, \quad (3.84)$$

Where \underline{U}_C is the output voltage of the converter in volts, and

$\underline{W}_C(p)$ is the transfer function of the converter.

The form taken by $\underline{W}_C(p)$ depends on the system of control (adjustment) adopted.

Let us consider two possible systems of control:

Firstly, control according to the error and its time derivative. Here and in the future we will take the error to mean the angle of deviation of the gyroscope housing from its desired orientation in inertial space. As is known, the inclusion

of the time derivative of the error with respect to the control system helps to increase damping. To bring this about, the converter unit changes the incoming voltage \underline{U} into the output voltage

$$\underline{U}_c = \underline{a}\underline{U} + \underline{b}\dot{\underline{U}}, \quad (3.85)$$

where \underline{a} and \underline{b} are constant coefficients. For this the transfer function of the converter in the ideal case ought to take the form

$$W_c(p) = a \left(1 + \frac{b}{a} p \right). \quad (3.86)$$

But in practice in the case under consideration the transfer function of the converter unit, which represents a correcting circuit, takes the form

$$W_c(p) = K_{U, U_c} \frac{nT_c p + 1}{T_c p + 1}, \quad (3.87)$$

where K_{U, U_c} is the amplification factor,

T_c is the time constant in sec, and

n is the constant coefficient.

Secondly, control according to the error and the derivative and integral of the error with respect to time. The integral of the error with respect to time is included in the control system with a view to eliminating the static (steady-state) error of the system. In this case the output voltage of the converter unit should take the form

$$U_c = aU + b\dot{U} + c \int U dt. \quad (3.88)$$

for which, in an ideal case, the transfer function is

$$W_c(p) = a \left(1 + \frac{b}{a} p + \frac{c}{a} \frac{1}{p} \right).$$

where a , b , and c are constant coefficients.

It is possible to obtain a voltage proportional to the integral with respect to time of the input voltage U by using an integrating circuit as part of the converter unit. Assuming that the transfer function of the integrating circuit is for practical purposes equal to $\frac{K_{in}}{p}$ and adding it to (3.87), we obtain the transfer function of the converter unit in the following form:

$$W_c(p) = \frac{K_U \cdot K_c (nT_c p + 1) p + K_{in} (T_c p + 1)}{f_c (p + 1) p}. \quad (3.89)$$

Of the two control systems considered, the second, i.e. control according to the error and the derivative and integral of the error with respect to time is the more perfect. It is the one which should be adopted since under this system there is more possibility of fully ensuring that the integrator functions properly in actual conditions. Naturally, the entire servodrive in this case should be correctly designed and should have a fairly high amplification factor. A high amplification factor enables the servodrive to work at low output voltages U_{out} from the integrating gyroscope, or in other words, at very small angles of rotation β of the floating gyroassembly with respect to the instrument housing.

Turning to the power amplifier, let us assume that it is linear and for practical purposes inertialess, by virtue of which its equation will take the form

$$I_a = K_{U_c} U_c, \quad I_a U_c, \quad (3.90)$$

where \underline{I}_a is the output current of the power amplifier in amp, and

\underline{K}_{U_C} , \underline{I}_a is the amplification factor in amp/volt.

Successively substituting Eqs. (3.84) and (3.83) into Eq. (3.90), we obtain an equation for the whole amplifier

$$\underline{I}_a = \underline{W}_a(p) \underline{U}_{out}, \quad (3.91)$$

in which the transfer function of the amplifier

$$\underline{W}_a(p) = \underline{K}_{U_{cut}} \underline{U} \underline{K}_{U_C} \underline{I}_a \underline{W}_C(p). \quad (3.92)$$

3. Slave Motor with Reducer

Taking the slave motor to be inertialess, we obtain

$$\underline{M}_{mot} = - \underline{K}_{I_a} \underline{M}_{mot} \underline{I}_a, \quad (3.93)$$

where \underline{M}_{mot} is the moment on the output shaft of the reducer in gf-cm, and

\underline{K}_{I_a} , \underline{M}_{mot} is the amplification factor of the slave motor with the reducer in gf-cm/amp.

The minus sign in Eq. (3.93) means that the output shaft of the reducer turns the housing of the floating integrating gyroscope in the opposite direction to its absolute angular velocity ω , since positive ω produce corresponding currents \underline{I}_a , which are also taken as positive.

4. Platform

Let us consider that the only external moment which may act upon the platform about the input axis y of the integrator is the moment \underline{M}_{mot} transferred to it by

the output shaft of the reducer. The equation for the motion of the platform with respect to the base of the integrator about its input axis y can then be written in the form

$$J_{ref} \ddot{\omega}_{rel} = \underline{M}_{mot}, \quad (3.94)$$

where J_{ref} is the reference moment of inertia equal to

$$J_{ref} = J_{pl} + J'_{ref} \text{ gf-cm-sec}^2. \quad (3.95)$$

Here,

J_{pl} is the moment of inertia of the platform with all the rigidly attached parts of the construction with respect to the input axis y of the integrator in gf-cm-sec^2 , and

J'_{ref} is the sum of the moments of inertia of the slave motor rotor, referred to the output axis y of the integrator, and all the parts of the reducer rotated by it in gf-cm-sec^2 .

In the form of an operator Eq. (3.94) becomes

$$\omega_{rel} = W_{pl}(p) M_{mot} \quad (3.96)$$

where the transfer function of the platform is

$$W_{pl}(p) = \frac{1}{J_{ref}}. \quad (3.97)$$

If it is necessary to take into account the effect of any disturbing moments (which we will denote M_{dist}) on the platform, for example, the moment of imbalance, the following equation should be used instead of Eq. (3.96)

$$\omega_{rel} = W_{pl}(p) [M_{mot} + M_{2:rel}] \quad (3.98)$$

Thus, we have considered all the parts of the integrator. A functional diagram of the instrument, compiled from the equations obtained and on the assumption that the transfer function of the converter unit is defined by Eq. (3.89), is given in Fig. 3.6.

Let us now formulate the equation for the integrator - the differential equation of motion of the platform, or what is the same thing, the gyroscope housing, about the input axis y of the integrator. This equation can either be obtained by the normal methods on the basis of the functional diagram in Fig. 3.6, or by successively substituting Eqs. (3.93), (3.91), and (3.82) into Eq. (3.96). In either case the desired equation is obtained in the form

$$[W'(p) + 1] \omega_{rel} = -W'(p) [\omega_{tra} - k_{con} I_{con} - k_{1, \dots} \ddot{\gamma} - k_{M, \dots} M_1] \quad (3.99)$$

where the transfer function is

$$W'(p) = K_{ra} W_{mot}(p) W_2(p) W_{pl}(p). \quad (3.100)$$

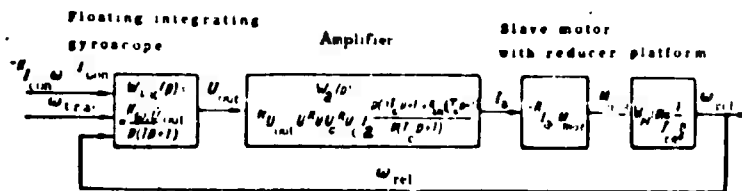


Fig. 3.6. Functional diagram of uniaxial space integrator of angular velocity with floating integrating gyroscope and servodrive.

Replacing the transfer function $W(p)$ in Eq. (3.99) by the expression for it (3.100) and applying Eqs. (3.46), (3.92), (3.89), and (3.97), this equation can be reduced to the form

$$\begin{aligned} & \left\{ p^2 (T_p + 1)(T_c p + 1) + K_0 \left[p(nT_c p + 1) + \frac{K_{in}}{K_{u, u_c}} (T_c p + 1) \right] \right\} \omega_{rel} = \\ & = -K_0 \left[p(nT_c p + 1) + \frac{K_{in}}{K_{u, u_c}} (T_c p + 1) \right] \times \\ & \quad \times (\omega_{tra} - k_{tra} - I_{con} - k_{tr} \ddot{\gamma} - k_{M_1} M_1), \end{aligned} \quad (3.101)$$

where

$$K_0 = K_{\omega, u_{con}} K_{u_{con}, u} K_{u, u_c} K_{u_c, I_{con}} K_{I_{con}, \ddot{\gamma}} K_{\ddot{\gamma}, M_1} \frac{1}{J_{rel}} \frac{1}{r_{ad} \omega_{rel}^2}. \quad (3.102)$$

As agreed, the orientation of the input axis of the integrator in space is invariable, as a result of which $\dot{\gamma} = \ddot{\gamma} = 0$. At first, however, let us take it that the acceleration $\ddot{\gamma} \neq 0$ and see, in principle, how its effect on the work of the instrument can be eliminated. If $\omega_{tra} = \text{constant}$, $I_{con} = \text{constant}$, $\ddot{\gamma} = \text{const}$ and $M_1 = \text{const}$, then, taking $p = 0$ in Eq. (3.101), we find that the work of the integrator in the steady state is described by the equation

$$\omega_{rel} = -(\omega_{tra} - k_{tra} - I_{con} - k_{tr} \ddot{\gamma} - k_{M_1} M_1). \quad (3.103)$$

In an ideal integrator the angular velocity ω_{rel} should be a function of the angular velocity ω_{tra} and the current I_{con} alone. In actual fact, as is clear from Eqs. (3.99) and (3.103), both in the transient and steady states the velocity ω_{rel} depends on the moment M_1 and the acceleration $\ddot{\gamma}$, and this leads to corresponding errors in the integrator. The moment M_1 causes drift. The components of this moment are due to various causes, but they can all be divided into two basic categories: systematic components and random components. Thus,

$$\underline{M}_1 = \underline{M}_1 \text{ syst} + \underline{M}_1 \text{ rand}, \quad (3.104)$$

where $\underline{M}_1 \text{ syst}$ is the systematic component, and

$\underline{M}_1 \text{ rand}$ is the random component of the moment \underline{M}_1 .

It follows from Eqs. (3.99) and (3.103) that if the current $\underline{I}_{\text{con}} = \underline{I}_{\text{con}} \underline{M}_1 \text{ syst}$ impressed upon the secondary winding of the microsyn-torquer is such that the equality $-k_{\underline{I}_{\text{con}}} \omega \underline{I}_{\text{con}} \underline{M}_1 \text{ syst} - k_{\underline{M}_1} \omega \underline{M}_1 \text{ syst} = 0$ is satisfied, i.e.

$$\underline{I}_{\text{con}} \underline{M}_1 \text{ syst} = - \frac{k_{\underline{M}_1} \omega}{k_{\underline{I}_{\text{con}}} \omega} \underline{M}_1 \text{ syst} \quad (3.105)$$

the effect of $\underline{M}_1 \text{ syst}$, the systematic component of moment \underline{M}_1 , will be eliminated. In other words, the systematic component of the angular velocity of drift will be eliminated. The moment $\underline{M}_1 \text{ rand}$ cannot be compensated, on the other hand. The random component of the angular velocity of drift produced by it determines the maximum performance of the integrator (stabilizer) in the region of small angular velocities.

In this way, complete compensation for the effect of the moment \underline{M}_1 is not possible due to the random components in it. In adjusting the floating integrating gyroscope every attempt should be made to reduce the moment \underline{M}_1 and particularly its random component $\underline{M}_1 \text{ rand}$.

To compensate the effect of the acceleration $\ddot{\gamma}$ on the functioning of the integrator, as is clear from Eqs. (3.99) and (3.103), a current $\underline{I}_{\text{con}} = \underline{I}_{\text{con}} \ddot{\gamma}$ should be supplied to the control winding of the microsyn-torquer such that will satisfy the equality $-k_{\underline{I}_{\text{con}}} \omega \underline{I}_{\text{con}} \ddot{\gamma} - k_{\ddot{\gamma}} \omega \ddot{\gamma} = 0$,
i.e.

$$\underline{I}_{\text{con}} = - \frac{k_{\ddot{\gamma}} \omega}{k_{\underline{I}_{\text{con}}} \omega} \ddot{\gamma}. \quad (3.106)$$

If the acceleration $\ddot{\gamma}$ changes in a random way while the integrator is working, in order to compensate for it, it is essential to measure the acceleration in some way or other and in accordance with its current values vary the current I_{con} $\ddot{\gamma}$ in such a way that Eq. (2.106) is always satisfied.

Assuming that in the integrator the moment $M_{\underline{1}}$ syst is compensated, the moment $M_{\underline{1}}$ rand is for practical purposes zero, and that the acceleration is $\ddot{\gamma} = 0$, or is compensated, instead of Eqs. (3.99) and (3.103) we obtain respectively

$$[W(p) + 1] \omega_{rel} = -W(p) [\omega_{tra} - k_{I_{con}} I_{con}] \quad (3.107)$$

$$\omega_{rel} = -\omega_{tra} + k_{I_{con}} I_{con} \quad (3.108)$$

In these equations I_{con} denotes the current supplied to the control winding of the microsyn-torquer, apart from the current supplied to it for purposes of the given compensation. This current I_{con} can be called the input current of the gyroscope or integrator.

From Eq. (3.107) for the dynamics of the integrator and Eq. (3.108) describing its statics, we can easily obtain equations for the two possible special working regimes of the integrator: the geometrical-stabilization regime ($I_{con} = 0$) and the spatial-integration regime ($\omega_{tra} = 0$). Assuming the current $I_{con} = 0$ in Eq. (3.107), we obtain the following equation describing the dynamics of the integrator in the geometrical-stabilization regime:

$$[W(p) + 1] \omega_{rel} = -W(p) \omega_{tra} \quad (3.109)$$

Correspondingly, when $I_{con} = 0$, we find from Eq. (3.108) that in the steady geometrical-stabilization regime, i.e. when $\omega_{tra} = \text{const}$,

$$\omega_{rel} = -\omega_{tra} \quad (3.110)$$

and, consequently, the orientation of the platform (the gyroscope housing) in inertial space remains unchanged. In practice, however, this equality is only fulfilled with a high degree of accuracy in the working range of the integrator. Hence the basic value describing the work of the gyroscope when tested within the integrator system in the steady geometrical-stabilization regime is the factor

$$(K_{\omega_{tra} = \omega_{rel}})_{exp} = \frac{|\omega_{rel, exp}|}{|\omega_{tra, exp}|} = \left| \frac{\omega_{rel}}{\omega_{tra}} \right|_{exp} \quad (3.111)$$

To evaluate the deviation of this factor from a particular value

$$(K_{\omega_{tra} = \omega_{rel}})_{cal} = \frac{|\omega_{rel, cal}|}{|\omega_{tra, cal}|} = \left| \frac{\omega_{rel}}{\omega_{tra}} \right|_{cal} \quad (3.112)$$

taken as the calibration value, let us introduce the relative dimensionless factor in accordance with Formula (3.56)

$$(K_{\omega_{tra} = \omega_{rel}})_{rel} = \frac{(K_{\omega_{tra} = \omega_{rel}})_{exp}}{(K_{\omega_{tra} = \omega_{rel}})_{cal}} \quad (3.113)$$

Alongside this factor, it is convenient to consider as well the relative error of the output value ω_{rel} which according to Formulas (3.58) and (3.59) will be

$$\epsilon_{\omega_{rel}} = \frac{\Delta \omega_{rel}}{\omega_{rel}} = (K_{\omega_{tra} = \omega_{rel}})_{rel} - 1 \quad (3.114)$$

Assuming $\omega_{tra} \approx 0$ in Eq. (3.107), and, consequently, $\omega_{rel} \approx \omega$, we obtain the equation

$$[W(p) + 1] \omega = W(p) k_{comp} / c_{gn} \quad (3.115)$$

which describes the dynamics of the integrator in the spatial-integration regime.

From Eq. (3.108) it follows that in the steady state with $\underline{I}_{con} = \text{constant}$

$$\omega = k_{I_{con}} \underline{I}_{con}.$$

Consequently, the steady-state spatial-integration regime is characterized by the factor $k_{I_{con}} \omega$, which has been given fairly thorough consideration above.

Equation (3.101), which describes for the general case the dynamics of the integrator (stabilizer), shows that the dynamic properties of the latter are determined by the dynamic properties of the parts composing it. The dynamics of the integrating gyroscope are characterized by the time constant T which is determined by Eq. (3.18). As a rule, it only amounts to a few milliseconds. Hence the integrating gyroscope has a much greater speed of reaction than the other components of the integrator, by dint of which its influence on the dynamics of the integrator will be insignificant. The same can be said of any other kind of device using a floating integrating gyroscope coupled with a servodrive.

The dynamic and static properties of the floating integrating gyroscope are such that when coupled with a carefully selected servodrive it is possible to solve successfully any problem to do with geometrical stabilization with respect to inertial space. Furthermore, as will be shown in the next chapter, a floating integrating gyroscope fitted with a feedback circuit can be converted into the most improved form of differentiating gyroscope. It can be stated that the floating integrating gyroscope coupled with a servodrive is capable of providing a more successful solution to many technical problems which are solved at the present time by ordinary gyroscopes, and opens up new horizons in the development of gyroscopes.

Let us now assume that a servodrive without integral control is used in the integrator, and that the only control is according to the error and its derivative

with respect to time. The transfer function of the converter unit is then determined by Eq. (3.87). Let us see how this integrator will work when the disturbing moments M_{dist} are acting on the platform. Successively substituting Eqs. (3.93), (3.91), (3.92), and (3.82) into Eq. (3.98), and assuming that $\dot{\psi}_{rand} = \ddot{\gamma} = 0$, and that the influence of M_{syst} is compensated by supplying a corresponding current to the control winding of the microsyn-torquer, we obtain the following equation for the dynamics of the integrator in the presence of the moment M_{dist} :

$$[W(p) + 1] \omega_{rel} = -W(p) [\omega_{tra} - k_{tra} \dot{\gamma}] + W_{pl}(p) M_{dist} \quad (3.116)$$

where the transfer function $W(p)$ determined by Eq. (3.100) can be presented as

$$W(p) = K_{U_{out}, U} K_{U_{in}, I} K_{I, M} W_{tra}(p) W_c(p) W_{pl}(p). \quad (3.117)$$

Equation (3.116) is valid for any control system since the transfer function $W_c(p)$ of the converter unit is contained in it in general form.

In the case concerning us $W_c(p)$ is determined by Eq. (3.87). Substituting this and also the values of the transfer functions $W_{tra}(p)$ and $W_{pl}(p)$ into Eq. (3.116), and applying the equalities

$$\omega_{tra} = p \alpha_{tra}; \quad \omega_{rel} = p \alpha_{rel},$$

where α_{tra} is the angle of rotation of the integrator housing in inertial space about the input axis y , and

α_{rel} is the angle of rotation of the gyroscope housing with respect to the integrator housing about the input axis y ,

we obtain

$$\begin{aligned}
[p^2(Tp+1)(T_c p+1) + K_0(nT_c p+1)] a_{rel} = \\
= -K_0(nT_c p+1) \left(a_{rel} - \frac{1}{p} K_{int} I_{con} \right) + \\
+ \frac{1}{p} (Tp+1)(T_c p+1) M_{dist}
\end{aligned}
\quad (3.118)$$

Here K_0 is determined as before by Eq. (3.102).

It is clear from Eq. (3.118) that if $M_{dist} = 0$, in the steady state, when $I_{con} = 0$, $a_{rel} = -a_{tra}$, that is to say, the orientation of the platform (gyro-scope housing) remains unchanged in inertial space, as in the case of the servo-drive with integral control.

Now let $a_{tra} = 0$, that is to say, let the orientation of the base of the integrator remain unchanged in inertial space, let the current $I_{con} = 0$ and the platform be subjected to the effect of the constant moment M_{dist} . Then, assuming $p = 0$ in Eq. (3.118), we find that in a state of equilibrium

$$a_{rel} = \frac{M_{dist}}{K_{st}} \quad (3.119)$$

where

$$K_{st} = K_{u,u_{int}} K_{u,u} K_{u,u_c} K_{u,c} K_{I_2} K_{I_1} K_{u_{int}} \quad (3.120)$$

This angle is the steady static error. The greater the amplification factor K_{st} , the less it will be. If a servodrive with integral control is used, this steady error will be zero.

In the practical investigation of Eq. (3.118) the terms Tp and $T_c p$ can be ignored in view of the small value of the time constants T and T_c . In this case Eq. (3.118) assumes the form

$$(T_{01}^2 p^2 + \pi T_c p + 1) z_{111} = -(\pi T_c p + 1) \left(z_{112} - \frac{1}{p} k_{111} z_{111} \right) + \frac{M_{111}}{K_{01}} \quad (3.121)$$

where the time constant

$$T_{01} = \sqrt{\frac{1}{K_0}} \dots \quad (3.122)$$

The same thing can be done in Eq. (3.101).

CHAPTER IV

THEORY OF THE FLOATING DIFFERENTIATING GYROSCOPE

The present chapter deals with the floating differentiating gyroscope, taking its specific features into account and singling out the parameters of interest from the standpoint of its practical application, testing, and analysis of the test results.

The floating differentiating gyroscope differs from the floating integrating gyroscope in that it contains an electrical or mechanical unit or arrangement which imposes upon the floating gyroassembly, when the latter deviates from its initial position (corresponding to a zero angular velocity ω), a moment proportional to the angle of deflection tending to return the gyroassembly to its initial position. As before, we will call this the elastic moment and denote it M_e . We will consider below two types of arrangement for creating an elastic moment in the floating differentiating gyroscope:

1) the gyroscope in which the elastic moment is created by a torsion rod (or any other mechanical spring or springs); this type of instrument we shall call the floating differentiating gyroscope with torsion rod;

2) the gyroscope in which the elastic moment is created by an electrical arrangement using a rigid electric feedback circuit; this instrument we shall call the floating differentiating gyroscope with feedback circuit.

Section 1. Differential Equation of Motion of the Floating
Differentiating Gyroscope With Torsion Rod

One of the variations in the design of this instrument and its working principle is given in Figs. 2.20 and 2.21. As in the case of the floating integrating gyroscope, in Fig. 2.21 \underline{x} , \underline{y} and \underline{z}_0 are the axes attached to the instrument housing, \underline{z} is the spin axis, \underline{y} is the input (measurement) axis, \underline{x} is the output axis, and \underline{z}_0 is the initial position of the spin axis \underline{z} , corresponding to a zero angular velocity ω , a zero microsyn-torquer control current I_{con} and a zero output voltage U_{out} from the microsyn-pickoff. The angle of deflection of the spin axis \underline{z} from its initial position \underline{z}_0 is represented as β . In Fig. 2.21 this angle is shown in the positive sense of its vectors.

The elastic torsion rod, shown separately in Fig. 4.1, is rigidly attached by one end to the floating gyroassembly (Figs. 2.20 and 2.21) and by the other to the instrument housing. Hence the moment imposed by it on the floating gyroassembly is in proportion to the angle β and directed in such a way as to return the gyroassembly to its initial position. Thus, the moment imposed by the torsion rod on the floating gyroassembly is

$$M_e = k\beta. \quad (4.1)$$

where k is the rigidity of the elastic torsion rod in gf-cm/rad. When the angles β are positive, the moment M_e lies along the \underline{x} -axis.

If a system of springs is used to create the elastic moment by acting on the floating gyroassembly via a lever (or levers), Eq. (4.1) will contain, instead of k , an expression for the moment imposed by them on the gyroassembly with $\beta = 1$ rad. This moment, if we follow the method adopted earlier, can conveniently be

denoted $\frac{K}{\theta} \cdot \frac{M_e}{\theta}$ and called the amplification factor of the arrangement creating the elastic moment. In future, therefore, we will use the following expression for M_e :

$$M_e = K_p \cdot \omega_e \beta. \quad (4.2)$$

In the case under consideration

$$K_p \cdot \omega_e \equiv k \quad (4.3)$$

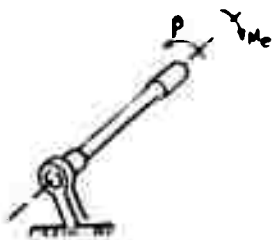


Fig. 4.1. Elastic torsion rod.

The interrelationship between the individual parts of the floating differentiating gyroscope with torsion rod is clearly illustrated in Fig. 4.2 which shows the purpose of the component parts and their interrelationship (we assume that the instrument is equipped with a microsyn-torquer). The diagram shows all

the physical values affecting the work of the instrument and determining the moments acting on the floating gyroassembly. The symbols used are the same as before.

The physical values given in Fig. 4.2 are subdivided into three groups.

1. Basic values. These are the angle θ , the angular velocities ω and $\dot{\theta}$, the current I_{con} , the voltage U_{out} and the moments I , M_d , M_t and M_e . The interconnection between these values is shown by thick lines.

2. Auxiliary values. These are the currents I'_{ex} and I_{ex} , the intake P_{gyr} and the temperature τ . The interconnection between these values is shown by broken lines.

3. Interference. These are velocity ω_{z0} and acceleration $\ddot{\gamma}$. Their interconnection is shown by lines consisting of dots and dashes.

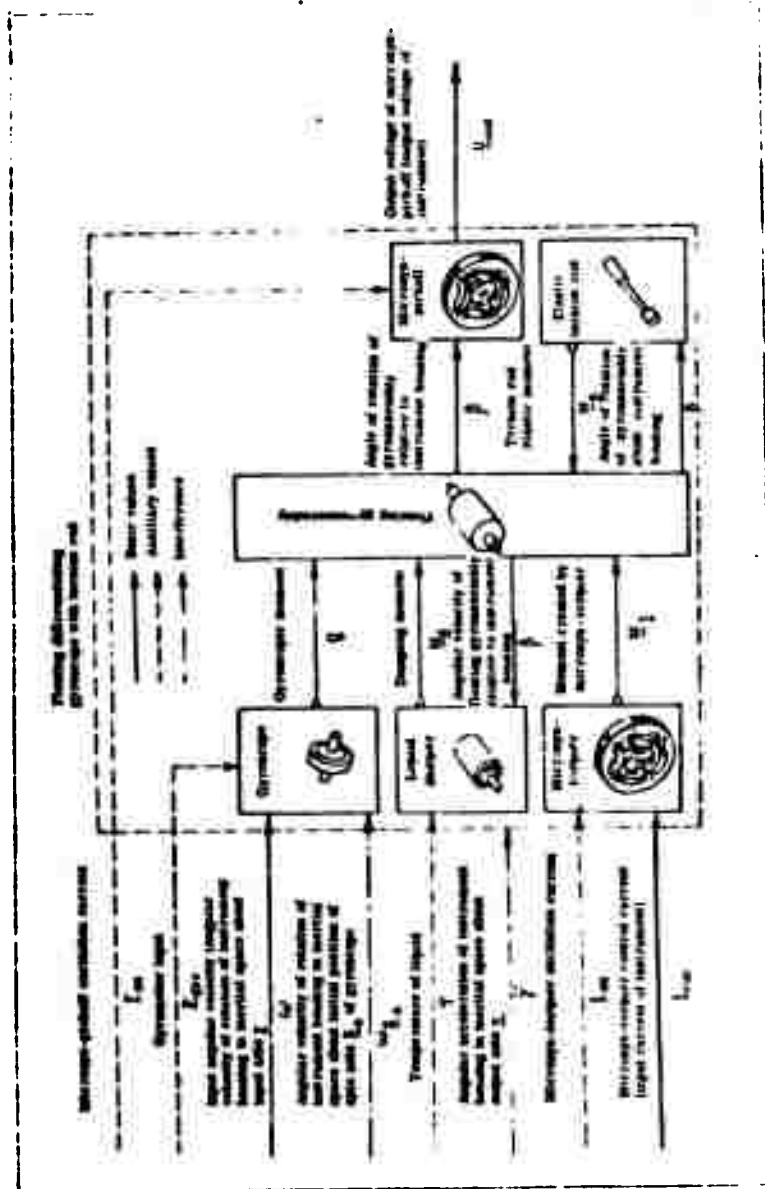


Fig. 4.2. Component parts of floating differentiating gyroscope.

The lines showing the interconnection (or influence) of the values have arrows to indicate the direction of their effect. Those of the moments have small circles on them in addition. This means that according to Newton's third law the parts which are sources of moments experience an equal and oppositely directed reaction from the parts on which they impose those moments. The moments of inertia and the components of the interference moment M_{\perp} , which inevitably arise when the instrument is functioning, have been left out of the diagram.

Let us formulate the equation of motion of the floating gyroassembly about its x axis of rotation with respect to the instrument housing. Since the only difference between the floating differentiating gyroscope we are dealing with and the integrating gyroscope considered in Chapter III is the torsion rod, to obtain a differential equation of motion we have to add to the left-hand side of Eq. (3.16) the moment M_e determined by Eq. (4.2). The differential equation of motion for the floating gyroassembly of the floating differentiating gyroscope with torsion rod will assume the following form

$$\begin{aligned} J(\ddot{\beta} + \ddot{\gamma}) + K_{\beta} M_{\beta} \dot{\beta} + K_{\gamma} M_{\gamma} \dot{\gamma} = \\ = H_0 \left(\cos \beta - \frac{\omega_y}{\omega} \sin \beta \right) - K_{t_{ex}} M_t I_{ex} - M_j. \end{aligned} \quad (4.4)$$

The numerical values of J , K_{β} , M_{β} , K_{γ} , M_{γ} = k for floating differentiating gyroscope Type 10⁴ No. 55 are given in Tables 4 and 5 (Chapter II, Section 2). The amplification factors in Eq. (4.4) will be considered constant, for which we must make

$$\begin{aligned} \frac{P}{\omega_y} = \text{const}, \quad \frac{f}{\omega_y} = \text{const}, \quad \tau = \text{const} \\ I_{ex} = \text{const}, \quad \frac{f}{\omega_t} = \text{const}. \end{aligned}$$

Dividing Eq. (4.4) by J and transposing the terms, we obtain the differential equation of motion for the floating differentiating gyroscope with torsion rod in the following form:

$$\begin{aligned} \beta + 2b\omega\beta + \omega^2\beta = \omega^2 K_{\omega, \beta} \left(\cos \beta - \frac{\omega_0}{\omega} \sin \beta \right) \omega - \\ - \omega^2 K_{I_{con}, \beta} I_{con} - \omega^2 K_{M_1, \beta} M_1. \end{aligned} \quad (4.5)$$

The constant coefficients in this equation are the following:

$$\omega_0 = \sqrt{\frac{K_{\beta, M_0}}{J}} = 2\pi f_0 \text{ rad/sec} \quad (4.6)$$

is the angular frequency of the undamped oscillations of the floating gyroassembly;
 f_0 is the frequency of the free undamped oscillations of the gyroassembly in cps
 (this numerical value for gyroscope Type 10⁴ No. 55 is given in Tables 4 and 5,
 Chapter II, Section 2).

$$b = \frac{K_{\beta, M_1}}{2J\omega_0} = \frac{K_{\beta, M_1}}{2\sqrt{JK_{\beta, M_0}}} \quad (4.7)$$

is the damping ratio of the floating gyroassembly which is the ratio of the actual
 damping factor to the critical damping factor (this numerical value for gyroscope
 Type 10⁴ No. 55 is given in Table 5, Chapter II, Section 2).

$$K_{\omega, \beta} = \frac{H}{K_{\beta, M_0}} = \frac{H}{k} \text{ ...} \quad (4.8)$$

$$K_{I_{con}, \beta} = \frac{K_{I_{con} M_1}}{K_{\beta, M_0}} = \frac{K_{I_{con} M_1}}{k} \text{ 1/amp} \quad (4.9)$$

$$K_{M_1, \beta} = \frac{1}{K_{\beta, M_0}} = \frac{1}{k} \text{ 1/ef.cm} \quad (4.10)$$

The amplification factors $K_{\omega, \beta}$; $K_{I_{con}, \beta}$ and $K_{M_1, \beta}$ describe the dependence of the
 angle β on the input angular velocity ω , the control current I_{con} of the
 microsyn-torquer and the moment M_1 respectively.

Equation (4.5) is not investigated because it is not the angle β which is of
 interest in the final analysis, but the output voltage U_{out} of the microsyn-pickoff.

Section 2. Equation for Floating Differentiating

Gyroscope With Torsion Rod

As in the case of the floating integrating gyroscope, the output voltage of the floating differentiating gyroscope \underline{U}_{out} emitted by the microsyn-pickoff is determined by Eq. (3.13). The numerical value of the amplification factor $\underline{K}_{\beta, \underline{U}_{out}}$ for floating differentiating gyroscope Type 10⁴ No. 55 is given in Table 4, (Chapter II, Section 2).

Replacing β , $\dot{\beta}$ and $\ddot{\beta}$ from Eq. (3.13), (3.14), and (3.15) in the lefthand side of Eq. (4.5), and substituting for $\underline{K}_{M_1, \beta}$ the value given by Eq. (4.10), we find the equation for the floating differentiating gyroscope with torsion rod:

$$\begin{aligned} \ddot{U}_{out} + 2\left(b\gamma_0 - \frac{\Delta_i \dot{\beta}}{K_{\beta, U_{out}} + \Delta_i}\right)\dot{U}_{out} + \gamma_0^2\left(1 + \frac{\Delta_i}{K_{\beta, U_{out}}}\right)U_{out} = \\ = \left(1 + \frac{\Delta_i}{K_{\beta, U_{out}}}\right)\left[\gamma_0^2 K_{\omega, U_{out}}\left(\cos \beta - \frac{\omega_{\Delta}}{\omega} \sin \beta\right) - \gamma_0^2 K_{I_{con}, U_{out}} I_{con} - \right. \\ \left. - K_{M_1, U_{out}} \ddot{\gamma} - \gamma_0^2 K_{M_1, U_{out}} M_1\right] + \Delta_i'' + 2b\gamma_0 \Delta_i' + \gamma_0^2\left(1 + \frac{\Delta_i}{K_{\beta, U_{out}}}\right)\Delta_i \end{aligned} \quad (4.11)$$

where

$$K_{\omega, U_{out}} = K_{\omega, \beta} K_{\beta, U_{out}} \frac{\gamma_0^2 \eta}{\gamma_0^2 \omega^2} \quad (4.12)$$

$$K_{I_{con}, U_{out}} = K_{I_{con}, \beta} K_{\beta, U_{out}} \text{ volt/amp} \quad (4.13)$$

$$K_{M_1, U_{out}} = K_{M_1, \beta} K_{\beta, U_{out}} \text{ volt/gr-sec} \quad (4.14)$$

The amplification factors $\underline{K}_{\omega, \underline{U}_{out}}$, $\underline{K}_{I_{con}, \underline{U}_{out}}$ and $\underline{K}_{M_1, \underline{U}_{out}}$ define the dependence of the output voltage \underline{U}_{out} on ω , I_{con} , and M_1 respectively. The numerical value of the factor $\underline{K}_{\omega, \underline{U}_{out}}$ for gyroscope Type 10⁴ No. 55 is given in Table 5 (Chapter II, Section 2). This factor represents the sensitivity of the floating differentiating gyroscope with torsion rod with respect to the input (measurement) angular velocity ω .

Disregarding in Eq. (4.11) the term $\frac{\Delta_p}{K_{\theta, U_{out}} + \Delta_p}$, which is small compared to the product bV_0 , which is many times greater than one, let us rewrite the equation for the gyroscope with the torsion rod in the following final form:

$$\begin{aligned} \ddot{U}_{out} + 2bV_0\dot{U}_{out} + V_0^2\left(1 + \frac{\Delta_p}{K_{\theta, U_{out}}}\right)U_{out} = V_0^2K_{\omega}U_{out}\left(1 + \frac{\Delta_p}{K_{\theta, U_{out}}}\right) \times \\ \times \left[\left(\cos\beta - \frac{\omega_{\theta}}{V_0}\sin\beta\right)\omega - k_{I, con}\omega - k_{I, \omega} - k_{M, -M}\right] + \\ + \ddot{\Delta}_p + 2bV_0\dot{\Delta}_p + V_0^2\left(1 + \frac{\Delta_p}{K_{\theta, U_{out}}}\right)\Delta_p \end{aligned} \quad (4.15)$$

where

$$k_{I, con} = \frac{K_{con}U_{out}}{K_{\omega, U_{out}}} = \frac{K_{I, con}M_{\theta}}{H} \quad \frac{\text{rad/sec}}{\text{amp}} \quad (4.16)$$

$$k_{I, \omega} = \frac{K_{\theta, U_{out}}}{V_0^2 K_{\omega, U_{out}}} = \frac{J}{H} \quad \text{sec} \quad (4.17)$$

$$k_{M, -M} = \frac{K_{M, U_{out}}}{K_{\omega, U_{out}}} = \frac{1}{H} \quad \frac{\text{rad/sec}}{\text{amp}} \quad (4.18)$$

The second expression in each of Formulas (4.16), (4.17), and (4.18) for these amplification factors are obtained by substituting the corresponding Eqs. (4.6), (4.8), (4.9), (4.10), (4.12), (4.13), and (4.14) into the first expression for the factors.

By comparing Eqs. (4.16), (4.17), and (4.18) respectively with Eqs. (3.32), (3.33), and (3.34), we see that the amplification factors $k_{I, con}\omega$; $k_{I, \omega}\omega$, and $k_{M, -M}\omega$ are the same in the case of the floating differentiating gyroscope as they are for the floating integrating gyroscope.

Section 3. Transfer Function and Frequency Characteristic of the Floating Differentiating Gyroscope With Torsion Rod

Assuming that the microsyn-pickoff is working ideally, in which case

$\Delta = \Delta' = \Delta'' = \Delta''' = 0$, and using the differential symbols

$$P = \frac{d}{dt}, \quad P^2 = \frac{d^2}{dt^2}$$

we will rewrite Eq. (4.15) in the form of an operator:

$$(p^2 + 2b_0 p + \gamma_0^2) U_{out} = \gamma_0^2 K_{in} U_{in} \left[\left(\cos \beta - \frac{\omega_0}{\omega} \sin \beta \right) - \right. \\ \left. - k_{l, out} J_{out} - k_{i, out} \bar{I} - k_{M, out} M \right].$$

Dividing this equation by $p^2 + 2b_0 p + \gamma_0^2$, we obtain

$$U_{out} = W_{e.g.}(p) \left[\left(\cos \beta - \frac{\omega_0}{\omega} \sin \beta \right) - k_{l, out} J_{out} - \right. \\ \left. - k_{i, out} \bar{I} - k_{M, out} M \right]. \quad (4.19)$$

where

$$W_{e.g.}(p) = \frac{\gamma_0^2 K_{in} U_{in}}{p^2 + 2b_0 p + \gamma_0^2} \quad (4.20)$$

is the transfer function of the floating differentiating gyroscope with torsion rod. In actual working conditions, a small, and, in the general case constant, voltage of an indeterminate nature due to the reasons given above will be added algebraically to the voltage U_{out} , determined by Expression (4.19).

Proceeding in the same way as in Chapter III, Section 3, we can obtain from Expression (4.20) the following expression for the frequency characteristic of the floating differentiating gyroscope with torsion rod:

$$W_{e.g.}(jf) = \frac{K_{in} U_{in}}{1 - p^2 + j2bp} = A(f) e^{j\varphi(f)}, \quad (4.21)$$

where

$$p = \frac{2\pi f}{\gamma_0} \text{ is the relative frequency} \quad (4.22)$$

$$A(f) = \frac{K_{in} U_{in}}{\sqrt{(1-p^2)^2 + (2bp)^2}} \quad (4.23)$$

or

$$A(f) = K_{in} U_{in} A_2(f). \quad (4.24)$$

(4.25)

$$\varphi(\omega) = -\arctan\left(\frac{2b\omega}{1-\omega^2}\right). \quad (4.26)$$

Expressions (4.23) and (4.24) are the amplitude-frequency characteristic of the floating differentiating gyroscope with torsion rod. The phase-frequency characteristic is given by Eq. (4.26). The physical meaning of these characteristics is the same as for the floating integrating gyroscope.

Section 4. Floating Differentiating Gyroscope With Torsion Rod Operating in the Steady State

Let us take the steady state to mean the working conditions under which $\ddot{U}_{out} = \ddot{U}_{out} = 0$, the control current I_{con} of the microsyn-pickoff (or there may be no pickoff at all) and the angular acceleration of the instrument housing $\ddot{\gamma}$ being equal to zero at the same time.

Taking $\ddot{U}_{out} = \ddot{U}_{out} = I_{con} = \ddot{\gamma} = 0$ in Eq. (4.15), we obtain the following equation for the steady-state operation of the floating differentiating gyroscope with torsion rod:

$$U_{out} = K_{\omega} U_{out} \left(\cos \beta - \frac{\omega_{d0}}{\omega} \sin \beta - k_{\omega i} - \frac{M_i}{\omega} \right) + \frac{\Delta_H + 2b\omega_{d0}}{\omega^2 \left(1 + \frac{\Delta_\theta}{K_\theta U_{out}} \right)} + \Delta. \quad (4.27)$$

In so doing, on the basis of Eq. (4.12) and (4.8) we have:

$$K_{\omega} U_{out} = \frac{H}{k} K_\theta U_{out} \frac{\omega_{d0}}{\text{rad/sec}}. \quad (4.28)$$

If we take $\Delta'_t = \Delta''_{tt} = 0$ in Eq. (4.27), which will be the case if the voltage Δ is not dependent on time, we will obtain the equation of equilibrium for the floating gyroassembly (on condition $I_{con} = \dot{\Psi} = 0$). The state of equilibrium which it defines occurs a short while after the instrument housing has begun to rotate with a constant input angular velocity ω . Thus, if Δ is not dependent on t , the steady state is merely the state of equilibrium of the floating gyroassembly for any constant value of the angular velocity ω when $\ddot{\Psi} = I_{con} = 0$.

But if the voltage Δ does depend on time, Eq. (4.27), strictly speaking, will not be the equation of equilibrium for the floating gyroassembly. This equation has been obtained on the basis of the condition that $\ddot{U}_{out} = \dot{U}_{out} = 0$, i.e. $U_{out} = \text{const.}$ If, however, Δ depends on time, then with the equilibrium of the floating gyroassembly which occurs when $\omega = \text{const.}$, the voltage U_{out} cannot remain constant. But since in an instrument working normally the values Δ , Δ'_t , and Δ''_{tt} are fairly small, the oscillations of the voltage U_{out} obtained when the floating gyroassembly is in a state of equilibrium will also be comparatively small. They will only have an effect to any great degree when the values of ω are small; the latter in the steady state correspond to small angles β , and, consequently, to small output voltages U_{out} . In order to reduce the relative error in the voltage U_{out} , caused by the voltage Δ and its derivatives, the factor $K_{\beta, U_{out}}$ has to be increased, but this must be done in such a way that there is no equivalent increase in Δ and its derivatives. We should note that in the gyroscopes of the Massachusetts Institute of Technology $K_{\beta, U_{out}}$ for the differentiating gyroscopes is double what it is in the integrating gyros.

Thus, when Δ depends on time, it is only possible for Eq. (4.27) to be accurately fulfilled, when the angular velocities ω vary with Δ and its derivatives.

Hence, it is vital to see to it that Δ in practice does not depend on time.

Let us assume that this is in fact the case to a high degree. Then, in Eq. (4.27) we can assume $\Delta''_{tt} = \Delta'_t = 0$, after which the equation will take the form:

$$U_{out} = K_{\omega, U_{out}} \left(\cos \beta - \frac{\omega_{z0}}{\omega} \sin \beta - k_{M, \omega} \frac{M_1}{\omega} \right) \omega + \Delta. \quad (4.29)$$

From this equation it will be clear that when

$$\cos \beta \approx 1, \quad \omega_{z0} = M_1 = \Delta = 0$$

$$U_{out} = K_{\omega, U_{out}} \omega,$$

i.e. here the dependence of U_{out} on ω in the steady state is fully determined by the factor $K_{\omega, U_{out}}$. But if $\cos \beta \approx 1, \omega_{z0} \neq 0, M_1 \neq 0, \Delta \neq 0$, then in the steady state [see (4.29)]

$$U_{out} = K_{\omega, U_{out}} \left(\cos \beta - \frac{\omega_{z0}}{\omega} \sin \beta - k_{M, \omega} \frac{M_1}{\omega} + \frac{\Delta}{K_{\omega, U_{out}} \omega} \right) \omega.$$

i.e. here the dependence of U_{out} on ω is determined by the factor values

$$K'_{\omega, U_{out}} = K_{\omega, U_{out}} \left(\cos \beta - \frac{\omega_{z0}}{\omega} \sin \beta - k_{M, \omega} \frac{M_1}{\omega} + \frac{\Delta}{K_{\omega, U_{out}} \omega} \right).$$

It is not possible to calculate the value of this factor in theory since M_1 and Δ are indeterminate; it can only be found by experiment, for which purpose we have to determine the ratio $\frac{U_{out \exp}}{\omega_{\exp}}$, which we shall denote $\left(\frac{U_{out}}{\omega}\right)_{\exp}$ (the index "exp" denotes a value found from experiment). Clearly, this ratio will be equal to the factor $K'_{\omega, U_{out}}$. The values of this factor derived in this way can be conveniently taken as the experimental values of $K'_{\omega, U_{out}}$, and we are then relieved of the need to introduce another coefficient into the discussion; we are also able to study and take into account experimentally the deviations of $K_{\omega, U_{out}}$ from its nominal value which are possible when $\cos \beta \approx 1$ and $\omega_{z0} = \frac{M_1}{\omega} = \Delta = 0$. Thus, taking the ratios $\left(\frac{U_{out}}{\omega}\right)_{\exp}$ as the experimental values of $K_{\omega, U_{out}}$, and marking them "exp," we obtain (provided none of the terms of Eq. (4.27) can be ignored) the following

$$(K_{\omega, U_{out}})_{exp} = \left(\frac{U_{out}}{\omega} \right)_{exp} =$$

$$= K_{\omega, U_{out}} \left(\cos \beta - \frac{\omega_{L_1}}{\omega} \sin \beta - k_{M, \omega} \frac{M_1}{\omega} + \frac{\Delta}{K_{\omega, U_{out}} \omega} \right).$$

In the last term on the right-hand side it may be taken that $K_{\omega, U_{out}} = U_{out}$. After substitution we obtain

$$(K_{\omega, U_{out}})_{exp} = \left(\frac{U_{out}}{\omega} \right)_{exp} \quad (4.30)$$

$$= K_{\omega, U_{out}} \left(\cos \beta - \frac{\omega_{L_1}}{\omega} \sin \beta - k_{M, \omega} \frac{M_1}{\omega} + \frac{\Delta}{U_{out} \omega} \right).$$

The numerical values of the amplification factor $(K_{\omega, U_{out}})_{exp}$ may vary with ω . For a quantitative evaluation of the variation we will use the concept of the relative dimensionless amplification factor, which, according to Formula (3.56), will be in the given case

$$(K_{\omega, U_{out}})_{exp, rel} = \frac{(K_{\omega, U_{out}})_{exp}}{(K_{\omega, U_{out}})_{cal}}, \quad (4.31)$$

where the calibration value of $(K_{\omega, U_{out}})_{exp}$ determined experimentally is

$$(K_{\omega, U_{out}})_{cal} = \frac{U_{out, cal}}{\omega_{cal}} = \left(\frac{U_{out}}{\omega} \right)_{cal}. \quad (4.32)$$

The value of $(K_{\omega, U_{out}})_{cal}$ should be determined under conditions where the angle β is so small that we can assume

$$\cos \beta \approx 1; \quad \sin \beta \approx 0$$

and where

$$\omega_{L_1} = 0, \quad \left| K_{M, \omega} \frac{M_1}{\omega} \right|_{max} < 1, \quad \left| \frac{\Delta}{U_{out} \omega} \right|_{max} < 1,$$

i.e. where the influence of angle β , the moments M_1 and the voltage Δ are insignificant.

In such a case, as is clear from the Eq. (4.30), the amplification factor $(K_{\omega}, U_{out})_{cal}$ will be in practice equal to the theoretical value of K_{ω}, U_{out} determined from Eq. (4.28) and taken in all preceding arguments as constant. It is also possible, however, to have cases when it will not be constant. For example when the core of the microsyn-pickoff is saturated, the dependence of its output voltage U_{out} on the angle θ ceases to be proportional. Hence, in the given case the amplification factor K_{θ}, U_{out} becomes variable, which, in its turn, causes variability in the factor K_{ω}, U_{out} , as is clear from Eq. (4.28). Therefore, in order to cover all feasible values of K_{ω}, U_{out} when considering $(K_{\omega}, U_{out})_{exp, rel}$, we will mark it and also the values used to express it with the subscript "cur" (current value). Then, in accordance with Equality (4.28)

$$K_{\omega, U_{out}} = (K_{\omega, U_{out}})_{cur} = \frac{H_{cur}}{h_{cur}} (K_{\theta, U_{out}})_{cur}. \quad (4.33)$$

In practice, we should choose as $(K_{\omega}, U_{out})_{cal}$ a value of the factor $(K_{\omega}, U_{out})_{exp}$ in the working range of the instrument, i.e. the range in which $U_{out, exp}$ is practically proportional to the angular velocity ω_{exp} . In this range $(K_{\omega}, U_{out})_{exp}$ is to a sufficient degree of accuracy constant and for practical purposes equal to the theoretical value of K_{ω}, U_{out} , determined by Eq. (4.28). Hence, according to Equality (4.28) we can assume

$$(K_{\omega, U_{out}})_{cal} = \frac{H_{cal}}{h_{cal}} (K_{\theta, U_{out}})_{cal}. \quad (4.34)$$

Since in the general case $(K_{\omega}, U_{out})_{exp}$ is determined by Eq. (4.30), substituting it into Formula (4.31), we obtain

$$(K_{\omega, U_{out}})_{exp, rel} = \frac{K_{\omega, U_{out}}}{(K_{\omega, U_{out}})_{cal}} \left(\cos \beta - \frac{\omega_{rel}}{\omega} \sin \beta - k_{M1} \frac{M_1}{\omega} + \frac{\Delta}{U_{out}} \right). \quad (4.35)$$

Substituting the value of $(K_{\omega}, U_{out})_{cal}$ determined by Eq. (4.34), marking $K_{\omega, U_{out}}$ with the subscript "cur" and substituting its value in (4.33), we obtain

$$(K_{\omega, U_{out}})_{exp} = \frac{H_{cur}}{H_{cal}} \frac{k_{cal} (K_{\theta, U_{out}})_{cur}}{k_{cur} (K_{\theta, U_{out}})_{cal}} \times$$

$$\times \left(\cos \beta - \frac{\omega_0}{\omega} \sin \beta - k_{M, \omega} \frac{M_1}{\omega} - \frac{\Delta}{U_{out}} \right). \quad (4.36)$$

For practical purposes $\frac{H_{cur}}{H_{cal}}$ is always roughly equal to unity, but we will leave this ratio in Formula (4.36) in its general form so that it may apply in all cases.

Analysis of Eq. (4.36) shows that at small angles β , when $\cos \beta \approx 1$, $\sin \beta \approx 0$, there are three characteristic regions of values for $(K_{\omega, U_{out}})_{exp}$ rel.

1. Working region. In this region

$$\left. \begin{aligned} \frac{H_{cur}}{H_{cal}} \approx \frac{k_{cal}}{k_{cur}} \approx \frac{(K_{\theta, U_{out}})_{cur}}{(K_{\theta, U_{out}})_{cal}} \approx 1, \\ \left| k_{M, \omega} \frac{M_1}{\omega} \right|_{max} < 1; \quad \left| \frac{\Delta}{U_{out}} \right|_{max} < 1 \end{aligned} \right\} \quad (4.37)$$

and, consequently,

$$(K_{\omega, U_{out}})_{exp} \approx 1. \quad (4.38)$$

Thus, in this case the output voltage U_{out} will be proportional to the input angular velocity ω .

If in Eq. (4.36)

$$\left| k_{M, \omega} \frac{M_1}{\omega} \right|_{max} < \cos \beta, \quad \left| \frac{\Delta}{U_{out}} \right|_{max} < \cos \beta$$

and

$$\frac{H_{cur}}{H_{cal}} \approx \frac{k_{cal}}{k_{cur}} \approx \frac{(K_{\omega, U_{out}})_{cur}}{(K_{\omega, U_{out}})_{cal}} \approx 1,$$

but the term $\frac{\omega_0}{\omega} \sin \beta$ cannot be ignored in comparison with $\cos \beta$ and $\cos \beta \approx 1$ cannot be assumed, then

$$(K_{\omega, U_{out}})_{exp} = 1 - \frac{\omega_0}{\omega} \sin \beta. \quad (4.39)$$

In this case U_{out} will not only depend on the input angular velocity ω , but also on the angular velocity ω_{z_0} , which is highly undesirable since it prevents us obtaining an idea of the angular velocity ω from the voltage U_{out} .

2. Region in which the influence of indeterminate (random) interference is considerable. In this region

$$\frac{H_{exp}}{H_{cal}} \approx \frac{k_{st}}{k_{exp}} \approx \frac{(K_{\theta, U_{out}})_{exp}}{(K_{\theta, U_{out}})_{cal}} \approx 1.$$

But the absolute values of both terms

$$k_{M_1} = \frac{M_1}{\omega} \Delta \omega \text{ and } \frac{\Delta}{U_{out}},$$

(or either one of them) are such that they cannot be ignored in comparison with unity i.e. in this region only one (or neither) of the equalities

$$\left| k_{M_1} = \frac{M_1}{\omega} \right|_{min} < 1; \quad \left| \frac{\Delta}{U_{out}} \right|_{max} \ll 1$$

is satisfied. In this region, therefore,

$$(K_{\omega, U_{out}})_{exp, rel} = 1 - k_{M_1} \frac{M_1}{\omega} + \frac{\Delta}{U_{out}}. \quad (4.40)$$

In this expression the two last terms, which are the indefinite (random) values, can be both positive and negative.

Thus, in the given region the factor $(K_{\omega, U_{out}})_{exp, rel}$ is a variable of a random nature on account of the random nature of the moment M_1 and the indeterminate character of the voltage Δ . This region occurs at small values of the input angular velocity ω when the gyroscopic moment is commensurate with or less than M_1 . The boundary of this region determines the minimum angular velocity ω_{min} which can be measured with the instrument.

3. Region in which the amplification factor of the microsyn-pickoff is a variable (region of saturation of core of microsyn-pickoff). In this region

$$\left| k_{M, \omega} = \frac{M_c}{\omega} \right|_{\max} \ll 1, \quad \left| \frac{\Delta}{U_{out}} \right|_{\max} \ll 1, \quad \frac{H_{out}}{H_{cal}} \approx \frac{k_{cal}}{k_{out}} \approx 1, \quad (4.41)$$

by virtue of which

$$(K_{\omega, U_{out}})_{cal} = \frac{(K_{\omega, U_{out}})_{out}}{(K_{\omega, U_{out}})_{cal}} \neq 1 \quad (4.42)$$

and, consequently, is a variable. This region occurs at high values of the measured angular velocity ω when the output voltage U_{out} induced in the secondary winding of the microsyn-pickoff reaches values at which there is saturation of the core. The boundary of this region determines the maximum angular velocity which the instrument can measure.

In order to increase the working region the boundary of the second region has to be reduced and that of the first region increased in every way. The former can be achieved by improving the design of the torsion rod with a view to increasing its transverse rigidity, by the greatest care in the manufacture, assembly and adjustment of the instrument, and by supplying it with power from stabilized sources. If a microsyn-torquer is used, the systematic interference component may be reduced by supplying an appropriate current I_{con} to its control winding. The second case can be made possible by using materials with high inductance which for practical purposes are not subject to hysteresis. Nevertheless, the upper boundary is still basically determined by the influence of the angular velocity ω_{z_0} , permitted, which fact requires limitation of the angle of rotation θ of the floating gyroassembly and the measured velocity ω .

Let us consider which conditions have to be fulfilled in order that the operation of the instrument under conditions of varying input angular velocity ω may correspond as closely as possible to operation in the steady state. In other words, under what conditions will the output voltage U_{out} be in practice

proportional to the angular velocity ω not only when the latter is constant, but also when it varies.

Dividing Eq. (4.15) by ψ_0^2 and assuming $\Delta'_{\theta} = \Delta'_{\dot{\theta}} = \Delta'_{\ddot{\theta}} = 0$, let us rewrite it in the form

$$T_0^2 \ddot{U}_{out} + T_1 \dot{U}_{out} + U_{out} = K_{\omega} U_{out} \left[\left(\cos \beta - \frac{\omega_{\dot{\theta}}}{\omega} \sin \beta \right) - \right. \\ \left. - k_{\omega \omega} \dot{\omega} - k_{\omega \ddot{\theta}} \ddot{\theta} - k_{M_1} M_1 \right] + \Delta, \quad (4.43)$$

where T_0 and T_1 denote the time constants

$$T_0 = \frac{1}{\omega_0} = \sqrt{\frac{J}{k}} \text{ sec.} \quad (4.44)$$

$$T_1 = \frac{2b}{\omega_0} = 2b T_0 = \frac{K_{\theta} M_d}{k} \dots \quad (4.45)$$

Clearly, for the operation of the instrument under conditions of a varying input angular velocity ω to correspond in practice to operation in the steady state, the first two terms in the left-hand side of Eq. (4.43) would have to be negligibly small compared with the third term U_{out} . For this the constants T_0 and T_1 have to be small for their part. It follows directly from Eqs. (4.44) and (4.45) that to obtain small time constants, the instrument has to be made in such a way that the moment of inertia J and the specific damping moment K_{θ} , M_d are as small as possible, and the rigidity of the torsion rod k is as large as possible. An ideal instrument would have $J = 0$; we could then take it that K_{θ} , $M_d = 0$. It is impossible, however, to make an instrument with $J = 0$, and if $J \neq 0$, it is also impossible for K_{θ} , $M_d = 0$. Moreover, the design itself of the floating gyroscope conditions the presence and necessity of damping, i.e. K_{θ} , $M_d \neq 0$. From this it

is clear why in the floating differentiating gyroscope the damping ($K_{\dot{\theta}}, \zeta_d$) should be less than in the floating integrating gyroscope.

In the ideal case, that is, when $T_0 = T_1 = 0$, the transfer function and the frequency characteristic of the floating differentiating gyroscope, as is clear from (4.20), (4.21), (4.22), and (4.44), would be equal to

$$W_{d,i}(p) = W_{d,i}(j\omega) = K_{d,i} \omega^{-1}.$$

Let us determine the values of T_0 and T_1 for the floating differentiating gyroscope with elastic torsion rod Type 10⁴ No. 55. Let us take the calculated values from Tables 4 and 5 (Chapter II, Section 2):

$$J = 0.035 \text{ gf-cm-sec}^2, K_{\theta, M_d} = k = 494 \text{ gf-cm-rad}, \\ K_{\dot{\theta}, M_d} = 5.1 \text{ gf-cm-sec}.$$

From Formula (4.6)

$$\omega_0 = 2\pi f_0 = \sqrt{\frac{K_{\theta, M_d}}{J}} = \sqrt{\frac{494}{0.035}} = 119 \text{ rad/sec}, \quad (4.46) \\ f_0 = \frac{2\pi}{\omega_0} = 19 \text{ cps}.$$

From Formula (4.7)

$$b = \frac{K_{\dot{\theta}, M_d}}{2\sqrt{JK_{\theta, M_d}}} = \frac{5.1}{2\sqrt{0.035 \cdot 494}} = 0.617. \quad (4.47)$$

Applying Formulas (4.44) and (4.45), we obtain

$$T_0 = \frac{1}{\omega_0} = \frac{1}{119} = 0.0084 \text{ sec}. \quad (4.48)$$

$$T_1 = \frac{2b}{\omega_0} = \frac{2 \cdot 0.617}{119} = 0.0104 \text{ sec}. \quad (4.49)$$

Section 5. Equation for Floating Differentiating

Gyroscope With Feedback Circuit

Figure 4.3 is a simplified block diagram of a floating differentiating gyroscope with feedback circuit. The instrument consists of a floating integrating gyroscope 1 and an amplifier 2. The output voltage U_{out} produced by the microsyn-pickoff of the integrating gyroscope is fed into the amplifier input 2. The amplifier output current I_a is passed through the feedback channel to the control winding of the microsyn-torquer of the integrating gyroscope. A detailed diagram of the parts of the instrument is given in Fig. 4.4. The diagram is similar in layout and symbols used to that of Fig. 4.2.

The output current from the amplifier is

$$I_a = K_{U_{out}} U_{out} \quad (4.50)$$

where K_{U_{out}, I_a} is the amplifier amplification factor in amp/volt.

Replacing the voltage U_{out} in Eq. (4.50) by the value for it obtained by Eq. (3.13), we get

$$I_a = K_{U_{out}} \beta (K_{\theta, U_{out}} \beta + \Delta) \quad (4.51)$$

From this it is clear that the current I_a is in direct proportion to the angle β with an accuracy continuing up to the value $K_{U_{out}, I_a} \Delta$, which in a normally working instrument is small because of the smallness of the voltage Δ . As has been said, the current I_a is passed along the feedback channel to the control winding of the microsyn-torquer. Under its influence the microsyn-torquer imposes a moment on the floating gyroassembly which on the basis of Formula (3.10) will be

$$M_1 = K_{I_{con}M_1} I_{con} = K_{I_{con}M_1} K_{U \dots U_1} I_1 (K_{\theta} U_{out} \beta + \Delta). \quad (4.52)$$

From this, disregarding the voltage Δ , we obtain

$$M_1 = K_{I_{con}M_1} K_{U \dots U_1} K_{\theta} U_{out} \beta. \quad (4.53)$$

Thus, the moment created by the microsyn-torquer under the influence of the current I_a will be directly proportional to the angle β and directed in such a way as to reduce that angle to zero, i.e. to return the floating gyroassembly to its initial position. In other words, this moment is in nature exactly the same as the elastic moment created in the previous version of the floating differentiating gyroscope by the elastic torsion rod (or by a spring or springs). In this version of the instrument this moment is created purely by electrical means, without the use of any elastic mechanical parts.

It should be pointed out that this instrument should work better than the previous one since both its gyroassembly supports are rigid, whereas in the torsion-rod gyroscope one of the supports -- the one constituted by the rod -- is elastic.

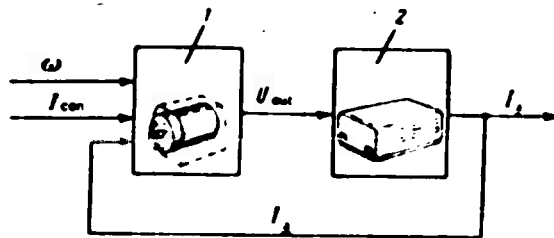


Fig. 4.3. Simplified diagram of parts of floating differentiating gyroscope with feedback circuit.

1) Floating differentiating gyroscope; 2) amplifier.

Besides the current I_a , the control winding, in the general case, may receive another current I_{con} , for example, to compensate for the interference moment. In the general case the current received by the control winding of the corrector is

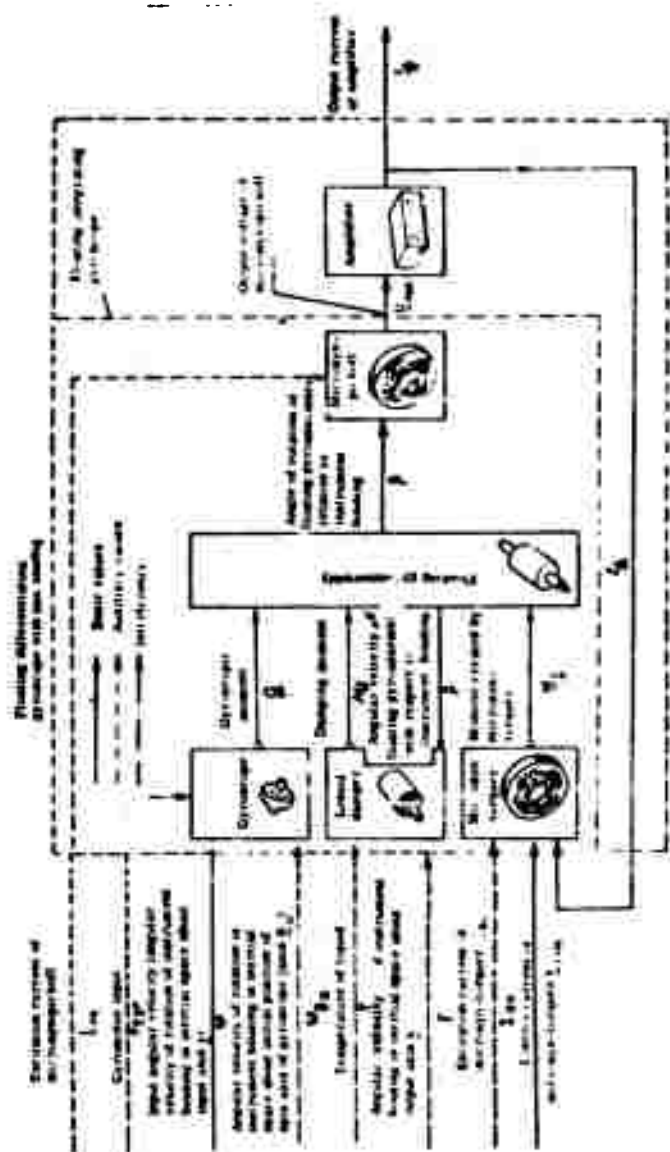


Fig. 4.4. Block diagram of floating differentiating gyroscope with feedback circuit.

$$I_{con} = I_p + I_{con} = K_{I_{con}} U_{out} + I_{con} \quad (4.54)$$

Both the voltage U_{out} and the current I_a can be taken as the output signal proportional to the angular velocity ω . It is preferable, however, to take the current I_a .

Let us formulate the equation for the floating differentiating gyroscope with feedback. To do so, we have to replace the current I_{con} in Eq. (3.24) by the current I'_{con} determined by Eq. (4.54). Next, transposing the term containing U_{out} , which is the "elastic moment," to the left-hand side of the equation, we obtain the desired equation in the following form

$$\begin{aligned} T\ddot{U}_{out} + \dot{U}_{out} + K_{I_{con}} \dot{U}_{out} K_{U_{out}} \left(1 + \frac{\Delta_p}{K_{p, U_{out}}}\right) I'_{con} = \\ = \left(1 + \frac{\Delta_p}{K_{p, U_{out}}}\right) [K_{\omega} \dot{U}_{out} - K_{I_{con}} \dot{U}_{out} I_{con} - K_{I_{con}} \dot{U}_{out} I - \\ - K_{M, U_{out}} M] + \Delta_i \end{aligned} \quad (4.55)$$

The first term on the right-hand side of Eq. (4.55) should be multiplied by the term in brackets

$$\left(\cos \beta - \frac{v_k}{\omega} \sin \beta\right),$$

which in deriving the equation for the floating integrating gyroscope was taken as equal to unity assuming angle β is small. The reason for this is that the floating differentiating gyroscope operates at angles β which, though small, are finite, whereas the floating integrating gyroscope operates at angles β close to zero. Dividing Eq. (4.55) by the time constant T and introducing parameters similar to those introduced earlier for the floating differentiating gyroscope with torsion rod, we obtain

$$\begin{aligned}
 & U_{out} + 2b\omega_0 U_{out} + \omega_0^2 \left(1 + \frac{\Delta_0^2}{K_{\theta} U_{out}} \right) U_{out} = \\
 & = \left(1 + \frac{\Delta_0^2}{K_{\theta} U_{out}} \right) \left[\omega_0^2 K_{\omega} U_{out} \left(\cos \beta - \frac{\omega_0}{\omega} \sin \beta \right) \omega - \right. \\
 & \left. - \omega_0^2 K_{I_{con}} U_{out} I_{con} - K_{\theta} U_{out} \Gamma - \omega_0^2 K_{M_1} U_{out} M_1 \right] + 2b\omega_0 \Delta_0^2.
 \end{aligned} \tag{4.56}$$

The constant coefficients in this equation are determined by the following equalities

$$\omega_0 = \sqrt{\frac{K_{U_{out}, I_{con}} K_{I_{con} U_{out}}}{J}} = \sqrt{\frac{K_{\theta, M_1}}{TK_{\theta, M_1}}} \tag{4.57}$$

or

$$\omega_0 = \sqrt{\frac{K_{\theta, M_1}}{J}} \text{ rad/sec} \tag{4.58}$$

is the angular frequency of the free undamped oscillations of the floating gyro-assembly. The second variation of Eq. (4.57) is obtained by using Formulas (3.26) and (3.20).

$$K_{\theta, M_1} = K_{\theta, U_{out}} K_{U_{out}, I_{con}} K_{I_{con}, M_1} \text{ gf-cm/rad} \tag{4.59}$$

is the amplification factor equivalent to the rigidity of the torsion rod k , or, what amounts to the same thing, the amplification factor $\frac{K_{\theta, M_1}}{J}$.

Expressions (4.58) and (4.59) are obtained by successive substitution of Eqs. (3.26), (3.18), and (3.20) into Formula (4.57).

$$\delta = \frac{1}{2T\omega_0} = \frac{1}{2T} \sqrt{\frac{J}{K_{\theta, M_1}}} = \frac{K_{\theta, M_1}}{2J\omega_0} = \frac{K_{\theta, M_1}}{2\sqrt{JK_{\theta, M_1}}} \tag{4.60}$$

is the damping ratio of the floating gyroassembly.

$$\tag{4.61}$$

$$K_{\omega, U_{out}} = \frac{K_{\omega, U_{out}}}{T\omega_0^2} = \frac{H}{K_{I_{con}, M_1} K_{U_{out}, I_{con}}} \frac{\text{volt}}{\text{rad/sec}}$$

The second expression for the given amplification factor is obtained by the successive application of Eqs. (3.25), (4.57), (3.19), (3.26), and (3.20). This factor describes the sensitivity of the floating differentiating gyroscope with feedback with respect to the input angular velocity ω .

$$K_{L_{out}, U_{out}} = \frac{K_{L_{out}, U_{out}}}{T_0^2} = \frac{1}{K_{U_{out}, I_{in}}} \text{ volt/rad/sec} \quad (4.62)$$

The second expression for the amplification factor $K_{I_{con}, U_{out}}$ is obtained by means of Eq. (4.57)

$$K_{M_{I, U_{out}}} = \frac{K_{M_{I, U_{out}}}}{T_0^2} = \frac{1}{K_{U_{out}, I_{in}} K_{I_{con}, U_{in}}} = \frac{K_{U_{out}, U_{in}} \text{ volt}}{K_{I_{con}, M_{I, U_{out}}} \text{ rad/sec}} \quad (4.63)$$

The second expression for $K_{M_{I, U_{out}}}$ is obtained by the successive application of Eqs. (3.28), (4.57), (3.23), and (3.20), and the third expression by substituting Eq. (4.59) into the second expression.

Reducing Eq. (4.56) to a form similar to Eq. (4.15), we arrive at the final form of the equation for the floating differentiating gyroscope with feedback for the case when the output voltage U_{out} of the microsyn-pickoff serves as the output value of the instrument:

$$U_{out} + 2b_0 \dot{U}_{out} + \nu_0^2 \left(1 + \frac{\Delta_0}{K_{U_{out}, I_{in}}} \right) U_{out} = \nu_0^2 K_{M_{I, U_{out}}} \left(1 + \frac{\Delta_0}{K_{U_{out}, I_{in}}} \right) \times \\ \times \left[\left(\cos \beta - \frac{\omega_0}{\omega} \sin \beta \right) - k_{L_{out}, I_{con}} - k_{I_{con}, U_{in}} - k_{M_{I, U_{out}}} \right] + 2b_0 \Delta_0 \quad (4.64)$$

where

$$k_{L_{out}, I_{con}} = \frac{K_{L_{out}, I_{con}}}{H} \frac{\text{rad/sec}}{\text{amp}}, \quad k_{I_{con}, U_{in}} = \frac{J}{H} \text{ sec}, \quad k_{M_{I, U_{out}}} = \frac{1}{H} \frac{\text{rad/sec}}{\text{volts}}$$

These three amplification factors are exactly equal to the corresponding factors (4.16), (4.17), and (4.18) of the floating differentiating gyroscope with torsion rod, and to those of the floating integrating gyroscope (3.32), (3.33),

and (3.34). Equation (4.64) is similar to Eq. (4.15) except that on the right-hand side there is no term proportional to Δ , as there is in Eq. (4.15) for the floating differentiating gyroscope with torsion rod. This shows that the voltage Δ affects the operation of the differentiating gyroscopes under consideration in different ways. The absence of the derivative Δ''_{tt} in the right-hand side of Eq. (4.64) is explained by the fact that when deriving the equation for the integrating gyroscope we ignored the product $T \Delta''_{tt}$ [see the derivation of Eq. (3.24)].

The dependence of the voltage U_{out} on the angular velocity ω in the steady state is determined by the amplification factor K_{ω} , U_{out} . However, as can be seen from Equality (4.61), this factor depends on the amplifier parameters, specifically on the amplifier amplification factor $K_{U_{out}}$, I_a . This dependence can be eliminated if the output current I_a of the amplifier, determined by Eq. (4.50), is taken as the output signal instead of the voltage U_{out} . Taking this current as the output value of the floating differentiating gyroscope with feedback, we replace the voltage U_{out} in Eq. (4.64) by the value of it determined from Eq. (4.50), as a result of which we obtain the equation for the floating differentiating gyroscope with feedback for the case when the amplifier output current I_a acts as the output value:

$$\begin{aligned} I_a + 2b\omega I_a + \omega^2 \left(1 + \frac{\Delta_p}{K_{\beta, U_{out}}} \right) I_a = \omega^2 K_{\omega, I_a} \left(1 + \frac{\Delta_p}{K_{\beta, U_{out}}} \right) \times \\ \times \left[\left(\cos \beta - \frac{\omega^2}{\omega_0^2} \sin \beta \right) \omega - k_{I_{cm}, \omega} I_{cm} - k_{I, \omega} \ddot{\omega} - k_{M, \omega} \dot{\omega} \right] + \\ + 2b\omega K_{U_{out}, I_a} \Delta_p \end{aligned} \quad (4.65)$$

where

$$K_{\omega, I_a} = \frac{H}{K_{I_{cm}, M_1}} \frac{\text{amp}}{\text{rad. sec}} \quad (4.66)$$

This amplification factor represents the sensitivity of the floating differentiating gyroscope with feedback with respect to the angular velocity ω for the case when the amplifier output current I_a serves as the output value. It is clear from Eq. (4.66) that this factor only depends on the angular momentum H of the gyroscope and on the amplification factor of the corrector K_{I_{con}, M_t} and does not depend in the least on the parameters of the other parts of the instrument, in particular, the amplifier. It should be pointed out, as can be seen from Eqs. (3.32) and (4.66), that

$$K_{\omega, I_a} = \frac{1}{H_{con, t}}$$

Thus, by taking I_a rather than U_{out} as the output value, we obtain a differentiating gyroscope whose sensitivity with respect to the angular velocity ω does not depend on the amplifier parameters.

It is immediately clear from Eq. (4.65) that the influence of Δ'_t is directly proportional to the magnitude of the amplifier amplification factor K_{U_{out}, I_a} .

It should be pointed out that Eqs. (4.50) and (4.54) only apply to the steady-state operation of the amplifier, although in practice this state does not always occur. Equations (4.64) and (4.65) for floating differentiating gyroscopes with feedback circuit can be expressed in the form of Eq. (4.43), but since this does not provide us with anything new, we will merely find the expression for the time constants T_0 and T_1 for floating differentiating gyroscopes with feedback. As in the case of the floating differentiating torsion-rod gyroscopes, they will be determined by the first expression in Formulas (4.44) and (4.45), i.e.

$$T_0 = \frac{1}{\gamma}; \quad T_1 = \frac{2b}{\gamma} = 2bT_0.$$

Substituting Eqs. (4.58) and (4.60) into these expressions, we have

$$T_0 = \frac{1}{\omega_0} = \sqrt{\frac{J}{K_{\theta} M_1}} \dots \quad (4.67)$$

and

$$T = 2bT_0 = \frac{K_{\theta} M_d}{K_{\theta} M_1} \dots \quad (4.68)$$

Section 6. Transfer Functions and Frequency Characteristics of Floating Differentiating Gyroscopes With Feedback

Let us first consider the floating differentiating gyroscope with feedback in which the output voltage U_{out} of the microsyn-pickoff serves as the output value. Using the differential symbols

$$p = \frac{d}{dt} \text{ and } p^2 = \frac{d^2}{dt^2}$$

and assuming that $\Delta'_\theta = \Delta'_t = 0$, we will rewrite Eq. (4.64) as an operator:

$$(p^2 + 2b\omega_0 p + \omega_0^2) U_{out} = \\ = \frac{1}{2} K_{\theta} U_{out} \left[\left(\cos \beta - \frac{\omega_0}{\omega} \sin \beta \right) - k_{\theta out} I_{out} - k_{1, out} \dot{I} - k_{\theta, out} M_1 \right].$$

When the equation has been divided by $p^2 + 2b\omega_0 p + \omega_0^2$, it can be represented in the form:

$$U_{out} = W_{dq}(p) \left[\left(\cos \beta - \frac{\omega_0}{\omega} \sin \beta \right) - k_{\theta out} I_{out} - k_{1, out} \dot{I} - k_{\theta, out} M_1 \right]. \quad (4.69)$$

where $W_{d.g.}(p)$ is the transfer function of the differentiating gyroscope under consideration, determined, as before, by Eq. (4.20). Now, however, the values ν_0 , \underline{b} and \underline{K}_ω , \underline{U}_{out} in the expression for $W_{d.g.}(p)$ have to be taken from Formulas (4.57) or (4.58), (4.60), and (4.61).

Equation (4.69) fully coincides with the corresponding Eq. (4.19) for the floating differentiating gyroscope with a torsion rod.

In actual conditions, as in the case of the torsion rod gyroscope, a certain small, and in the general case, variable, voltage of an indeterminate nature due to reasons considered earlier will be algebraically added to the voltage \underline{U}_{out} determined by Eq. (4.69).

The frequency characteristic of this instrument and also its amplitude-frequency and phase-frequency characteristics, as in the differentiating gyroscope with a torsion rod, are determined by Formulas (4.21), (4.22), (4.23), (4.24), (4.25), and (4.26). In the case given, however, the values \underline{K}_ω , \underline{U}_{out} , ν_0 , and \underline{b} in them should be taken from Formulas (4.61) and (4.57) or (4.58) and (4.60).

Now let us consider the differentiating gyroscope with feedback in which the output current \underline{I}_a of the amplifier serves as the output value. Assuming that in Eq. (4.65) $\Delta'_\theta = \Delta'_t = 0$, and using the differential symbols

$$p = \frac{d}{dt}, \quad p^2 = \frac{d^2}{dt^2},$$

we can rewrite this equation as an operator:

$$(p^2 + 2b_0 p + \nu_0^2) I_a = \nu_0^2 K_{\omega, I} \left[\left(\cos \beta - \frac{\nu_0}{\omega} \sin \beta \right) \omega - \right. \\ \left. - k_{t, \omega} I_{\omega} - k_{t, \ddot{\theta}} \ddot{\theta} - k_{M, \omega} M_1 \right].$$

Dividing it by $p^2 + 2b_0 p + \nu_0^2$, we obtain

$$I_a = W_{a.s.}(p) \left[\left(\cos \beta - \frac{v_0}{\omega} \sin \beta \right) - k_{t_{0a}} I_{0a} - k_{t_{0a}} \ddot{M}_1 - k_{M_1} M_1 \right], \quad (4.70)$$

where

$$W_{a.s.}(p) = \frac{K_{a.s.}}{p^2 + 2b_0 p + v_0^2} \quad (4.71)$$

is the transfer function of the floating differentiating gyroscope with feedback in which the output current I_a of the amplifier serves as the output value. The values $K_{a.s.}$, I_{0a} , v_0 , and b in (4.71) should be taken from Formulas (4.66) and (4.57) or (4.58) and (4.60). If Δ'_g and Δ'_t do not equal zero, a small indeterminate current caused by these derivatives from the voltage Δ will be added algebraically to the current I_a determined by Eq. (4.70).

The transfer function (4.71) coincides exactly in form with the transfer function (4.20) for the floating differentiating torsion-rod gyroscope and the feedback gyroscope in which the voltage U_{out} serves as the output value. Hence, if we leave aside the slight effect of the voltage Δ and its derivatives, which are impossible to take into account theoretically, we find that all three types of floating differentiating gyroscope considered have the same dynamic properties.

To obtain the frequency characteristic and also the amplitude-frequency and the phase-frequency characteristics of the floating gyroscope with feedback in which the output current I_a of the amplifier is taken as the output value, we should apply Formulas (4.21), (4.22), (4.23), (4.24), (4.25), and (4.26), substituting $K_{a.s.}$, I_a for $K_{a.s.}$, U_{out} into them, and taking b and v_0 from Formulas (4.60) and (4.57) or (4.58).

Section 7. Steady-State Operation of a Differentiating Gyroscope

With Feedback

Let us consider that the output current \underline{I}_a of the amplifier is taken as the instrument's output value. We will take the steady state to mean the operating conditions of the instrument under which $\ddot{\underline{I}}_a = \dot{\underline{I}}_a = 0$ with the control current \underline{I}_{con} of the microsyn-torquer and the angular acceleration $\ddot{\gamma}$ of the instrument housing equal to zero at the same time. In setting the condition $\underline{I}_{con} = 0$ we do not in any way count out the use of the microsyn-torquer to compensate the systematic component of the moment \underline{M}_1 . Given this compensation, \underline{I}_{con} is taken to mean the value of the control current over and above the value necessary for the said compensation.

Thus, assuming $\ddot{\underline{I}}_a = \dot{\underline{I}}_a = \underline{I}_{con} = \ddot{\gamma} = 0$ in Eq. (4.65), we obtain the following equation for the steady state of operation of the floating differentiating gyroscope with feedback in which the output current \underline{I}_a of the amplifier serves as the output value:

$$\begin{aligned} I_a = K_{a,1} \left[\left(\cos \beta - \frac{\omega_{z0}}{\omega} \sin \beta \right) \omega - k_{w,1} M_1 \right] + \\ + \frac{2bK_{U_{out},1} \dot{\Delta}_t}{\omega \left(1 + \frac{b}{K_{\theta,U_{out}}} \right)} \end{aligned} \quad (4.72)$$

Let us first assume that $\underline{M}_1 = \dot{\Delta}_t = \omega_{z0} = 0$. Then there is a corresponding value of the current \underline{I}_a for each constant value of the angular velocity ω in the steady state. If $\omega_{z0} \neq 0$ when $\dot{\Delta}_t = 0$, but is constant, and $\underline{M}_1 \neq 0$, but does not depend on time, then the steady-state value of \underline{I}_a will not only depend on ω , but also on ω_{z0} and \underline{M}_1 .

Let us now consider what happens if $\dot{\Delta}_t \neq 0$ and is a function of time. For this purpose let us first take a look at the physical side of the operation of the

instrument when $\omega = \dot{\theta} = \dot{\phi} = 0$. When there is an angular velocity ω , a gyroscopic moment $H \omega \cos \theta$ is created which causes the gyroassembly to deviate from the position $\theta = 0$, which it occupies when $\omega = 0$. Let us assume that the possible values of the angle θ are such that we can take $\cos \theta \approx 1$ with a high degree of accuracy, and, consequently, that the gyroscopic moment is $H \omega$ and does not depend on the angle θ .

At the output of the microsyn-pickoff there is created a voltage U_{out} which, reaching the input of the amplifier, causes a current I_a at its output. The secondary winding of the microsyn-torquer is connected to the amplifier output. Given a current I_a , the microsyn-torquer will impose a counteracting gyroscopic moment $K_{I-con}, M_t I_a$ on the floating gyroassembly. When the torquer moment becomes equal to the gyroscopic moment, i.e. when

$$K_{I-con}, M_t I_a = H \omega, \quad (4.73)$$

the floating gyroassembly will enter a state of equilibrium, in which the current

$$I_a = \frac{H}{K_{I-con}, M_t} \omega = K \omega, \quad I_a \omega. \quad (4.74)$$

Thus, the rotation of the floating gyroassembly continues until the current I_a acquires the value necessary for the creation of a moment by the microsyn-torquer equal and opposite to the gyroscopic moment. Since neither of these moments depends on the angles θ , the current I_a will not do so either, but will be determined by the input angular velocity ω alone. For example, if in a state of equilibrium with $\omega = \text{constant}$ the voltage U_{out} for any reason changes, this will first and foremost cause a change in the current I_a , and, consequently, a disturbance of Eq. (4.73) of the moments. Since the gyroscopic moment remains unchanged,

the equality of the moments may only be restored by returning I_a to its previous value. The current I_a is a single-valued function of the voltage U_{out} which is in turn a function of the angle β . Hence to restore the disturbed equality of the moments, the floating gyroassembly has to turn to a new position in which the voltage U_{out} and the current I_a assume the old values at which Eq. (4.73) is satisfied. It is quite clear that the design of the instrument ensures that Eq. (4.73) is automatically restored when disturbed through a change in U_{out} . Thus, any possible changes in the voltage U_{out} lead in the long run to the floating gyroassembly occupying a new equilibrium position in which the current I_a and the voltage U_{out} assume their old values.

Let us determine the value of the angle β in the equilibrium position. Solving Eq. (4.51) with respect to β , we obtain

$$\beta = \frac{I_a - K_{U_{out}, I_a} \Delta}{K_{\beta, U_{out}} K_{U_{out}, I_a}}. \quad (4.75)$$

The value of the current I_a in the equilibrium position is determined by Eq. (4.74). Substituting it in (4.75), we obtain the value of the angle β in the equilibrium position:

$$\beta = \frac{K_{\alpha, I_a} \omega - K_{U_{out}, I_a} \Delta}{K_{\beta, U_{out}} K_{U_{out}, I_a}}. \quad (4.76)$$

It follows directly from this that with the variation in Δ and K_{U_{out}, I_a} , β will also vary, but the variation in the latter does not affect the steady-state value of I_a , which remains unchanged.

Thus, the possible nonlinearity of the microsyn-pickoff, i.e. the absence of direct proportionality between the voltage U_{out} and the angle β , has no effect whatsoever on the dependence of the output signal -- the current I_a -- on the

input angular velocity ω . This also explains the fact that the voltage Δ is not directly a part of Eqs. (4.64) and (4.65), and, accordingly, Eq. (4.72). The fact that the voltage Δ is not directly a part of Eq. (4.15) for the differentiating gyroscope with a torsion rod (or some other mechanical spring) can be explained by the following: in this instrument the moment counteracting the gyroscopic moment is created by a torsion rod and, consequently, is a single-valued function of the angle ϑ of its twist. Hence in the steady state there is one definite value of the angle ϑ for each value of $\omega = \text{const}$. The voltage U_{out} serves as the output signal; this voltage is obtained at the given value of angle ϑ and has, as pointed out (see 3.13), an indeterminate component Δ . Thus, the difference is that in the torsion-rod gyroscope the output signal is the voltage U_{out} obtained at an equilibrated value of angle ϑ and not directly dependent on ω , while in the feedback gyroscope the output signal U_{out} or I_a is directly determined by the value of the gyroscopic moment, i.e. the angular velocity ω . We can now answer the question, posed earlier, as to what happens if $\Delta'_t \neq 0$; in other words we can ascertain the physical meaning of the last term in the right-hand side of Eq. (4.72). To make the argument simpler, let us assume that $\omega = M_1 = 0$, $\Delta'_t = \text{const}$, and that when $t = 0$ the angle $\vartheta = 0$. In this case the amplifier input begins to receive a voltage which varies at a constant rate. A current ΔI_a will therefore begin to flow through the control winding and the torquer will impose a moment $K_{I_{\text{con}}} M_t \Delta I_a$ on the floating gyroassembly. The gyroassembly will begin to rotate with velocity $\dot{\vartheta}$ and will do so in a direction tending to reduce the voltage reaching the amplifier input. As a result there will be established a regime under which the gyroassembly will rotate with a velocity $\dot{\vartheta} = \text{const}$ such that [see (3.14)]

$$\dot{U}_{\text{in}} = (K_0 U_{\text{in}} + \Delta'_t) \dot{\vartheta} + \Delta'_t = 0$$

and the moment of the torquer will be balanced by the damping moment, i.e.

$$K_{t, \text{com}}, \Delta I_s + K_{\phi, \text{com}} \beta = 0.$$

Excluding β from these equations, we obtain

$$\Delta I_s = \frac{K_{\phi, \text{com}} \Delta I_s}{K_{t, \text{com}}, (K_{\phi, \text{com}} + \Delta \phi)} = \frac{20 K_{U_{\text{ext}}, I_s}}{1 + \frac{\Delta \phi}{K_{\phi, \text{com}}}} \Delta I_s.$$

This is in fact the current determined by the last term on the right-hand side of Eq. (4.72). Consequently, the condition $\Delta'_{t_s} = \text{const}$ leads to the appearance of the current $\Delta I_s = \text{const}$. The error produced in the instrument by this current will be $\omega = \Delta I_s (K_{\omega}, I_s)$. A case in which $\Delta'_{t_s} = \text{const}$ is highly improbable. Much more likely is $\Delta'_{t_s} \neq \text{constant}$. If Δ'_{t_s} varies according to a periodic law, the current I_s will vary correspondingly.

Strictly speaking, if $\Delta'_{t_s} \neq \text{const}$, \ddot{I}_s and \ddot{I}_s cannot equal zero, and Eq. (4.72) cannot therefore be satisfied. Thus, $\Delta = \text{const}$ does not influence I_s , and does not therefore cause any error. But if Δ is a function of time, it causes an error -- the greater the instantaneous values of Δ_{t_s} , the larger the error will be. The aim should therefore be to make $\Delta'_{t_s} = 0$, i.e. the voltage Δ should not depend on time. We will assume from now on that this is the case.

Up to the present we have assumed that the angle ϕ has been small enough to enable us to consider $\cos \phi = 1$. But in actual fact $\cos \phi \neq 1$ and the gyroscopic moment is therefore a function of ϕ . We will show that in this case the current I_s will depend on the voltage Δ . We should point out in passing that this dependence cannot be seen directly from Eq. (4.72) since the angle ϕ is not expressed in it through the voltage.

In the equilibrium position the torquer moment equals the gyroscopic moment,
i.e.

$$K_{I_{\text{out}}} I_a = H \omega \cos \beta$$

or

$$I_a = K_{\omega, I_a} \omega \cos \beta. \quad (4.77)$$

The dependence of the current I_a and the angle β is given, as before, by Eq. (4.75). Substituting the value of β determined by this equality into (4.77), we obtain

$$I_a = K_{\omega, I_a} \omega \cos \left(\frac{I_a - K_{U_{\text{out}}, I_a} \Delta}{K_{\beta, U_{\text{out}}, I_a} I_a} \right). \quad (4.78)$$

The current I_a will be the root of this transcendental equation. It is quite clear that it will depend on Δ . If in practice the current I_a is not to be dependent on Δ , the instrument must operate at small β angles at which for practical purposes $\cos \beta = 1$. In order for this to be the case, as is clear from Eq. (4.78), the factor $K_{\beta, U_{\text{out}}}$ (the sensitivity of the microsyn-pickoff) must in turn be large enough and the current I_a and the amplification factor K_{U_{out}, I_a} small enough for the cosine of the fraction in brackets equal to the angle β to equal unity, for practical purposes. When this condition is met, Eq. (4.78) becomes (4.74), i.e. the current I_a ceases to be dependent on the angle β , and, therefore, also on the voltage Δ .

A direct influence on the nature of the dependence of the output signal on the input angular velocity is exerted in a differentiating gyroscope with feedback by the microsyn-torquer characteristic, i.e. by the nature of the dependence of

the moment created by it on the current I_{con} (when the instrument is operating this is the amplifier output current I_a) fed to the control winding. If this dependence is not proportional, the dependence of the output signal (the current I_a or the voltage U_{out}) on the input angular velocity ω will not be proportional either. Thus the strictest possible fulfillment of the condition $K_{I_{\text{con}}}, M_t = \text{const}$ is essential. And so the differentiating gyroscope with a feedback circuit has to operate at angles β for which $\cos \beta \approx 1$. In this instrument serious attention has to be given to the microsyn-torquer to ensure that $K_{I_{\text{con}}}, M_t = \text{const}$. In the microsyn-pickoff the voltage Δ should not depend on time. It is better, of course, if it equals zero.

It is clear from (4.72) that when $\cos \beta \approx 1$ and $\omega_{z0} = M_1 = \Delta_t' = 0$

$$I_a = K_{\omega}, I_a \omega,$$

i.e., in this case the dependence of I_a on ω in the steady state is fully determined by the factor K_{ω}, I_a . But when $\cos \beta \neq 1$, $\omega_{z0} \neq 0$, $M_1 \neq 0$ and $\Delta_t' \neq 0$, then, as is clear from Eq. (4.72), in the steady state (in the term containing Δ_t' we assume

$$K_{\omega, I_a} \approx I_a \text{ and } \frac{I_a}{K_{U_{\text{out}}, I_a}} = U_{\text{out}})$$

$$I_a = K_{\omega, I_a} \omega,$$

where

$$K_{\omega, I_a} = K_{I_a} \left[\cos \beta - \frac{\omega_{z0}}{\omega} \sin \beta - k_{M, I_a} \frac{M_1}{\omega} + \frac{2b\Delta_t'}{\omega_{\text{out}} \left(1 + \frac{\Delta_t'}{K_{\phi, U_{\text{out}}}} \right)} \right].$$

Thus, in the given case the dependence of I_a on ω is determined not by the factor K_{ω}, I_a , but by the values of the factor K_{I_a}, I_a , the numerical values of which cannot be determined theoretically since $M_1, \Delta_t',$ and Δ_t' are indeterminate values. It can only be determined experimentally, for which purpose we

have to determine the ratio $\frac{I_a \exp}{\omega \exp}$, which we shall denote $\left(\frac{I_a}{\omega}\right)_{\exp}$. Obviously, this ratio will be equal to the factor K'_{ω, I_a} . The values of K'_{ω, I_a} derived this way will be taken as the experimental values of K_{ω, I_a} , which relieves us of the need to introduce another factor into the discussion, and enables us to study and take into account experimentally the possible deviations of the factor K_{ω, I_a} from its nominal value determined by Eq. (4.66), which also occur when $\cos \beta \approx 1$ and

$$\omega_{z0} = \frac{M_1}{t} = \Delta \frac{1}{t} = 0.$$

Thus, by taking the ratios $\left(\frac{I_a}{\omega}\right)_{\exp}$ as the experimental values of the factor $K_{\omega, U_{out}}$ and giving them the subscript "exp," we obtain for the case in which none of the terms of Eq. (4.72) can be disregarded

$$(K_{\omega, I_a})_{exp} = \left(\frac{I_a}{\omega}\right)_{exp} = -K_{\omega, I_a} \left[\cos \beta - \frac{u_z}{u} \sin \beta - k_{M_1} - \frac{M_1}{u} + \frac{2b\delta'_1}{u U_{out} \left(1 + \frac{b}{K_{\theta, U_{out}}}\right)} \right]. \quad (4.79)$$

To evaluate the deviation of this factor from any value

$$(K_{\omega, I_a})_{cal} = \frac{I_a \text{ cal}}{u_{cal}} = \left(\frac{I_a}{u}\right)_{cal}, \quad (4.80)$$

taken as a calibration value, we have to introduce the relative dimensionless amplification factor in accordance with Formula (3.56)

$$(K_{\omega, I_a})_{exrel} = \frac{(K_{\omega, I_a})_{exp}}{(K_{\omega, I_a})_{cal}}. \quad (4.81)$$

The value $(K_{\omega, I_a})_{cal}$ should be determined under conditions where the angle β is so small that we can assume $\cos \beta \approx 1$ and $\sin \beta \approx 0$ and where

$$u_z = 0, \left| k_{M_1} - \frac{M_1}{u} \right|_{max} < 1, \left| \frac{2b\delta'_1}{u U_{out} \left(1 + \frac{b}{K_{\theta, U_{out}}}\right)} \right|_{max} < 1,$$

i.e. where the influence of angle β , the moments M_i and the derivative Δ_t' are insignificantly small. In this case, as is clear from Eq. (4.79), the value of $(K_{\omega, I_a})_{cal}$ will be practically the same as the theoretical value of K_{ω, I_a} determined by Formula (4.66). However, since K_{ω, I_a} cannot remain constant at large values of ω (of current I_a), as $(K_{\omega, I_a})_{cal}$ we have to choose a value of the factor corresponding to the working range of the instrument, i.e. the range in which the current $I_a \exp$ is for practical purposes directly proportional to the angular velocity $\omega \exp$.

If these conditions are met, on the basis of Formula (4.66) we can assume

$$(K_{\omega, I_a})_{cal} = \frac{H_{cal}}{(K_{I_{con} M_i})_{cal}} \quad (4.82)$$

We will show that values of the factor $(K_{\omega, I_a})_{exp, rel}$ fall into three characteristic regions similar to those for the factor $(k_{I_{con}, \omega})_{exp, rel}$ (we will recall that $K_{\omega, I_a} = \frac{1}{k_{I_{con}, \omega}}$) considered in Chapter II, Section 5.

In order to cover all feasible values of the factor K_{ω, I_a} in Expression (4.79), we will mark the factor and the values used to express it with the subscript "cur" (current value). Then, according to (4.66)

$$K_{\omega, I_a} = (K_{\omega, I_a})_{cur} = \frac{H_{cur}}{(K_{I_{con} M_i})_{cur}} \quad (4.83)$$

Substituting (4.83) into (4.79) and then (4.79) and (4.82) into (4.81), we obtain

$$(K_{\omega, I_a})_{exp, rel} = \frac{H_{cur}}{H_{cal}} \frac{(K_{I_{con} M_i})_{cal}}{(K_{I_{con} M_i})_{cur}} \times \left[\cos \beta - \frac{a_2}{\omega} \sin \beta - k_{M_i} - \frac{M_i}{\omega} + \frac{2\Delta_t'}{\omega U_{out} \left(1 + \frac{\Delta_p}{K_{p, U_{out}}} \right)} \right] \quad (4.84)$$

It is clear from this that at small angles ϑ , for which $\cos \vartheta \approx 1$ and $\sin \vartheta \approx 0$, the three following characteristic regions of $(K_{\omega}, I_a)_{\text{exp.rel}}$ values may occur, in a similar way to the regions for the factor $(k_{I_{\text{con}}, \omega})_{\text{exp.rel}}$.

1. Working region. Here

$$\frac{H_{\text{cur}}}{H_{\text{cal}}} \approx \frac{(K_{I_{\text{con}}, M_1})_{\text{cal}}}{(K_{I_{\text{con}}, M_1})_{\text{cur}}} \approx 1, \quad (4.85)$$

$$\left| k_{M_1} - \frac{M_1}{\omega} \right|_{\text{max}} \ll 1, \quad \left| \frac{2b\delta'_t}{\omega U_{\text{out}} \left(1 + \frac{\delta_\theta}{K_{\theta, U_{\text{out}}}} \right)} \right|_{\text{max}} \ll 1, \quad (4.86)$$

and, consequently,

$$(K_{\omega, I_a})_{\text{exp. rel}} \approx 1,$$

by virtue of which the current I_a will be proportional to the angular velocity ω .

2. Region in which the influence of the indeterminate (random) interference is considerable. This region is characterized by the fact that when the conditions (4.85) are met, only one (or neither) inequality (4.86) is satisfied. Hence in this region

$$(K_{\omega, I_a})_{\text{exp. rel}} = 1 - k_{M_1} = \frac{M_1}{\omega} + \frac{2b\delta'_t}{\omega U_{\text{out}} \left(1 + \frac{\delta_\theta}{K_{\theta, U_{\text{out}}}} \right)},$$

and, consequently, is a variable of a random nature due to the random nature of M_1 and Δ'_t . This region occurs at small values of ω when the gyroscopic moment is commensurate with the moment M_1 . The boundary of this region determines the minimum angular velocity which the instrument can measure.

3. Region in which the amplification factor of the microsyn-torquer is variable (region of saturation of the microsyn-corrector). In this region the inequalities (4.76) are satisfied and

$$\frac{H_{cor}}{H_{sat}} \approx 1.$$

However

$$\frac{(K_{L_{cor}M_r})_{sat}}{(K_{L_{cor}M_r})_{cor}} \neq 1.$$

Therefore

$$(K_{\omega, I_a})_{cor, sat} = \frac{(K_{L_{cor}M_r})_{sat}}{(K_{L_{cor}M_r})_{cor}}$$

and is therefore a variable. This region occurs at large values of $\frac{I_a}{-a}$ which cause saturation of the magnetic circuit of the microsyn-torquer.

If

$$\left| k_{M_r} = \frac{M_r}{\omega} \right|_{\max} < \cos \beta \left| \frac{2M_r'}{\omega_{out} \left(1 + \frac{L_p'}{K_{\beta, U_{out}}} \right)} \right|_{\max} < \cos \beta$$

and the conditions (4.85) are satisfied, but the term $\frac{\omega_{\Sigma 0}}{\omega} \sin \beta$ cannot be ignored when compared with $\cos \beta$, and $\cos \beta \approx 1$ cannot be assumed, then (4.84) will take the form

$$(K_{\omega, I_a})_{cor, sat} = \cos \beta - \frac{\omega_{\Sigma 0}}{\omega} \sin \beta. \quad (4.87)$$

This value of $(K_{\omega, I_a})_{cor, sat}$ fully coincides with the value $(K_{\omega, U_{out}})_{exp, rel}$ in the torsion-rod differentiating gyroscope obtained under similar conditions [see (4.39)].

Section 8. Comparison of the Two Types of Differentiating Gyroscope

Let us determine the frequency of the natural undamped oscillation f_0 , the damping ratio \underline{b} and the time constants T_0 and T_1 for the floating differentiating gyroscope with feedback containing the floating integrating gyroscope, Type 10⁴ No. 79 developed by the Massachusetts Institute of Technology. For convenience in comparing the values obtained with those of the floating differentiating gyroscope with torsion rod, Type 10⁴ No. 55, let us assume that the amplification factor $\underline{K}_{\underline{U}_{out} \underline{I}_a}$ is chosen in such a way that the factor $\underline{K}_\theta, \underline{M}_t$ [see Formula (4.59)] equals the calculated value of the torsion rod rigidity \underline{k} . Thus we take it that

$$\underline{K}_\theta, \underline{M}_t = \underline{k} = 1.94 \text{ gf-cm/rad} \quad (4.88)$$

Let us first determine the values enumerated above from calculated data for the integrating gyroscope, and then from the values as measured.

1) From Table 1 (Chapter II, Section 1) we have the following values for the integrating gyroscope parameters:

$$\underline{J} = 0.036 \text{ gf-cm-sec}^2,$$

$$\underline{K}_\theta, \underline{M}_t = 20.39 \approx 20.4 \text{ gf-cm-sec.}$$

From Formula (4.58)

$$\omega_0 = \sqrt{\frac{\underline{K}_\theta, \underline{M}_t}{\underline{J}}} = \sqrt{\frac{20.4}{0.036}} = 117 \text{ rad/sec}$$

Consequently,

$$f_0 = \frac{\omega_0}{2\pi} = \frac{117}{2\pi} = 18.7 \text{ cps}$$

From Formula (4.60)

$$b = \frac{K_{\theta, M_d}}{2J\omega_0} = \frac{20.4}{2 \cdot 0.036 \cdot 117} = 2.45.$$

Applying Eqs. (4.67) and (4.68), we find

$$T_0 = \frac{1}{\omega_0} = \frac{1}{117} = 0.0086 \text{ sec},$$

$$T_1 = 2bT_0 = 2 \cdot 2.45 \cdot 0.0086 = 0.0421 \text{ sec}.$$

The calculated values of the frequency f_0 and the time constant T_0 coincide for practical purposes with those of the differentiating gyroscope with torsion rod, which are 19 cps and 0.0084 sec respectively. The slight discrepancy is explained by the difference in the moments of inertia J of the floating gyroassemblies in the instruments. The calculated values of the damping ratio b and time constant T_1 are approximately four times greater than those of the differentiating gyroscope with torsion rod. This is due to the fact that in the integrating gyroscope the specific damping moment $\frac{K_{\theta}}{J}, \frac{M_d}{J}$ is more than four times greater than in the differentiating gyroscope with torsion rod.

2) From Tables 1 and 2 (Chapter II, Section 1) we have the following actual values of the integrating gyroscope parameters:

$$\frac{K_{\theta}}{J}, \frac{M_d}{J} = 22.12 \approx 22.1 \text{ gf-cm-sec (computed value)}$$

$$T = 0.0027 \text{ sec}.$$

Applying Formula (4.57), we find

$$\omega_0 = \sqrt{\frac{K_{\theta, M_d}}{TK_{\theta, M_d}}} = \sqrt{\frac{494}{0.0027 \cdot 22.1}} = 91.2 \text{ rad/sec}.$$

Correspondingly

$$f_0 = \frac{\omega}{2\pi} = \frac{91.2}{2\pi} = 14.5 \dots \quad (4.89)$$

From Formula (4.60)

$$b = \frac{1}{2T_0} = \frac{1}{2 \cdot 0.0027 \cdot 91.2} = 2.03. \quad (4.90)$$

From Formulas (4.67) and (4.68)

$$T_0 = \frac{1}{\omega} = \frac{1}{91.2} = 0.011 \dots$$

$$T_1 = 2bT_0 = 2 \cdot 2.03 \cdot 0.011 = 0.0447 \dots$$

Comparing the actual values of f_0 , b and T_0 , T_1 with their calculated values we see that the actual values of f_0 and b are smaller than the calculated values while the true values of T_0 and T_1 are somewhat greater than the calculated values. This is mainly due to the fact that the actual value of the time constant T is greater than its theoretical value.

Thus, if an ordinary floating integrating gyroscope is converted into a floating differentiating gyroscope with feedback, the result is an instrument which has too great a damping ratio b and, correspondingly, too large a time constant T_1 . From Formulas (4.60), (4.59), and (4.68) it is clear that these values can be reduced either by increasing the amplifier amplification factor K_{U_{out}, I_a} or by reducing the specific damping moment K_g, M_d , or by both methods together.

The following point, however, should be kept in mind. When the amplification factor of the amplifier is increased and the time constants T_0 and T_1 reduced at the same time, there is an increase in the factor K_g, M_t (see Eq. 4.59) equivalent to the rigidity of the torsion rod k . The factor K_g, M_t increases as many times as the amplifier amplification factor. But one should not think of increasing the amplifier amplification factor alone since this would also lead to an

increase in the current fed by the amplifier to the microsyn-torquer, and this in turn could lead to saturation of the torquer core even at comparatively small input angular velocities ω . In order to reduce the damping ratio ζ (2.03) in the instrument under consideration to its calculated value in the torsion rod gyroscope (0.617), the amplification factor of the amplifier $\frac{K_{U-out}}{I_a}$ has to be increased 10.8 times. In the process the time constant T_1 will decrease 10.8 times.

If nothing in the design of the instrument is to be changed, the specific damping moment can only be reduced by decreasing the viscosity of the filler liquid. This can either be done by raising the working temperature of the liquid or by using a less viscous liquid. But filling the instrument with a less viscous liquid will limit its use since it will be impossible to use it as an integrating gyroscope. The only instruments which can be filled with a less viscous liquid, therefore, are those specifically intended for use as differentiating gyroscopes with feedback. Consequently it may sometimes be more practical to raise the working temperature of the liquid. However, a considerable increase in the temperature in comparison with its calculated value will decrease the efficiency of the instrument at small angular velocities on account of an increase in friction in the floating gyroassembly bearings. The latter fact is explained by a reduction, accompanying the temperature increase, in the buoyancy of the liquid as compared with its calculated value, which for practical purposes is equal to the weight of the gyroassembly.

Tests carried out at the Massachusetts Institute of Technology on a gyroscope intended for use in an automatic pilot have shown that an increase in the temperature of the liquid of approximately 9°C will not decrease its efficiency and will not to any significant degree affect the characteristics of the instrument of importance in its operation as an automatic pilot (the drift increases by 0.05 mrad/sec).

From Formula (4.60) it is clear that the damping ratio ζ is directly

proportional to the specific damping moment $\underline{K}_\beta, \underline{M}_\beta$ and inversely proportional to the square root of $\underline{K}_\beta, \underline{M}_\beta$. The time constant \underline{T}_1 is in direct proportion to $\underline{K}_\beta, \underline{M}_\beta$ and in inverse proportion to $\underline{K}_\beta, \underline{M}_\beta$ [see Formula (4.68)]. Hence a variation in $\underline{K}_\beta, \underline{M}_\beta$ has an identical effect on both \underline{b} and \underline{T}_1 ; a variation in $\underline{K}_\beta, \underline{M}_\beta$ affects \underline{T}_1 more than \underline{b} .

The operation of both types of floating differentiating gyroscope considered is described by the identical second-order differential equations, (4.15) and (4.65). In both cases the increase in the input value is caused by an increase in the angle β of rotation of the floating gyroassembly with respect to the instrument housing. Hence the influence of angle β on the operation of the floating differentiating gyroscope becomes noticeable and, in this connection, very important. The influence shows up, firstly, in the fact that instead of sensing the full value of the measured angular velocity ω , the instrument only senses part of it, $\omega \cos \beta$, and secondly, in the fact that it partially reacts to the angular velocity ω_{z_0} , which it should not sense at all.

The influence of angle β on the operation of both types of instrument is the same, as can be seen immediately from the expressions (4.39) and (4.87). Hence the quantitative aspect of this influence may be determined on the basis of either one. Let us do so for the floating differentiating gyroscope with torsion rod. In the steady state the output value \underline{U}_{out} is determined by Eq. (4.29). Let us assume that $\underline{M}_1 = \Delta = 0$; this equation then assumes the form

$$\underline{U}_{out} = K_{out} \left(\cos \beta - \frac{\omega_{z_0}}{\omega} \sin \beta \right) \omega. \quad (4.91)$$

or, if we apply Eq. (4.39),

$$\underline{U}_{out} = K_{out} \omega_{out}. \quad (4.92)$$

Let us denote the voltage U_{out} which would have been obtained if $\beta \approx 0$ as $(U_{out})_0$; from (4.91) we obtain

$$(U_{out})_0 = K_{\omega} u_{out} \omega. \quad (4.93)$$

In evaluating the influence of the angle β and the angular velocity ω_{z0} on the U_{out} , it is convenient to use the coefficient κ and the concept, introduced earlier, of the relative error in the output value. According to Formula (3.58) the relative error in the voltage U_{out} resulting from the influence of angle β and the angular velocity ω_{z0} is

$$u_{out} = \frac{\Delta U_{out}}{(U_{out})_0} = \frac{U_{out} - (U_{out})_0}{(U_{out})_0} = \frac{U_{out}}{(U_{out})_0} - 1. \quad (4.94)$$

Substituting Eqs. (4.91) and (4.93) into this, we obtain

$$u_{out} = \cos \beta - \frac{\omega_{z0}}{\omega} \sin \beta - 1. \quad (4.95)$$

From Eq. (4.92) after substitution of Eq. (4.93) we find

$$\kappa = \frac{U_{out}}{(U_{out})_0}.$$

The right-hand side of the equality, as is clear from Expression (4.94) is

$1 + u_{out}$. Thus,

$$\frac{U_{out}}{(U_{out})_0} = \kappa = 1 + u_{out} \quad (4.96)$$

When $\omega_{z0} = 0$

$$\kappa = \kappa_0 = \cos \beta. \quad (4.97)$$

The influence of angle φ and the angular velocity ω_{z0} on the voltage U_{out} can be conveniently evaluated by means of the graph in Fig. 4.5. The broken line shows the dependence of ω_0 on φ . The continuous lines show the relative error $\delta_{U_{out}}$, plotted from Formula (4.95), for different values of the ratio of the angular velocities $\frac{\omega_{z0}}{\omega}$ and with the condition $\frac{\omega_{z0}}{\omega} \sin \varphi > 0$. Knowing the values of $\delta_{U_{out}}$ it is easy to calculate the values of the factor κ from Formula (4.96).

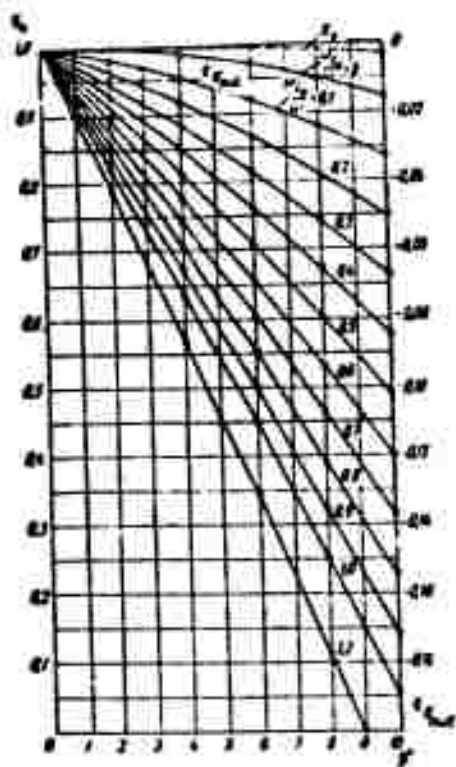


Fig. 4.5. Graph for evaluation of influence of angle φ and angular velocity ω_{z0} on output voltage U_{out} .

From the graph and Formulas (4.92) and (4.96) it is clear that the output voltage U_{out} , when $\frac{\omega_{z0}}{\omega} \sin \varphi > 0$ and other conditions are equal, decreases as the angle φ and the ratio of the angular velocities $\frac{\omega_{z0}}{\omega}$ increases.

The comparison of the two types of instrument considered enables us to conclude that the differentiating gyroscope with feedback has considerable advantages over the differentiating gyroscope with torsion rod (or any other mechanical spring). In view of the dependence of the modulus of elasticity on temperature and mechanical hysteresis it is extremely difficult to find a spring in which the rigidity remains constant with the required degree of accuracy. The manufacture of springs with strictly identical rigidity and slight hysteresis involves great technological difficulties. This,

in its turn, makes it difficult to manufacture differentiating gyroscopes with a mechanical spring which have strictly identical characteristics. It is in practice impossible to make the torsion rod in such a way that its rigidity can be altered by simple means. Any change in the rigidity k of the torsion rod is accompanied by a change in the factor $K_{\omega, U_{out}}$ determined by Eq. (4.28). None of the difficulties involved in the use of a torsion rod apply to the differentiating gyroscope with a feedback circuit.

In the differentiating gyroscope with a torsion rod or any other kind of mechanical spring the value of the output signal voltage U_{out} is proportional to the angle φ of deviation of the floating gyroassembly from its initial position and this angle, if we leave aside the subsidiary factors, is proportional to the input angular velocity ω . If the parameters of the instrument when it is being designed are so chosen that the angle φ_{max} corresponding to the upper limit of the input angular velocity ω_{max} is small, the instrument will have a low amplification factor $K_{\omega, U_{out}}$, i.e., it will not be highly sensitive. On the other hand, if the chosen angle φ_{max} is large, then, as pointed out, instead of sensing the full value of the angular velocity ω , the instrument will only sense part of it, $\omega \cos \varphi$, and will react at the same time to the angular velocity ω_{z_0} about the axis z_0 perpendicular to the y input and the x output axes of the instrument. The angle φ_{max} can only be increased when the angular momentum of the gyroscope H is constant by decreasing the rigidity of the torsion rod k , which will be accompanied by an unwanted increase in the time constants T_0 and T_1 [see Eq. (4.44) and (4.45)], i.e. the dynamic properties of the instrument will be poorer. All this leads to the frequent impossibility of producing a differentiating gyroscope with torsion rod which fully meets all the specified requirements of the system in which it is to work. In such cases a differentiating gyroscope with feedback should be used. This instrument is very sensitive, i.e. it has a high amplification factor $K_{\omega, I_{-2}}$, for what balances the gyroscopic moment is not

the voltage U_{out} , i.e., the angle β , which serves as the output signal proportional to the angular velocity ω , but rather the output current I_a of the amplifier, which is fed to the microsyn-torquer, and serves to measure the moment M_t which it generates. The current I_a attains considerable values (but, as pointed out, this current should not be large) and is to a considerably lesser degree subject to the influence of various factors than the output voltage U_{out} produced by the microsyn-pickoff. In short, greater accuracy is obtained here in the measurement of the input angular velocity ω on account of the fact that we are not measuring the angle of rotation of the floating gyroassembly by means of U_{out} but rather we are measuring the current I_a at which there is created a moment M_t which balances the gyroscopic moment. This method brings better results than the method of measuring the angular velocity by means of a floating differentiating gyroscope with torsion rod. The gyroscope with feedback circuit can operate at fairly small values of the angle β and, consequently, is to a considerable extent free from the influence of the angular velocity ω_{z0} .

CHAPTER V

ANALYSIS OF FLOATING GYROSCOPES

The characteristics of floating gyroscopes may be divided into three groups: static characteristics, drift characteristics, and dynamic characteristics.

Analyses of floating gyroscopes are also performed in three ways, as follows:

1. Static analysis.
2. Analysis for drift.
3. Dynamic analysis.

The static characteristics describe the behavior of the floating gyroscope during time intervals in which the input and output quantities are either constant or change so slowly that the behavior of the gyroscope is, in this case, essentially analogous to its behavior in steady-state operation. Two groups of static characteristics, corresponding to their two possible operating regimes, are registered in static analyses of floating integrating gyroscopes: the spatial integration regime and the geometric-stabilization regime.

The drift characteristics describe the relatively slow, spontaneous change in the output signal which is observed during time intervals in which all of the input quantities of the floating gyroscope are held constant.

The dynamic characteristics describe the behavior of a floating gyroscope during time intervals in which a change occurs in the output quantities as a result of a change in the input quantities. These characteristics must be determined from

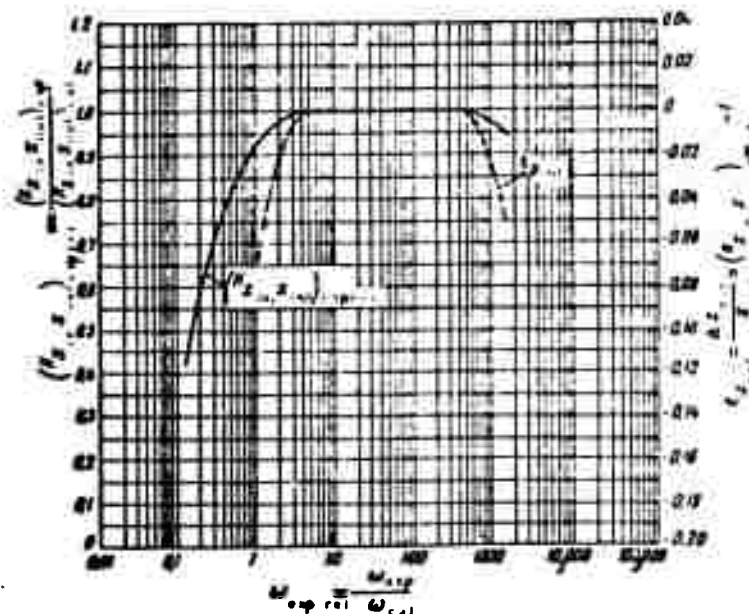
the results of analysis of devices operating under known and carefully controlled conditions. The following must be precisely regulated and maintained constant: the temperature of the surrounding medium, the power requirement of the gyroscope motor, the excitation currents of the pickoff and torquer, the condition of the mechanical mountings, the values of vibrational and shock loads, and other extraneous factors acting upon the device.

Given the characteristics of any specific floating gyroscope, we may make inferences concerning the influence exerted upon it by external factors and form a clear idea of the difference between changes in the various values peculiar to the gyroscope itself and changes due to other causes. Experimental floating-gyroscope characteristics obtained under typical conditions by the Massachusetts Institute of Technology are presented below.

Section 1. An Outline of Static Analysis

The static characteristics of floating gyroscopes are given as curves of the dependency of the relative dimensionless amplification factors $(K_{x_{in}}, x_{out})_{exp. rel}$ and the corresponding relative errors $\epsilon_{x_{out}}$ of the output values upon the relative angular velocity $\omega_{exp. rel}$. These values are generally determined from the corresponding formulas (3.56), (3.59), and (3.61).

The static characteristics of floating gyroscopes of all types are plotted on a semilogarithmic grid of the type shown in Fig. 5.1. Values of the relative velocity $\omega_{exp. rel}$ are ranged along the axis of abscissas, which is calibrated logarithmically for the interval 0.01 to 100,000. The left-hand axis of ordinates, which has a uniformly calibrated scale reading from 0 to 1.2, carries the values of the relative dimensionless amplification factor $(K_{x_{in}}, x_{out})_{exp. rel}$ under consideration. The right-hand axis of ordinates carries a uniform scale for the interval



• Fig. 5.1. Semilogarithmic grid for plotting static characteristics of floating gyroscopes.

(-0.20)-0-(+0.04). The zero point of this scale is placed opposite 1.0 on the scale for the factor $(K_{x_{in}}, x_{out})_{exp. rel.}$. This right-hand scale carries values of the relative error Δx_{out} of the output quantity. The curve of the dependency of the factor $(K_{x_{in}}, x_{out})_{exp. rel.}$ upon the relative angular velocity $\omega_{exp. rel.}$ is represented by the solid line, and the dependency of x_{out} upon $\omega_{exp. rel.}$ by the broken line.

The conditions under which the static characteristic was obtained and the values of $(K_{x_{in}}, x_{out})_{cal}$ and ω_{cal} should be indicated in each case. It is also necessary to indicate $x_{in. cal.}$, the calibrating value of the input quantity, unless the input quantity is the angular velocity $\omega_{exp.}$. Knowledge of the last two values permits the use of the static characteristics to determine, in addition, the values of $(K_{x_{in}}, x_{out})_{exp.}$ and Δx_{out} for any desired value of $\omega_{exp.}$ encompassed by the static characteristics. Thus Formula (3.56) gives

$$(K_{x_{in}, x_{out}})_{exp} = (K_{x_{in}, x_{out}})_{cal} (K_{x_{in}, x_{out}})_{exp} \quad (5.1)$$

Since the subdivisions of the x_{out} scale are one fifth the size of those of the $(K_{x_{in}, x_{out}})_{exp}$ rel scale, the value of the last factor is determined more conveniently not from its curve, but from the x_{out} curve, obtained in this case by the use of Formula (3.60).

It should be noted that it follows from this particular formula that the deviation of the factor $(K_{x_{in}, x_{out}})_{exp}$ from unity, expressed as a percentage, is given by

$$\delta = \epsilon_{out} 100\%. \quad (5.2)$$

It follows from the Eq. (3.58) that $\Delta x_{out} = x_{out} \epsilon_{out}$. By successive substitution of Eqs. (3.57), (3.56), and (3.55) into this, we obtain

$$\Delta x_{out} = (K_{x_{in}, x_{out}})_{cal} x_{in, rel} \epsilon_{out} x_{in, exp} \quad (5.3)$$

where

$$x_{in, rel} = x_{in, exp} / x_{in, cal} \quad (5.4)$$

is the relative value of the input quantity. If the input quantity is the angular velocity ω_{exp} , it follows from Formula (5.3) that

$$\Delta x_{out} = (K_{x_{out}}) \cdot \epsilon_{x_{out}} = \epsilon_{x_{out}} \quad (5.5)$$

The sign of the absolute error Δx_{out} of the output quantity is determined by the sign of its relative error $\epsilon_{x_{out}}$.

Section 2. Static Analyses of Differentiating Gyroscopes

The Differentiating Gyroscope With Torsion Rod

The steady-state operation of this device is characterized by the coefficient $K_{\omega, U_{out}}$. Thus the following two curves constitute its static characteristics: first, the dependence of the relative dimensionless amplification factor $(K_{\omega, U_{out}})_{exp. rel}$ as determined from Eq. (4.31) upon the relative angular velocity $\omega_{exp. rel}$, and, second, the dependence of the relative error $\epsilon_{U_{out}}$ of the output voltage U_{out} upon the relative angular velocity $\omega_{exp. rel}$. According to Formula (3.59), $\epsilon_{U_{out}} = (K_{\omega, U_{out}})_{exp. rel} - 1$.

A device which permits the instrument under analysis to be rotated about its input (measurement) axis at various angular velocities ω_{exp} is required to record these characteristics. Devices capable of measuring the resulting output voltages U_{out} with sufficient accuracy are also required.

Differentiating Gyroscope With Feedback Circuit

This device is characterized in the steady operating state by an amplification

factor K_{ω, I_a} . Its static characteristics are accordingly as follows: first, the curve of the dependence of the relative dimensionless amplification factor $(K_{\omega, I_a})_{\text{exp. rel}}$ upon $\omega_{\text{exp. rel}}$, and, second, the curve of the dependence of the relative error ϵ_{I_a} of the amplifier output current I_a upon $\omega_{\text{exp. rel}}$. The factor $(K_{\omega, I_a})_{\text{exp. rel}}$ is determined by Eq. (4.81). According to Formula (3.59),

$$\epsilon_{I_a} = (K_{\omega, I_a})_{\text{exp. rel}} - 1. \quad (5.6)$$

The same turntable mechanism is required for registration of these characteristics as in the case of the preceding device. Also necessary is a device capable of measuring the output current I_a of the amplifier with sufficient accuracy.

The turntable mechanism used in the analysis of floating gyroscopes is represented schematically in Fig. 5.2. As far as the operating principle is concerned, it is a single-axis spatial angular-velocity integrator with integrating gyroscope and servo-system, shown schematically in Fig. 2.19.

The base 2 of the device takes the form of a pedestal and is mounted on a pier. The slave motor, which consists of the stator 14 and the rotor 13, is mounted within the base. The rotor is fastened to the shaft 10, which occupies a fixed vertical position. The geometrical axis of this shaft is the input axis of the device considered as an integrator. This axis is designated by the letter y in Fig. 5.2, as it was in Fig. 2.19.

The platform 9 is carried on the shaft 10 in a rigidly horizontal position. To this platform is attached the thermostat 11, which contains the floating integrating gyroscope 12 (if the device has its own heating system, the thermostat is unnecessary). The gyroscope is mounted in such a way that its input axis coincides with the y axis or is parallel to it. The x axis, the output axis of the gyroscope, is perpendicular to the y axis. The z_0 axis is perpendicular to both the x and y axes

and is consequently horizontal. In some analyses it is necessary to fix the axis of rotation of the platform (the shaft 10) in a horizontal position, and also at various angles ($\neq 90^\circ$) to the horizontal. Thus the design of an actual turntable differs from the scheme shown in Fig. 5.2 in that it permits the axis of rotation of the platform to be adjusted to a horizontal position or at angles other than 90° to the horizontal, and reliably fixed in these positions. For this purpose, the housing of the motor (which carries the platform 9 on its shaft 10) is not mounted directly on the base 2, as shown schematically in Fig. 5.2, but is carried on a

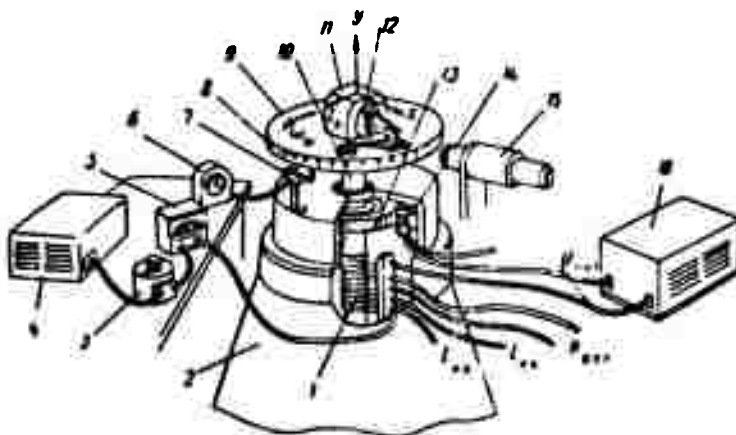


Fig. 5.2. Turntable device for analysis of floating gyroscopes. 1) Contact brushes and rings; 2) base; 3) rheostat for regulation of current I_{con} ; 4) I_{con} current supply; 5) milliammeter; 6) electric clock; 7) contact device; 8) graduated circle; 9) platform; 10) shaft of slave motor; 11) thermostat; 12) floating integrating gyroscope; 13) rotor of slave motor; 14) stator of slave motor; 15) read-off microscope; 16) amplifier.

horizontal pivot-axis perpendicular to the axis of rotation of the platform. The structural elements which carry the bearings of the motor-housing pivot axis are conveniently mounted on a plate equipped with adjustable legs, which are used to ensure the axis is truly horizontal. The plate is mounted on the base 2. The base should be fully protected from vibration and tremors in the building and in the earth.

In other cases the axis of rotation of the platform 9 (the y axis) should be strictly vertical.

The apparatus should permit rotation of the platform 9 in inertial space about the y axis at any constant angular velocity ranging from a small fraction of the earth's diurnal-rotational velocity to velocities of the order of 10 to 20 rad/sec. The required velocity of rotation is imparted to the platform 9 by impressing the appropriate current I_{con} from the current supply 4 upon the control winding of the microsyn torquer of the gyroscope 12. The size of this current is regulated by means of the rheostat 3 and checked at the milliammeter 5. Under the influence of the current I_{con} , the microsyn torquer applies a moment M_t to the floating gyro-assembly, deflecting it from its original position. A voltage U_{out} appears at the output of the microsyn pickoff and is delivered to the input of the amplifier 16. The amplifier output feeds the control winding of the stator 14 of the slave motor. The slave-motor rotor proceeds to rotate at a velocity at which the moment M_t is compensated by the moment of the gyroscope. At a constant current I_{con} , this velocity will also be constant. Thus there is a specific velocity of rotation of the platform 9 for each value of the current I_{con} . The rotational velocity of the platform is determined by measurement of the angle through which it rotates in a certain

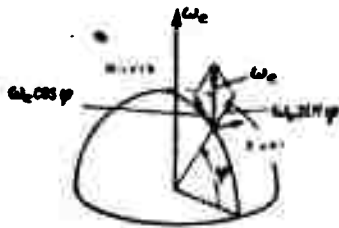


Fig. 5.3. Decomposition of angular velocity of earth's diurnal rotation into vertical ($\omega_e \sin \varphi$) and horizontal ($\omega_e \cos \varphi$) components (φ = latitude).

interval of time. The angle of rotation is read through the microscope 15 from the circle 8, which is calibrated in degrees. The electric clock 6 and its contact device 7 serve to determine the elapsed time. The angular sensitivity threshold of the apparatus should be no higher than 6 seconds of arc. In the actual apparatus,

all feed sources and their controls are built into a single console. The turntable apparatus and all measuring devices incorporated in it must ensure high precision in

the necessary measurement ranges. Only when this condition is met may we depend on obtaining the true static characteristics of the gyroscopes. Specifically for this purpose, the effect exerted on the operation of the apparatus by the moments $M_{-d.syst}$ acting upon the floating gyroassembly of the integrating gyroscope are compensated by application of a current $I_{-con-d.syst} \left[\text{see Eq. (3.105)} \right]$ to the control winding of the microsyn torquers. The accuracy with which the gyroscope is positioned on the turntable platform is of great importance.

Due to the high sensitivity of the floating integrating gyroscope and its servo-system, the vertical component of the angular velocity of the earth's diurnal rotation will exert an influence on the operation of the turntable apparatus (Fig. 5.3). To examine this influence let us assume that the current $I_{-con} = 0$. The apparatus rotates with the earth about a vertical in inertial space, in other words, about the input axis y (see Fig. 5.2), with a velocity $\omega_e \sin \varphi$ (Fig. 5.3). Under these circumstances a gyroscopic moment $H\omega_e \sin \varphi$ arises, deflecting the floating gyroassembly from its original position. This leads to the appearance at the output of the microsyn pickoff of the output voltage U_{out} , which results in actuation of the servodrive. The latter begins to return the platform 9 to its original position, i.e. to rotate it at a velocity $-\omega_e \sin \varphi$ with respect to the base. Thus the platform 9 of an apparatus in good working order should, at $I_{-con} = 0$, revolve with respect to the base at an angular velocity equal in magnitude and opposite in sign to the vertical component of the angular velocity of the earth's diurnal rotation. With $I_{-con} \neq 0$, therefore, the angular velocity of the platform as determined by time and angle measurements during its rotation must be corrected for the vertical component of the angular velocity of the earth's diurnal rotation.

An explanatory block diagram of the turntable apparatus is presented in Fig. 5.4. It is analogous in principle to the diagram shown in Fig. 3.5. In both cases the amplifiers consist of elements which perform analogous functions. The converter

element of the turntable amplifier has a transfer function which is determined by

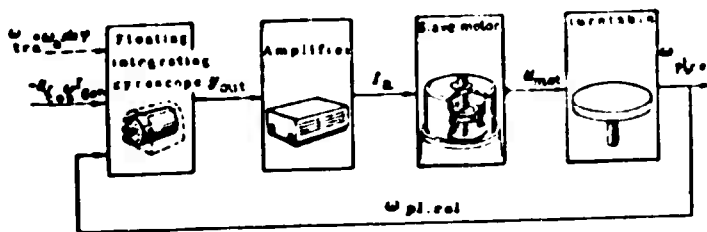


Fig. 5.4. Block diagram of turntable apparatus.

Eq. (3.87). The slave motor of the turntable operates without reduction gearing.

Assuming in Eq. (3.99) that

$$\omega_{tra} = \omega_e \sin \varphi,$$

$$\omega_{rel} = \omega_{pl,rel},$$

where $\omega_{pl,rel}$ is the angular velocity of the platform with reference to the base of the apparatus, we obtain the differential equation of motion of the rotary platform in the form

$$[W(p) + 1] \omega_{pl,rel} = -W(p) [\omega_e \sin \varphi - k_{com} \omega_{com}]. \quad (5.7)$$

By successive substitution in this equation of the expressions (3.100), (3.46), (3.92), (3.97), and (3.87) [or supposing in (3.101) that $K_{in} = \frac{M_d}{J} = \ddot{\gamma} = 0$, $\omega_{tra} = \omega_e \sin \varphi$, $\omega_{rel} = \omega_{pl,rel}$], we obtain

$$\begin{aligned} [p^2(Tp + 1)(T_c p + 1) + K_0(\pi T_c p + 1)] \omega_{pl,rel} = \\ = -K_0(\pi T_c p + 1)(\omega_e \sin \varphi - k_{com} \omega_{com}) \end{aligned} \quad (5.8)$$

In practical studies of the dynamics of the rotating platform we may consider the terms \underline{T}_p and $\underline{T}_{\underline{C}}p$ in Eq. (5.8) negligible by comparison with unity, since this is assured by the small values of the time constants \underline{T} and $\underline{T}_{\underline{C}}$. In this case, the differential equation of motion of the turntable platform (5.8) is considered simplified:

$$(T_{01}^2 p^2 + nT_C p + 1) \omega_{p,rel} = -(nT_C p + 1) (\omega_0 \sin \varphi - k_{I_{con}} \int \omega_0 dt) \quad (5.9)$$

Here, T_{01} is determined by Equality (3.122).

Considering $\underline{I}_{con} = \text{const}$ and assuming in either Eq. (5.8) or (5.9) that $p = 0$, we find that the angular velocity of the rotary platform in the steady state is given by

$$\omega_{p,rel} = k_{I_{con}} \int \omega_0 dt - \omega_0 \sin \varphi. \quad (5.10)$$

With $\underline{I}_{con} = 0$, it follows from this that

$$\omega_{p,rel} = -\omega_0 \sin \varphi. \quad (5.11)$$

The absolute angular velocity of the platform is

$$\omega_{p,abs} = \omega_{p,rel} + \omega_0 \sin \varphi = k_{I_{con}} \int \omega_0 dt \quad (5.12)$$

This velocity must also be taken as the angular velocity ω_{exp} .

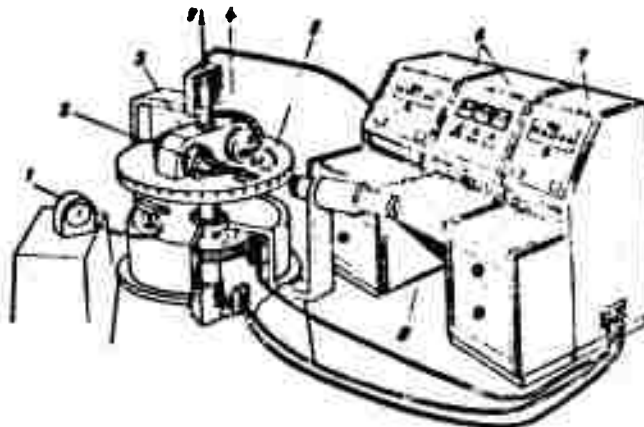


Fig. 5.5. General view of apparatus for analysis of floating differentiating gyroscopes. 1) Electric clock; 2) floating differentiating gyroscope, acting as component of turntable; 3) thermostat; 4) gyroscope under analysis; 5) rotary platform; 6) feeding, regulating, and monitoring units for gyroscope under analysis; 7) feeding, regulating, and monitoring unit for turntable apparatus; 8) three-unit console.

Integrating Eq. (5.10) for zero initial conditions, we find that the angle of rotation of the platform relative to the base of the apparatus is

$$\alpha_{p1} = (k_{1..n} \int_{t_0}^t -\omega \sin \varphi) f. \quad (5.13)$$

A general view of the apparatus for the static analysis of floating differentiating gyroscopes is presented schematically in Fig. 5.5. It consists of the turntable device described above and shown separately in Fig. 5.2, plus the three-section console 8. All the components necessary to feed, regulate, and monitor the turntable apparatus are incorporated in section 7. The two sections 6 contain everything necessary for feeding, regulating, and monitoring the gyroscope being analyzed.

The floating differentiating gyroscope being tested (4) is mounted on the

rotary platform 5 (Fig. 5.5) inside a common thermostat 3 with the floating integrating gyroscope 2, which acts as an accessory component of the turntable apparatus. The input (measurement) axis of the test gyroscope is oriented parallel to the axis (y) of rotation of the platform 5. Its x and z_0 axes are parallel to the corresponding axes of the gyroscope 2, whose directions are indicated in Fig. 5.2.

Static analyses of floating differentiating gyroscopes in the apparatus shown in Fig. 5.5 proceed as follows: the platform 5 is made to rotate at various constant angular velocities $\omega_{pl. rel}$ by supplying various currents I_{con} to the microsyn torquer of the floating integrating gyroscope 2. The output signal of the floating differentiating gyroscope being analyzed is measured for each value of $\omega_{pl. rel}$. For torsion-rod gyroscopes this signal will be the voltage U_{out} , and for feedback gyroscopes it will be the output current I_a of the amplifier. The static characteristics of the devices tested are constructed on the basis of the results of analysis.

Static characteristics obtained by the above method for floating differentiating gyroscopes are presented below. Figure 5.6 shows static characteristics for a floating differentiating gyroscope with a torsion rod -- Type 10⁴, No. 55. Data concerning this gyroscope were given previously in Tables 4 and 5 (Chap. II, Sec. 2). The static characteristics were recorded under the following conditions:

Frequency of current fed to gyromotor	$f_{gyr} = 400$ cps
Phase voltage of gyromotor	$U_{ph} = 4.0$ volts
Phase current of gyromotor	$I_{ph} = 0.6$ amp
Excitation current of microsyn pickoff	$I'_{ex} = 250$ ma
Frequency of current fed to excitation winding of microsyn pickoff	$f_p = 400$ cps
Temperature of fluid	$t = 71.1^\circ C$

In calculating the numerical values of the relative angular velocity $\omega_{exp. rel}$ [see Equality (3.61)] and the relative dimensionless amplification factor $(K_{\omega, y_{out}})_{exp. rel}$ [see Eq. (4.31)], it was assumed that

$$\omega_{\text{cal}} = 1 \text{ mrad/sec} = 0.0573^\circ/\text{sec} = 13.8 \omega_e$$

Here and henceforth, $\omega_e = 7.29 \cdot 10^{-5}$ rad/sec is the angular velocity of the diurnal rotation of the earth.

$$(K_{\omega} U_{\text{out}})_{\text{cal}} = 0.819 \frac{\text{mV}}{\text{mrad/sec}} = 819 \frac{\text{mV}}{\text{rad/sec}} = 0.239 \frac{\text{mV}}{\text{min}}$$

Static characteristics for torsion-rod floating differentiating gyroscope, Type 10⁴, No. 26, produced by the Massachusetts Institute of Technology, which is similar in design to the No. 55, are presented in Fig. 5.7. The characteristics were recorded under the following conditions:

Frequency of current fed to gyromotor	$f_{\text{gyr}} = 400$ cps
Phase voltage of gyromotor	$U_{\text{ph}} = 3.5$ volts
Phase current of gyromotor	$I_{\text{ph}} = 0.5$ amp
Excitation current of microsyn pickoff	$I'_{\text{ex}} = 250$ ma
Frequency of current fed to excitation winding of microsyn pickoff	$f_p = 400$ cps
Temperature of fluid	$t = 71.1^\circ\text{C}$

In plotting these curves it was assumed that

$$\omega_{\text{cal}} = 1 \text{ mrad/sec} = 0.0573^\circ/\text{sec} = 13.8 \omega_e$$

$$(K_{\omega} U_{\text{out}})_{\text{cal}} = 1.15 \frac{\text{mV}}{\text{mrad/sec}} = 1150 \frac{\text{mV}}{\text{rad/sec}} = 0.335 \frac{\text{mV}}{\text{min}}$$

In the analyses of both gyroscopes, the upper limit of the measured angular velocities ω_{exp} was 1950 mrad/sec = 1.95 rad/sec; this was imposed by the

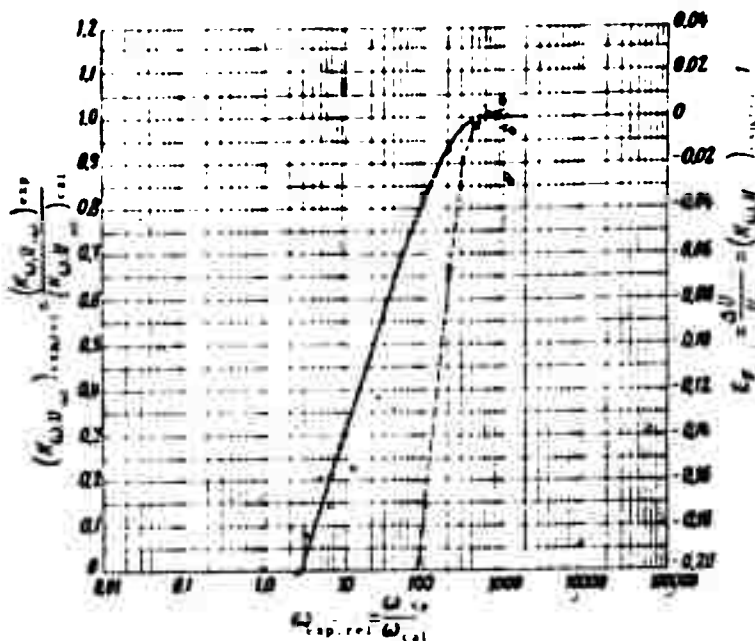


Fig. 5.6. Static characteristics of Massachusetts Institute of Technology torsion-rod floating differentiating gyroscope, Type 10⁴, No. 55. o-points for $(K_{U, out} - K_{U, in}) / K_{U, in}$; •-points for U_{out} / U_{in} .

presence of stops which prevented deflection of the floating gyroassembly through more than 2.5° from its initial position with reference to the housing of the mechanism. It will be remembered that the upper-limit restriction on the velocities to be measured with the differentiating gyroscope was occasioned in practice by the necessity of avoiding effects on its operation due to the angular velocity of the rotation of the instrument housing about the axis z_0 , i.e. about the initial position of the spin axis z . The greater the measured angular velocity, the greater will be the angle of deflection of the floating gyroassembly from its initial position, and, consequently, the greater the effect of the angular velocity about the z_0 axis. It would seem that floating differentiating torsion-rod gyroscopes should operate well beginning at very small values of the measured velocity ω_{exp} . However, as shown by the curves in Figs. 5.6 and 5.7, this is not the case. It

develops that the lower limit of the working range is rather high. Thus in the case of Gyroscope No. 55 it is 0.390 rad/sec, provided that a relative output-voltage

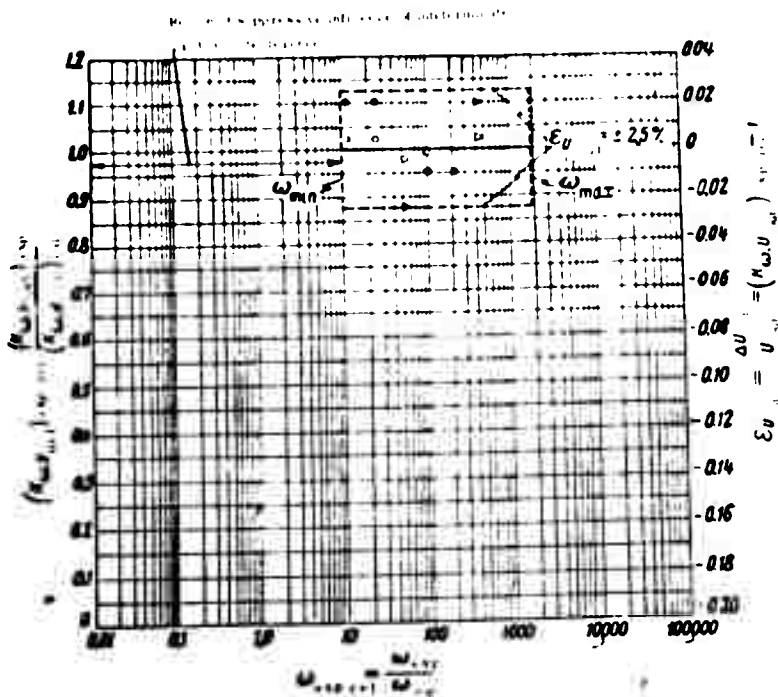


Fig. 5.7. Static characteristics of floating differentiating gyroscope with torsion rod, Type 10⁴, No. 26. o-points for $(K \cdot \omega, U_{out} \exp. rel)$; •-points for U_{out} .

error $U_{out} \gg 0.01$ is tolerated, and 0.170 rad/sec for $U_{out} \gg 0.1$. Gyroscope No. 26 gave the best results. The relative output-voltage error U_{out} for this device does not exceed ± 0.025 at angular velocities above 0.010 rad/sec. At smaller angular velocities, the discrepancy of the results of measurement is so great that it becomes impossible to make inferences regarding the operation of the device from these data. It should be noted, however, that the wide scattering of the experimental results at small values of the measured angular velocity is due not only to imperfections in the gyroscope itself, but also to imperfections in the apparatus used to measure the output voltage U_{out} of the gyroscope. This voltage was measured with the aid of an ordinary thermionic voltmeter without special

modification of the measurement apparatus. As a result, indeterminate electrical disturbances of various types showed up in the experimental results. These disturbances were particularly intense in measurements of the voltages U_{out} for small measured angular-velocity values. It is necessary to exercise extreme care in designing the layout for analysis of differential gyroscopes in order to reduce these disturbances.

According to information furnished by the persons who conducted them, no special conditions were created for the gyroscope analyses, i.e. the gyroscopes were tested under conditions similar to those encountered in actual use.

Most important among the factors which exert a negative influence on the operation of torsion-rod floating differential gyroscopes at small values of the measured angular velocity are the following: lack of rigidity (elasticity) in the mounting of the floating gyroassembly, which is formed by the elastic torsion rod, and undue influence on the value of the output voltage U_{out} arising from dynamic imbalance of the gyromotor rotor, since the electrical noise created by this condition results in considerable distortion and suppression of the voltage U_{out} , which is relatively small at small values of the measured angular velocity. Other such negative factors are torsion-rod hysteresis, the zero-point errors of this rod and the microsyn pickoff, mechanical vibrations, etc.

Thus the lower limit of the working range of the device under consideration is determined both by the imperfections of the device itself and by disturbances of various types in the measurement circuits. It is possible that refinement of the instruments and technique used in measuring the output voltage will permit a certain reduction in the lower limit of the working range of torsion-rod floating differential gyroscopes. In the opinion of C. S. Draper and the specialists working with him, however, the peculiarities of the torsion-rod floating differentiating gyroscope itself will, in all probability, prevent the device working efficiently at measured angular velocity values significantly lower than 0.005 rad/sec. This

statement should be regarded as applicable solely to the specific design of the device analyzed.

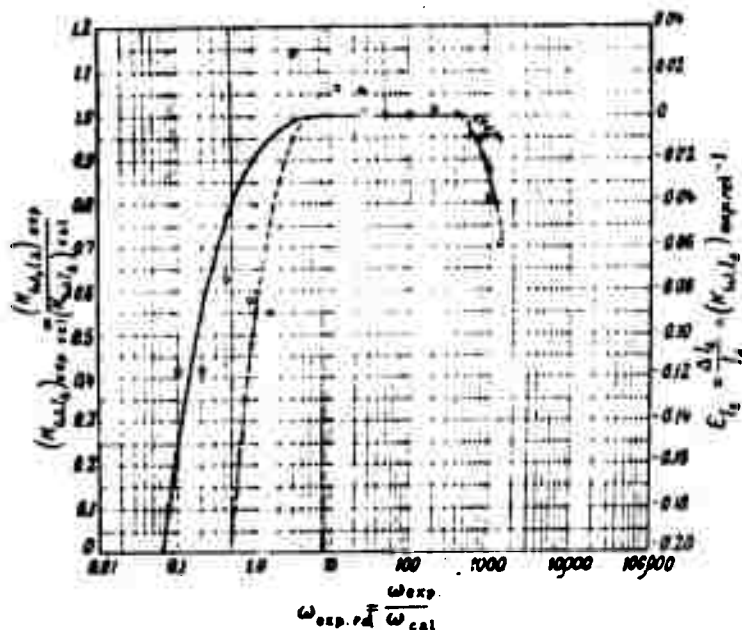


Fig. 5.8. Static characteristics of floating differentiating gyroscope with feedback circuit. \circ -points for $(K_{\omega, I_a})_{exp. rel}$; \bullet - points for ϵ_{I_a} .

Figure 5.8 shows the static characteristics of a floating differentiating gyroscope with a feedback circuit, formed from the floating integrating gyroscope (Type 10⁴, No. 79) whose characteristics were presented earlier in Tables 1 and 2 (Chapter II, Sec. 1). The static characteristics were recorded under the following conditions:

Frequency of current fed to gyromotor	$f_{\text{gyr}} = 400$ cps
Phase voltage of gyromotor	$U_{\text{ph}} = 7.5$ volts
Phase current of gyromotor	$I_{\text{ph}} = 0.2$ amp
Excitation current of microsyn pickoff	$I'_{\text{ex}} = 125$ ma
Frequency of current fed to excitation winding of microsyn pickoff	$f_p = 400$ cps

Excitation current of microsyn-torquer	I_{ex}	=	200 ma
Temperature of fluid	θ	=	71.1°C
Amplification factor of amplifier	$K_{U-out} \frac{I_a}{I_a}$	=	0.0952 ma/mv

In computing the numerical values of the relative angular velocity $\omega_{exp.rel}$ [see Equality (3.61)] and the relative dimensionless amplification factor $(K_{\omega}, I_a)_{exp.rel}$ [see Eqs. (4.81) and (4.80)], it was assumed that

$$\begin{aligned} \omega_{rel} &= 1 \text{ rad/sec} = 0.0573^\circ \text{ sec} = 13.8 \omega_0 \\ (I_a)_{rel} &= 0.1181 \text{ ma} \\ (K_{\omega}, I_a)_{rel} &= 0.1181 \frac{\text{ma}}{\text{rad/sec}} = 118.1 \frac{\text{ma}}{\text{rad/sec}} = 0.344 \frac{\text{ma}}{\text{rad/sec}} \end{aligned}$$

The following conclusions may be drawn from consideration of the graph shown in Fig. 5.8. If it is specified that the relative error ϵ_{I_a} of the output signal (the current I_a) shall not exceed 0.01, the lower limit of measured angular velocities will be

$$\omega_{exp.min} = 0.003 \text{ rad/sec},$$

and the upper limit

$$\omega_{exp.max} = 0.700 \text{ rad/sec}.$$

If, however, we have $\epsilon_{I_a} > 0.1$,

$$\omega_{exp.min} = 0.0009 \text{ rad/sec},$$

$$\omega_{exp.max} = 1.800 \text{ rad/sec}.$$

In the latter case the value of $\omega_{exp.max}$ was obtained by extrapolation.

The static characteristics of the above device are generally similar to those of the torsion-rod floating differentiating gyroscope. In this device, however, $\omega_{exp.min}$ is considerably smaller. Its $\omega_{exp.max}$ value is determined not by the positions of the stops which limit the rotation of the floating gyroassembly, but by a saturation phenomenon in the core of the microsyn torquer due to the drop in the

static characteristic at large values of the measured angular velocity.

Thus the floating differentiating gyroscope with a feedback circuit permits us to exploit the advantages afforded by the efficiency of the floating integrating gyroscope in the region of low values of the measured angular velocity. It has been noted above that the microsyn pickoff can operate on either alternating or direct current, i.e. if the current I_a delivered from the amplifier output to the secondary winding of the microsyn-pickoff is an alternating current, the experimental values for the input angular velocity determined by the measurement of this current will depend on the mode of alternation of this current. In principle, therefore, we are faced here with the same difficulties in measuring alternating currents as are encountered with torsion-rod floating differentiating gyroscopes. However, the floating differentiating gyroscope with feedback generally permits more accurate measurement of the input angular velocity, since measurement of it in this case amounts to measurement of a comparatively large I_a current ($I_{a \min} \approx 100 \mu \text{ amp}$), and also by virtue of the advantages which this device offers in principle over the torsion-rod differentiating gyroscope, and which were discussed in Chapter IV, Sec. 7.

Difficulties due to magnetic hysteresis arise in cases when the microsyn torquer and, consequently, the feedback circuit, are operated on direct current. These may prove to be just as troublesome as the difficulties which arise when working with alternating current. Special measures are necessary to eliminate magnetic-hysteresis effects.

In measurement of high angular velocities, the operation of the device would be limited only by the potentialities of the gyroscope itself, or, more precisely, by those of the microsyn torquer, provided that the feedback circuit and the system used to measure the amplifier-output current are chosen correctly. In practice, however, it may prove unnecessary to provide for the measurement of the maximal angular velocities permitted by the gyroscope. When this is the case, a simplified

electrical layout may be employed in the feedback circuit.

Section 3. Static Analyses of Integrating Gyroscopes in Spatial-Integration Regime

The steady spatial-integration regime is characterized by the amplification factor $k_{I_{-con}}$. Thus the curves of the dependence of the relative nondimensional amplification factor $(k_{I_{-con}}, \omega)_{exp.rel}$ as determined by Eq. (3.70) and the relative error ϵ_{rel} upon the relative angular velocity $\omega_{exp.rel}$ are the static characteristics of this regime.

Analysis is conducted with the turntable apparatus illustrated schematically in Fig. 5.2. The device 12 undergoing analysis is mounted on the platform 9 in the manner shown in Fig. 5.2. The analytical process ought to consist in delivery of various currents I_{con} to the control winding of the microsyn torquer and measurement of the corresponding steady values of the angular velocity of the platform. The current I_{ex} fed to the excitation winding of the microsyn torquer ought to be held strictly constant, as is usually the case when the floating integrating gyroscope is normally used in its effective (linear) working range. However, when the windings of the microsyn torquer are fed separately, its working range, which is characterized by a proportional dependence of the moment M_t generated by it on the control current I_{con} , is significantly smaller than when its windings are series-connected and fed by a common current I_{con} .

The restriction of the working range of an integrating gyroscope resulting from reduction of the working range of the microsyn torquer, due to the use of separate current supplies for its windings, amounts to at least two modules of the $\omega_{exp.rel}$ scale, and in some cases even more (see Fig. 5.1). Thus the use of separate feeds for the windings of the microsyn torquer prevents full exploration of the potential of the floating integrating gyroscope undergoing analysis.

In the analyses, therefore, the two windings of the microsyn torquer are connected in series and supplied with a common current I_{con} . This permits complete study of the full potential of the floating integrating gyroscope under examination, or, in other words, full coverage of the angular-velocity range inherent to it, except for certain restrictions imposed even in this case by the microsyn torquer. The effect of the moment $M_{\text{I syst}}$ on the floating gyroassembly is compensated by the delivery of the appropriate current to the microsyn torquer.

Accordingly, static analyses of floating integrating gyroscopes in the spatial-integration regime, using the apparatus shown in Fig. 5.2, consists in delivery of various currents I_{con} to the series-connected primary and secondary windings of the microsyn torquer and measurement of the resulting steady angular velocities of the platform. Accordingly, the curve of the dependence of the relative nondimensional amplification factor

$$(k_{\text{I con}})_{\text{exp. rel}} = \frac{(k_{\text{I con}})_{\text{exp}}}{(k_{\text{I con}})_{\text{cal}}} \quad (5.14)$$

on the relative angular velocity $\omega_{\text{exp. rel}}$ is used as the static characteristic which describes the steady spatial-integration regime, and not the curve of the factor $(k_{\text{I con}})_{\text{exp. rel}}$. Here,

$$(k_{\text{I con}})_{\text{exp}} = \frac{\omega_{\text{exp}}}{(I_{\text{con}})_{\text{exp}}} \quad (5.15)$$

$$(k_{\text{I con}})_{\text{cal}} = \frac{\omega_{\text{cal}}}{(I_{\text{con}})_{\text{cal}}} \quad (5.16)$$

Let us establish the relationship between the factors $(k_{\text{I con}})_{\text{exp. rel}}$ and $(k_{\text{I ex-con}})_{\text{exp. rel}}$. Applying Eq. (3.39), we may rewrite Expression (5.14) in

$$(k_{I_{con}})_{exp. rel} = \frac{(k_{I_{con}})_{exp. cal}}{(k_{I_{con}})_{cal} \frac{I_{exp. cal}}{I_{exp. rel}}}$$

It follows from this upon application of Eq. (3.70) that

$$(k_{I_{con}})_{exp. rel} = (k_{I_{con}})_{exp. rel} \frac{I_{exp. cal}}{I_{exp. rel}} \quad (5.17)$$

Since the windings of the microsyn torquer are series-connected and fed with a single current I_{con} during the analysis,

$$I_{con} = I_{cm} \quad (5.18)$$

and Eqs. (5.14), (5.15), (5.16), and (5.17) take the form

$$(k_{I_{con}})_{exp. rel} = \frac{(k_{I_{con}})_{exp. cal}}{(k_{I_{con}})_{cal}} \quad (5.19)$$

$$(k_{I_{con}})_{exp. rel} = \frac{\omega_{exp. rel}}{(I_{con})_{exp. rel}} \quad (5.20)$$

$$(k_{I_{con}})_{cal} = \frac{\omega_{cal}}{(I_{con})_{cal}} \quad (5.21)$$

$$(k_{I_{con}})_{exp. rel} = (k_{I_{con}})_{exp. rel} \frac{I_{con. cal}}{I_{con. exp.}} \quad (5.22)$$

In addition to the graph of the dependence of the relative dimensionless amplification factor $(k_{I_{con}})_{exp. rel}$ on the relative velocity $\omega_{exp. rel}$, we also construct a curve of the dependence of the relative error ϵ_{ω} of the angular velocity upon this factor; according to Formula (3.59), this will be given by

$$\epsilon_{\omega} = (k_{I_{con}})_{exp. rel} - 1. \quad (5.23)$$

Figure 5.9 presents the static characteristics of a floating integrating gyroscope of Type 10⁴, No. 79 (data for which were presented in Chapter II, Sec.

1, Tables 1 and 2), as registered by the described method using the apparatus illustrated schematically in Fig. 5.2. The characteristics were recorded under the following conditions:

Frequency of current fed to gyromotor	$f_{\text{gyr}} = 400 \text{ cps}$
Phase voltage of gyromotor	$U_{\text{ph}} = 7.5 \text{ volts}$
Phase current of gyromotor	$I_{\text{ph}} = 0.2 \text{ amp}$
Excitation current of microsyn pickoff	$I'_{\text{ex}} = 125 \text{ ma}$
Frequency of current fed to excitation winding of microsyn pickoff	$f_p = 400 \text{ cps}$
Temperature of fluid	$\tau = 71.1^\circ\text{C}$

The windings of the microsyn torquer were supplied with direct current during the analyses. A high-quality direct-current voltage stabilizer of the type used under normal operational conditions was employed as a current supply. The use of direct current considerably simplified the task of obtaining exact measurements of the I_{con} currents which arise in the series-connected windings of the microsyn torquer. It should be noted that the integrating gyroscope analysis was conducted under conditions which approximated to normal working conditions just as closely as in the case of differentiating gyroscopes.

In computing the numerical values of the relative angular velocity $\omega_{\text{exp.rel}}$ [see Eq. (3.61)], the relative dimensionless amplification factor $(k_{I_{\text{con}}}^2)_{\text{exp.rel}}$ [according to Eqs. (5.19) and (5.20)], and the relative error ϵ , which is determined by Formula (5.23), it was assumed that

$$\epsilon_{\text{cal}} = 1 \text{ rad/sec} = 0.0573^\circ/\text{sec} = 13.8\omega_e$$

$$(I_{\text{con}})_{\text{cal}}^2 = 24.47 \text{ ma}^2$$

$$(k_{I_{\text{con}}}^2, \omega)_{\text{cal}} = 0.04087 \frac{\text{mrad/sec}}{\text{ma}^2} = 4.087 \cdot 10^{-5} \frac{\text{rad/sec}}{\text{ma}^2} = 0.234 \frac{^\circ/\text{min}}{\text{ma}^2}$$

It will be seen from the curves in Fig. 5.9 that the factor $\left(\frac{k_{I,2}}{I_{con, \omega}}\right) \exp. rel$ remains equal to unity with an error of $\pm 1\%$ in the angular-velocity range from 0.0001 to 4 rad/sec. In other words, the relative error ϵ_{rel} of the output quantity, the angular velocity ω , does not exceed ± 0.01 ($\pm 1\%$) in this range. At angular velocities greater than 4 rad/sec, the curve of the factor $\left(\frac{k_{I,2}}{I_{con, \omega}}\right) \exp. rel$,

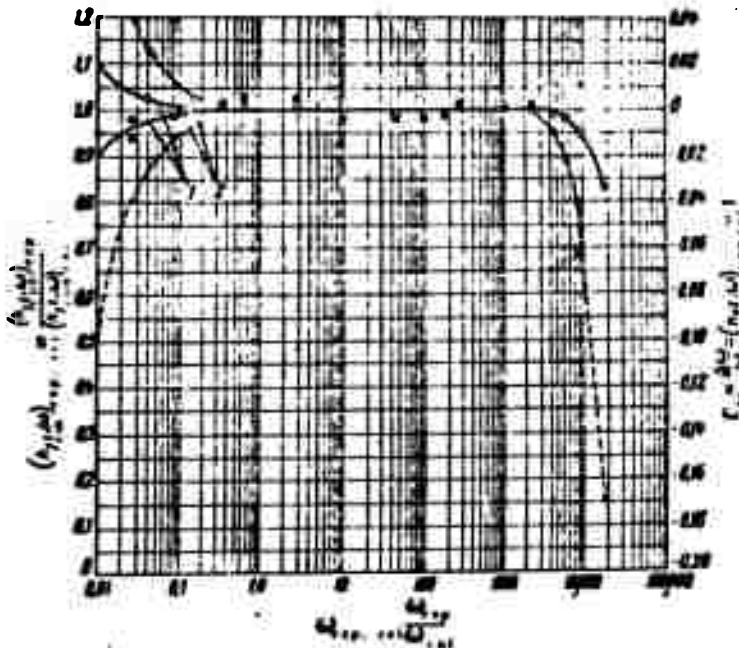


Fig. 5.9. Static characteristics of operation of floating integrating gyroscope of Type 10^4 , No. 79, in spatial-integration regime. o-points for $\left(\frac{k_{I,2}}{I_{con, \omega}}\right) \exp. rel$; ●-points for ϵ_{rel} ; 1 and 2) Envelopes of points for $\left(\frac{k_{I,2}}{I_{con, \omega}}\right) \exp. rel$ and ϵ_{rel} , corresponding to an absolute error $\Delta\omega$ of the output quantity equal to ± 0.000001 rad/sec.

and, consequently, that of the relative error ϵ_{rel} , turn sharply downward; this is accounted for by a saturation effect in the core of the microsyn torquer which reduces the moment which it generates, and also by friction due to the radial load on the bearings which results from the increase in the magnetic reactive moment.

At angular velocities smaller than 0.0001 rad/sec the distribution of the

points assumes a random character. However, all of them occur between enveloping curves which correspond to absolute errors $\Delta\omega$ of the angular velocity ω of ± 0.000001 rad/sec. This signifies that the influence of various indeterminate electrical disturbances prevents us at small angular velocities from maintaining the output quantity of the spatial integrator, i.e., the angular velocity ω , with an error smaller than ± 0.000001 rad/sec. Among the principal factors which cannot be taken into account due to their indeterminate nature, and which, consequently, belong to the class of indeterminate disturbances, are the following: friction in the bearings of the floating gyroassembly; radial displacement of the floating gyroassembly, which results in asymmetry of the magnetic flux in the gaps of the microsyn torquer and microsyn pickoff and, consequently, in the development of a moment acting upon the floating gyroassembly; and finally, electrical disturbances of various types which produce indeterminate output-signal components and thereby affect the operation of the gyroscope.

The region of indeterminate values of the factor $\left(\frac{k_{I2}}{I_{con}}, \omega\right)_{exp. rel}$ which is found at angular velocities smaller than 0.0001 rad/sec could, in all probability, be reduced by more careful manufacture, adjustment, and monitoring both of the floating integrating gyroscope itself and of the servodrive. It may be assumed, however, that a certain region of indeterminate values of the factor $\left(\frac{k_{I2}}{I_{con}}, \omega\right)_{exp. rel}$, i.e., a region of indeterminate operation of the device in the spatial-integration regime, will always exist at low angular velocities. Refinement of the device may lead to the region shifting toward lower angular-velocity values, but the general nature of the static characteristics of the device will remain the same as that indicated in Fig. 5.9.

It should also be borne in mind that the error of measurement is also a function of the accuracy with which the turntable circle is graduated and the interval of time which elapses between successive microscope readings.

If a $\pm 2.5\%$ deviation of the factor $\left(\frac{k_{I2}}{I_{con}}, \omega\right)_{exp. rel}$ from unity [see

Formula (5.2)] is considered tolerable in the working range of the Type 10⁴, No. 79 device, this working range will extend (as seen from Fig. 5.9) from $\omega_{\text{exp. min}} = 0.00004$ rad/sec to approximately $\omega_{\text{exp. max}} = 7$ rad/sec. The ratio of these limits is $N_{79} = \frac{\omega_{\text{exp. max}}}{\omega_{\text{exp. min}}} = 175,000$.

Applying the same tolerance to the working range of the floating torsion-rod differential gyroscope whose characteristics were presented in Fig. 5.7, we find that it extends from $\omega_{\text{exp. min}} = 0.010$ rad/sec to $\omega_{\text{exp. max}} = 1.950$ rad/sec.

Thus for this device

$$N_{26} = \frac{\omega_{\text{exp. max}}}{\omega_{\text{exp. min}}} = 195.$$

Accordingly, $N_{79} : N_{26} = 897.5$.

The significantly wider working range of the floating integrating gyroscope operating in a uniaxial spatial-integrator system as compared to the working range of the floating torsion-rod differential gyroscope used to measure angular velocity is accounted for on the one hand by the superior design of the integrating gyroscope, and on the other by the larger error in an ordinary thermionic voltmeter reading for an alternating output voltage U_{out} as compared with a direct-current voltage. The analyses of the differentiating and integrating gyroscopes were conducted on the same turntable apparatus. The angular velocities of the rotary platform were imparted by the same integrating gyroscope in both cases; in one case, this functioned as a component of the apparatus, and in the other as the object of analysis. The angular velocities of the turntable apparatus were thereby maintained with the same degree of accuracy in the analyses of both devices.

Even when the difficulties involved in measurement of the input and output quantities are taken into account, the range in which the integrating gyroscope functions satisfactorily is far wider than the same range for the differentiating gyroscope. This is explained by numerous factors which affect the operation of the

differential gyroscope but not that of the integrating gyroscope. As was noted previously, these include torsion-rod hysteresis, the zero-point error of this rod and the microsyn-pickoff, vibration, etc.

Differentiating gyroscopes with feedback circuits are superior in that they do not have torsion rods or mechanical springs of any other type. The basic disadvantage of all types of differentiating gyroscopes, however, is the necessity of limiting the angle of rotation of the floating gyroassembly in order to eliminate the influence on their operation of the angular velocity of rotation of the instrument housing about the z_0 axis perpendicular to the input (measurement) and output axes of the device; this lowers the upper limit of the working range of the device by a considerable margin. This limitation does not generally apply to the integrating gyroscope, provided that it operates in conjunction with a correctly computed servosystem equipped with an integral control having an adequate amplification factor. The use of large amplification factors renders it possible to actuate the servodrive at small values of the microsyn-pickoff output voltage U_{out} , or, in other words, at extremely small (near-zero) angular deflections of the floating gyroassembly from its initial position.

Since the integrating gyroscope does not possess a torsion rod or any other mechanical springing device, it is completely free from the drawbacks inherent in them: hysteresis, nonlinearity, difficulties in connection with the adjustment of the torsion rod. Another advantage of the integrating gyroscope is that it makes use of a heavy fluid having a considerably higher viscosity than that used in the differentiating gyroscope. This results in appreciable reduction of the influence which the vibration of the gyromotor rotor during its rotation exerts upon the operation of the integrating gyroscope.

Section 4. Static Analysis of Integrating Gyroscopes in the Geometric-Stabilization Regime

In the steady state, the geometric-stabilization regime is characterized by the relative dimensionless amplification factor $(K_{\omega_{tra}} \omega_{rel})_{exp. rel}$ determined by Eqs. (3.113) and (3.111) and the relative error $\epsilon_{\omega_{rel}}$ given by Eq. (3.114). Thus the static characteristics of this regime are the curves of $(K_{\omega_{tra}} \omega_{rel})_{exp. rel}$ and $\epsilon_{\omega_{rel}}$ as functions of $\omega_{exp. rel}$, as obtained from Eq. (3.61). It should be noted that the geometrical-stabilization regime is, by nature, a particular case of the spatial-integration regime which occurs when the current I_{con} delivered to the secondary winding of the microsyn torquer is given zero value. As a rule, the various disturbing moments M_1 due to mechanical imbalance, the reactions of the pickoff and torquer, the gyromotor leads, etc., affecting the floating gyroassembly, lead, as noted previously, to the appearance of drift in the servodrive which controls the integrating gyroscope. It was also pointed out that a suitable current $I_{con M_1 syst}$ is supplied to the control winding of the microsyn torquer in order to compensate the effect of the systematic component $M_1 syst$ of the interference moment M_1 . The presence of this current does not alter the operating regime of the device, which remains one of geometric stabilization, as in the case $I_{con} = 0$.

The analysis of integrating gyroscopes in the geometrical-stabilization regime is conducted in the apparatus represented schematically in Fig. 5.10. This consists of the familiar turntable, illustrated separately in Fig. 5.2, and the three-section console 17. These are complemented by the independent uniaxial spatial angular-velocity integrator mounted on the rotary platform 16 with its servosystem and

the floating integrating gyroscope 10 to be analyzed. The input axis y of this integrator coincides with the geometrical axis of rotation of the platform 16. The base 3 of the integrator is rigidly attached to the platform 16. The slave motor 15 and its speed reducer, which consists of the servosystem gears 14 and 13, are mounted in the base 3. The shaft of the gear 13 is vertical and directed along the input axis y of the integrator. The thermostat 12 is rigidly mounted on the gear 13, and plays the part of the object which has to be stabilized geometrically in inertial space with reference to the y axis. The gyroscope 10 undergoing analysis is mounted within the thermostat. Its measurement axis is directed along the y

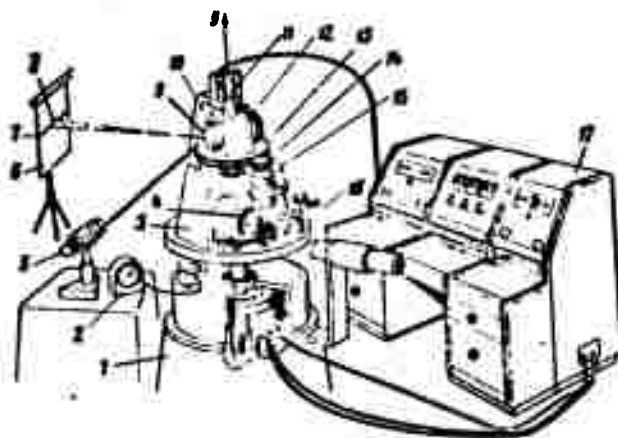


Fig. 5.10. Apparatus for static analysis of floating integrating gyroscopes in the geometric-stabilization regime. 1) Base; 2) electric clock; 3) base of integrator; 4) floating integrating gyroscope; 5) light source; 6) screen; 7) scale; 8) light spot formed by beam reflected from mirror 9; 9) mirror; 10) integrating gyroscope undergoing analysis; 11) contact rings and brushes; 12) thermostat; 13), 14) servomechanism reduction gearing; 15) slave motor of servosystem; 16) rotary platform; 17) three-section console.

axis. A mirror 9 is affixed to the face of the gyroscope. The angles through which the thermostat 12 and gyroscope 10 rotate with respect to the base 1, i.e. with respect to the earth, are determined by observation of the spot 8 (formed by the pencil of light reflected from the mirror 9) as it moves along the scale 7 on the fixed screen 6.

Let us examine the steady-state operation of the integrator mounted on the rotary platform 16, which is characterized in the general case by Eq. (3.103). $\dot{\gamma} = 0$ for the integrator under consideration. Let us assume that the moment $M_{-1 \text{ syst}}$ acting on the floating gyroassembly of the test gyroscope 10 is compensated by supplying the appropriate current $I_{\text{con } M_{-1 \text{ syst}}}$ as determined by Eq. (3.105) to the control winding of its microsyn torquer. The transfer angular velocity ω_{tra} of the integrator base 3 is identical to the absolute angular velocity of rotation of the platform 16, which is determined by Eq. (5.12). Thus,

$$\omega_{\text{tra}} = \omega_{\text{pl. abs}} = \omega_{\text{pl. rel}} + \omega \sin \varphi. \quad (5.24)$$

Taking all of the above factors into account, we find that the steady-state operation of the integrator under examination is characterized in the general case, provided that $M_{-1 \text{ rand}} = 0$, by the equation

$$\omega_{\text{rel}} = -(\omega_{\text{pl. rel}} + \omega \sin \varphi - k_{\text{tr}} I_{\text{con}}). \quad (5.25)$$

Here ω_{rel} is the angular velocity of the thermostat 12 carrying the gyroscope 10 (i.e. velocity of the mirror 9) about the y axis with reference to the integrator base 3 or, which amounts to the same thing, to the platform 16.

Setting $I_{\text{con}} = 0$ in Eq. (5.25), we obtain the steady-state equation of the geometric-stabilization regime. Thus for ideal operation of the integrator in the steady-state geometric-stabilization regime,

$$\omega_{\text{rel}} = -(\omega_{\text{pl. rel}} + \omega \sin \varphi) = -\omega_{\text{pl. abs}}. \quad (5.26)$$

In actuality, the value of the angular velocity ω_{rel} will deviate somewhat from its ideal value as given by Eq. (5.26), simply because $M_{-1 \text{ rand}} \neq 0$. Let the corresponding absolute error be denoted by $\Delta \omega_{\text{rel}}$. Now ω_{rel} will be determined in practice by the equality

$$\omega_{rel} = -(\omega_{pl. abs} - \Delta\omega_{rel}) = -(\omega_{pl. rel} + \omega_r \sin \varphi - \Delta\omega_{rel}). \quad (5.27)$$

In order to determine the values of $(K_{\omega_{tra}, \omega_{rel}})^{exp. rel}$ which correspond to various relative angular velocities

$$\omega_{exp. rel} = \frac{\omega_{pl. abs. exp}}{\omega_{pl. abs. cal}}, \quad (5.28)$$

it is necessary to know the corresponding values of the factor $(K_{\omega_{tra}, \omega_{rel}})^{exp.}$. Proceeding from Eqs. (3.111), (5.27), and (5.24), we find that

$$(K_{\omega_{tra}, \omega_{rel}})^{exp.} = \left(\frac{\omega_{pl. abs} - \Delta\omega_{rel}}{\omega_{pl. abs}} \right)_{exp} = 1 - \left(\frac{\Delta\omega_{rel}}{\omega_{pl. abs}} \right)_{exp} \quad (5.29)$$

Thus the problem comes down to one of measuring $\omega_{pl. abs}$ and $\Delta\omega_{rel}$. The technique used in measuring $\omega_{pl. abs}$ is evident from Formula (5.12), and also from the earlier descriptions of the use of the apparatus shown in Fig. 5.2. $\Delta\omega_{rel}$ should not be measured with reference to the platform 16, which would be difficult, but with reference to the earth, i.e. by means of the light spot moving along the scale 7 of the screen 6 (Fig. 5.10).

Let us find the relationship between $\Delta\omega_{rel}$ and the angular velocity of the mirror 9 about the y axis with reference to the earth, measured in corresponding units with the aid of the scale 7 and the light spot formed by the beam of light reflected from the mirror 9. The velocity of rotation of the mirror 9 about the y axis with respect to the earth is given by $\omega_{mir} = \omega_{rel} + \omega_{pl. rel}$. Substituting Eq. (5.27) in the above, we obtain

$$\omega_{mir} = -(\omega_r \sin \varphi - \Delta\omega_{rel}). \quad (5.30)$$

Thus ω_{mir} differs from $\Delta\omega_{rel}$ by the vertical component of the angular velocity of the earth's diurnal rotation, $\omega_e \sin \varphi$. As a result it is necessary to correct the measured values for the angular velocity ω_{mir} mathematically for the vertical component of the earth's diurnal rotation in order to obtain values for $\Delta\omega_{rel}$. In practice, however, it is considerably more convenient to proceed in such a way that the angular velocity ω_{mir} is not a function of $\omega_e \sin \varphi$, and therefore directly equal to $\Delta\omega_{rel}$, i.e.

$$\omega_{mir} = \Delta\omega_{rel} \quad (5.31)$$

To accomplish this, a current $I_{con} = I_{con. comp}$ sufficient to compensate the vertical component $\omega_e \sin \varphi$ of the earth's diurnal rotation should be supplied to the control winding of the microsyn torquer of the gyroscope 10 undergoing analysis. It follows from Eq. (5.25) that this current

$$I_{con. comp} = \frac{\omega_e \sin \varphi}{k_{con}} \quad (5.32)$$

On the basis of all the above considerations, therefore, the analysis of a floating integrating gyroscope in the geometric-stabilization regime should consist of the following: various constant angular velocities in the inertial space about the y axis are imparted to the platform 16 by supplying the appropriate currents I_{con} to the control winding of the microsyn torquer of the gyroscope 4. The velocity $\Delta\omega_{rel}$ is measured by observation of the light spot (formed by the beam of light reflected from the mirror 9) as it moves along the scale 7, and of the electric clock 2, referring, in this case, to Formula (5.31), since this is permissible by virtue of application of the current $I_{con. comp}$ determined from Eq. (5.32) to the control winding of the microsyn-torquer of the gyroscope 10. Next, the values of $(K_{tra}, \omega_{rel})_{exp}$ which correspond to the various values of $\omega_{exp. rel}$

determined from Eq. (5.28) are computed from Formula (5.29). Then the values for $(K_{\omega_{tra}}, \omega_{rel})_{exp. rel}$ and $\epsilon_{\omega_{rel}}$ are calculated and curves plotted accordingly.

Figure 5.11 shows static characteristics for a floating integrating gyroscope of Type 10⁴, No. 79 (data for which were given in Chapter II, Sec. 1, Tables 1 and 2), operating in the geometric-stabilization regime; these were recorded by the method outlined previously in the apparatus represented schematically in Fig. 5.10.

The characteristics were registered under the following conditions:

Frequency of current fed to gyromotor	$f_{gyr} = 400$ cps
Phase voltage of gyromotor	$U_{ph} = 8.2$ volts
Phase current of gyromotor	$I_{ph} = 0.3$ amp
Excitation current of microsyn pickoff	$I_{ex} = 125$ ma
Frequency of current fed to excitation winding of microsyn pickoff	$f_p = 400$ cps
Excitation current of microsyn torquer	$I_{ex} = 100$ ma
Frequency of current fed to excitation winding of microsyn torquer	$f_t = 400$ cps
Vertical component of angular velocity of earth's diurnal rotation, compensated by application of current $I_{con. comp} =$ = const to secondary winding of microsyn torquer	$\omega_e \sin \varphi = 4.87 \times 10^{-5}$ rad/sec
Temperature of fluid	$\tau = 71.1^\circ\text{C.}$

In calculating the numerical values of the relative angular velocity $\omega_{exp. rel}$ and the relative nondimensional amplification factor $(K_{\omega_{tra}}, \omega_{rel})_{exp. rel}$ it was assumed that

$$\omega_{pl. sh. cal} = 1 \text{ mrad/sec} = 0.0573^\circ/\text{sec} = 13.8 \text{ } \omega_e$$

$$(K_{\omega_{tra}}, \omega_{rel})_{cal} = 1.00 \frac{\text{mrad/sec}}{\text{mrad/sec}}.$$

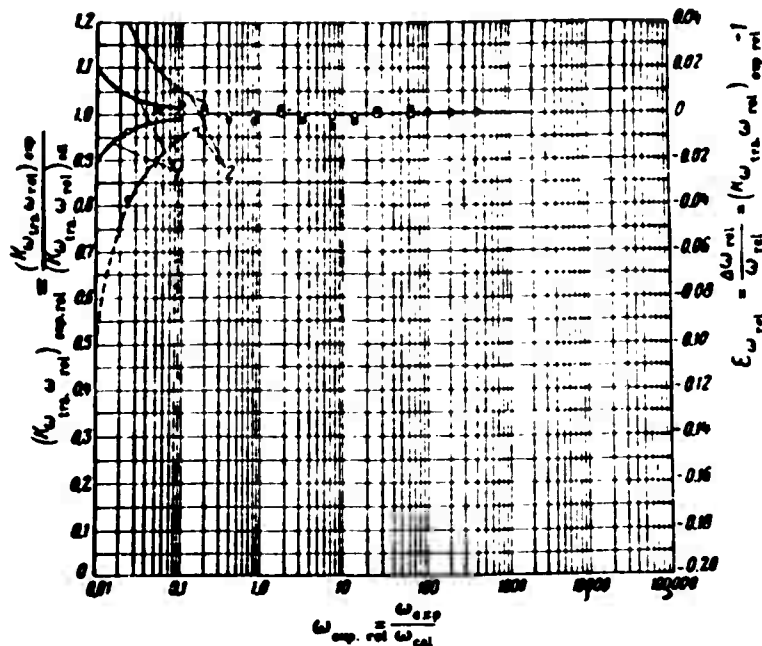


Fig. 5.11. Static characteristics of operation of floating integrating gyroscope, Type 10⁴, No. 79 in geometric-stabilization regime. o-points for $(K \omega_{tra} \omega_{rel})_{exp. rel}$; ● -points for ω_{rel} ; 1), 2) envelope curves of points for $(K \omega_{tra} \omega_{rel})_{exp. rel}$ and ω_{rel} , which correspond to an absolute output-quantity error $\Delta \omega_{rel}$ of ± 0.000001 rad/sec.

It can be seen from comparison of the curves of Fig. 5.11 and those of Fig. 5.9 that for $\omega_{exp. rel} < 4$ rad/sec, the operation of the floating integrating gyroscope in the geometric-stabilization regime is similar to its operation in the spatial-integration regime. In the range of angular velocities from 0.0001 to 4 rad/sec the factor $(K \omega_{tra} \omega_{rel})_{exp. rel}$ remains equal to unity within $\pm 1\%$, i.e. the relative error ω_{rel} of the output quantity (the angular velocity ω_{rel}) does not exceed ± 0.01 , or $\pm 1\%$, in this range. At angular velocities lower than 0.0001 rad/sec, the experimental points fall between envelope curves which correspond to absolute errors $\Delta \omega_{rel}$ of ± 0.000001 rad/sec. The reason for this is

essentially the same as in the case of the spatial-integration regime.

At higher angular velocities, and particularly at angular velocities in excess of 4 rad/sec, the operation of the integrating gyroscope in the geometric-stabilization regime, as distinguished from its operation in the spatial-integration regime, proceeds normally, without deteriorating in any way. It may be stated that the operation of the device in the geometric-stabilization regime is not subject to an upper angular-velocity limit. This is in consequence of the fact that imperfections in the operation of the microsyn pickoff, gyromotor, fluid damper, or the mechanical components of the design by which these elements are linked exert hardly any detrimental influence on the operation of the integrator as a whole. In any concrete geometric-stabilization system the upper velocity limit is imposed by the capacity of the servosystem to reproduce this high angular velocity and large angular accelerations.

Section 5. Drift Analysis of Differentiating Gyroscopes

By the angular velocity of drift of a differentiating gyroscope we mean the input angular velocity which would necessarily result, under ideal conditions, in the appearance of that output signal of the gyroscope which is actually obtained at zero value of the input angular velocity ω . Let us use $U_{out, dr}$ to denote the output voltage obtained from the differentiating gyroscope at zero input angular velocity ω , and by ω_{dr} the angular velocity of drift which corresponds to it. It follows from Eq. (4.29) that in the ideal case, i.e. for $M_1 = \Delta = 0$ and angles β near zero, $U_{out} = K_{out} \omega$, $U_{out} = \omega_{dr}$. Proceeding from this equality, we may write

$$\omega_{dr} = \frac{U_{out, dr}}{K_{out, U_{out}}} \quad (5.33)$$

Accordingly, the angular velocity of drift of a floating differential gyroscope with a feedback circuit is

$$\omega_{dr} = \frac{I_{a, dr}}{K_{a, I_2}} \quad (5.34)$$

where $I_{a, dr}$ is the output current of the amplifier at zero value of the input angular velocity ω .

In accordance with the above, measurement of the drift of a floating differentiating gyroscope is accomplished by measurement of its output signal for zero value of the input angular velocity ω . The analysis is performed in the apparatus illustrated schematically in Fig. 5.5. The velocity of the platform 5 in inertial space about the y axis should be adjusted to zero. The corresponding angular velocity $\omega_{pl. rel}$ should be equal to $-\omega_e \sin \psi$. The occurrence of drift in a torsion-rod floating differential gyroscope is a result of inaccurate assembly and adjustment of the device, torsion-rod hysteresis, noncorrespondence between the zero-points of the torsion rod and the microsyn-pickoff, etc.

The systematic component of drift may be compensated by application of an appropriate current $I_{con M_1 syst}$ to the microsyn torquer (if there is one). The random drift component cannot be compensated. The drift of a floating differentiating gyroscope with feedback may also be basically compensated in a similar manner. Analyses of a floating differentiating gyroscope with a torsion rod -- No. 26 -- showed that its ω_{dr} was 0.0014 rad/sec. Drift data for the differentiating gyroscope Type 10⁴, No. 55, were given in Table 5 (Chapter II, Sec. 2).

Section 6. Drift Analysis of Integrating Gyroscopes

By the angular velocity of drift of a floating integrating gyroscope, which we

denote by ω_{dr} , we mean the absolute angular velocity at which it is necessary to rotate the device about its input axis in order to maintain the output signal of the gyroscope (the voltage U_{out}) constant (specifically, for example, equal to zero) when the current $I_{con} = 0$. In other words, it is the velocity at which it is necessary to rotate the device about its input axis in order to create a gyroscopic moment equal in value and opposite in sign to the interference moment acting upon the floating gyroassembly about its axis of rotation. Accordingly, the floating gyroassembly will be in equilibrium when the device is rotated at a velocity ω_{dr} with $I_{con} = 0$, and U_{out} will be constant as a result. If the device were an ideal one, i.e. if M_1 were zero, its ω_{dr} would become zero. The angular velocity ω_{dr} is the sum of systematic and random components. The systematic component of ω_{dr} is an effect of moment components $M_{1\text{ syst}}$ due, first, to imbalance of the floating gyroassembly with respect to its axis of rotation and, second, to moments exerted on the floating gyroassembly by the leads of the gyromotor and the pickoff and torquer, and also to moments resulting from elastic deformation of the floating gyroassembly. The systematic component of ω_{dr} due to the second group of factors may be compensated by supplying an appropriate current to the control winding of the microsyn torquer. The systematic component of ω_{dr} due to imbalance of the floating gyroassembly, which we shall designate the gravitational component of the drift velocity and denote by $\omega_{dr\text{ gr}}$, depends on the orientation of the floating gyroassembly with respect to the vector of the force of gravitation. This component of ω_{dr} may also be compensated if we take the above orientation into account. Thus the entire systematic component may be compensated by supplying the appropriate current to the control winding of the microsyn torquer. It is readily seen that this compensation does not complicate the normal operation of the device. As was noted previously, however, there are also random, indeterminate components of ω_{dr} which cannot be compensated. These also determine the ultimate potential of the gyroscope.

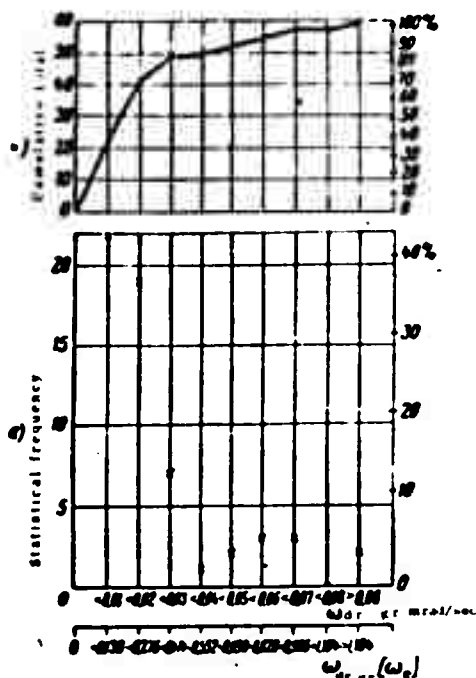


Fig. 5.12. Results of measurement of angular velocity of gravitational drift in 38 floating integrating gyroscopes of Type 104. (a) Graph of statistical-frequency distribution; (b) graph of cumulative sums.

As a rule, drift velocity should be determined with the output axis of the device (the axis of rotation of the floating gyroassembly) in both the vertical and horizontal positions. When this axis is horizontal, the observed drift velocity $\omega_{dr. hor}$ will be due to all of the factors enumerated above, including imbalance of the floating gyroassembly with respect to its axis of rotation. With the output axis of the device in a vertical position, the drift velocity $\omega_{dr. vert}$ will not contain the gravitational drift component, since the moments of gravity and lift are zero with respect to the axis of rotation of the floating gyroassembly when it occupies this position. The drift observed in this case is due to

all of the causes discussed above with the exception of imbalance of the floating gyroassembly with respect to its axis of rotation.

Accordingly, if $\omega_{dr. hor}$ and $\omega_{dr. vert}$ are known, the gravitational drift component $\omega_{dr. gr}$ is $\omega_{dr. hor} - \omega_{dr. vert}$. In drift analyses, the device undergoing test 12 should be mounted on the platform 9 in the manner indicated in Fig. 5.2. The output axis x of the device should be perpendicular to the axis of rotation of the platform, and the input axis y should be disposed along or parallel to the axis of rotation of the platform. Thus the axis of rotation of the platform should be vertical for determination of $\omega_{dr. hor}$ when drift is being determined with the z_0 axis in the horizontal position, and horizontal when drift

is determined for the vertical position of the z_0 axis. The y and z_0 axes should lie in the plane of the meridian in both cases. The axis of rotation of the platform must be situated horizontally in the plane of the meridian for determination of $\omega_{dr. vert}$.

Setting $I_{con} = \tilde{\gamma} = 0$ in Expression (3.103) and applying Eq. (3.34), we find that the relative angular velocity of the platform $\omega_{rel} = -\omega_{tra} + (M_1/H)$ for drift analysis. The absolute angular velocity of the platform, which is the drift velocity sought, is equal to

$$\omega_{dr} = \omega_{rel} + \omega_{tra} = M_1/H.$$

It is evident from this, among other things, that the larger H is, the smaller will be the drift velocity under otherwise identical conditions. This is accounted for by the fact that the larger H becomes, the smaller the angular velocity ω_{dr} required to create a gyroscopic moment equal in value and opposite in sign to the moment M_1 .

Thus, to determine ω_{dr} we must measure the relative angular velocity ω_{rel} of the platform with $I_{con} = 0$ and add to it the transfer velocity of the platform ω_{tra} . If the x and z_0 axes are horizontal, $\omega_{tra} = \omega_e \sin \varphi$; when the x axis is horizontal and the z_0 axis vertical, and also when the x axis is vertical,

$$\omega_{tra} = \omega_e \cos \varphi.$$

Given ω_{dr} , we may also determine the disturbance moment $M_1 = H \omega_{dr}$. The gravitational moment M_1 gr acting about the axis of rotation of the floating gyro-assembly is accordingly $H \omega_{dr. gr}$.

The diagrams in Fig. 5.12 present experimental values for angular velocity of gravitational drift for 38 Type 10⁴ floating integrating gyroscopes (Massachusetts Institute of Technology) with their z_0 axes in the horizontal position. The graphs are constructed on the basis of 59 measurements. The lower diagram shows the distribution of statistical frequencies, and the one above the distribution of

cumulative totals. The common axis of abscissas is calibrated in values of the gravitational component of the angular velocity of drift $\omega_{dr. gr}$ in mrad/sec on the upper scale and in fractions of ω_e (the angular velocity of the diurnal rotation of the earth) on the lower scale.

Let us recall the importance of the concepts "statistical frequency" and "cumulative total." Statistical frequency refers to the number of values of a continuous random quantity (in our case the angular velocity $\omega_{dr. gr}$) in each of the equal intervals into which the region of practical occurrence of these values is divided. The value of the statistical frequency is plotted on the ordinate of the point which represents the right-hand boundary of the interval in question. In Fig. 5.12, the region in which $\omega_{dr. gr}$ values occurred in the analyses is divided into intervals of 0.01 mrad/sec. It is pointed out that the term "continuous random quantity" refers to a variable random quantity which may assume any value within a given interval.

By cumulative total or cumulative frequency we mean the number of values of a continuous random quantity occurring to the left of a given point in the region in which values of this quantity occur in practice. The cumulative sums are calculated for the points which represent the boundaries of the above-mentioned intervals, with the exception of the point forming the left-hand boundary of the first interval. Accordingly, the cumulative sum for any given point is equal to the sum of statistical frequencies for all intervals lying to the left of this point. The cumulative sum is plotted on the ordinate of the point in question.

It can be seen from Fig. 5.12 that 95% of all measured values of the gravitational component of the angular velocity of drift do not exceed the angular velocity of the earth's diurnal rotation, while 70% are smaller than approximately one-fourth of this velocity. The results of measurement of the gravitational component of drift angular velocity with the z_0 axis in a vertical position agree with the data given in the graphs of Fig. 5.12.



Fig. 5.13. Apparatus for drift analysis of precision floating gyroscopes, mounted on a concrete pier.

Drift analysis of integrating gyroscopes requires high-precision equipment.

In order to carry out drift measurements for the modern high-precision floating gyroscopes designed for use in the inertial-navigation systems of guided missiles, it was necessary to take extraordinary measures to insulate the test apparatus from the inevitable vibrations of the building. To accomplish this it was necessary to mount the test apparatus on a specially constructed concrete pier built on a rock base which was buried deep underground and not in contact with the building.

A photograph of an apparatus of this type used by the Minneapolis-Honeywell firm is shown in Fig. 5.13. The apparatus in which the gyroscopes are drift-tested is mounted on the pier. It must be noted that as floating gyroscopes of even higher precision are developed, the problem of insulating the test stands from the various possible types of vibration and accidental shock grows considerably more complicated.

The creation of stable, high-precision feed sources is a very important

and difficult matter.

Section 7. Dynamic Testing

The general procedure for determining the dynamic characteristics of floating gyroscopes consists in the following: a certain input signal is supplied to the input of the gyroscope, i.e. the input quantity of the gyroscope is varied according to a definite pattern, and the resulting variation of the output quantity of the gyroscope with time registered with the aid of an oscillograph. Inferences concerning the dynamic properties of the gyroscope are made on the basis of the curve obtained in this way, and the parameters which characterize these properties of the gyroscope are determined. Either the input angular velocity ω or the input current I_{con} of the gyroscope (the current supplied to the secondary winding of the microsyn-torquer) may serve as the signal delivered to the input of the gyroscope.

The input signal (the input quantity) is varied in such a way as to produce an output curve from which it will be possible to ascertain the dynamic properties of the gyroscope. Step-displacement, pulse, uniform-sinusoidal, and certain other modes of input-quantity variation are most suitable from this standpoint. We proceed now to consideration of the reactions of floating gyroscopes to step displacement of input angular velocity as a means of determining the parameters which characterize their dynamic properties.

Analysis of Integrating Gyroscopes

It is evident from Eq. (3.24) for the floating integrating gyroscope that its dynamic properties are characterized by a single parameter, namely, the time

constant T . The time constant is most conveniently determined from the curve of the transient process which occurs upon step displacement of the input angular velocity ω . Let us consider how this is done.

The analysis is conveniently performed in the apparatus represented schematically in Fig. 5.5. The floating integrating gyroscope 4 undergoing the test is mounted on the rotary platform 5 in a common thermostat 3 with the floating integrating gyroscope 2 which is functioning as a component of the turntable apparatus. The input (measurement) axis of the test gyroscope should be parallel to the y axis of rotation of the platform 5. The platform is set into rotary motion with a certain constant angular velocity ω by the procedure described earlier. In this method, the control winding of the microsyn-torquer is supplied with an input current I_{con} such that the output signal of the gyroscope (the voltage U_{out}) remains equal to zero within the limits of the accidental components, which cannot be compensated. Under these circumstances, the gyroscopic moment and the systematic component of the moment M_1 are in equilibrium with the moment M_t of the microsyn torquer. The instant registration of the transient process begins, the input current I_{con} is switched off, with the result that the floating gyroassembly is freed from the influence of the moment M_t . In this way the test gyroscope is subjected to a step-displacement reaction of the angular velocity at which the platform 5 is rotating. The transient process which results from this -- a variation in time of the output voltage U_{out} of the test gyroscope -- is recorded with the aid of the oscillograph. For exposition of the procedure by which the time constant T is determined from the curve of the transient process, we will refer to Eq. (3.24). In our case the acceleration $\ddot{\gamma} = 0$.

Up to cutoff of the current I_{con} , the entire right-hand member of Eq. (3.24) is equal to zero; the voltage U_{out} is likewise zero within the limits of the random components, which are not subject to compensation. The voltage U_{out} , which is governed by the input angular velocity ω , is measured after cutoff of the I_{con}

current. As seen from Eq. (3.24), however, this voltage will also be a function of the moment M_1 and the derivatives Δ'_t and Δ'_β . The dependence of U_{out} on M_1 could have been eliminated by application of a suitable current $I_{con} = I_{con. comp}$, but this would have complicated the procedure, since it would necessitate effecting a momentary drop in the value of the current to $I_{con. comp}$ instead of a complete cutoff. Moreover, the application of a current $I_{con. comp}$ would merely compensate the influence of the constant components of the moment M_1 , whose presence does not produce errors in the determination of the time constant T from the experimental graph of the transient process.

Thus it is more convenient in practice to make Δ'_t and the term containing M_1 negligibly small in comparison with the term containing ω . The velocity ω must be sufficiently high to fulfil this condition. Assuming that this condition is met and the current I_{con} is completely cut off, and also considering the term containing Δ'_β negligible by comparison with unity, we may rewrite Eq. (3.24) in the form

$$T\ddot{U}_{out} + \dot{U}_{out} = K_{\omega} \dot{\omega}_{in} \omega.$$

Integrating this equation with the assumption that at the instant $t = 0$, when the current I_{con} is switched off, $\dot{U}_{out} = U_{out} = 0$, and that the input angular velocity instantly assumes a value ω , we obtain an equation which describes the transient process resulting from step displacement of the input angular velocity:

$$U_{out} = K_{\omega} \dot{\omega}_{in} \omega \left[t - T(1 - e^{-t/T}) \right]. \quad (5.35)$$

It will be seen from this equation that if the time constant T were equal to zero, the transient process would be determined by the equation

$$U_{out} = K_{\omega} \dot{\omega}_{in} \omega t. \quad (5.36)$$

In this case the voltage U_{out} would increase as a linear function of time. This relationship is represented graphically by the broken line in Fig. 5.14. With $T \neq 0$, the graph of the transient process takes the form of the curve indicated by the heavy line in Fig. 5.14. This curve is asymptotic. Letting $t \rightarrow \infty$ in Eq. (5.36), we obtain the equation of the asymptote in the form

$$U_{out} = K_{\omega} \dot{\omega}_{in} (t - T). \quad (5.37)$$

It follows from this equation that the asymptote cuts off a segment on the axis of abscissas equal to the time constant T expressed in corresponding units.

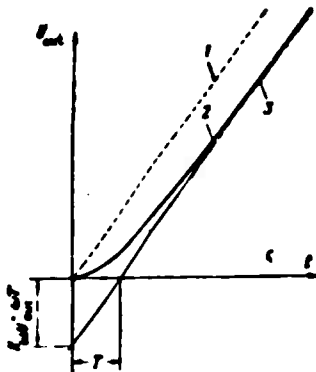


Fig. 5.14. Transient process in floating integrating gyroscope upon step displacement of input angular velocity ω . 1) For $T = 0$; 2) for $T \neq 0$; 3) asymptote of curve of transient process for $T \neq 0$.

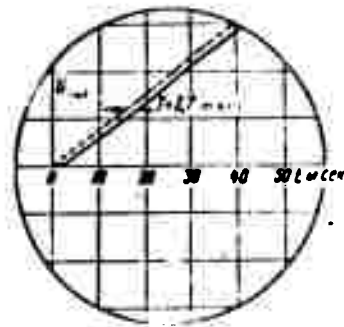


Fig. 5.15. Oscillogram of transient process in floating integrating gyroscope of Type 10⁴, No. 79, upon step displacement of input angular velocity ω .

This fact may also be used to determine the time constant T from the curve of the transient process obtained experimentally by the procedure described above. The slope of the asymptote is equal to the slope of the straight line which represents the transient process for $T = 0$.

Figure 5.15 shows the experimental transient-process curve which appears upon step displacement of the input angular velocity ω for a Type 10^4 floating integrating gyroscope, No. 79, as obtained by the above procedure. The broken line is drawn parallel to the asymptote and represents the curve of the transient process which would occur for $T=0$. We find from the curve that the time constant \underline{T} for the gyroscope in question is 0.0027 sec.

This experimental value for the time constant \underline{T} is larger than its calculated value, which is 0.0017 sec. Similar results in the sense of increased time-constant values (with reference to their calculated values) were also obtained in tests of other devices of the same type, but larger in dimension. The causes of the time-constant increase are not yet fully explained. The basic factors are apparently the following:

- 1) The shaft of the gyromotor rotor, the housing (frame) of the gyroscope, and the axis of the floating gyroassembly are to a certain degree elastic, rather than absolutely rigid, which gives rise to a lag in the transmission of moments;
- 2) the presence of play in the bearings;
- 3) the time lag inherent in the electrical measuring equipment used to measure and record the output signal (the voltage U_{out}).

It is noted that since the integrating gyroscope possesses a large specific damping moment, moderate changes in temperature cannot produce any essential changes in its dynamic characteristics.

Analysis of Differentiating Gyroscopes

It is evident from Eqs. (4.15) and (4.65) that the dynamic characteristics of differentiating gyroscopes of both the torsion-rod and feedback types are determined by two parameters: the angular frequency of free undamped vibration ω_0

and the dimensionless damping ratio \underline{b} . It follows from Eq. (4.43) that the dynamic properties of differentiating gyroscopes may also be characterized by the two time constants \underline{T}_0 and \underline{T}_1 . The parameters ν_0 and \underline{b} or the corresponding \underline{T}_0 and \underline{T}_1 may be determined from the curve of the transient process which results from step displacement of the input angular velocity ω . The analysis is performed in the apparatus represented schematically in Fig. 5.5. As before, the test gyroscope is the one keyed with the numeral 4. A certain constant angular velocity ω is imparted to the platform 5; as in the analysis of the integrating gyroscope, this must be sufficiently large to render insignificant the influence of \underline{M}_1 , Δ , and the derivatives of Δ on the transient process. In analyses of torsion-rod differentiating gyroscopes, which do not have (microsyn) torquers, the step displacement of the input angular velocity ω is brought about by abrupt reduction of this velocity from a value equal to the angular velocity of the platform to zero, which results in sharp deceleration by means of special mechanical devices.

In the case of differentiating gyroscopes with feedback circuit, step displacement of the input angular velocity ω is accomplished, as with the integrating gyroscopes, by switching off the current \underline{I}_{con} . Thus the differentiating gyroscope with torsion rod is tested on the basis of step-displacement nullification of the input angular velocity ω , and the feedback gyroscope on the basis of the step-displacement appearance of this velocity. The transient process, the time-curve of the voltage \underline{U}_{out} , is registered in either case by means of an oscillograph.

Figure 5.16 shows the experimental curve (oscillogram) of the transient process which occurs in a Type 10^4 floating differentiating gyroscope (No. 55) upon step displacement of its input angular velocity, as registered by the above method. The transient process is of the character of a damped harmonic vibration. Thus the dimensionless damping ratio is $\underline{b} < 1$ for this gyroscope. Let us derive formulas for determination of the values of \underline{b} and ν_0 from the transient-process oscillogram. It is known that the period of damped harmonic vibrations is given by

$$T_d = \frac{2\pi}{\omega \sqrt{1-b^2}},$$

and the damping decrement by

$$D = e^{-\delta \frac{T_d}{2}}.$$

Substituting the value of T_d in this and solving the resulting expression for b , we obtain

$$b = \frac{1}{\sqrt{1 + \left(\frac{\pi}{\ln \frac{1}{D}} \right)^2}}. \quad (5.38)$$

If b is known, we obtain

$$\omega = \frac{2\pi}{T_d \sqrt{1-b^2}}. \quad (5.39)$$

from the expression for T_d .

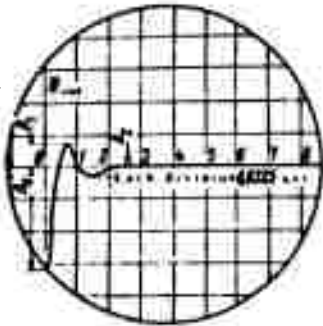


Fig. 5.16. Oscillogram of transient process occurring in floating differentiating gyroscope with torsion rod (Type 10⁴, No. 55) upon step displacement of input angular velocity.

In order to compute b and ω_0 from Formulas (5.38) and (5.39) it is necessary to know T_d and D . The period T_d is determined directly from the transient-process oscillogram. To establish D on the basis of the oscillogram we determine the values A_0, A_1, A_2, \dots -- the amplitudes of the initial and succeeding half-waves. Then the formula is employed to calculate

$$D_{n,n+1} = \frac{A_{n+1}}{A_n} (n=0, 1, 2, \dots) \quad (5.40)$$

the values of the damping decrement for each pair of successive amplitudes. The arithmetical mean of the values $D_{n, n+1}$ is taken as the damping decrement D .

Knowing τ_0 and b , we may compute the time constants T_0 and T_1 from Formulas (4.44) and (4.45).

Referring to Fig. 5.16, we find that

$$T_d \approx 0.044 \text{ sec}, A_0 = 32, A_1 = 7, A_2 = 3.$$

According to Formula (5.40),

$$D_{0,1} = 7/32 = 0.219; D_{1,2} = 3/7 = 0.429.$$

The value of $D_{1,2}$ is nearly double that of $D_{0,1}$. The most immediate explanation for this is the influence on the vibration of the gyroassembly of the moments M_1 , the voltage Δ and its derivatives, and also of the errors of the measurement apparatus. Consequently, we shall not take $D_{1,2}$ into consideration in determining the values of b and τ_0 , but shall consider

$$D = D_{0,1} = 0.219.$$

Substitution of this value for D in Formula (5.38) yields

$$b = \frac{1}{\sqrt{1 + \left(\frac{\pi}{\ln \frac{1}{0.219}} \right)^2}} = 0.436.$$

Referring to Formula (5.39), we find that

$$\nu_0 = \frac{2\pi}{0.044 \sqrt{1 - 0.436^2}} = 158.5 \text{ rad/sec}$$

Consequently,

$$f_0 = \frac{\nu_0}{2\pi} = \frac{158.5}{2\pi} = 25.2 \text{ cps.}$$

According to Formulas (4.44) and (4.45),

$$T_0 = \frac{1}{\nu_0} = \frac{1}{158.5} = 0.0063 \text{ sec.}$$

$$T_1 = \frac{2b}{\nu_0} = \frac{2 \cdot 0.436}{158.5} = 0.0055 \text{ sec.}$$

The experimental value for the natural undamped-vibration frequency f_0 was found to be higher than its calculated value of 19 cps. Thus the experimental

value of the time constant T_0 is found to be smaller than its calculated value, which was 0.0084 sec. The experimental value of the dimensionless damping ratio \underline{b} is approximately 30% lower than its theoretical value, while the time constant T_1 is approximately half its theoretical value. The discrepancies between the experimental and calculated values of f_0 , T_0 , \underline{b} , and T_1 are explained by the fact that their calculated values do not include the effective values of the radial clearance δ of the damper, the moment of inertia J , and the rigidity k of the torsion rod; the failure of the computation formulas to take into account secondary factors which influence the vibration of the floating gyroassembly, and the errors of the test apparatus.

Figure 5.17 shows the experimental curve (oscillogram) obtained by the above procedure for the transient process which occurs upon step displacement of the input

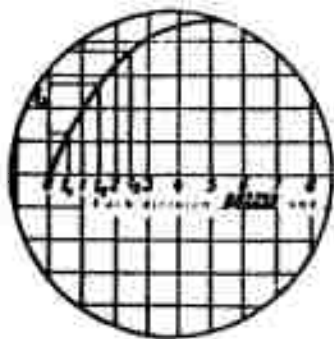


Fig. 5.17. Oscillogram of transient process in floating differentiating gyroscope with feedback circuit on step displacement of input angular velocity.

angular velocity of a floating differentiating gyroscope with feedback circuit formed from a floating integrating gyroscope of Type 10^4 (No. 79). The transient process is aperiodic (monotonic) in nature. Hence the dimensionless damping ratio $\underline{b} > 1$ for this device.

If the anticipated value of the dimensionless damping ratio $\underline{b} \leq 2$, C. S.

Draper recommends the use of graphs of the type shown in Fig. 5.18 to determine its value, and also the value of the angular frequency of natural undamped vibration f_0 from the curve of the transient process which accompanies step displacement of the input quantity. We note that these graphs are suitable for both nonoscillatory and oscillatory transient processes (for $0.5 \leq \underline{b} \leq 2$). Let us consider how the graph shown in Fig. 5.18 is applied. From

the graph of the transient process, we determine the three time values (denoted by t_1 , t_2 , and t_3) at which the output quantity x_{out} becomes equal to

a) for the transient process which occurs when the output quantity is step-reduced to zero (Fig. 5.19a):

$$\left. \begin{aligned} x_{1 \text{ out}} &= 0.736 x_{0 \text{ out}}' \\ x_{2 \text{ out}} &= 0.406 x_{0 \text{ out}}' \\ x_{3 \text{ out}} &= 0.199 x_{0 \text{ out}}' \end{aligned} \right\} \quad (5.41)$$

where $x_{0 \text{ out}}$ is the steady-state value of the output quantity at the moment at which the step-displacement reduction of the input quantity occurs (i.e. at the instant $t = 0$);

b) for the transient process which occurs when a constant value is imparted to the input quantity by step displacement (Fig. 5.19b):

$$\left. \begin{aligned} x_{1 \text{ out}} &= 0.264 x_{out \text{ sdy}}' \\ x_{2 \text{ out}} &= 0.594 x_{out \text{ sdy}}' \\ x_{3 \text{ out}} &= 0.801 x_{out \text{ sdy}}' \end{aligned} \right\} \quad (5.42)$$

where $x_{out \text{ sdy}}$ is the steady-state value of the output quantity which is established after step displacement of the input quantity to a constant value.

The next step is to determine the ratios

$$\frac{t_2}{t_1}, \frac{t_3}{t_1}, \frac{t_3 - t_2}{t_3 - t_1} \quad (5.43)$$

Then the dimensionless damping ratios b are determined for each of these ratios from the graphs shown in Fig. 5.18, and their arithmetical mean taken as the experimental value of b .

The graphs in Fig. 5.18 are used to determine the values of the products

$${}^0t_1', \quad {}^0t_2', \quad {}^0t_3', \quad (5.44)$$

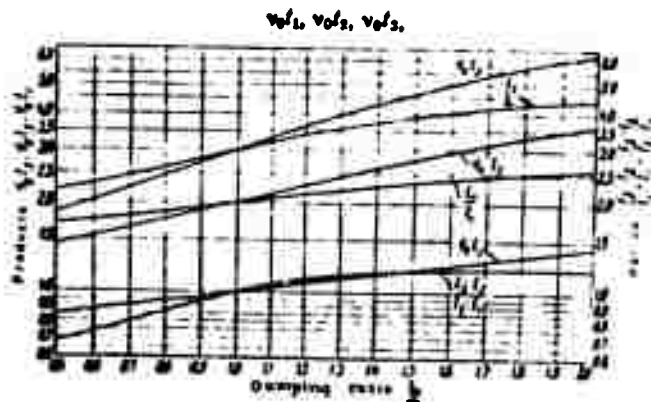


Fig. 5.18. Graphs for determination of b and ν_0 from oscillogram of transient processes with $0.5 \leq b \leq 2$.

which correspond to the values of the ratios (5.43) at this value of b . This yields three values for the angular frequency of natural undamped vibration ν_0 equal to

$$\nu_0 = \frac{\nu_1}{t_1}; \quad \nu_0 = \frac{\nu_2}{t_2}; \quad \nu_0 = \frac{\nu_3}{t_3}. \quad (5.45)$$

The arithmetic mean of these values is taken as the experimental value of ν_0 .

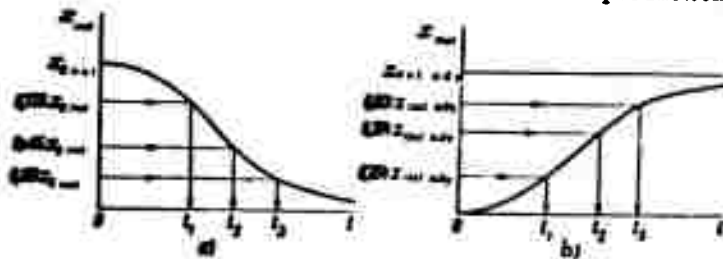


Fig. 5.19. Determination of values for t_1 , t_2 , and t_3 .
(a) For step-displacement reduction of input quantity;
(b) for step-displacement application of constant input quantity.

Referring to the transient-process oscillogram shown in Fig. 5.17 and applying Formulas (5.42), we obtain $t_1 = 0.0136$ sec, $t_2 = 0.0339$ sec, $t_3 = 0.0553$ sec.

Computing the ratios (5.43),

$$\frac{t_2}{t_1} = 2.5, \quad \frac{t_3}{t_1} = 4.1, \quad \frac{t_3}{t_2} = \frac{t_3}{t_1} \cdot \frac{t_1}{t_2} = 1.1.$$

Referred to the curves in Fig. 5.18, these ratios give $\underline{b}_1 = 1.8$, $\underline{b}_2 = 1.62$, $\underline{b}_3 = 1.2$.

The value for \underline{b}_3 will not be taken into consideration, as it differs significantly from \underline{b}_1 and \underline{b}_2 . Then the value of \underline{b} becomes

$$\underline{b} = \frac{\underline{b}_1 + \underline{b}_2}{2} = \frac{1.8 + 1.62}{2} = 1.7.$$

Referred to the curves in Fig. 5.18, this value of \underline{b} yields $\tau_{0-2} = 3.15$, $\tau_{0-3} = 5.4$.

According to Formulas (5.45),

$$\omega_n = \frac{\omega_d}{\tau_1} = \frac{3.15}{0.0339} = 92.9 \text{ rad/sec},$$

$$\omega_n = \frac{\omega_d}{\tau_2} = \frac{5.4}{0.0553} = 97.6 \text{ rad/sec}.$$

Let us assume

$$\omega_n = \frac{\omega_n + \omega_n}{2} = \frac{92.9 + 97.6}{2} = 95.3 \text{ rad/sec}.$$

Consequently,

$$f_n = \frac{\omega_n}{2\pi} = \frac{95.3}{2} = 15.2 \text{ cps}.$$

Thus the undamped natural vibration frequency f_0 for the feedback differential gyroscope analyzed is 15.2 cps, and its dimensionless damping ratio \underline{b} is 1.7. It would be desirable to have $\underline{b} = 0.7$ to obtain proper dynamic properties in the device. The value of \underline{b} may be reduced by the methods discussed earlier. It should be noted, however, that a gyroscope with a dimensionless damping ratio $\underline{b} = 0.7$ could no longer be used as an integrating gyroscope, since it would have an excessively large time constant \underline{T} .

CHAPTER VI

INERTIAL SYSTEM OF NAVIGATION

Section 1. General Outline

The inertial system of navigation is a method of automatically and semi-automatically guiding aircraft and guided missiles, and directing them towards their target. The chief feature of the system is that it is completely self-contained and is not dependent on any ground equipment. The inertial-system instruments installed in the moving object make it possible without any contact with the ground or any orientation with respect to celestial bodies to direct the object to its target solely on the basis of Newton's laws of motion in absolute (inertial) space. The inertial system of navigation is based exclusively on equipment installed in the aircraft or guided missile. This equipment measures distance and direction without the use of optical or magnetic radio communication, or any other contact with the earth or the celestial bodies.

In the United States the inertial system was originally developed for use in medium-range guided missiles as well as in conventional piloted craft. But the system is chiefly intended for long-range guided missiles.

The inertial system of navigation has several important advantages over conventional systems. The main advantages are its invulnerability to intentional

interference, the absence of any need for ground equipment, and the absence of radio emissions, making it difficult for the aircraft or rocket to be detected by the enemy. At the present stage of development the weight of the inertial navigation equipment installed in the aircraft or rocket, according to American sources, varies between 34 and 900 kg, depending on the purpose, accuracy required, and time needed to complete the task assigned.

The inertial system of navigation consists of roughly the following familiar instruments: gyroscopes, accelerometers, computing devices, and servodrives. They are all used in one form or another in modern aircraft. In an inertial system of navigation, however, the demands made upon these instruments are considerably more complex. The chief requirement is great accuracy. The accuracy required in the manufacture, adjustment, and maintenance of the set parameters of inertial-system instruments is so great that it can only be compared with the accuracy of precision instruments in the laboratory. At the same time this equipment must operate correctly under conditions where there are great changes in the surrounding temperature and under the conditions of vibration and shocks which occur in high-speed aircraft and rockets.

Any inertial system of navigation is basically a device for reckoning the path traversed by the object from the point of departure to its point of destination. For the system to be effective the geographical position (longitude and latitude or equivalent data) and the departure and destination points have to be known. These data have to be incorporated into the system in the right way. From what has been said it follows that the inertial system of navigation cannot home the object it is guiding (for instance, an aircraft or rocket) onto a moving target unless at the final homing stage some other automatic searching device working on a different principle is used (radar, infrared etc.)

An operating inertial system of navigation supplied with data on the initial position of the guided object and on the location of the point of destination is

able to determine and produce the following data: the geographical position of the moving object, the ground speed, the distance already traversed and the distance left to the point of destination, the direction of the point of destination, and the position of the aircraft or rocket with respect to the plane of the horizon.

Given these data, it is comparatively easy to work out a system which will emit command signals that can be fed to the automatic pilot of the craft to ensure automatic flight to the point of destination. Thus, this system of navigation can direct a guided object from one fixed point to another. In its purest form, as pointed out, it is a self-contained system unconnected with any devices outside the guided object. In its ideal form it should work at any point on the globe at any time and in any weather. It should be completely insensitive to any outside interference, either random or intentional; it should be accurate and reliable, and should be able to make unlimited deviations from the planned course and ensure guidance of the object at any height. In its completed form the system must ensure accurate guidance of the aircraft or rocket from a certain point to another point of destination or to any subsequent points on the earth's surface along any chosen path. The path may be predetermined or decided during flight.

A system answering this specification will not require complex ground equipment either at the point of departure or along the line of flight. The only ground equipment necessary is the instruments used to determine the geographical coordinates of the launching point. Information regarding the coordinates of the point of destination will also be required.

The inertial system of navigation should not be confused with navigation by the stars or with automatic computing systems for dead reckoning.

The distinction between the inertial system of navigation and navigation by the stars (astronavigation) is obvious. When flying at a low altitude in bad weather the possibility of using astronavigational equipment is limited whereas this is not the case in inertial navigation.

The computing instruments for automatic dead reckoning (aviagraphs), which have now been in use for several years, provide data similar to those supplied by the inertial system, but they carry out the computation using entirely different input signals. The automatic dead-reckoning computers receive indications of the air speed from the speed data unit. The signals are automatically corrected for drift by means of a radar unit using the principle of the Doppler effect. The actual speed, thus measured, is broken down by means of coordinates into southern and northern components which are then integrated with respect to time. In this way data is obtained on the distances traversed in the North-South and East-West directions. Other automatic dead-reckoning systems do not use the air-speed indicator and rely entirely on radar readings.

Without radar measurement of the ground speed by the use of equipment in the flying object (aircraft or rocket), the work of the computer will depend on the action of the air pressure recorder used to measure the air speed. But the use of air pressure recorders in high-speed aircraft, and all the more so in guided missiles, involves many difficulties. In practice it is impossible in such cases to obtain exact data on the speed and continuous data on the drift relative to ground at a great height without using external radiation, which involves the danger of intentional interference or detection.

The inertial system of navigation uses a completely different method of pinpointing a moving object, eliminating the need for data on the movement of the object relative to the stars or the earth obtained by optical, radar or other means.

Section 2. Working Principle of Inertial System of Navigation

The working principle of any inertial system lies in measurement of the acceleration of a moving object. As is known, the only value describing the motion

of a body in space which can be measured inside the body is the acceleration. By continuous measurement of the acceleration it is possible to obtain initial data with which to determine the velocity and path. The acceleration of a moving object can be measured with an instrument called an accelerometer.

The velocity of a moving object is the integral of the acceleration with respect to time, and the distance traversed is the integral of the velocity with respect to time. Thus, the distance can be expressed as a double integral of the acceleration with respect to time. Let us assume, for example, that there is a power truck standing on a straight section of railway track. We will equip it with an accelerometer which can measure its acceleration in the direction of motion, and two integrators 5 and 6 (Fig. 6.1). We will attach a device with contacts to the integrator output shaft which turns to form an angle proportional to the distance traversed; one contact must be connected to the integrator shaft and the other to the instrument housing. We will turn the second contact with respect to the first contact to form an angle corresponding to the prescribed path of the truck.

When the truck begins to move the accelerometer immediately begins to measure the acceleration and the output shaft of the second integrator turns, forming an angle proportional to the distance traveled. As soon as the truck has traveled the predetermined distance, the contact device is actuated, switching off the motor and stopping the truck. Thus the truck reaches a set point, guided solely by equipment installed inside it and without any contact with the outside; the external conditions, on which the velocity of the truck is dependent, may differ (for instance, head wind, variation in the contact circuit voltage), but none of them can affect the halting of the truck at a given point along the track. This example illustrates the simplest inertial system with one degree of freedom, and shows that it is possible in practice to direct the guided object to a fixed point by previously setting the instruments for a given distance; the operation of the instruments does not in any way involve the direct measurement of the velocity by contact

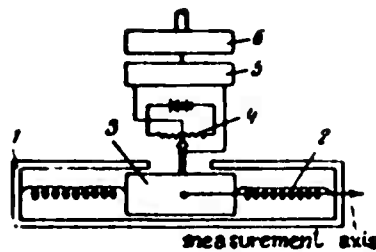


Fig. 6.1. Accelerometer and integrator. 1) Accelerometer housing connected to moving object; 2) springs; 3) mats; 4) potentiometer; 5) and 6) first and second integrators.

with the rails or other external means. The measurement — the dead reckoning — is made here by means of self-contained equipment installed in the moving object and is not connected with the surrounding medium. This principle of measuring and integrating the acceleration is the basis of present-day systems of inertial navigation.

Section 3. Problems of the Practical Application of the Inertial Navigation System

In an elementary example of the inertial guidance of an object along a straight line, it is enough, as pointed out, to equip it with a single accelerometer to measure the acceleration acting in the direction of motion.

If it is necessary to furnish inertial guidance to an object moving in a plane along two mutually perpendicular axes, we shall require two accelerometers and two pairs of integrators. Each accelerometer with its two integrators will in the given case control the movement of the object along its own axis.

If we now imagine an inertial system of navigation intended for aircraft or rockets with as many as six degrees of freedom and capable of flying in different positions, further problems arise in connection with the choice of working principles and the development of the essential units of the system, and also in connection with ensuring that they operate with a very high degree of accuracy. An aviation inertial system must contain two or three accelerometers to determine the corresponding acceleration of the aircraft along two or three mutually perpendicular

axes (e.g. S-N, W-E, upward-downward). The output signals from the accelerometers may be integrated by separate integrators or in certain cases by integrators which are part of the accelerometers themselves.

We will take it from now on that the inertial system contains two accelerometers — one to measure the acceleration \dot{v}_N in the direction S-N, and the other to measure the acceleration \dot{v}_E in the direction W-E. The northern and southern accelerations are considered positive. For the accelerometers to measure the given accelerations, they should be installed on a horizontally stabilized platform permanently orientated with respect to the line S-N. The measurement axis of one accelerometer lies along the line S-N, and the other along the line W-E. We will call the first one the northern accelerometer and the second one the eastern accelerometer. Since the accelerometers cannot distinguish the acceleration of the moving object, which they are intended to measure, from the acceleration of gravity, which they are not supposed to measure, even a slight deviation of the platform with the accelerometers from horizontal may give rise to large errors. The proper orientation of the platform and accelerometers relative to the S-N and W-E axes or relative to some other initial system of coordinates selected must also be strictly maintained.

The northern and eastern velocities of the object relative to the ground (see Fig. 1.13) are determined by continuous integration of the accelerations \dot{v}_N and \dot{v}_E effected by the integrators. Thus, with zero initial conditions

$$v_N = \int \dot{v}_N dt, \quad (6.1)$$

$$v_E = \int \dot{v}_E dt. \quad (6.2)$$

The distance L_N and L_E traversed by the object in the northern and southern directions are obtained by continuous integration of the velocities v_N and v_E . With zero initial conditions

$$L_n = \int \dot{v}_n dt, \quad L_e = \int \dot{v}_e dt.$$

The true course of the object K_{tr} can be determined by a computing device on the basis of the equality

$$\cos K_{tr} = \frac{v_e}{v_n}.$$

Dropping in Formula (1.11) the minus sign, which depended on the choice of the direction of the ξ axis (Fig. 1.13), we find that the rate of change in latitude is

$$\dot{\varphi} = \frac{v_n}{R}.$$

Integrating, we obtain

$$\varphi = \varphi_0 + \frac{1}{R} \int \dot{v}_n dt, \quad (6.3)$$

where φ_0 is the latitude of the launching point.

This integration is carried out by the second northern acceleration integrator. Substituting into (6.3) the value of \dot{v}_n emitted by the first northern acceleration integrator and determined by Eq. (6.1), we find

$$\varphi = \varphi_0 + \frac{1}{R} \int \int \dot{a}_n dt^2. \quad (6.4)$$

Thus, the latitude of the position of the object is determined by double integration of the northern acceleration. The value φ_0 is introduced into the system at the take-off.

Let us see how the longitude λ of the position of the object is determined. To obtain the rate of change in longitude determined by Eq. (1.12), the eastern velocity signal emitted by the first eastern acceleration integrator and the latitude signal emitted by the second northern acceleration integrator are fed to an automatic computing device which calculates $\dot{\lambda}$ from Formula (1.12). Thus, the computing device output emits a signal indicating the rate of change in longitude

$$\dot{\lambda} = \frac{v_E}{R \cos \varphi}. \quad (6.5)$$

This signal is fed to the input of the second eastern integrator which continuously integrates Eq. (6.5). Thus the second eastern integrator calculates the longitude of the object's position from the formula

$$\lambda = \lambda_0 + \int_0^t \frac{v_E}{R \cos \varphi} dt, \quad (6.6)$$

where λ_0 is the longitude of the launching point introduced into the system at the take-off.

Consequently, the longitude λ is determined by double integration of the eastern acceleration, i.e.

$$\lambda = \lambda_0 + \int_0^t \frac{1}{R \cos \varphi} \int_0^t \ddot{v}_E dt^2. \quad (6.7)$$

The distance and direction required to the point of destination are calculated by spherical trigonometry by the automatic computing device which receives signals from the acceleration integrators. In addition, the inertial system of navigation continuously and automatically determines the angles ψ , θ and γ (see Fig. 1.6), describing the object's position with respect to the planes of the horizon and meridian, knowledge of which (in addition to knowledge of the distance and required direction to the point of destination) is essential for automatic guidance of the object by means of an autopilot.

It will be clear from the foregoing that for the practical implementation of the inertial navigational system the first essential is a triaxially stabilized platform which maintains its horizontal position with a great degree of accuracy and is permanently orientated with respect to the line S-N. Let us suppose that an aircraft takes off at the equator (Fig. 6.2) and that the stabilized platform 2 with the accelerometers mounted on it inside the aircraft is horizontal at take-off. If the platform is to continue to maintain faithfully in inertial space the position in which it was set at take-off, when the aircraft moves along the meridian

through, let us say, the angle ψ , the platform will incline towards the horizon by angle ψ . Hence, for the platform to remain horizontal during any movement of the aircraft with respect to the earth, it must be stabilized not with respect to

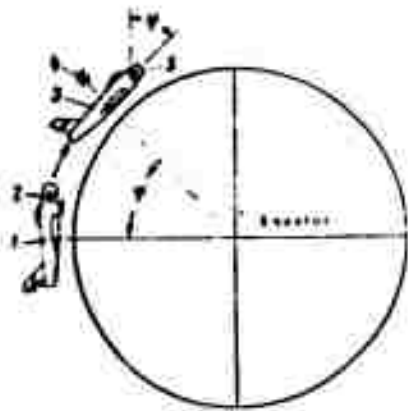


Fig. 6.2. Platform with accelerometers in an aircraft. 1) Aircraft at take-off point; 2) platform with accelerometers; 3) position of aircraft after movement along meridian through angle ψ ; 4) position of platform stabilized in inertial space; 5) position of horizontally stabilized platform.

inertial space, but to the plane of the horizon. In other words, the position of the platform with the accelerometers when the geographical coordinates of the aircraft change must also be changed in such a way as to remain horizontal and permanently orientated relative to the line S-N.

A similar problem is encountered in the conventional gyrohorizon in which the verticality of the direction of the gyroscope spin axis must be maintained during arbitrary movement of the aircraft relative to the ground. The problem in the gyrohorizon is solved by using a small corrector pendulum (or some similar arrangement) which serves to determine the direction of the vertical and to switch on the slave motor which sets the gyroscope spin axis in this direction. As is known, however, when lengthy turns are made, the gyrohorizon does not show the true vertical. The reason for this is that the correction pendulum deviates from vertical under the influence of the transfer forces of inertia. The gyroscope also deviates from vertical in its wake.

Unfortunately, in inertial systems of navigation intended for high-speed aircraft and rockets it is impossible to use a simple pendulum arrangement to determine the true vertical and keep the stabilized platform in an exactly horizontal position. The reason for this is that the pendulum will be affected by the transfer forces of inertia and made to deviate from the true vertical. Thus if the

accelerometers are to work properly, the stabilized platform must always be horizontal and must be orientated invariably with respect to the S-N line. Unless the platform is horizontal the accelerometers will start measuring, besides the acceleration of the object, the projection of the acceleration of gravity onto the plane of the platform. For example, if the platform swings from the horizontal through $1'$, the effect of the projection of the acceleration of gravity onto the plane of the platform may cause an error in determination of the distance of 18.5 km by the end of an hour's flight.

Let us consider the two main methods of ensuring the desired direction of the measuring axes of the accelerometers used in the inertial system of navigation.

In the first method the accelerometers 8 and 9 (Fig. 6.3) are situated on the platform 7 which is mounted in the frame 6 on the gyrostabilized platform 1 orientated permanently in inertial space so that its ζ' axis is parallel to the earth's diurnal rotation. For the sake of simplicity the gyrostabilized platform 1 in Fig. 6.3 has been drawn without the gimbal in which it is mounted. The platform is shown diagrammatically in Fig. 1.21, and its operation is dealt with in Chapter I, Sec. 7. The ξ' axis in Fig. 6.3 corresponds to the ξ axis in Fig. 1.21. Since the platform 1 remains permanently orientated in inertial space, the floating gyroscopes used on it should operate in the geometrical-stabilization regime.

The platform 7 with the accelerometers has two degrees of freedom with respect to the platform 1; one is rotation about the ζ' axis together with the frame 6, and the other is rotation about the ξ axis with respect to the frame 6. Rotation of the platform 7 about the ξ axis is effected by the servodrive 10 controlled by the output signal of the second northern accelerometer 12. Rotation of the frame 6 about the ζ' axis is effected by the servodrive 16 controlled by the signals emitted by the clock 14 and the computing device 4. The ξ , η , and ζ axes are permanently fixed to the platform 7 and are similarly orientated to those in Fig. 1.13. The ξ axis is the measurement axis of the eastern accelerometer 8,

and η the measurement axis of the northern accelerometer 9.

In order to understand how in the given system the horizontal position and the desired orientation of the platform 2 in the azimuth are maintained, let us look at Fig. 6.4. Let us consider that the take-off point of the aircraft is located on

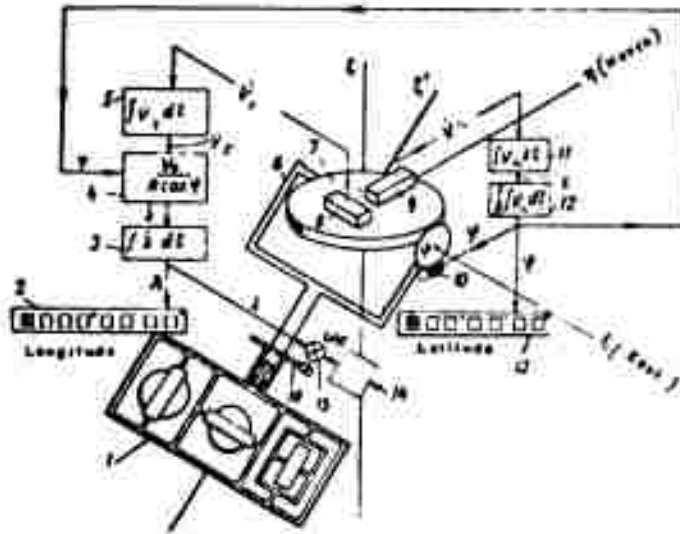


Fig. 6.3. Diagram showing principle of inertial navigation system with gyrostabilized platform orientated permanently in inertial space. 1) Gyro-stabilized platform orientated permanently in inertial space so that the ξ' axis is parallel to the axis of the earth's diurnal rotation; 2) longitude indicator; 3) second eastern-acceleration integrator; 4) computing device; 5) first eastern-acceleration integrator; 6) frame; 7) platform with accelerometers; 8) eastern accelerometer; 9) northern accelerometer; 10) servodrive; 11) first northern-acceleration integrator; 12) second northern-acceleration integrator; 13) latitude indicator; 14) clock; 15) summation device; 16) servodrive of frame 6.

the equator (in Fig. 6.4. the aircraft is not shown). The gyrostabilized platform 1 is mounted in such a way that its ξ' axis is parallel to the axis of the earth's diurnal rotation. The platform 2 with the accelerometers is set horizontal at the take-off. Since the platform 2 is mounted on the platform 1 gyrostabilized in inertial space, to prevent disturbance of the horizontal position of the platform 2 through the earth's diurnal rotation, it is essential to turn it in inertial space about the ξ' axis at the rate of the earth's diurnal rotation, i.e. at a rate of $15^\circ/\text{hour}$. This rotation is effected by the servodrive 6 (in Fig. 6.3 it is

marked item 16) controlled by the clock 7. In such a case the platform 2 on the equator will remain horizontal. In Figs. 6.3 and 6.4 the ξ , η and ζ axes have the same meaning.

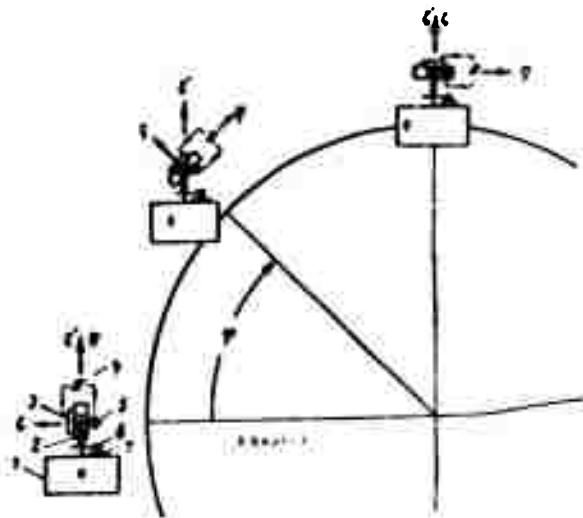


Fig. 6.4. Diagram illustrating integral correction: 1) gyrostabilized platform orientated permanently in inertial space so that the ξ axis is parallel to the axis of the earth's diurnal rotation; 2) platform with accelerometers; 3) northern accelerometer; 4) northern integrators; 5) servodrive; 6) servodrive; 7) clock.

Let us suppose that the aircraft has begun to move uniformly along a meridian in a northerly direction in such a way that the northern acceleration is $\underline{v}_N = 0$. When the aircraft has moved through a small angle $\Delta \varphi$, the platform 2 is no longer horizontal since it has maintained its original position in inertial space. As a result, the projection of the force of gravity will begin to act on the measurement axis η of the northern accelerometer. The accelerometer will send a signal to the first integrator which, in its turn, will send one to the second integrator (in Fig. 6.3 the two integrators are represented by a double integral sign). The signal from the second integrator output sets going the servodrive 5 (item 10 in Fig. 6.3) which begins to turn the platform 2 to a horizontal position. As a result, a regime is established in which the second integrator output emits a

constant signal ensuring that the servodrive 5 (Fig. 6.4) keeps turning platform 2 about the ξ axis (Fig. 6.3) at a rate equal to the rate of change, $\dot{\varphi}$, in the latitude. Hence the platform 2 stays horizontal the whole time. The signals from the accelerometer and the first integrator will be zero at this point. This method of keeping the platform horizontal is conventionally called integral correction. Integral correction ensures the horizontal position of the platform in similar fashion when the aircraft is moving with an acceleration of \dot{v}_H . In this case the signals from the accelerometer and the first integrator will no longer be equal to zero, and the signal from the second integrator will not be constant.

Let us go back to Fig. 6.3. The northern accelerometer signal is twice integrated by the integrators 11 and 12. The output signal of the integrator 12 is sent to the servodrive 10 and to the latitude indicator 13. The latter shows the aircraft's latitude. The first window shows whether the latitude is northern (by the letter N) or southern (by the letter S). The other windows indicate the degrees, minutes and seconds of the latitude.

The signal from the eastern accelerometer 8 is sent to the input of the first eastern integrator 5. Its output signal, which is proportional to the eastern speed of the aircraft, is sent to the input of the computing device 4. This device simultaneously receives a signal from the output of the accelerometer 12 proportional to the latitude φ . The computing device 4 emits a signal proportional to the rate of change $\dot{\lambda}$ in the longitude, calculated from Formula (6.5). This signal is sent to the input of the second eastern integrator 3. The signal from the integrator output is sent to the longitude indicator 2, which is similar to the latitude indicator 13, and is fed to the summation device 15 where it is algebraically added to the signal indicating the rate of the earth's diurnal rotation

ω_e received from the clock. The signal from the output of the summation device 15 switches on the servodrive 16 which turns the frame 6 about the ξ' axis at a rate of $\omega_e + \dot{\lambda}$, ensuring the horizontal position and required orientation of

the platform 7 in the azimuth, together with the servodrive 10.

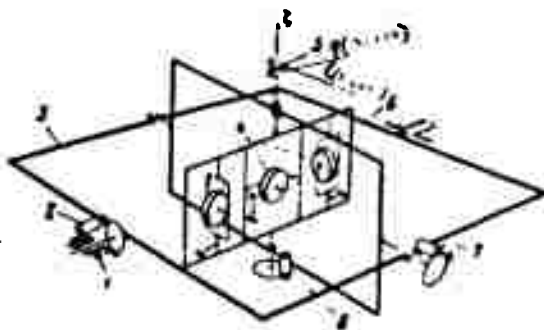


Fig. 6.5. Gyro-stabilized platform. 1) Body of guided object; 2) slave motor of roll servo-system; 3) frame of roll axis; 4) gyroscopes; 5) accelerometers; 6) stabilized platforms; 7) slave motor of pitch servo-system; 8) slave motor of course servo-system.

The second way of making certain that the accelerometer measurement axes retain their horizontal position and required orientation in the azimuth is to place the accelerometers directly on the gyro-stabilized platform 6 (Fig. 6.5) which, in this case, is stabilized with respect to the plane of the horizon and the S-N direction. In other words, in this case the ξ , η , and ζ axes (Figs. 1.13 and 6.5) are materially reproduced directly by the gyro-stabilized platform. The working principle of this kind of platform has been described in Chapter I, Sec. 7. The diagram in Fig. 6.5 is a slightly altered version of the platform shown in Fig. 1.21. It was pointed out in Chapter I, Sec. 7 that in order to ensure the required orientation of the ξ , η , and ζ axes relative to the earth, it is essential to turn the platform correspondingly in inertial space, for which corresponding currents I_{con} have to be fed to the gyroscope torquers. In the case under consideration these currents are supplied by the output signals of the first integrators of the northern and eastern accelerations of the object (aircraft or guided missile). The gyroscopes on this platform will operate both in the geometrical-stabilization and spatial-integration regimes. A great advantage of this version is the invariant nature of the position of the gyroscopes and the platform itself with regard to the gravitational field.

In principle the integral system is set in operation in the following way. The stabilized platform is set in a horizontal position and is mounted in the azimuth with the measurement axis of the northern accelerometer lying from south to north, which also orientates the eastern accelerometer. Next, the longitude and latitude of the departure point and the destination point are fed into the computer and the integrators are set at zero. As soon as the aircraft begins its take-off run the accelerometers start working and emit the signals necessary for the system to operate. The computer will keep determining the current coordinates, the course and the angles of pitch and roll of the aircraft, and will emit the necessary signals for the automatic pilot to guide the flight.

The distance traversed, measured by double integration of the accelerometer signals, is proportional to the square of the time; this results in an inadmissible accumulation of errors in dead reckoning. But it is not yet possible to manufacture accelerometers, integrators, and gyroscopes with the accuracy needed to prevent these errors during prolonged flight by a guided object.

A practical solution to the problem of reducing the accumulation of errors and maintaining the horizontal position of the stabilized platform has only been possible through the implementation by designers of inertial systems of navigation of the idea put forward by Dr. M. Schuler in 1923. Schuler's principle of a pendulum with an oscillation period of 84.4 min is the basis of all the known practical systems of inertial navigation being developed at the present time for guiding aircraft and rockets. The principle of this pendulum has made it possible to establish the direction of gravity (vertical) with precision in a moving object irrespective of the acceleration acting in any direction, due to any cause. When this principle is applied, the platform and its accelerometers with a period of 84.4 min will uninterruptedly follow the true vertical and thereby set the accelerometers perpendicular to this vertical. Furthermore, the application of this principle is a guarantee against the inadmissible accumulation of errors in the computed position, which

would otherwise occur through the drift of the gyroscopes, the lack of balance of the accelerometers and instrument errors. In practice the inertial navigation system is arranged in such a way that it functions as a pendulum with an oscillation period of 84.4 min. Schuler formulated his principle approximately as follows:

"An oscillating mechanical system, the center of gravity of which is being acted upon by a central force, when moving along the surface of a sphere around the center of the forces, will not be drawn into an oscillating motion if the period of its natural undamped oscillations is equal to the oscillation period of a pendulum of a length equal to the radius of the sphere and subject to the effect of its field of forces."

For bodies moving along the earth's surface or flying above the earth at a height which is insignificantly small compared to the radius R of the Earth, this period is

$$T = 2\pi \sqrt{\frac{R}{g}} = 2\pi \sqrt{\frac{6,371,000}{9.81 \cdot 3600}} = 84.4 \text{ min}$$

Section 4. Application of the Principle of the Pendulum With an Oscillation Period of 84.4 Min to the Inertial System of Navigation

By the correct selection of the parameters for the separate parts of the inertial system its natural oscillation period can be made to equal 84.4 min. If this is done, the system, like Schuler's classical pendulum, will find the vertical of a point and maintain its position or oscillate with respect to it, irrespective of the movement of the object. Furthermore, this oscillating system will not accumulate errors proportional to the square of the time; any accumulation will be of an oscillatory nature.

This oscillatory nature can be demonstrated by considering the system with one

degree of freedom, shown diagrammatically in Fig. 6.6. The system consists of a platform, turning by means of a servodrive about an axis perpendicular to the plane of the drawing, to which is attached an accelerometer equipped with an acceleration indicator. The accelerometer signals are passed successively from the potentiometer-pickoff to two integrators equipped with indicators showing the speed and distance traversed.

Let us transpose the whole system to the North Pole and suppose that the accelerometer has a slight error in balance which creates a small output signal at the accelerometer output (Fig. 6.6g) when the object and the accelerometer are stationary. This output signal cannot be distinguished from the signal which is obtained if the object begins to turn to the right (clockwise around the earth). After the second integration the accelerometer signal will indicate the apparent change in the latitude of the object. If this signal is passed as a correcting signal to the servodrive of the platform, the latter will begin to turn in a clockwise direction. If the platform deviates from the horizontal, the elastically suspended body of the accelerometer will be subject to the effect of gravity which will now act in the opposite direction to the initial imbalance of the accelerometer. As soon as the platform reaches the point where the effect of gravity exactly compensates for (cancels) the initial imbalance (Fig. 6.6h), the accelerometer signal will become zero. The rate of change in the output signal of the first integrator will also drop to zero in the process. The second integrator will record this as a continuation of the object's motion at a constant speed in a clockwise direction and will gradually increase the "distance gone" output signal, through which the platform will be forced to continue turning in the previous direction.

As the platform turns, the elastically suspended body of the accelerometer swings by the force of gravity to the right, producing a signal of the opposite polarity at the accelerometer output which makes it appear that the object has slowed down. When the angle through which the platform swings to the right is

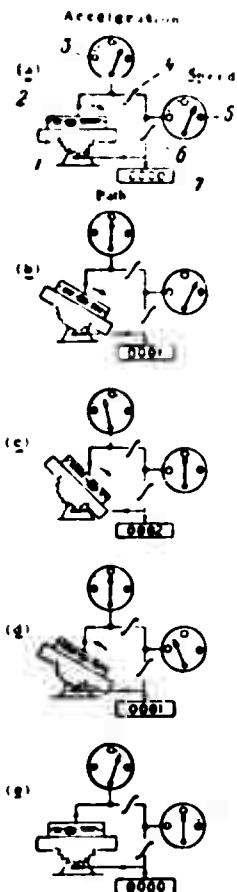


Fig. 6.6. Diagram illustrating oscillations of platform. 1) Stabilized platform; 2) accelerometer; 3) acceleration indicator; 4) first integrator; 5) speed indicator; 6) second integrator; 7) indicator of distance traversed.

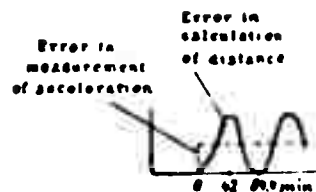


Fig. 6.7. Graph showing errors in system with oscillation period of 84.4 min.

such that the body of the accelerometer moves away from the center by a value equal in absolute terms and opposite in sign to the initial harmful deviation, the signal at the output of the first integrator becomes zero (Fig. 6.6c). A signal with a negative sign will then begin to appear at the first integrator output, showing that the object has seemingly begun to move in the reverse direction.

As a result, the output signal of the second integrator is reduced, which makes the platform turn in the reverse direction, i.e. counterclockwise. During this reversal the platform will again pass a

point where the imbalance of the elastically suspended body of the accelerometer will be exactly compensated by gravity (Fig. 6.6d). At this point the acceleration will be zero and the speed in absolute values will be equal to the speed in Fig. 6.6a, being different only in sign. When the platform moves further in a counterclockwise direction it will reach the position shown in Fig. 6.6e, after which the

whole cycle will be repeated.

If the parameters of the oscillatory system under consideration are selected in such a way that its oscillation period is 84.4 min, the system will behave like Schuler's pendulum. The error in the calculated distance will also oscillate with a period of 84.4 min. A rough graph of these errors is given in Fig. 6.7. The amplitude of the oscillation of the error depends on the sensitivity and the precision of the accelerometer, gyroscopes (if the system is constructed as in Fig. 6.5), servodrives, and integrators.

Section 5. Effect of the Coriolis Acceleration and the Nonspherical Shape of the Earth on the Operation of the Inertial System of Navigation

Rotational acceleration (Coriolis acceleration) affects the operation of the inertial system of navigation to a certain extent.

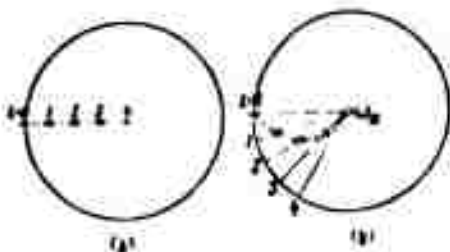


Fig. 6.8. Effect of Earth's rotation on the path of a guided object in absolute space when flying from the Equator to the North Pole on a steady course. (a) Path relative to ground (the absolute path would be the same if the Earth did not rotate); (b) actual absolute path.

If the Earth did not turn on its own axis, an object flying, let us say, from the Equator to the North Pole along a straight ground course would follow the straight path shown in Fig. 6.8a. In actual fact, however, on account of the rotation of the Earth, while flying along a meridian the object describes a curved path in absolute space (Fig. 6.5b). An observer located in space above the Pole

would see it as such. This path testifies to the constant change in the magnitude and direction of the object's speed in inertial space and to the effect of Coriolis (rotational) acceleration on the object; to compensate for this the output signals of the S-N and W-E accelerometers have to be corrected.

The nonspherical shape of the Earth has a certain effect on the operation of

the inertial system of navigation. If the Earth were perfectly spherical, the vertical fixed by means of a pendulum with an oscillation period of 84.4 min would be the same as a line from a point on the surface of the earth to its center. As a result of the slightly flattened shape of the Earth, however, a vertical line does not correspond to a line to the center of the Earth. The angle between them at a latitude of 45° is approximately 11 minutes. The noncoincidence of the lines gives rise to a harmful acceleration. The inertia caused thereby affects the S-N accelerometer and this effect in long-range inertial systems must also be corrected.

Section 6. Combining Inertial Systems of Navigation With Other Navigational Systems

A purely inertial system of navigation (Fig. 6.9) requires its component units --the accelerometers, gyroscopes, computing devices, servodrives, and other instruments --to possess a very high degree of accuracy compared with similar instruments used in aircraft at the present time. The problem of achieving the required accuracy in the inertial system components has not yet been fully solved; at the moment, therefore, so-called combined systems have appeared alongside designs of purely inertial systems, in which the accumulation of errors inherent in

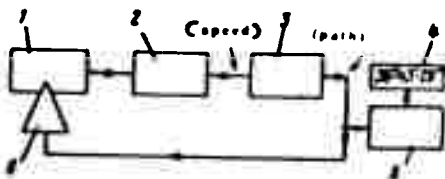


Fig. 6.9. Block diagram of purely inertial system of navigation. 1) Accelerometer; 2) first integrator; 3) second integrator; 4) position indicator; 5) computing device; 6) stabilized platform.

the latter type of system is compensated for by the use of signals from a radar unit on board the guided object, or by additional verification of the speed and path from celestial or ground reference points.

The combined inertial system of navigation lacks the chief advantage of the purely inertial system, to wit, complete independence from outside emission and the absence of any need for external

reference points. In certain areas, however, the use of combined inertial systems is fully justified on account of the small size, simplicity, and low cost of the equipment required as compared to the equipment used in purely inertial systems of navigation. Civil aviation, for instance, is a field in which combined systems can be used predominantly. They can also be used in military aviation.

One of the best-known combined systems is formed by the addition to the inertial system of a radar unit working on the principle of the Doppler effect. The radar antenna is mounted on the lower surface of the aircraft or rocket and faces forwards or backwards at an angle to the line of flight, but not directly downwards. When the guided object is in flight, the antenna of the radar unit emits a continuous-wave signal. Part of the signal is reflected from the earth's surface back to the antenna, its frequency differing slightly from that of the original signal on account of the Doppler effect. The difference between the frequencies of the original and reflected signals is proportional to the speed of the object above the earth. By measuring the different signals along an axis parallel to the longitudinal axis of the object and also along its transverse axis and their vector summation it is possible to obtain the true ground speed.

As already pointed out, the purely inertial system calculates the ground speed of a guided object by continuous integration of the output signals from two accelerometers with the necessary correction for the earth's rotation and other factors. The ground speed signal, calculated by the first integrator is sent to the servo-drive of the gyrostabilized platform carrying the accelerometers and turns the platform with an angular velocity equal to the angular velocity of the movement of the object around the earth, which is essential to maintain the horizontal position of the accelerometers. In order to give a reading of the distance traveled, the speed signal is integrated by the second integrator. That is what happens in a purely inertial system of navigation in which, as already pointed out, the accuracy with which the speed and the distance traveled are determined will gradually

deteriorate as the flight continues on account of the inevitable accumulation of errors.

In a combined system of navigation it is possible to make a continuous or periodic ground-speed correction which is calculated by the acceleration integrator. In the radar system making use of the Doppler effect this is done in the following way. The ground speed signal from the radar unit is compared with the speed signal calculated by the acceleration integrator. If there is any discrepancy, the relevant correction is made so that the speed signals emitted by the radar unit and the integrator become the same.

If the guided object is flying over friendly territory where detection of the radar emission from the object is of no danger to it, the radar unit can be left on the whole time. Under the circumstances the unit can act as the basic ground-speed indicator, and the accelerometer-integrator system can be used to average the momentary errors and interference created by the radar unit when flying over rugged terrain.

When the guided object is flying over foreign territory the radar unit may not work the whole time on account of the danger of instant detection. But it can be automatically switched on from time to time for a few seconds, and then be switched off for considerably longer, irregular periods, say from 10 to 15 min. Under these operating conditions the periodic correction of the inertial-system readings is kept up, and the chances of the guided object being spotted are greatly reduced at the same time. A block-diagram of an inertial system of navigation combined with a radar unit working on the principle of the Doppler effect is shown in Fig. 6.10.

A (US) firm working in the field of inertial navigation reports that the combined system incorporating both inertial and radar principles has a navigational error not greater than 1.5% of the distance traveled in 10 hr. This means that a bomber flying at 965 km/hr towards a target 4800 km from the take-off point will reach it with an error not greater than 72 km. Inertial systems of navigation can

be combined with other types of radar. For example, an inertial system intended for long-range bombers or transport planes can be further equipped with a radar unit of the type installed in similar aircraft for observation of the terrain being flown over and for bombing purposes. By keeping a watch on certain known landmarks and ground radar beacons with the aid of this radar unit the navigator can determine the exact position of his aircraft. The aircraft's coordinates determined in this way can then be compared with data calculated by the inertial system. If there is any discrepancy, the readings of the inertial system can be corrected accordingly.

Another way of obtaining a fix in order to make periodic corrections to the inertial system is by astronavigation. As is known, if the height and azimuth of two stars are known, the geographical coordinates of the object at any point on the earth's surface can be determined. One of the most important problems of astronavigation -- obtaining an exact standard for the horizontal -- is solved by using the gyrostabilized platform of the inertial system. The main component in the astronavigational system is the system for observing the heavenly bodies or automatic photoelectric sextant. This device can automatically follow the chosen star or planet at night, or the sun during the day. A fully automatic system of astronavigation requires two stellar observation systems mounted on a repeating stabilized platform which follows in movement the basic gyrostabilized platform of the inertial system. The system contains a computing device which solves the problems of spherical trigonometry in the calculations.

The observation of two stars makes it possible in principle to achieve a fully automatic system of astronavigation. If the astronavigational system is solely used to correct the inertial system, a simplified system following only one star can be used. A rough block diagram of a combined inertial system of navigation with astronomic correction is shown in Fig. 6.11.

Inertial-astronomic systems of navigation are being used at the present time in some of the guided missiles produced in the USA.

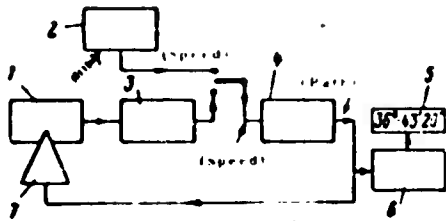


Fig. 6.10. Block diagram of system of inertial navigation combined with radar unit working on the principle of the Doppler effect. 1) Accelerometer; 2) radar unit; 3) first integrator; 4) second integrator; 5) position indicator; 6) computer; 7) stabilized platform.

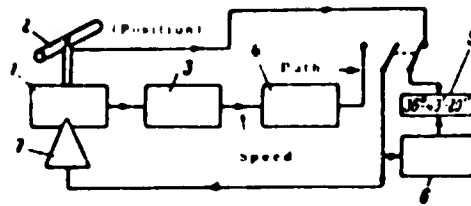


Fig. 6.11. Rough block diagram of inertial system of navigation combined with automatic system for following a celestial body. 1) Accelerometer; 2) automatic photosextant; 3) first integrator; 4) second integrator; 5) position indicator; 6) computer device; 7) stabilized platform.

Section 7. Some Components of Inertial Navigation Systems

The above-described working principles of inertial systems of navigation do not constitute anything new. As is well known, a navigational system of this kind was first developed in the Soviet Union by E. B. Levental' in 1932. Nor is the equipment used in inertial systems original in principle. It has been possible to manufacture a complete gyroscope from the structural point of view for about fifteen years; the principle of the pendulum with an oscillation period of 84.4 min was put forward by Schuler in 1923, and integrators, servodrives, and other kinds of measuring instruments were known before the Second World War; nevertheless, despite the fact that the general principles of the system of inertial navigation and its components have long been familiar, even by the beginning of the War the problem of the practical realization of these systems had not been emphasized sufficiently anywhere.

This may seem strange at first sight since the advantages of the inertial system considered above far outweigh those of all the known systems of navigation.

Simple calculations, however, will show that in spite of the simplicity of the principles of the system, the implementation of it involves the greatest difficulties. It has taken many years to develop the theory and to perfect the designs and technology of production of the gyroscopes, accelerometers, servodrive and other instruments making up the inertial navigation system. The reason for the great difficulty in actually constructing inertial systems is first and foremost that the demands made upon the instruments in the system are inordinately severe.

The main requirement is an extremely high degree of accuracy in manufacturing and adjusting the instruments. Gyroscopes, accelerometers, servodrives, and integrators have long been used in modern navigational systems, but the accuracy required from them in inertial systems must be one or two orders greater than that attained at the present time. Standard and batch-produced components for inertial systems can only be compared as to accuracy required with precision instruments used in the laboratory. On the other hand, the high degree of accuracy has to be combined with exceptional shock and vibration resistance so that the instruments can work in the exacting conditions encountered in high-speed aircraft and rockets. Moreover, inertial-system instruments intended for conventional and pilotless aircraft must be small in size and low in weight.

The second and no less important requirement in these instruments is that they should operate accurately and reliably over an unusually wide range of input values. The ratio of the maximum measured input value (e.g. acceleration, angular velocity, etc.) to the minimum in some instruments may reach 100,000. This is an entirely new requirement and not even the most accurate instruments come up to it. It is difficult to imagine, for instance, a voltmeter with a scale reading up to 100 kv which could measure with great accuracy voltages of both up to 10 v and up to 100,000 v without changing the measurement range (scale). In this connection it is of interest to recall that the most remarkable natural "instrument" as regards the range of values which can be sensed is the human ear, in which the ratio of the

maximum audible value (sound intensity) to the minimum is 10^{13} .

At present the development of instruments for inertial systems of navigation is proceeding along two lines: on the one hand, the instruments of familiar design now used in aircraft are being perfected from the point of view of accuracy, speed of action and range of response. These instruments (accelerometers, gyroscopes, integrators, computers and servodrives) are being carefully analyzed from the standpoint of maximum accuracy attainable in mass production. On the other hand, many experts are seeking new principles in the construction of mechanical and electrical instruments specially adapted to work in inertial systems of navigation.

The high accuracy required in inertial system instruments has given rise to the need for special precision test apparatus without which verification and adjustment of these instruments is impossible. Such apparatus includes turntables for testing gyroscopes with precision devices to measure the angular velocity with an accuracy of several milliradians per day; stands for testing synchronous coupling systems with an accuracy in transmitting the component angle of several minutes; equipment for measuring the gyroscopic moment with an accuracy of mill millionths of a gram-centimeter; potentiometers (compensators) measuring ac current with an accuracy of hundredths of a percent, and so on. In its turn, the building of such test apparatus may require the development of completely new devices, such as reducerless silent electric motors, ultra-accurate dc and ac voltage regulators, optical instruments for measuring slight movement and so on. Thus the development of inertial systems of navigation cannot be compared with the development of a system which, although new, does not differ very much in principle from existing types. Compared with known methods the development of inertial systems is a technological jump forward demanding solutions different in principle in the field of the designing, production technique and testing of aircraft instruments.

Let us consider in general terms some of the basic elements of inertial navigation systems, with the exception of the gyroscopes, since all the preceding chapters of the book have been devoted to them.

Accelerometers

Devices for measuring acceleration, or accelerometers, are important components in inertial systems. To measure acceleration of motion in a straight line, so-called linear accelerometers are used. These include, for example, accelerometers which work by measuring the movement of an elastically suspended body. These accelerometers have been known for a long time and are widely used in research of various kinds. In the old type of design direct methods of recording were often used, for example, a diamond tip which made scratches on a glass plate.



Fig. 6.12. Linear accelerometer.

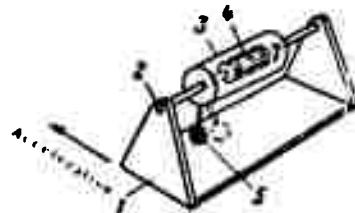


Fig. 6.13. Illustration of working principle of accelerometer with electric spring. 1) Instrument housing; 2) low friction bearings; 3) electric motor stator; 4) armature of motor; 5) pendulum weight.

The accelerometers intended for aircraft usually use electric output-signal pick-offs. Figure 6.12 shows an industrially produced linear accelerometer with an electric output signal pickoff. This accelerometer is intended for aircraft and short-range rockets and measures positive and negative accelerations acting in a horizontal and vertical plane, or in both planes at once. Accelerometers of this kind are produced in batches with upper limits of measurement varying from 5 g to 50 g. The total error of these instruments (scale, hysteresis, and also nonlinearity) is a maximum of 2%.

In developing a new accelerometer or adapting an existing one for an inertial system, the problem immediately arises of the range of measurable acceleration or

the ratio of the maximum measurable acceleration to the minimum. It is considered that this ratio should be of the order of 100,000 if the system is to operate satisfactorily. It is extremely difficult to construct an accelerometer with an elastically suspended body with this ratio since at small accelerations the operation of the instrument will be detrimentally affected by friction and at high accelerations there will be errors caused by hysteresis of the elastic suspension. Moreover, the designing and manufacture of springs or spring systems with a satisfactory performance over such a wide range of accelerations involves great complications. One of the practical ways of overcoming this difficulty is to use a mechanical spring with low rigidity together with a so-called "electric spring."

Figure 6.13 is an illustration of one of the possible applications of the electric-spring method in the construction of a linear accelerometer. The part of the electric spring in the diagram is played by a small dc electric motor. The armature 4 of the motor is attached immovably to the instrument housing. The stator 3 and the load 5 attached to it is suspended on two supports in the low-friction bearings 2. If there is no acceleration, the pendulum thus formed hangs vertical, i.e., in its initial position. If the device is shifted horizontally in the plane of the swing of the pendulum with acceleration, the pendulum will swing and take up the position shown in Fig. 6.13 by the dotted line. The stator 4 will turn with it. Let us now impress upon the armature a voltage of a polarity and magnitude such that the motor develops a moment sufficient to return the stator-pendulum to its initial position, corresponding to absence of acceleration. The voltage which is impressed upon the armature and which causes the moment of the motor, compensating in this case for the moment of inertia, will be proportional to the linear acceleration with which the device moves. Thus the device acts as an accelerometer and the measurement of the acceleration is the value of the voltage needed by the armature to return the stator to its initial position.

Since moments tending to return the stator immediately to its initial position

are always impressed upon it when there is acceleration, the angle of deflection of the stator will always be small. This means that the accelerometer measures the linear acceleration and does not experience the undesirable effect of the acceleration of gravity. In order to impress a voltage on the armature, use can be made in the accelerometer of contact-type or other pickoffs which react to the deviation of the stator-pendulum from its initial position and in response send a voltage to the armature which keeps increasing until the stator returns to its initial position.

One of the methods of the measurement of acceleration is the use of the so-called resonance accelerometer. This instrument contains a vibrating unit, the resonance frequency of which varies with the acceleration with which it moves. The deviation of the resonance frequency is proportional to the acceleration. Hence, if we calculate the difference between the number of oscillations which would have occurred in a given time interval if there were no acceleration and the number of oscillations occurring over the same period when there is oscillation, it will be proportional to the integral of the acceleration, i.e., proportional to the variation in speed over the given time interval. Thus, the resonance accelerometer is a representative of the so-called integrating accelerometers whose use can simplify the problem of the instruments needed for the inertial system of navigation. Certain experts believe that resonance accelerometers eventually may replace conventional accelerometers.

Integrators

At the present time there are various types of integrators in existence and in actual use. Methods of "machine" integration have been carefully studied, and any present-day computer can cope with integration processes. When this method of integration is used in inertial systems of navigation, however, we encounter the same

difficulties which perpetually accompany these systems, to wit, accuracy, resistance to vibration, range of response, and so on. The specific conditions in which inertial navigation systems operate make it difficult to utilize the conventional integrators used in the laboratory.

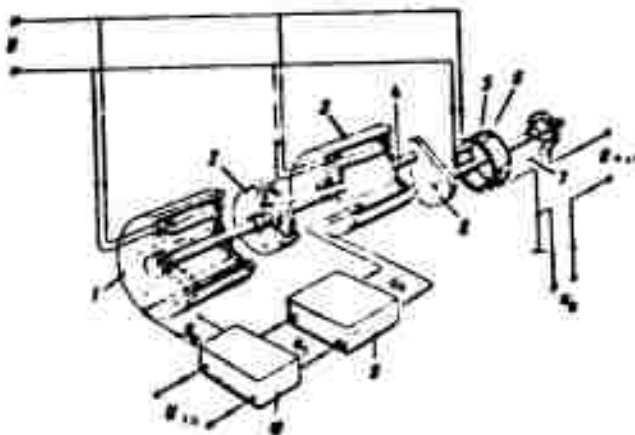


Fig. 6.14. Diagram showing components of electromechanical integrator of the integrating-drive type. 1) Two-phase tachometer generator; 2) liquid damper; 3) two-phase induction motor; 4) output shaft; 5) potentiometer pickoff; 6) output shaft of reducer; 7) potentiometer wiper; 8) reducer; 9) amplifier; 10) comparator.

One of the commonest integrators in inertial systems is the electromechanical integrator of the integrating drive type with an ac tachometer generator. It is a shaping-type integrator.

A diagram showing the component parts of this type of integrator is given in Fig. 6.14. The chief requirement is that the angular velocity of the output shaft 6 with respect to the instrument housing should be proportional with a high degree of accuracy to the input voltage U_{in} . The input voltage U_{in} is sent to the comparator 10. The latter simultaneously receives a voltage U_{tg} from the precision tachometer generator 1, mounted on the output shaft 4, proportional to the momentary value of the angular velocity of the output shaft. The difference voltage is picked off the comparator output and is sent after amplification by the amplifier 9 to the control winding of the two-phase induction motor 3, the rotor of which is

connected to the output shaft. The difference voltage and, consequently, the rotational moment of the motor become zero only when the velocity of the rotation of the shaft 1 (the motor rotor) is exactly proportional to the value of the input voltage U_{in} . Let us suppose that the output shaft at the moment under consideration is rotating at an angular velocity exactly proportional to the input voltage. On account of the difference voltage equalling zero, the rotation of the shaft will then begin to slow down and its angular velocity will cease to be proportional to the input voltage U_{in} . As a result of the voltage U_{tg} developed by the tachometer-generator will fall below the input voltage U_{in} . The result of this will be another difference voltage and the rotation of the output shaft will begin to accelerate. At the moment the angular velocity of the output shaft reaches a value proportional to the input voltage U_{in} , the difference voltage will again become zero. If the angular velocity of the output shaft exceeds the required value, there will again be a difference voltage, but this time its phase will be such that it will cause the motor to slow down; this will continue until the angular velocity of the output shaft becomes proportional to U_{in} .

Hence the difference voltage is always such that it brings the angular velocity of the output shaft to a value proportional to the input voltage U_{in} . Since the angular velocity of the output shaft ω is proportional to the input voltage U_{in} , its angle of rotation, and consequently the output voltage U_{out} picked off the potentiometer 5 (Fig. 6.14), will be proportional to the integral of the input voltage U_{in} with respect to time.

The parameters of the design are chosen in such a way that the deviations of the angular velocity of the output shaft from a value proportional to the input voltage are fairly small. The liquid damper 2 is mounted on the output shaft to reduce its free oscillations to a minimum.

This type of integrator works satisfactorily in conventional systems of aircraft navigation. Inertial systems of navigation, however, which require the

integration of signals from extremely small (thousandths of a g) up to very large (tens of g) accelerations, need an integrator with considerably greater accuracy which can work over a wide range of input values. One way to solve this problem is to use multistage integrators of the integrating drive type. The firm Bosch Arma has constructed a two-stage integrator in which each of the two tachometer-generators works in its own range of velocities and voltages, and which has a corresponding circuit for selecting the ranges.

Another analog-integrator is the dc integrating amplifier. The output signal of this amplifier is proportional to the integral of the input voltage with respect to time. A critical component in the integrating amplifier is the high-grade condenser connected to the feedback circuit. The leakage current from the condenser and the dielectric loss in the insulation must be very small in order to obtain the necessary accuracy in integration.

The most convenient instruments for integrating pulse signals, for instance resonance accelerometer signals, are integrators of the digital type or pulse counters. The digital integrators can provide any desired degree of accuracy whereas in the analog-integrator the required degree of accuracy is frequently unattainable through limitations in design and production technique.

Computing Devices

Analog computers, which make calculations involving problems of spherical trigonometry, have been used in aircraft for some time. In using them in inertial systems of navigation the greatest difficulty encountered is obtaining the desired accuracy. This problem frequently makes it impossible to use analog computers in inertial systems.

An obvious solution to the problem is to use binary digital computers which

can provide practically any desired degree of accuracy with only a slight increase in size, weight, and cost as compared with analog computers. An example of a modern aircraft digital computer is the differential analyzer made by the North American Aviation firm. This device, which contains 93 integrators, weighs 56.5 kg, takes up a volume of 0.028 m^3 , and consumes only 100 watts. An additional advantage of digital computers in inertial systems of navigation is that they can be used at the same time for calculations in connection with bombing, fire control, etc. besides navigational problems. Present-day digital computers work so rapidly that they can solve navigational problems in fractions of a second and then make a calculation connected with bombing, after which they can go back to inertial-navigation problems. The advantages of digital computers have earned them a prominent place in new inertial systems of navigation.

Servodrives

It is clear that although we have highly sensitive and reliable accelerometers and gyroscopes as well as integrators and computing devices, it is still impossible to construct an inertial system of navigation until we have developed servodrives which can stabilize the platform carrying the accelerometers sufficiently accurately and rapidly. The ability of gyroscopes to detect the slightest rotation about their axes and the capacity of accelerometers to record the slight accelerations will be of no avail unless the servodrives are able to react to the extremely weak signals emitted by these instruments and turn the platform appropriately in response. Servodrives must provide exact geometric stabilization of the platform no matter what computed changes in the position of the aircraft or rocket may occur in the air. The rapidity with which servodrives intended for inertial systems must work is very great and the dynamic errors must be very small. The whole

servosystem will not work well unless its component parts --the amplifier, slave motors, and reducer --possess the necessary accuracy, linearity, small time constant, and good dynamic characteristics.

In developing a servodrive for an inertial system of navigation we should not only make use of everything that is known in the theory of servosystems, but also devise entirely new methods of analysis and computation.

REFERENCES

Literature on the General and Applied Theory of Gyroscopes and Aircraft Gyroscopic Instruments

- D.A. Braslavskiy, S.S. Logunov and D. S. Pel'por, The Calculation and Design of Aircraft Instruments (Raschet i konstruktsiya aviatsionnykh priborov), Oborongiz (St. Press of Def. Indust.), 1954.
- B.V. Bulgakov, Applied Theory of Gyroscopes (Prikladnaya teoriya giroskopov), State Press for Technical and Theoretical Literature, 1955.
- P. Grammel', The Gyroscope, its Theory and Application, Parts I and II (Giroskop, yego teoriya i primeneniye, chast' I i II), Foreign Literature Press, Moscow, 1952.
- A.S. Kozlov, Theory of Aircraft Gyroscopic Instruments (Teoriya aviatsionnykh giroskopicheskikh priborov), Oborongiz, 1956.
- A.N. Krylov and Yu. A. Krutkov, General Theory of Gyroscopes and Some of Their Applications (Obshchaya teoriya giroskopov i nekotorykh tekhnicheskikh yikh primeneniye, Acad. Sci., USSR, 1932.
- Ye. L. Nikolai, Gyroscopes in Gimbals (Giroskop v kardanovom podvece), Technical and Theoretical Literature Press, 1944.
- Ye. L. Nikolai, The Gyroscope and Some of Its Applications (Giroskop i nekotoryye yego tekhnicheskikh primeneniye), Gostekhnizdat (State Tech. and Theor. Lit. Press), 1947.
- Ye. L. Nikolai, The Theory of Gyroscopes (Teoriya giroskopov), Gostekhnizdat, 1948.
- Ye. V. Ol'man, Ya. I. Solov'yev and V.P. Tokarev, Automatic pilots (Avtopiloty), Oborongiz, 1946.
- V.A. Pavlov, Aircraft Gyroscopic Instruments (Aviatsionnyye giroskopicheskiye pribory), Oborongiz, 1954.
- G.A. Slomvanskiy, Concerning the Deduction and Analysis of Equations for the Motion of the Symmetrical Gyroscope (K vyvodu i analizu uravneniy dvizheniya simmetrichnogo giroskopa), Papers of the Moscow Institute of Aviation Engineering, No. 6 (Trudy Moskovskogo aviatsionnogo tekhnologicheskogo instituta, vyp.6), Oborongiz, 1949.

G.A. Slomyanskiy, Concerning Integration of Equations of Motion for the Symmetrical Astatic Gyroscope (Ob integrirovaniⁱ uravneniy dvizheniya simmetrichnogo astati-cheskogo giroskopa), Applied Mathematics and Mechanics, No. 4, 1953, 17.

G.A. Slomyanskiy, Commentary on Greynakher's Article (Zamechaniya k stat'ye Grey-nakhera), Bull. Acad. Sci. USSR, Div. Tech. Sci. (Izv. AN SSSR, OTN), 1954, No. 11.

G.A. Slomyanskiy, Concerning Precession of Fast-Spinning Gyroscopes in Gimbals (O pretsessii bystrovrashchayushchegosya giroskopa v kardanovom podvece), sv. Akad. Nauk SSSR, OTN, No. 9, 1955.

G.A. Slomyanskiy, Shortened Equations of Motion for Fast-Spinning Gyroscopes in Gimbals and the Effect of Static Imbalance of the Gyromotor on the Behavior of the Gyroscope (Ukorochennyye uravneniy dvizheniya bystrovrashchayushchegosya giroskopa i vliyaniye staticheskoy neuravnoveshannosti giromotora na povedeniye giroskopa), Papers of Moscow Institute of Aviation Engineering, No. 27, Oborongiz, 1956.

S.S. Tikhmenev, Theory of Aircraft Instruments (Teoriya aviatsionnykh priborov), Zhukovsky Airforce Academy, 1940.

REFERENCES USED

1. Draper, C. S., Wrigley, W., Grohe, L. R. The floating integrating gyro and its application to geometrical stabilization problems on moving bases. IAS Preprint 503.
2. Draper, C. S., Wrigley, W., Grohe, L. R. The floating gyro and its application to geometrical stabilization problems on moving bases, Aeronautical Engineering Review, 1956, No. 6, V. 15.
3. Draper, C. S., McKay, Walter, and Lees, Sidney. Instrument Engineering, Vol. II.53, Vol. III.55, Part 1.
4. Steier, H. P., M. H. Tackles. Inertial Component Challenge, American Aviation, 11/II, 1957.
5. Aircraft Instruments and Systems, American Aviation, 22/X 1956.
6. Philip J. Klass, Inertial Guidance, Aviation Week, 2/I 1956, 9/I 1956, 16/I 1956, 23/I 1956.
7. Aero Digest, IV, 1954.
8. Electronics, XI, 1955.
9. Electronics, VII, 1955.
10. American Aviation, 30/I 1956.
11. American Aviation, 21/XI 1955.
12. Aviation Age, IX, 1954.
13. Aviation Age, I, 1955.
14. Aviation Week, 9/VIII, 1954.

15. Aviation Week, 3/I, 1955.
16. Aviation Week, 10/I, 1955.
17. Aviation Week, 24/I, 1955.
18. Aviation Week, 22/II, 1955.
19. Aviation Week, 14/III, 1955.
20. Aviation Week, 21/XI, 1955.
21. Aviation Week, 12/XII, 1955.
22. Aviation Week, 8/X, 1956.
23. Aviation Week, 10/VI, 1957.

CONTENTS

	Page
Preface	111
Chapter I. Brief Survey of the Characteristics and Certain Applications of Gyroscopes	1
Sec. 1. Brief consideration of gyroscopes with two degrees of freedom	1
Sec. 2. Brief consideration of gyroscopes with three degrees of freedom	4
Sec. 3. Certain specific applications of the gyroscope with three degrees of freedom	16
Sec. 4. The stabilized platform.	40
Sec. 5. The differentiating gyroscope.	45
Sec. 6. The integrating gyroscope.	53
Sec. 7. The spatial angular-velocity integrator and application of the integrating gyroscope to geometrical stabilization.	60
Chapter II. Design and Basic Parameters of Floating Gyroscopes	75
Sec. 1. Integrating gyroscopes	78
Sec. 2. Differentiating gyroscopes	115
Sec. 3. Floating gyroscopes with three degrees of freedom. . .	126
Chapter III. Theory of the Floating Integrating Gyroscope.	130
Sec. 1. Differential equation of motion of the floating gyroassembly	131
Sec. 2. Equation for the floating integrating gyroscope. . . .	146
Sec. 3. Transfer function and frequency characteristic of the floating integrating gyroscope	153

CONTENTS (cont)

	Page
Sec. 4. Relative dimensionless values	157
Sec. 5. Floating integrating gyroscopes operating in the steady state.	162
Sec. 6. Floating integrating gyroscopes coupled with a servodrive.	171
 Chapter IV. Theory of the Floating Differentiating Gyroscope.	 187
Sec. 1. Differential equation of motion of the floating dif- ferentiating gyroscope with torsion rod	188
Sec. 2. Equation for floating differentiating gyroscope with torsion rod	193
Sec. 3. Transfer function and frequency characteristic of the floating differentiating gyroscope with torsion rod	194
Sec. 4. Floating differentiating gyroscope with torsion rod operating in the steady state	196
Sec. 5. Equation for floating differentiating gyroscope with feedback circuit.	206
Sec. 6. Transfer functions and frequency characteristics of floating differentiating gyroscopes with feedback	214
Sec. 7. Steady-state operation of a differentiating gyro- scope with feedback	217
Sec. 8. Comparison of the two types of differentiating gyroscope	228
 Chapter V. Analysis of Floating Gyroscopes.	 237
Sec. 1. An outline of static analysis	238
Sec. 2. Static analyses of differentiating gyroscopes	241
Sec. 3. Static analyses of integrating gyroscopes in the spatial integration regime.	257
Sec. 4. Static analysis of integrating gyroscopes in the geometric-stabilization regime.	265

CONTENTS (cont)

	Page
Sec. 5. Drift analysis of differentiating gyroscopes	272
Sec. 6. Drift analysis of integrating gyroscopes	273
Sec. 7. Dynamic testing.	279
 Chapter VI. Inertial System of Navigation.	 291
Sec. 1. General outline.	291
Sec. 2. Working principle of inertial system of navigation . .	294
Sec. 3. Problems of the practical application of the inertial navigation system.	296
Sec. 4. Application of the principle of the pendulum with an oscillation period of 84.4 min to the inertial system of navigation.	307
Sec. 5. Effect of the Coriolis acceleration and the non- spherical shape of the Earth on the operation of the inertial system of navigation.	310
Sec. 6. Combining inertial systems of navigation with other navigational systems.	311
Sec. 7. Some components of inertial navigation systems	315
 REFERENCES: Literature on the general and applied theory of gyroscopes and aircraft gyroscopic instruments.	 326
References Used.	328